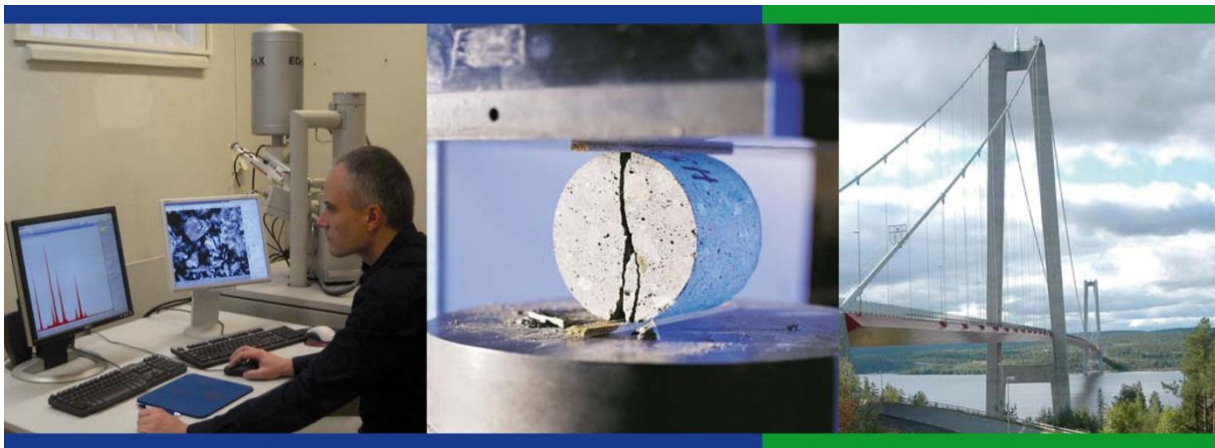




Chloride Ingress in Concrete Exposed to Marine Environment

-Field data up to 20 years' exposure



Dimitrios Boubitsas

Tang Luping

Peter Utgenannt

Chloride Ingress in Concrete Exposed to Marine Environment

-Field Data Up to 20 Years' Exposure

Dimitrios Boubitsas

010-516 68 50, dimitrios.boubitsas@cbi.se

Tang Luping

031-772 23 05, tang.luping@chalmers.se

Peter Utgenannt

010-516 68 70, peter.utgenannt@cbi.se

Final draft rapport: 2014-02-14

Preface

In the 1990s Swedish researchers have made great efforts to study chloride ingress and its consequences – chloride-induced corrosion of reinforcement steel and salt-frost scaling. The research projects covered not only fundamental studies but also intensive field investigations, including the establishment of a field exposure site in a marine environment at the Träslövsläge field site on the west coast of Sweden. At the test site a large number of concrete panels made of different concrete compositions have been exposed to the harsh marine climate. In a number of previous research projects the concrete slabs were periodically sampled for chloride penetration profiles after exposure for 0.5–2, 5 and 10 years. In this project, chloride penetration profiles in all of the available concrete slabs after exposure for over 20 years were measured again.

The work carried out in the laboratory was primarily carried out at CBI, the Swedish Cement and Concrete Research Institute in Borås, except for measurements of the moisture profiles, which were carried out at Chalmers University in Gothenburg.

This project was financially supported by SBUF – The Development Fund of the Swedish Construction Industry, the construction company Skanska AB, the cement producer Cementa and the microsilica powder producer Elkem. The financial support is gratefully acknowledged.

A special thanks to the very experienced reference group of this project and for all the participants' input and valuable guidance: Kyösti Tuutti (chairman), Magnus Alfredsson, Bo-Erik Eriksson, Per Fidjestöl, Jens Mejer Frederiksen, Hans Hedlund, Elisabeth Helsing, Ulf Jönsson, Christian Munch-Petersen, Lars-Olof Nilsson, Nils Rydén and Stefan Sandelin.

Abstract

This report presents the results from a research project dealing with chloride ingress in concrete exposed to a marine environment after exposure for over 20 years. In the beginning of the 1990s, some 40 types of concrete slabs were exposed to seawater at the Träslövsläge field site on the west coast of Sweden. Through a number of previous research projects the concrete slabs were periodically sampled for chloride penetration profiles after exposure for 0.5–2, 5 and 10 years. In this project, chloride penetration profiles in all of the available concrete slabs after exposure for over 20 years were measured again. These chloride profiles were used for validation of prediction models for chloride penetration. Two models, one empirical and another mechanism-based, were compared with the measured chloride profiles. In the study the corrosion conditions of the rebars embedded in the concrete slabs were measured using a non-destructive method developed based on the principle of galvanostatic pulse technique. A destructive visual examination was carried out to confirm the results from the non-destructive method.

The results show that the chloride ingress is in general more severe in the submerged zone than in the other zones. Multi-pozzolanic additions such as fly ash and silica fume can effectively reduce chloride ingress. The mechanism-based model gives reasonable prediction of chloride ingress from 1 up to 20 years whilst the empirical model based on short-term field data underestimates chloride ingress in concrete with low water-binder ratios and pozzolanic additions. From the predictions of the mechanism-based model, it has been demonstrated that the best measure to achieve 100 years' service life with a cover thickness of for example 60 mm is to use either 5% silica fume or 20% fly ash with reduced water-binder ratio ≤ 0.30 , or to use a combination of both fly ash and silica fume (w/b 0.35). It seems that a water-binder ratio lower than 0.30 does not further reduce chloride ingress.

The chloride threshold values were estimated from the analysis of corrosion conditions and chloride contents at the cover depth measured after 10 and 20 years' exposure. The results make it reasonable to assume a chloride threshold value of at least 1% by weight of binder for initiation of corrosion of reinforcement steel embedded in the marine concrete structures. This threshold value seems valid for various unitary and binary binders including ordinary Portland cement, sulphate resistance Portland cement and blended cement with 5% silica fume, and with different water-binder ratios in a range of 0.3 to 0.5. For the ternary binder blended with 5% silica fume and 10% fly ash with water binder ratio 0.35, the chloride threshold value can be as high as 2% by weight of binder content. These chloride threshold values were based on the results from thin cover thickness. A thicker cover provides a relatively more stable micro-climate with less variation in moisture and oxygen, implying that a higher chloride concentration is needed to initiate corrosion under such a stable climate condition. Therefore, it is reasonable to assume somewhat higher threshold values for steel embedded in concrete with greater cover thickness.

Sammanfattning (Summary in Swedish)

I denna rapport presenteras resultat från ett forskningsprojekt som behandlar kloridinträngning i betong utsatt för havsmiljö efter exponering i över 20 år. I början av 1990-talet placerades ett stort antal betongplattor av ca 40 olika betongsammansättningar, vid en fältprovplats i Träslövsläges hamn i Varberg på svenska västkusten. Betongplattorna har använts för provtagning i flera tidigare forskningsprojekt och kloridinträngningsprofiler är uppmätta efter exponering i 0,5–2; 5 och 10 år. I detta projekt har kloridinträngningsprofiler i alla tillgängliga betongplattor uppmätts efter ca 20 års exponering. Kloridprofilerna används för validering av modeller för kloridinträngning. Beräkningsresultat från två modeller, en empirisk och en mekanismbaserad, jämfördes med de uppmätta kloridprofilerna. I detta projekt undersöktes också korrosionsförhållandena för armeringsstål inbäddade i betongplattor med hjälp av en icke-förstörande metod. Metoden är baserad på principen om galvanostatisk pulsteknik. Dessutom genomfördes okulärbesiktning på ett stort antal armeringsstål som sågades fram och frigjordes från betongplattorna. Okulärbesiktningen genomfördes för att bekräfta resultaten från den icke-förstörande metoden.

Resultaten visar att kloridinträngningen i allmänhet är större i den zon av provplattorna som varit nedsänkta under vattenytan jämfört med skvalpzonen och den atmosfäriska zonen. Resultaten visar också på att de betongsammansättningar som innehåller puzzolanska tillsatsmaterial så som flygaska och/eller kiselstoft erhåller en långsammare kloridinträngning jämfört med övriga betongsammansättningar. Den mekanismbaserade modellen ger en rimlig bedömning av kloridinträngningen från 1 upp till 20 års exponering. Den empiriska modellen baserad på kortsiktiga fältdata underskattar däremot kloridinträngning i betong med låga vattenbindemedelstal och puzzolanska tillsatsmaterial. Resultat från den mekanismbaserade modellen för kloridinträngning visar att den bästa åtgärden för att erhålla 100 års livslängd med ett täcksikt på 60 mm är att använda en betongsammansättning med portlandcement tillsammans med antingen 5 % kiselstoft eller 20 % flygaska eller en kombination av båda flygaska och kiselstoft och med ett vattenbindemedelstal på 0,35.

Genom analys av korrosionsförhållanden och kloridhalt vid armeringsstålen efter 10 respektive 20 års exponering har en bedömning av kloridtröskelvärden utförts. Resultaten visar att för betongkonstruktioner i marin miljö är det rimligt att anta ett kloridtröskelvärde för initiering av korrosion på armeringsstål på åtminstone 1 % av bindemedelvikten. Detta tröskelvärde verkar gälla för betong med olika bindemedel med en eller två huvudbeståndsdelar såsom ordinära portlandcement, sulfatresistent portlandcement och portlandsilikacement med 5 % silikastoft, och för olika vattenbindemedelstal i intervallet 0,3 till 0,5. För betong med bindemedel sammansatt av de tre beståndsdelarna portlandcement, silikastoft (5 %) och flygaska (10 %) och med vattenbindemedelstalet 0,35 kan kloridtröskelvärdet vara så högt som 2 % av bindemedelvikten. Den bedömning som gjorts här gällande kloridtröskelvärden är baserad på resultat från undersökningar på provkroppar med i de flesta fall litet täckande betongskikt. För ingjutet stål i konstruktioner med större täckande betongskikt är det rimligt att förvänta sig något högre kloridtröskelvärde då förhållandena vid stålet med avseende på fukt- och syrehalt är mer stabila.

Contents

	Page
Preface	I
Abstract	II
Sammanfattning (Summary in Swedish)	III
1 Introduction.....	1
2 Concrete Specimens and Exposure Conditions	3
2.1 Concrete slabs.....	3
2.2 Exposure conditions at the Träslövsläge field site	7
3 Measurements of Chloride and Moisture Profiles	8
3.1 Sampling.....	8
3.2 Measurement of chloride profiles.....	9
3.3 Measurement of moisture profiles	10
4 Effect of exposure zones	11
4.1 Chloride profiles	11
4.2 Moisture profiles.....	14
4.3 Effect of water-binder ratio and entrained air	16
4.4 Effect of binder type	18
4.5 Distribution of other ions.....	19
5 Modelling of Chloride Ingress	21
5.1 Curve-fitted diffusion coefficient	21
5.2 Modelling of chloride ingress in concrete	24
5.3 Input parameters used for modelling	25
5.4 Modelled results	26
5.5 Prediction of chloride ingress after 100 years' exposure	31
6 Chloride induced corrosion.....	32
6.1 Measurement Methodology	32
6.2 Corrosion measurements	33
6.3 Chloride threshold values for corrosion initiation.....	37
6.4 Further visual examination and confirmation of corrosion conditions.....	41
7 Concluding Remarks.....	44
8 References.....	45

Appendix 1 - Method for determination of acid soluble chloride and calcium in concrete

Appendix 2 - Chloride profiles sampled 2012 (~20 years)

Appendix 3 - Curve-fitted parameters D_{F2} and C_s

Appendix 4 - Data from corrosion measurements

Appendix 5 - Visual examination and confirmation of corrosion conditions

1 Introduction

Chloride-induced reinforcement corrosion is one of the most important degradation processes in reinforced concrete structures exposed to a marine environment and road environment where de-icing salt is used in the winter (Hobbs, 2001). Concrete is a porous material in which the pores are partially filled with water. When concrete is exposed to salt solutions chloride ions migrate into the concrete changing the environment around the reinforcement, and causing a degradation of the reinforcement with time (Tuutti, 1982) (Bamforth et al., 1997). The degradation of reinforced concrete structures, especially infrastructures, has very important economic and social consequences due to the need for diverting resources for repairing damaged structures and sometimes the need to close the facility for carrying out the repair work. It is a common consensus that concrete structures should be built in an economical, sustainable and safe way. Therefore models for chlorides transport in concrete are needed to design new concrete structures and also to assess or redesign the existing structures. In order for these models to be robust and reliable they must be validated based on findings from research on concrete structures exposed in the field, especially after long-term exposure. Owing to Sweden's long coastline and intensive application of de-icing salt, the topic of chloride ingress in concrete has special significance. In the beginning of the 1990s, a Swedish national project called "BMB" – Durability of Marine Concrete Structures – was initiated (Sandberg, 1996). As a part of work in the BMB project, some 40 types of concrete specimens were exposed to seawater at the Träslövsläge field site on the west coast of Sweden. The specimens were periodically sampled for chloride penetration profiles, which served to provide "first-hand" information about chloride ingress into concrete and are believed valuable for the examination of modelling for chloride penetration. The chloride ingress profiles for samples exposed for up to five years to seawater at the field site have been measured during the lifetime of the BMB project.

After the BMB project, many concrete slabs were left at the field site for continuous long-term exposure. To collect the field data after 10 years' exposure, SP Technical Research Institute of Sweden (the parent company of CBI Betonginstitutet AB) together with Chalmers University of Technology (Chalmers) carried out a project under the financial support of Swedish National Road Administration (SP Report 2003:16). Further, to collect the field data after 20 years' exposure CBI together with SBUF (The Development Fund of the Swedish Construction Industry), Cementa and Elkem carried out this project with the main objectives to:

- measure chloride and moisture profiles in the concrete slabs after 20 years' exposure at the field site
- compare the new data with the previous data
- model chloride ingress using previously developed model
- perform the evaluation of chloride-induced corrosion of steel in concrete

The Träslövsläge field site is perhaps the first field exposure site in the world for systematic collection of chloride ingress profiles in various types of concrete. Nanukuttan et al. (2010) reported some chloride ingress data from one type of concrete (CEM I, w/c 0.4) after exposure under the North Sea tidal zone near the Dornoch bridge, Scotland, for 18 years. Baroghel-Bouny et al. (2013) reported some chloride ingress profiles from 15 different types of concrete after exposure under the Atlantic tidal zone in La Rochelle, France, for 10 years. It can be noticed that these published field data were taken from tidal zone which make the modelling and validation more complicated. On the other hand, the data from the Träslövsläge field site were taken mainly from the submerged zone, which supplies unique opportunity for validating chloride ingress models under clearer boundary conditions with the longest exposure time (over 20 years).

2 Concrete Specimens and Exposure Conditions

2.1 Concrete slabs

The original mixture proportions of concrete cast 20 years ago are summarised in Table 2.1. The main variations included water-binder ratio (0.25, 0.3, 0.35, 0.4, 0.5, 0.6 to 0.75), binder type (four types of cement with different additions of silica fume and fly ash), and air content (6% entrained air and non-AEA). The water-binder ratios in Table 2.1 were calculated assuming that the efficiency factor for silica fume is 1 and for fly ash 0.3. Nowadays, according to the European standard EN 206-1, the efficiency factor for silica fume is 1–2 and for fly ash 0.2–0.4. It should be noted that the moisture content in the fine and coarse aggregate was regarded as free accessible water for cement hydration, and was included in the calculation of the water-binder ratios. Concrete slabs of 1000×700×100 mm were cast at the SP Swedish Technical Research Institute. After moisture curing for about two weeks, the slabs were transported to the Träslövsläge field site and mounted on the sides of pontoons for exposure with the bottom side of the slab facing the seawater. A parallel set of slabs was transported to the laboratory at Chalmers for measurement of accelerated chloride transport as it is described in Tang (2003b).

Table 2.1 Mixture proportions of concrete exposed at the Träslövsläge field site in 1992.

Mix No.	Binder type	Binder kg/m ³	Water-binder ratio ¹⁾	Fine aggreg. 0-8 mm kg/m ³	Coarse aggreg. 8-16 mm kg/m ³	Sp ²⁾ % of binder	AEA ³⁾ % of binder	Air content %	28d compr. Strength ⁴⁾ MPa
1-35	100%Anl ⁵⁾	450	0.35	839	839	1	0.041	6.0	70
1-40		420	0.40	873	806	0.8	0.03	6.2	58
Ö		430	0.38	813	840	1	0.04	6.2	58
1-50		370	0.50	876	808	-	0.033	6.4	41
1-75		240	0.75	1013	796	-	0.029	6.1	21
2-35	100%Slite ⁶⁾	450	0.35	801	868	1.7	0.038	5.7	60
2-40		420	0.40	871	804	1.3	0.029	6.2	54
2-50		390	0.50	853	787	-	0.026	5.8	42
2-60		310	0.60	936	797	-	0.022	6.3	35
2-75		250	0.75	999	785	-	0.02	5.8	26
3-35	95%Anl+5%SF ⁷⁾	450	0.35	801	868	1.2	0.08	5.8	72
3-40		420	0.40	835	835	0.8	0.043	6.1	61
3-50		370	0.50	840	840	-	0.04	6.0	45
3-75		240	0.75	966	823	-	0.039	5.9	21
4-40	90%Anl+10%SF	420	0.40	803	870	1.17	0.043	6.6	65
5-40	95%Anl+5%SF	420	0.40	878	878	1.5	0.006	2.9	81
6-35	95%Anl+5%SF	450	0.35	858	929	1.5	-	2.1	93
6-40	95%Anl+5%SF	420	0.40	898	898	1.5	-	1.7	87

Table 2.1 (Continuation)

Mix No.	Binder type	Binder kg/m ³	Water-binder ratio ¹⁾	Fine aggreg. 0-8 mm kg/m ³	Coarse aggreg. 8-16 mm kg/m ³	Sp ²⁾ % of binder	AEA ³⁾ % of binder	Air content %	28d compr. Strength ⁴⁾ MPa
7-35	100%Anl ⁵⁾	450	0.35	898	898	1.5	-	2.4	91
7-40	100%Anl	420	0.40	939	867	1	-	2.1	79
7-75	100%Anl	265	0.75	1044	821	-	-	1.1	32
8-35	100%Slite ⁶⁾	470	0.35	847	918	1.8	-	2.1	73
8-40	100%Slite	440	0.40	882	882	1.5	-	2.1	67
8-50	100%Slite	410	0.50	893	924	-	-	1.4	56
8-60	100%Slite	330	0.60	977	833	-	-	1.6	45
8-75	100%Slite	270	0.75	1040	817	-	-	1.4	37
9-40	95%DK ⁸⁾ +5%SF ⁷⁾	420	0.40	839	839	1.2	0.037	6.5	63
10-40	78.5%DK+17%FA ⁹⁾ +4.5%SF	420	0.40	770	905	1.7	0.063	6.1	69
11-35	85%DK+10%FA+5%SF	450	0.35	781	917	2.33	0.04	5.7	84
12-35	85%Anl+10%FA+5%SF	450	0.35	781	917	1.87	0.055	6.4	73
H1	95%Anl+5%SF	500	0.30	836	942	2.3	-	0.8	112
H2	90%Anl+10%SF	500	0.30	820	963	2.1	-	1.1	117
H3	100%Anl	492	0.30	791	892	2.7	-	3.6	96
H4	95%Anl+5%SF	420	0.40	840	840	0.8	0.055	5.9	63
H5	95%Anl+5%SF	551	0.25	806	946	3	-	1.3	125
H6	95%Anl+5%FA	518	0.30	791	892	2.5	-	2.8	95
H7	95%Deg400 ¹⁰⁾ +5%SF	500	0.30	836	942	2.3	-	1.3	117
H8	80%Anl+20%FA	616	0.30	680	865	2.8	-	3.0	98
H9	100%Deg400	500	0.30	812	916	2.3	-	2.9	102

1) Assuming that the efficiency factor of silica fume is 1 and fly ash is 0.3

2) Sp – Super-plasticiser. Cementa 92M

3) AEA – Air-entraining agent. Cementa L14

4) According to SS 13 72 10

5) Anl – AnlÄggningscement (Swedish SRPC, CEM I 42,5 N MH/SR/LA)

6) Slite – Slite cement (Swedish OPC, CEM I 42,5 R)

7) SF – Silica fume (Elkem. Norway)

8) DK – Aalborg Lav cement (Danish SRPC)

9) FA – Fly ash (Aalborg, Denmark)

10) Deg400 – Degerhamn 400 cement (another type of Swedish SRPC, CEM I 52,5 N SR/LA)

It should be noted that the slurry silica fume was used in concrete H-series, while the powder one was used in the other types of concrete.

Additional concrete slabs were cast at SP and placed at Träslövsläge field site both in 1993 and 1994. The mixture proportions of concrete cast on both these occasion are summarised in Table 2.2.

Table 2.2 Mixture proportions of concrete exposed at the field site in 1993 and 1994.

Mix No.	Binder type	Binder kg/m ³	Water - binder ratio ¹⁾	Fine aggreg. 0-8 mm kg/m ³	Coarse aggreg. 8-16 mm kg/m ³	Sp ²⁾ % of binder	AEA ³⁾ % of binder	Air content %	28d compr. Strength ⁴⁾ MPa
Placed at the test site 1993									
30-5	95%AnI ⁵⁾ +5%SF ⁶⁾	500	0.30	763	896	2	0.1	6.2	90
35-5	95%AnI+5%SF	450	0.35	804	874	1.2	0.09	5.6	78
50-5	95%AnI+5%SF	370	0.50	840	840	-	0.07	5.8	47
Placed at the test site 1994									
94-1	Slag cement ⁷⁾	450	0.35	837	837	1.5	0.025	5.8	71.6
94-2	100%AnI	450	0.35	839	839	1.1	0.035	6.1	68.3
94-3	95%AnI+5%SF	450	0.35	800	867	1.06	0.055	6.3	79.1
94-4	85%AnI+5%SF+10%FA ⁸⁾	450	0.35	772	906	1.5	0.05	5.5	82.2
RHA2	85%AnI+15%RHA ⁹⁾	410.2	0.35	672 ¹⁰⁾	1207.2 ¹¹⁾	1.5	-		105.8

1) Assuming that the efficiency factor of silica fume is 1 and fly ash is 0.3

2) Sp – Super-plasticiser. Cementa 92M

3) AEA – Air-entraining agent. Cementa L14

4) According to SS 13 72 10

5) AnI – Anl ggningscement (Swedish SRPC, CEM I 42,5 N MH/SR/LA)

6) SF – Silica fume (Elkem. Norway)

7) Slagcement – Cementfabriek Ijmuiden, Holland (CEM III / B 42,5 N)

8) FA – Fly ash (Aalborg, Denmark)

9) RHA – Rice Husk Ash

10) Fine aggreg. 0–8 mm

11) Coarse aggreg. 8–12 mm

Except for mix RHA2, the slabs placed at the test site in 1994 were prepared in three different conditions: A=no cracks, B=with artificial cracks and C=natural cracks. Fig. 2.1 shows on the left-hand side a slab with artificial cracks (slab 94-1-B) and on the right-hand side a slab with so-called natural cracks (slab 94-3-C). The type B cracks were achieved by placing metal discs of different thickness (0.5, 0.3, 0.1 and 0.05 mm) in the concrete when it started to set. How the so-called natural cracks were achieved is not clear.

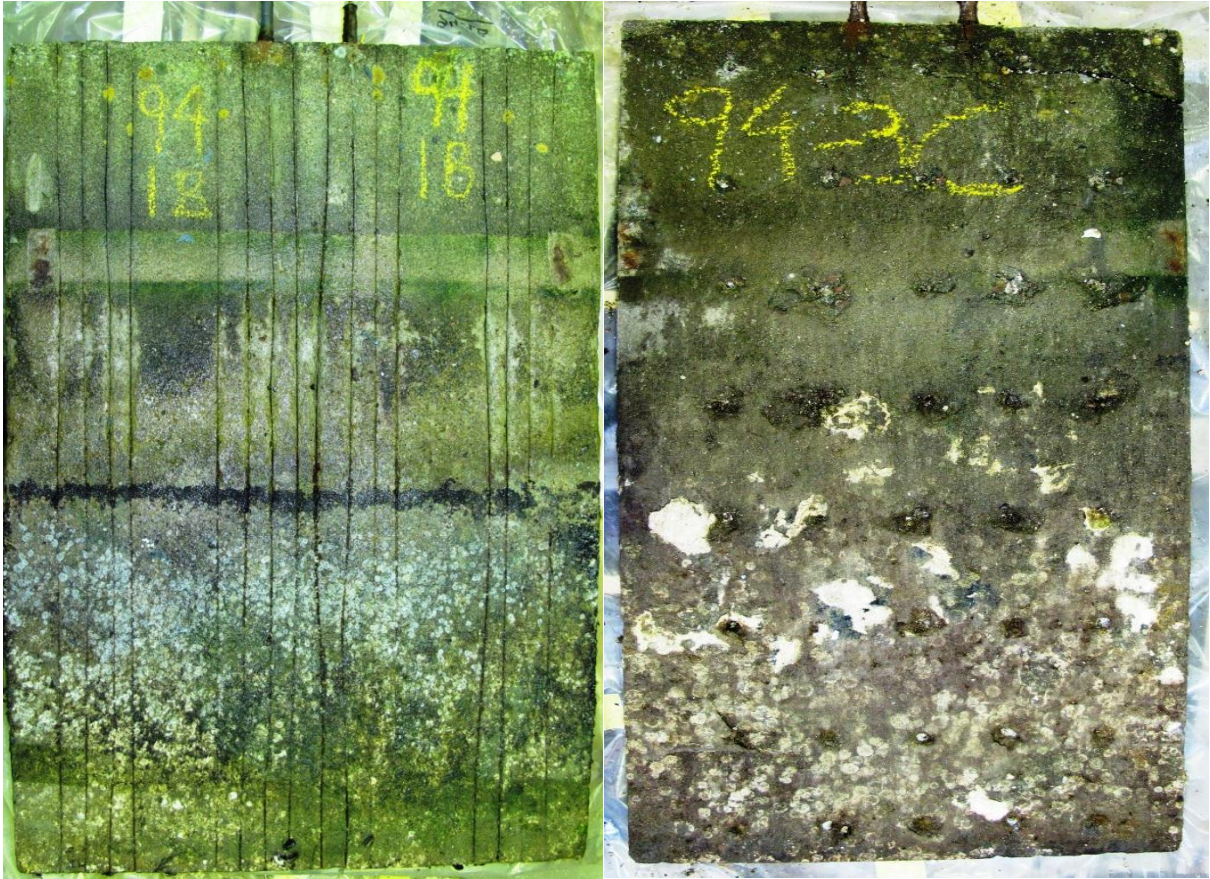


Figure 2.1 Slabs with different simulated cracks, the left slab 94-1-B with artificial cracks and the right slab 94-3-C with so-called natural cracks.

2.2 Exposure conditions at the Träslövsläge field site

An overview of the Träslövsläge field site is shown in Fig. 2.2. The chloride concentration in the seawater varies from 10 to 18 g Cl per litre, with an average value of about 14 g Cl per litre. The typical water temperature is illustrated in Fig. 2.3 and has an annual average of +11°C.



Figure 2.2 Overview of the Träslövsläge field site.

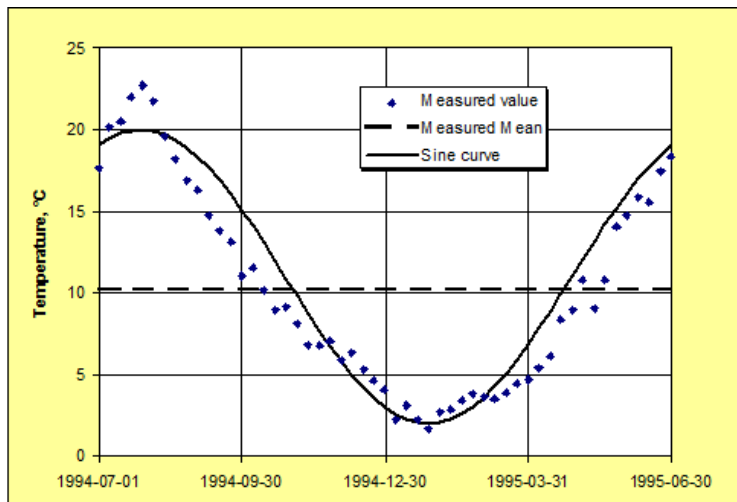


Figure 2.3 Annual temperature in the seawater.

3 Measurements of Chloride and Moisture Profiles

3.1 Sampling

In this investigation, the concrete slabs were sealed in thick plastic and stored outside the laboratory (up to 6 months) to perform corrosion rate measurements and then taken into the laboratory where cores (\varnothing 100 mm) were drilled. The exposure condition of the slabs was divided into three major zones as illustrated in Fig. 3.1. An atmospheric zone constantly above sea level, a splash zone with more unstable conditions (further sub-divided into three zones) and a submerged zone constantly under sea level. The splash zone was as mentioned divided into three zones: a zone mostly above sea level (Sa), a zone at sea level (splash), and a zone mostly below sea level (Su), see Fig. 3.1. For all concrete slabs one core for chloride profile was taken from the submerged zone, for some slabs cores from up to four exposure zones were taken. From some slabs cores for moisture profiling were also taken, Table 3.1 shows more specifically the experimental programme.

The sampling positions were chosen in such a way that the least distance between the curved surface of a core and the outermost side of a slab is about 150 mm to avoid the influence of two-dimensional penetration as much as possible.

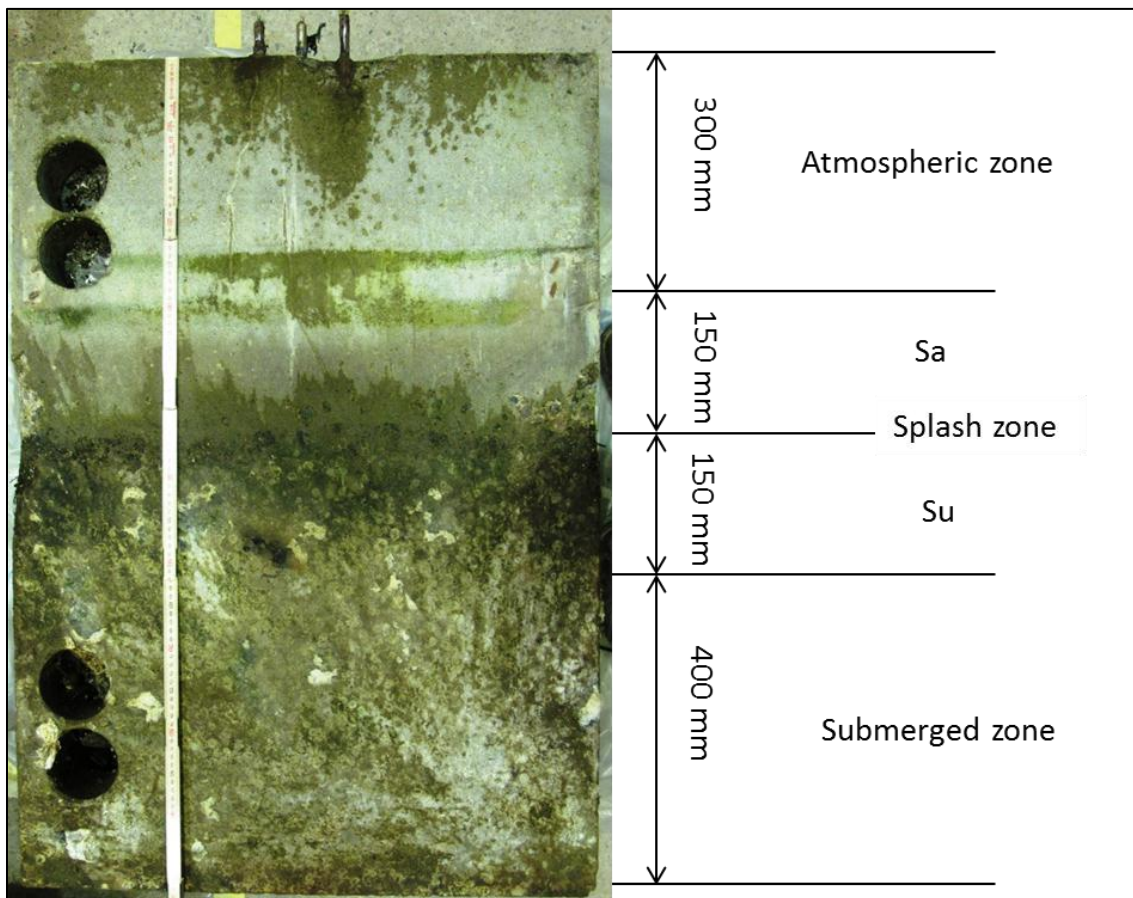


Figure 3.1 Sampling overview of a concrete slab after exposure.

Table 3.1 Experimental programme in this project, sampled cores and exposure zones.

Mix No.	Cores chloride profiles	Cores moisture profiles	Remarks regarding exposure zones ¹⁾
Placed at the test site 1992			
1-35	3	1	For Cl: A-, S-, and Sub-zone; For RH: Sub-zone
1-40	4	3	For Cl: A-, Sa-, Su, and Sub-zone; For RH: A-, Su-, Sa-zone
2-35	3	1	For Cl: A-, S-, and Sub-zone; For RH: Sub-zone
2-50	3		For Cl: A-, S-, and Sub-zone
3-35	3	1	For Cl: A-, S-, and Sub-zone; For RH: Sub-zone
5-40	4	3	For Cl: A-, Sa-, Su, and Sub-zone; For RH: A-, Su-, Sa-zone
6-35	1		Sub.-zone
6-40	1		Sub.-zone
7-35	1		Sub.-zone
7-40	1		Sub.-zone
8-35	1		Sub.-zone
8-40	1		Sub.-zone
12-35	1		Sub.-zone
H1	1		Sub.-zone
H2	1		Sub.-zone
H5	1		Sub.-zone
H8	1		Sub.-zone
Placed at the test site 1993			
30-5	1		Sub.-zone
35-5	1		Sub.-zone
50-5	1		A-zone
Placed at the test site 1994			
94-1	1		Sub.-zone
94-2	1		Sub.-zone
94-3	1		Sub.-zone
94-4	1		Sub.-zone
RHA2	1		Sub.-zone

1) Abbreviations (see also Fig. 3.1): A = Atmospheric zone, Sa = Upper part of the splash zone
S = Right on the splash zone (sea level), Su = Lower part of the splash zone, Sub. = Submerged zone.

3.2 Measurement of chloride profiles

The cores individually sealed in double thick plastic bags were stored in the laboratory at room temperature for no longer than two weeks prior to sampling. Powder samples were then taken from each core by means of dry grinding on a lathe with a diamond tool (Fig. 3.2), successively from the exposed surface to a certain depth. The depth of each sample was measured from the lathe with an accuracy of 0.5 mm. After grinding, the powder samples

were immediately dried at 105°C and then stored in a desiccator for further chloride and calcium analysis. The acid-soluble chloride content in each sample was determined principally in accordance with AASHTO T260 using potentiometric titration on an automatic titrator Metrohm Titrator 716 with chloride-selective electrode and Ag/AgCl reference electrode. A sample size of about 1.5 grams was used to facilitate the parallel calcium analysis. According to the results from a Nordic inter-comparison test (Tang, 1998) and an international inter-comparison test (Castellote and Andrade, 2001), this potentiometric titration technique reveals good precision.

The technique for determination of soluble calcium content parallel to the determination of chloride content was originally developed at Chalmers. In the past year, a Nordtest project was carried out to evaluate the precision of this technique (Tang, 2003a). The results from the Nordic inter-laboratory comparison test reveal satisfactory precision for this technique, whose pooled standard deviation of repeatability is 0.38 mass% of sample and pooled standard deviation of reproducibility is 0.90 mass% of sample. A more detailed description of the method for determination of chloride and calcium contents is given in Appendix 1. Since similar techniques were employed in the previous investigations even though by different operators, the obtained data from various investigations should be reliable and comparable.

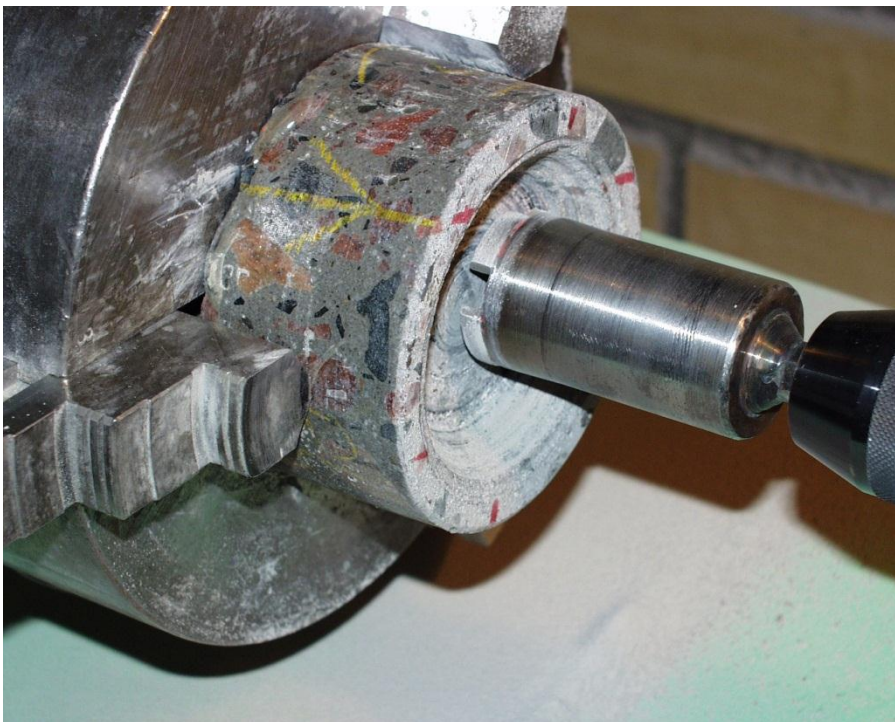


Figure 3.2 Illustration of grinding concrete samples on a lathe.

3.3 Measurement of moisture profiles

The measurement of moisture profiles was carried out at Chalmers. The cores, individually sealed in double thick plastic bags, were stored in the laboratory at room temperature for no longer than a few days prior to sampling. A slice of about 10~20 mm thick was split from

each concrete core, starting from one of the ends, with the help of a compression jack. A large piece of sample of about 10~30 g and a number of small pieces of sample were immediately taken, using hammer and chisel, from the central portion of the freshly split slice. The large piece was immediately weighed and then placed in a box for measurement of the degree of capillary saturation, while the small pieces were stored in a glass test tube for measurement of RH (Relative Humidity). The technique for measurement of RH has been well described by Nilsson (1980) and for degree of capillary saturation by Hedenblad and Nilsson (1985). After the above sampling, another slice was successively split and samples were taken. The above sampling process was repeated until all the samples were taken from each core.

4 Effect of exposure zones

4.1 Chloride profiles

The chloride profiles in concrete with three different types of binder and with the same water-binder ratio are summarised in Fig 4.1. It can be seen that the chloride ingress in the submerged zone is in general the severest among all the three exposure zones, while the chloride ingress in the splash zone may be similar to or less than that in the submerged zone. This is in agreement with the results from the previous investigations after 10 years' exposure, Tang (2003b).

From the previous investigations (Tang and Sandberg 1996) it has been known that the chloride profiles from the splash zone vary widely due to the unstable climate in this zone. Fig. 4.2 shows chloride profiles from two different concretes. In the splash zone two cores were taken, one in the upper splash zone (Sa) and one in the lower splash zone (Su) (see Fig. 3.1). It can be seen that the chloride profile taken in the Su zone coincides, and in some parts, even exceeds the chloride profile taken in the submerged zone. This is quite expected as this part of the slab most of the time will be under the sea level.

The chloride profile taken in the Sa zone is always lower than that taken from the submerged zone. However, the tendency of the chloride profiles from the Sa zone is not always consistent. For concrete 1-40 it is close to that from the submerged zone and in concrete 5-40 it is much lower, coinciding with the chloride profile taken in the atmospheric zone. The results in Fig. 4.2 imply that a small difference in the coring position may result in a large difference in the chloride profile.

Fig. 4.3 shows a comparison between chloride profiles from different exposure zones after 10 and 20 years. In the atmospheric zone a clear increase in the chloride levels can be observed. Whereas, for the submerged zone concretes 2-35 and 3-35, higher chloride levels are only seen further away from the exposed surface.

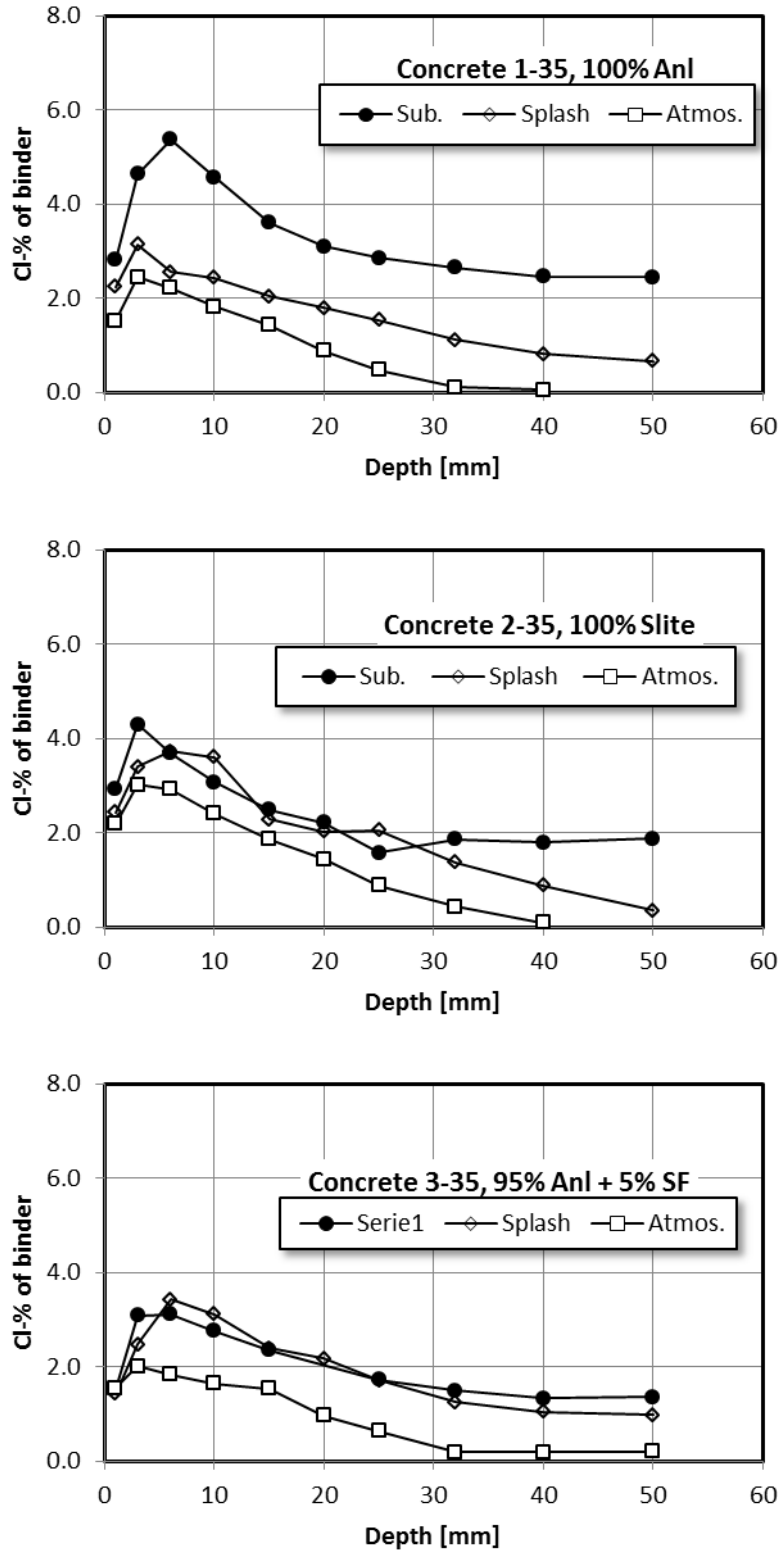


Figure 4.1 Profiles of chloride ingress in concrete under various exposure zones after 20 years' of exposure.

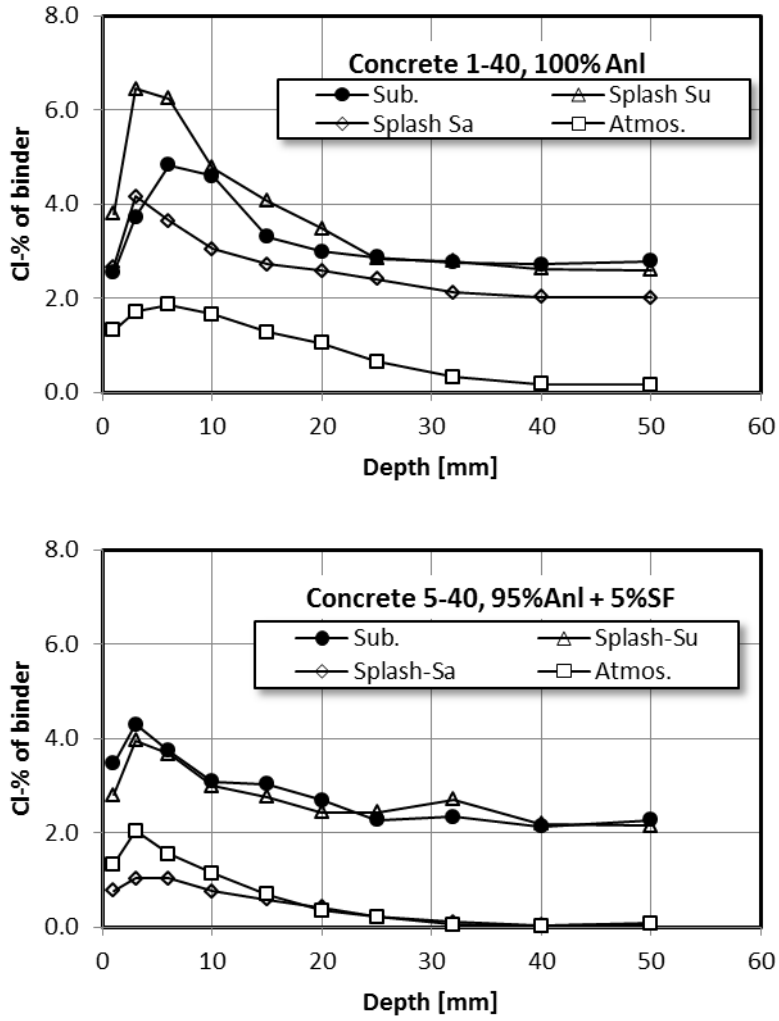


Figure 4.2 Profiles of chloride ingress in concrete under various exposure zones.

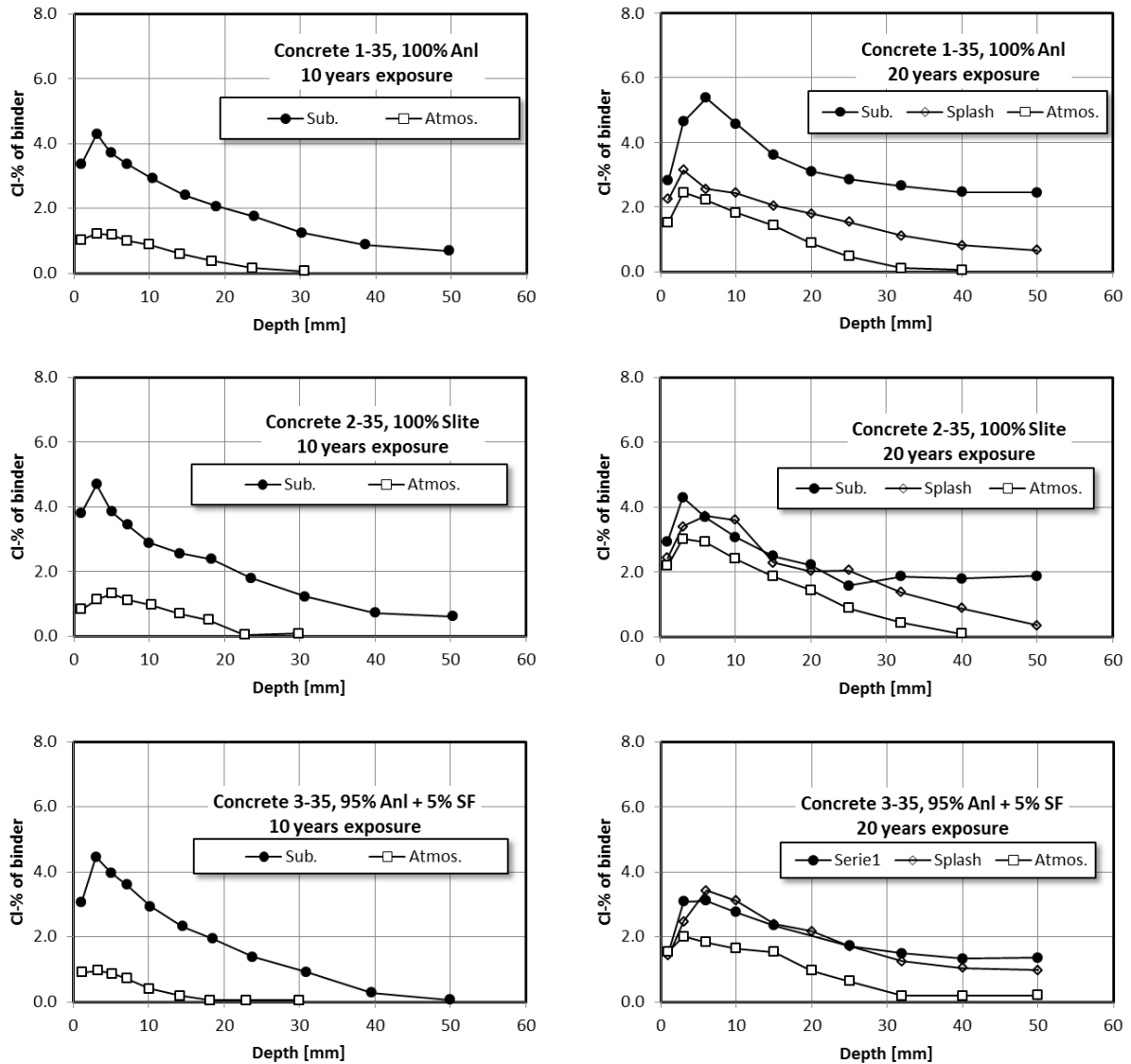


Figure 4.3 Comparison between chloride profiles from different zones after 10 and 20 years' exposure.

4.2 Moisture profiles

The moisture profiles in concrete with three different types of binder and with the same water-binder ratio (w/b 0.35) are summarised in Fig 4.4. It can be seen that the moisture level in the concrete with 5% silica fume (Concrete 3-35) is slightly lower than those in the concrete with plain cement (SRPC and OPC, i.e. concrete 1-35 and 2-35, respectively), which are close to the saturation conditions through the concrete. It is interesting to see that the degree of capillary saturation in the specimens after 20 years' exposure is lower than that after 10 years' exposure (Tang, 2003b), possibly due to different sampling conditions. In the report (Tang, 2003b) the cores for moisture profiles were taken immediately after lifting the slabs from the seawater at a low temperature, whilst in this study the slabs were transported to the laboratory and stored there for a period before taking cores. The effect of low temperature might make the degree of capillary saturation over 1 in the 10-year specimens.

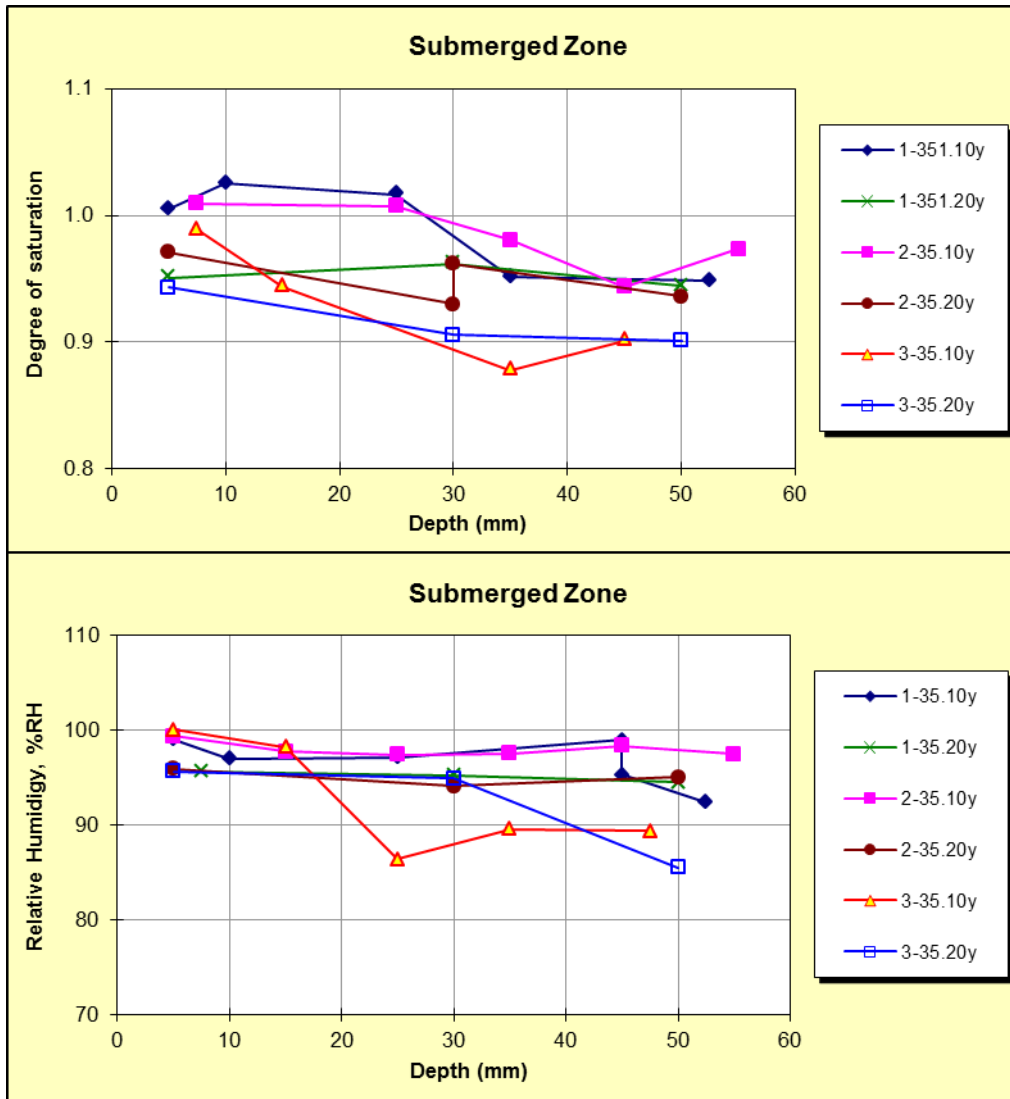


Figure 4.4 Comparison between moisture profiles from submerged zone after 10 and 20 years' exposure. 1 – SRPC; 2 – OPC; 3 – 95% SRPC + 5% silica fume.

Figure 4.5 shows the moisture profiles in the concrete taken from different exposure conditions. As expected, there is a significant difference in moisture profiles between atmospheric and submerged zones, while the moisture profiles taken from the splash zone can be close to the atmospheric zone or to the submerged zone, implying a high uncertainty in the moisture profiles from this zone.

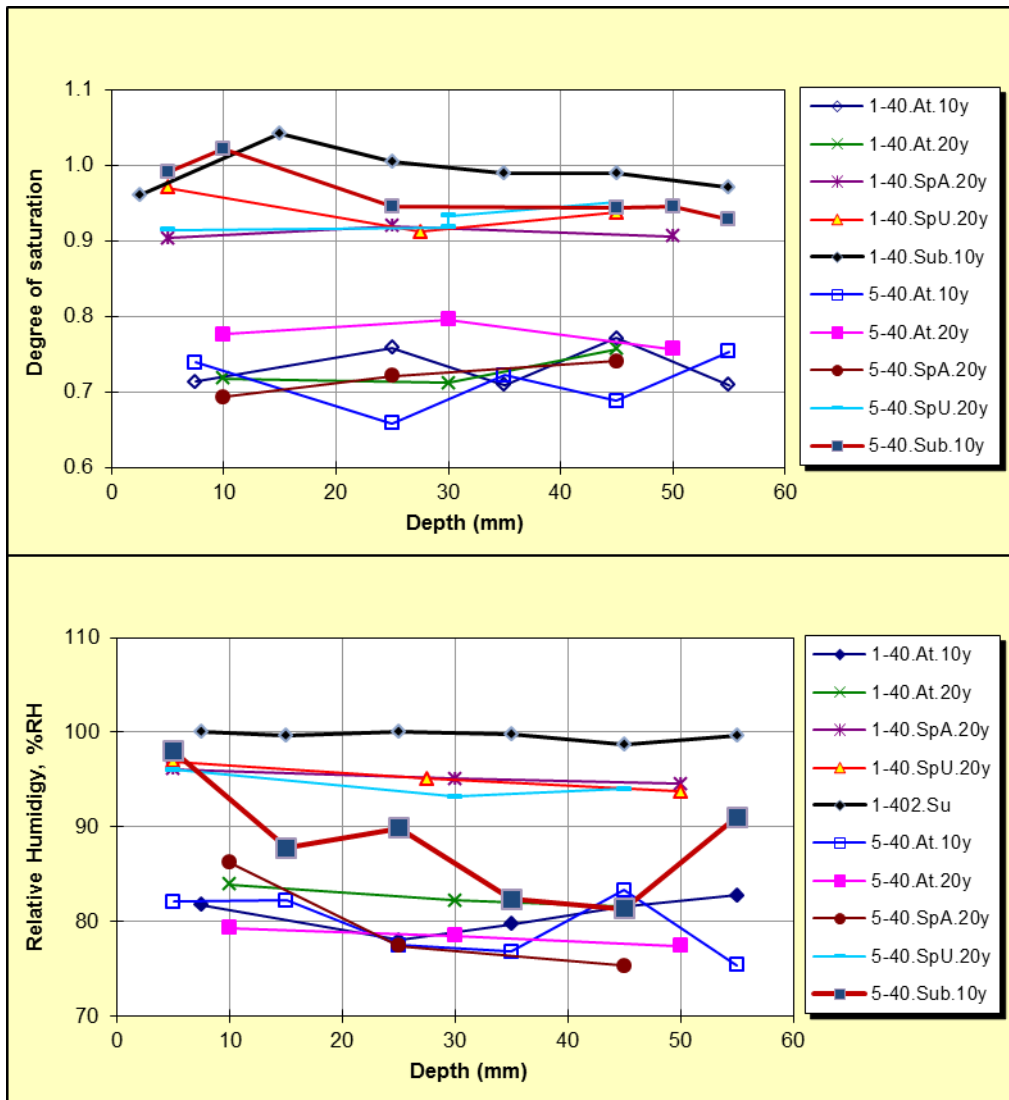


Figure 4.5 Comparison between moisture profiles from taken from different zones after 10 and 20 years' exposure. At = Atmospheric; SpA = Splash zone near atmospheric; SpU = Splash zone near submerged; Sub = submerged.

4.3 Effect of water-binder ratio and entrained air

The results and discussion hereafter will be limited to the submerged zone as the chloride ingress in this zone is in general the severest among all the three exposure zones (see Figs 4.1 and 4.2). Chloride profiles in concrete with different water-binder ratios are shown in Figs. 4.6 to 4.8. Not all concretes contained Air Entrained Agent (AEA) as indicated in the figures. In Fig. 4.8 concrete 5-40 contained a very small amount of AEA resulting in air content similar to the concretes without AEA. The results in Figs 4.6 and 4.8 show that lower water-binder ratio results in less chloride ingress. This is more evident in concretes with 95% Anl + 5%SF as binder. However, also in Fig. 4.7 for concretes with 100% Slite cement it can be seen that for a water-binder ratio of 0.5 the chloride ingress is much higher than for the lower water-binder ratios. Figs. 4.6 and 4.8 show also that the incorporation of AEA (air content ~6%) increases the chloride ingress. This is not evident in Fig. 4.7.

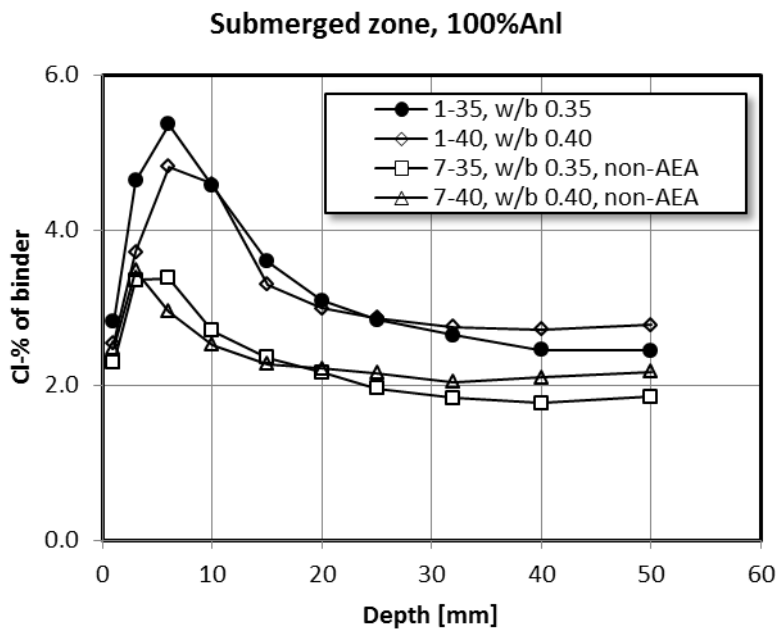


Figure 4.6 Chloride profiles in concrete with Anl cement with and without AEA.

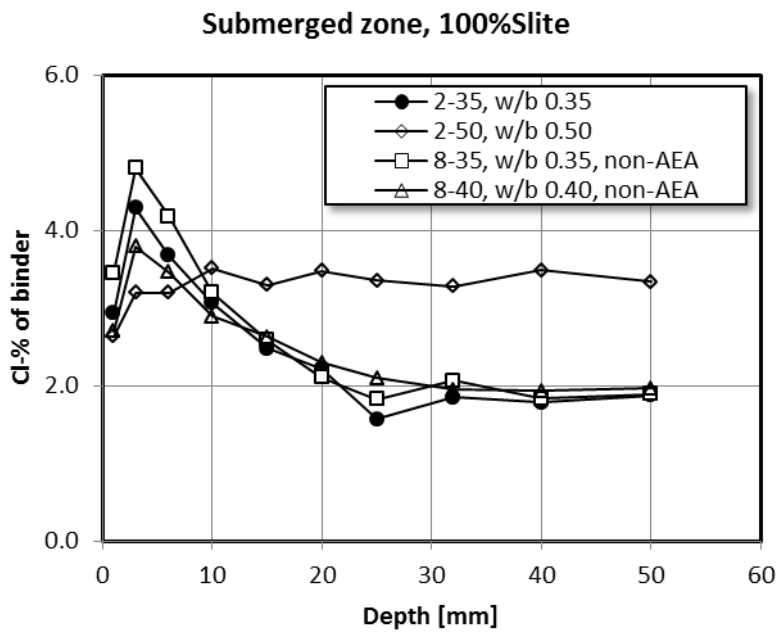


Figure 4.7 Chloride profiles in concrete with Slite cement with and without AEA.

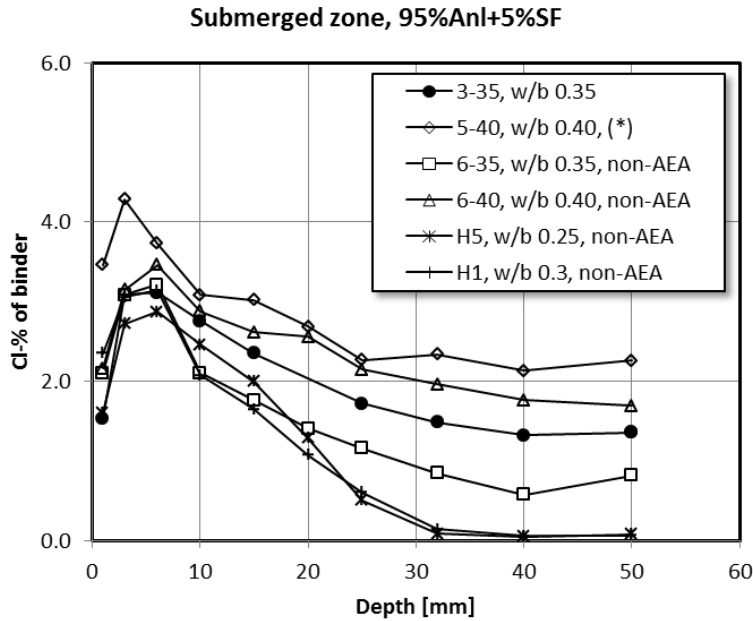


Figure 4.8 Chloride profiles in concrete with Anl cement blended with 5% silica fume (as powder) with and without AEA.

4.4 Effect of binder type

The chloride profiles in concrete with various types of binder are summarised in Figs. 4.9 and 4.10. It can be seen from Fig. 4.9 that Slite cement reveals a lower chloride profile than Anl cement. Further, the addition of silica fume and fly ash in Anl cement effectively increases the resistance to chloride ingress. Fig. 4.10 shows the lowest chloride profiles after 20 years of exposure. This is accomplished with a low water-binder ratio (w/b 0.30) and mineral additions, it must also be pointed out that concretes H2 and H8 did not contain any AEA.

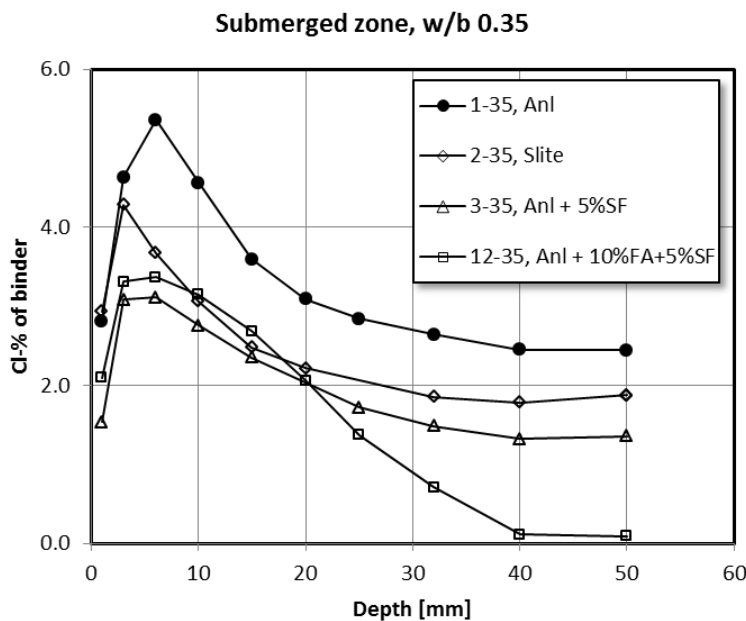


Figure 4.9 Chloride profiles in concrete with water-binder ratio 0.35.

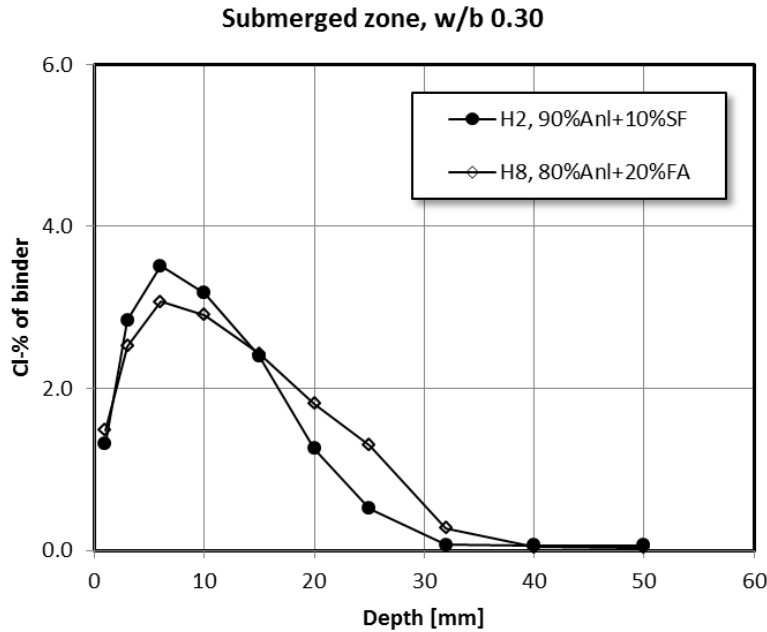


Figure 4.10 Chloride profiles in concrete with water-binder ratio 0.35.

4.5 Distribution of other ions

An attempt was made to try to press out pore water from one concrete (1-40), which was not successful. Further, ion chromatography analysis was performed at Chalmers on selective concretes. The same concrete powder samples as those used in chloride and calcium titration were used. The results are presented in Fig. 4.11. The general trend in Fig. 4.11 is:

- Higher concentrations of Mg^{2+} and SO_4^{2+} at the surface of the concretes and subsequently stable concentrations further in. This is due to the diffusion of those ions from the seawater.
- As expected from the titration results a gradually decrease of Cl^- with depth, and also a higher Ca^{2+} concentration at the surface of the concretes followed by a stable concentrations further in.
- The concentration of Na^+ seems to be evenly distributed throughout the concrete, while the concentration of K^+ tends to be lower at the surface than further in.

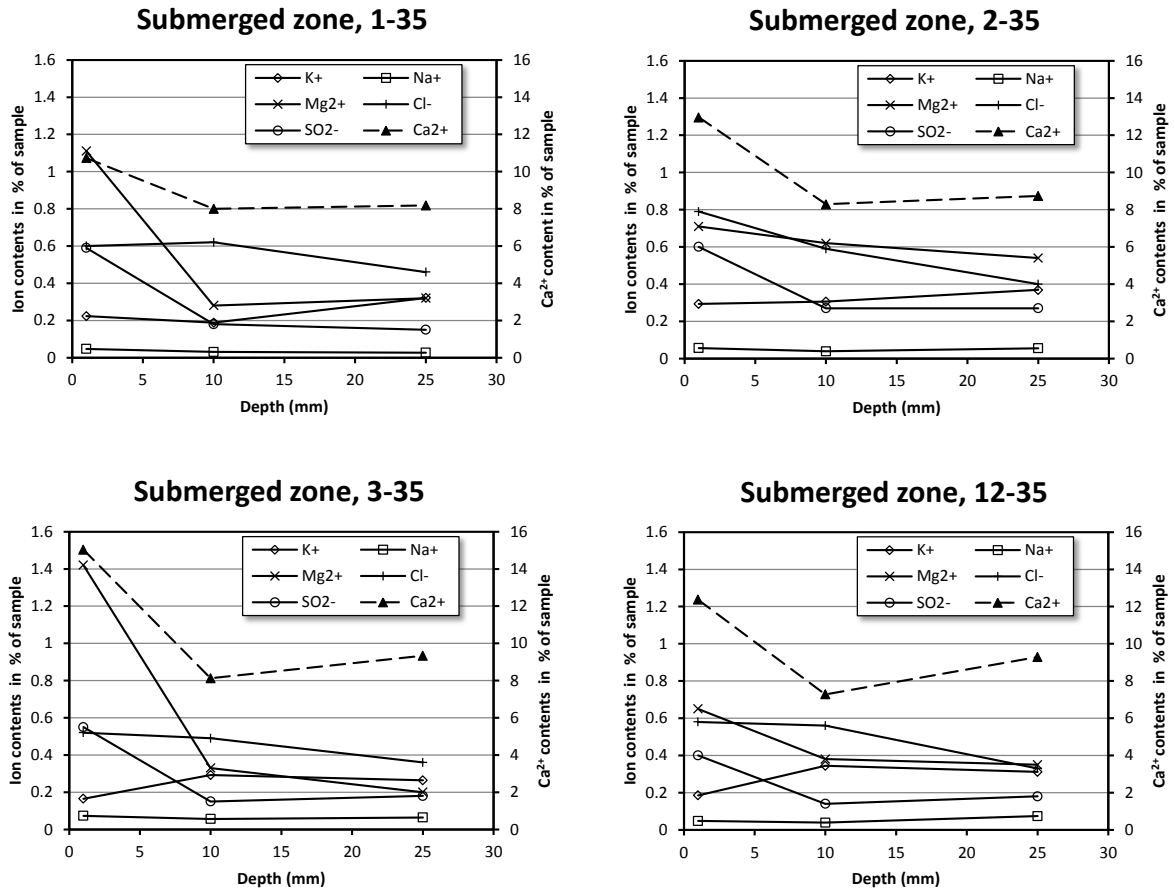


Figure 4.11 Distribution of ions from ion chromatography analysis in concretes with water-binder ratio 0.35.

5 Modelling of Chloride Ingress

5.1 Curve-fitted diffusion coefficient

According to Fick's second law, the following error function solution can be used to describe diffusion under the semi-infinite boundary:

$$C(x,t) = C_{\text{ini}} + (C_s - C_{\text{ini}}) \cdot \left[1 - \operatorname{erf} \left(\frac{x}{2\sqrt{D_{F2}t}} \right) \right] \quad (5.1)$$

where $C(x,t)$ is the chloride concentration at depth x after exposure period t , C_{ini} is the initial chloride concentration in concrete, C_s is the chloride concentration at the exposure surface, D_{F2} is the chloride diffusion coefficient, and erf is the error function. When a concrete slab with a limited thickness of $2L$ is exposed to the seawater, as in our case at the Träslövsläge field site, the chlorides from the seawater can penetrate into concrete from the both sides of the slab. If the chlorides have penetrated through the centre of the slab, the above equation cannot be used because the boundary is no longer the semi-infinite. Instead, the following equation should be used for such a case according to Nilsson's suggestion (2003):

$$C(x,t) = C_{\text{ini}} + (C_s - C_{\text{ini}}) \cdot U \left(\frac{x}{L}, F_0 \right) \quad (5.2)$$

where

$$U \left(\frac{x}{L}, F_0 \right) = 1 - \frac{4}{\pi} \sum_{n=0}^{\infty} \frac{(-1)^n}{2n+1} \exp \left(- (2n+1)^2 \left(\frac{\pi}{2} \right)^2 F_0 \right) \cos \left(\frac{(2n+1)\pi}{2} \left(1 - \frac{x}{L} \right) \right) \quad (5.3)$$

and the Fourier number F_0 is equal to

$$F_0 = \frac{D_{F2}t}{L^2} \quad (5.4)$$

Theoretically, only the gradient of free chloride concentration is contributed to the driving force for chlorides to penetrate into concrete. However, the free chloride profiles can, up to now, hardly be measured. The reported chloride profiles are normally based on the determination of total chloride content. The total chloride content is not necessarily proportional to the free chloride concentration due to the non-linear behaviour of chloride binding. Therefore, using the gradient of total chloride content as a driving force in Fick's law may not be theoretically correct, but just empirically convenient for describing the characteristics of penetration profiles. The models based on the above equations may be regarded as empiric models. Nevertheless, curve-fitting the measured chloride profile to equation (5.1) or (5.2), one can obtain two parameters, D_{F2} and C_s . These two parameters are

anyway a description of chloride ingress under a specific exposure condition and after a specific exposure period. A MS Excel-based program was used for curve-fitting calculations. For each chloride profile, the first one or two points were omitted prior to the calculation, if the values are significantly out of the diffusion curve. Fig. 5.1 shows two examples of curve-fitting procedures, one with eq. 5.1 for single side penetration and one with eq. 5.2 for double side penetration.

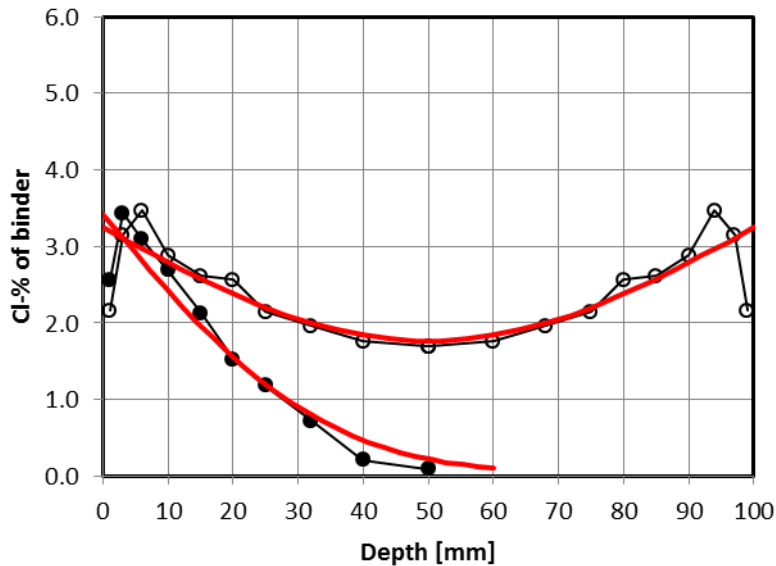


Figure 5.1 Example of curve fitting for single-side chloride penetration using eq. 5.1, and double side chloride penetration, using eq. 5.2.

The curve-fitted results are given in Appendix 3 and examples of relationships between curve-fitted parameters and exposure time is shown in Figs. 5.2 and 5.3. The curve-fitted parameters from previous exposure times can also be found in Tang (2003b), where also data for more concrete qualities can be found.

Fig. 5.2 shows that for the “higher” water-binder ratio (0.40) and 100% Anl cement the D_{F2} decreases gradually with exposure time, while for water-binder ratio 0.30 it seems that D_{F2} is quite steady after 10 years of exposure. Similar tendency of the D_{F2} can be observed for the concretes with 100% Slite cement. For the concretes containing mineral additions in the binder the results shows generally a lower D_{F2} then for the OPCs, and that D_{F2} don’t change much after 5 years of exposure.

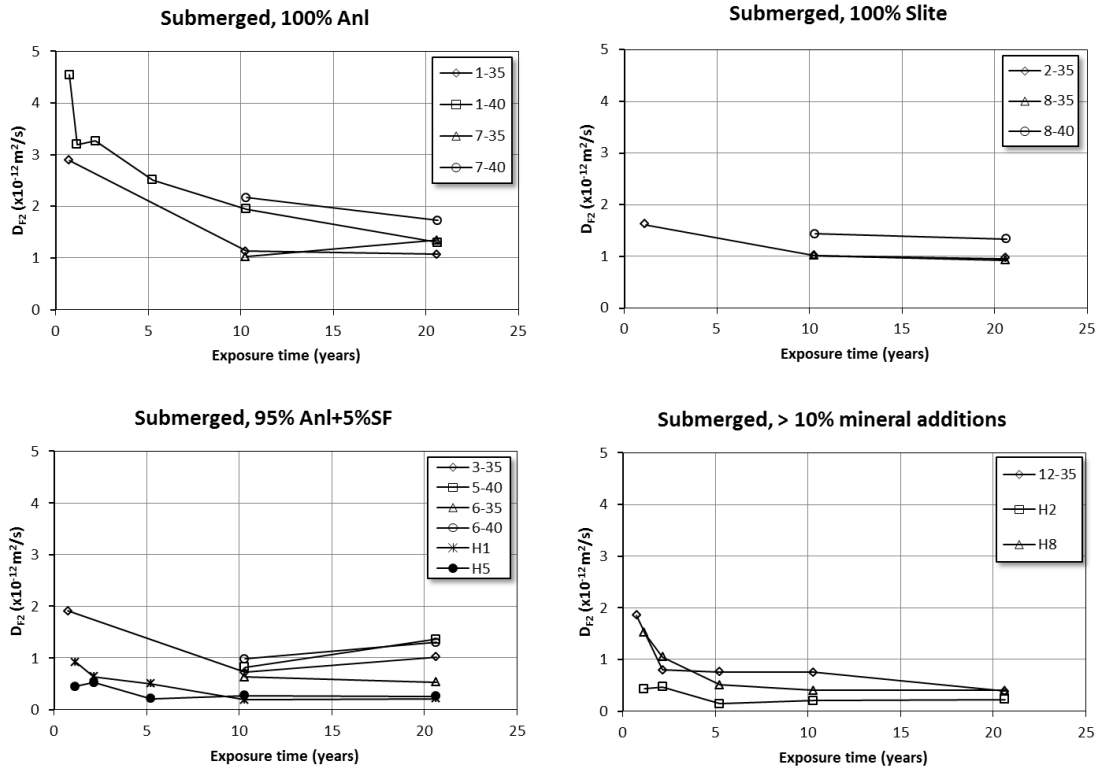


Figure 5.2 Relationship between the curve-fitted parameter D_{F2} and exposure time.

Fig. 5.3 shows that for most concretes C_s gradually increased in the first 5 years and then kept more or less unchanged. Exceptions from this general trend can be observed in some of the OPC concretes.

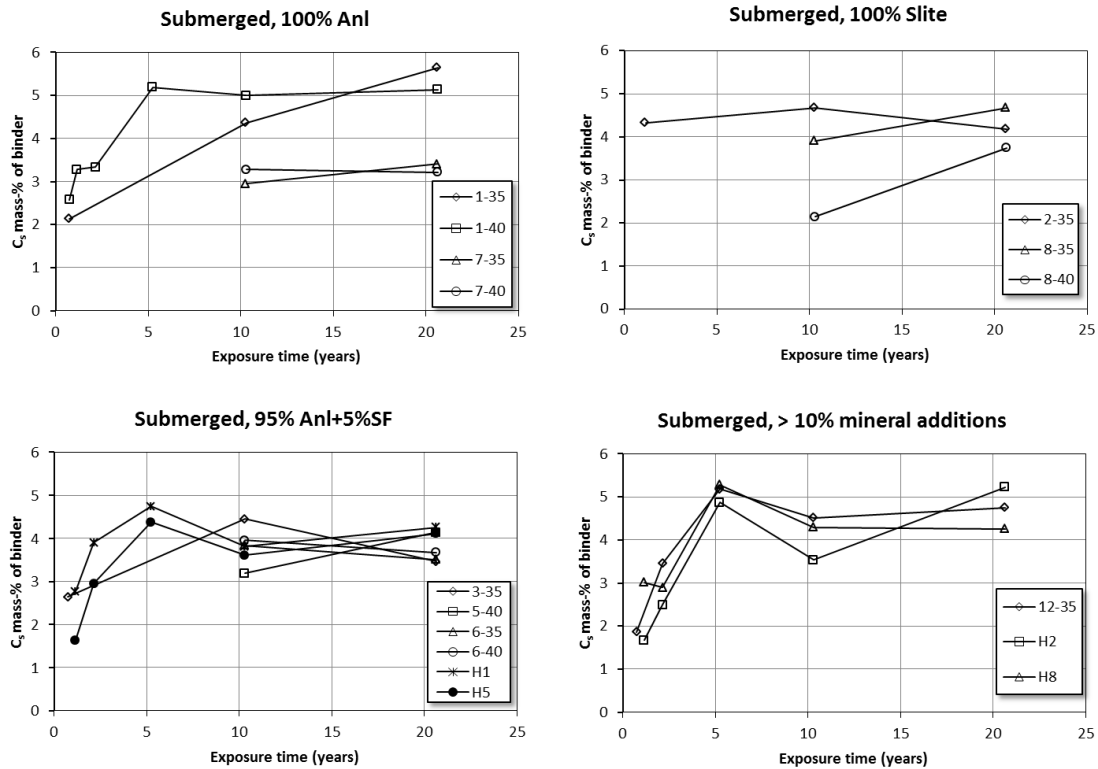


Figure 5.3 Relationship between the curve-fitted parameter C_s and exposure time.

5.2 Modelling of chloride ingress in concrete

Many models have been proposed in the past decades for predicting chloride ingress in concrete. As reported by Tang et al. (2012), DuraCrete model (2000) has been widely recognised in the world owing to its EU-project characteristics. This model has also been introduced by Betongföreningen (2007). On the other hand, a mechanism-based model the so called ClinConc model was developed at Chalmers (Tang and Nilsson 1994, Tang 1996, Tang 2008). These two models were used for modelling of chloride ingress in the concretes exposed under the seawater (sub-zone) at the Träslövsläge exposure site.

DuraCrete model

The DuraCrete model is based on an erfc solution to Fick's 2nd law of diffusion under the semi-infinite boundary condition:

$$C(x,t) = C_i + (C_s - C_i) \cdot \operatorname{erfc}\left(\frac{x}{2 \cdot \sqrt{D_a \cdot t}}\right) \quad (5.5)$$

where: C_i is the initial chloride content in the concrete (sometimes this chloride content is negligible), C_s is the surface chloride content, x is the depth, D_a is the apparent diffusion coefficient, t is the exposure duration. In this model the parameters C_s and D_a are assumed constant during the whole period of exposure.

The DuraCrete project (2000) recommended the following equation to express the apparent diffusion coefficient in equation (5.6):

$$D_a = k_{e,cl} \cdot k_{c,cl} \cdot D_{RCM,0} \cdot \left(\frac{t_0}{t + t_{ex}}\right)^{n_{cl}} \quad (5.6)$$

where: $D_{RCM,0}$ is the chloride migration coefficient measured by e.g. the Nordtest method NT BUILD 492, at the age $t_0 = 28$ days, $k_{e,cl}$ and $k_{c,cl}$ are constants considering the influence of environment and curing, respectively, on chloride ingress, t_0 is the reference period (concrete age of 28 days) at which $D_{RCM,0}$ is measured and n_{cl} is the age factor describing the time-dependency of the apparent diffusion coefficient.

ClinConc model

The ClinConc model (Cl in Concrete) was first developed in the mid-1990s (Tang and Nilsson 1994; Tang 1996). The ClinConc model consists of two main procedures: 1) Simulation of free chloride penetration through the pore solution in concrete using a genuine flux equation based on the principle of Fick's law with the free chloride concentration as the driving potential, and 2) Calculation of the distribution of the total chloride content in concrete using the mass balance equation combined with non-linear chloride binding.

Obviously, the ClinConc model uses free chloride as the driving force and takes non-linear chloride binding into account. Thus it describes chloride transport in concrete in a more

scientific way than the empirical or semi-empirical models. In past years, this model has been expressed in a more engineer-friendly way (Tang 2008) so as to make it possible for applications by practising engineers.

The free chloride concentration in the concrete at depth, x , is determined using the following equation:

$$\frac{c - c_i}{c_s - c_i} = 1 - \operatorname{erf} \left(\frac{x}{2 \sqrt{\frac{\xi_D D_{6m}}{1-n} \cdot \left(\frac{t_{6m}}{t}\right)^n \cdot \left[\left(1 + \frac{t_{ex}}{t}\right)^{1-n} - \left(\frac{t_{ex}}{t}\right)^{1-n} \right] \cdot t}} \right) \quad (5.7)$$

where c , c_s and c_i are the concentration of free chlorides in the pore solution at depth x , at the surface of the concrete and initially in the concrete, respectively, D_{6m} is the diffusion coefficient measured by the RCM test, e.g. NT BUILD 492, at the age of t_{6m} , ξ_D is the factor bridging the laboratory-measured D_{6m} to the initial apparent diffusion coefficient for the actual exposure environment, n is the age factor accounting for the diffusivity decrease with age, t_{ex} is the age of concrete at the start of exposure and t is the duration of the exposure.

In contrast to the empirical models, the factors ξ_D and n in the ClinConc can be calculated based on the physical properties of concrete including cement hydration, hydroxide content, water accessible porosity, time-dependent chloride binding, and the environmental parameters such as chloride concentration and temperature. Detailed descriptions of the factors ξ_D and n are given by Tang (2006).

The total chloride content is basically the sum of the bound chloride and free chloride and can be calculated based on the relationship between the free and total chloride content, i.e. a chloride-binding isotherm (Tang and Nilsson 1993).

5.3 Input parameters used for modelling

It should be noted that both the DuraCrete and the ClinConc models use the diffusion coefficient measured by the RCM test, e.g. NT BUILD 492, as an input parameter, but care should be taken that this parameter is tested at different concrete ages, i.e. 28 days in the former while 6 months in the latter. However, although in DuraCrete (2000) the concrete age t_0 is specified as 28 days, there should be no difference in the D_a values calculated using $D_{RCM28d} \cdot (t_{28d})^n$ and $D_{RCM6m} \cdot (t_{6m})^n$ when the same n value is adopted. Therefore, the values of D_{RCM6m} for the concretes exposed at the Träslövsläge field exposure site summarised in Tang (2003b) were used for both the DuraCrete and the ClinConc models.

The other input parameters for the DuraCrete model were taken from the guidelines recommended by DuraCrete (2000), whilst those for the ClinConc model were taken or

calculated in accordance with the previous studies published in Tang (2003b, 2006) as well as summarised in Appendix A in CBI Report 2:2012 (Tang et al. 2012).

5.4 Modelled results

Effect of binder type

The modelled results for the concretes with different types of binder are presented in Figs. 5.4 and 5.5. It can be seen that the ClinConc model gives predictions closer to the measured values than the DuraCrete model, which markedly underestimates the measured values after 20 years' exposure. For the concrete with 10% silica fume (Mix H2), both the DuraCrete and ClinConc models underestimate the actual chloride ingress, implying that further study is needed to invest the long-term behaviour of concrete with the addition of 10% silica fume.

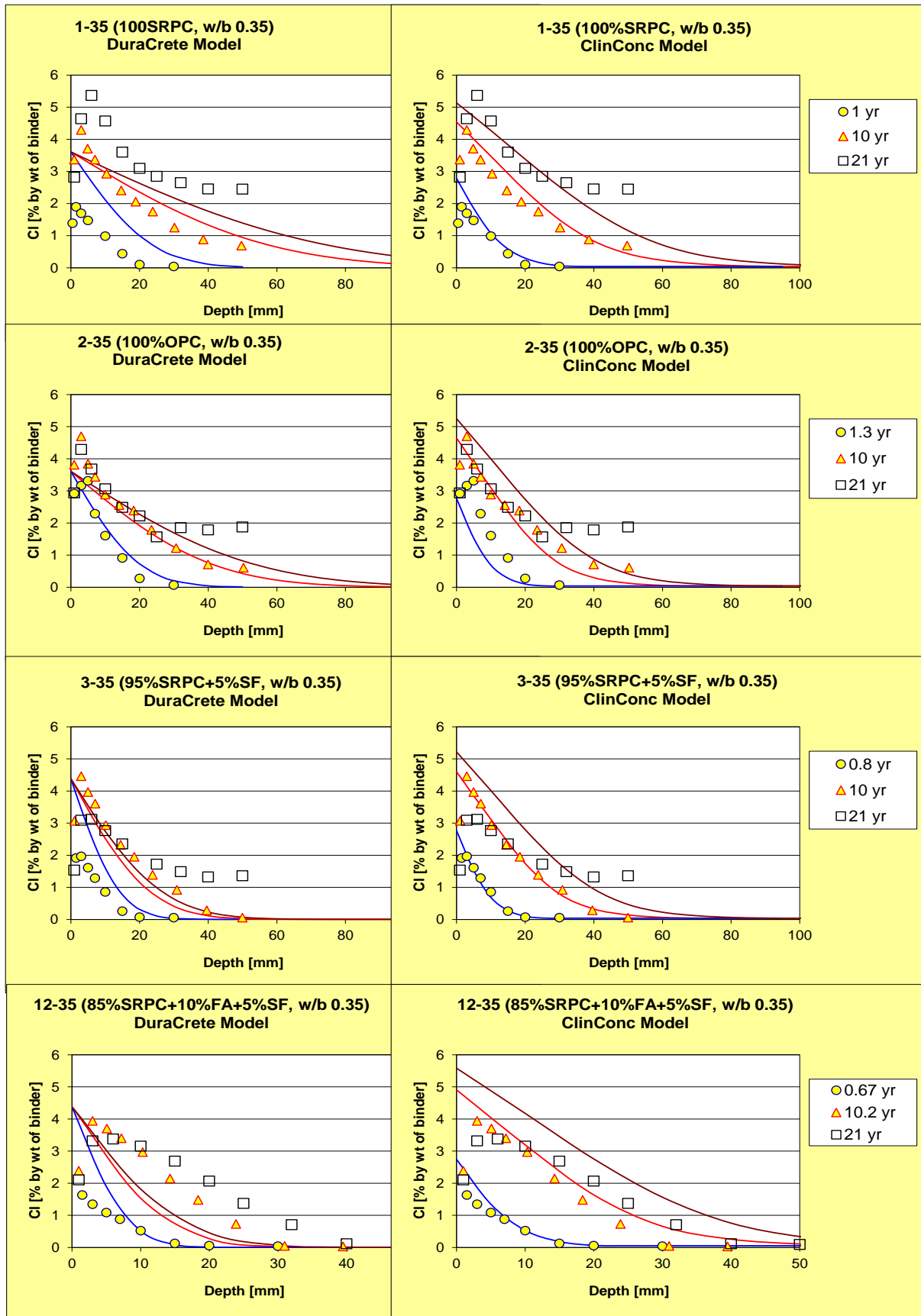


Figure 5.4 Modelled results for the concretes with different types of binder with water-binder ratio w/b 0.35.

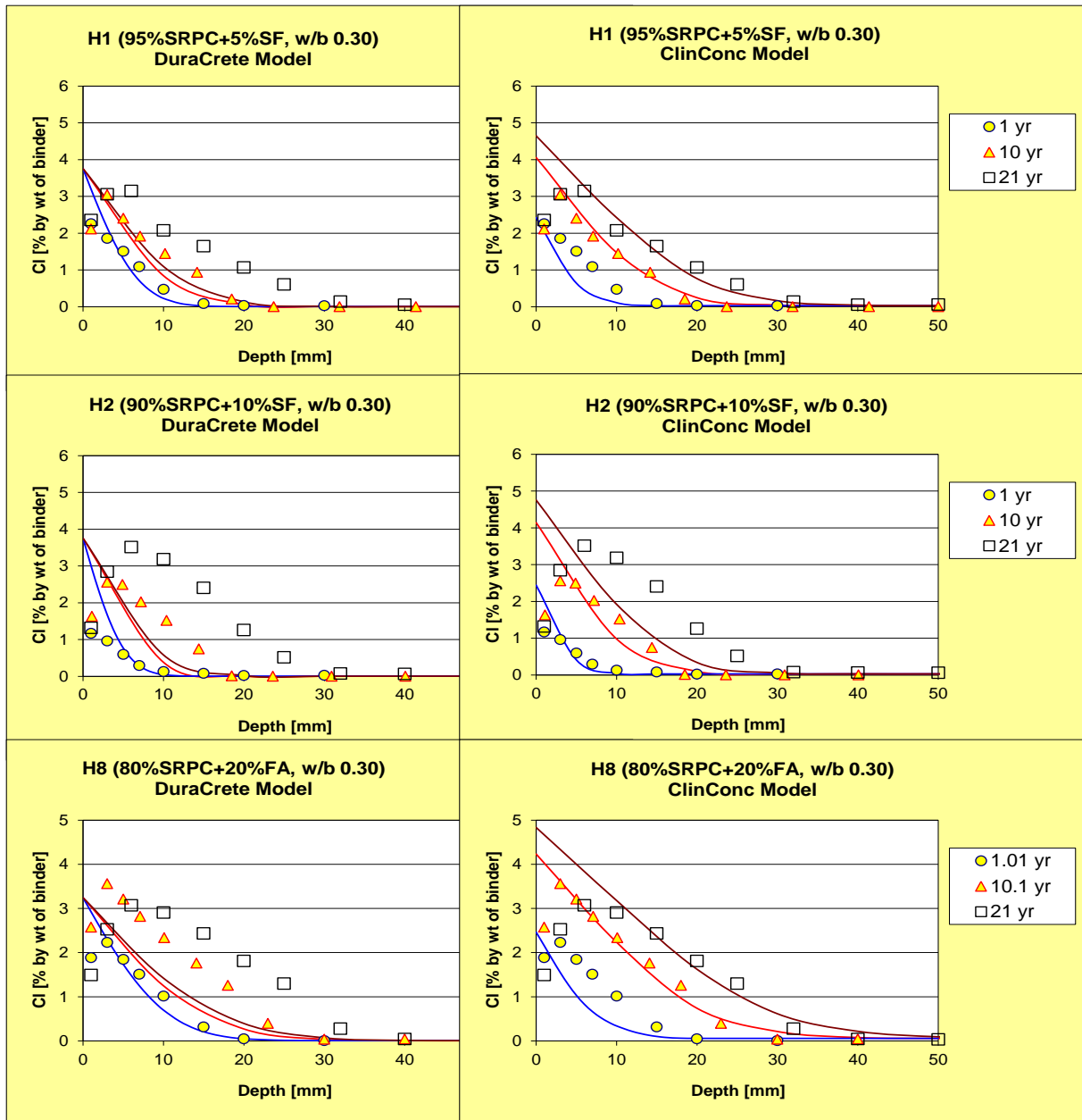


Figure 5.5 Modelled results for the concretes with different types of binder with water-binder ratio w/b 0.30.

Effect of water-binder ratio

The modelled results for the concretes with different water-binder ratios are presented in Figs. 5.6 to 5.7. It can be seen again that the ClinConc model gives predictions closer to the measured values than the DuraCrete model, which markedly underestimates the measured values after 20 years' exposure, especially for the concretes with low water-binder ratios (<0.40). For the concretes with w/b 0.40 and 0.50, the DuraCrete model gives predictions closer to the chloride profiles measured after 10 or 20 years' exposure, but overestimates the chloride profiles measured after a short exposure time. This is an indication that the uncertainty of extrapolation based on empirical models is usually larger than that with mechanistic models.

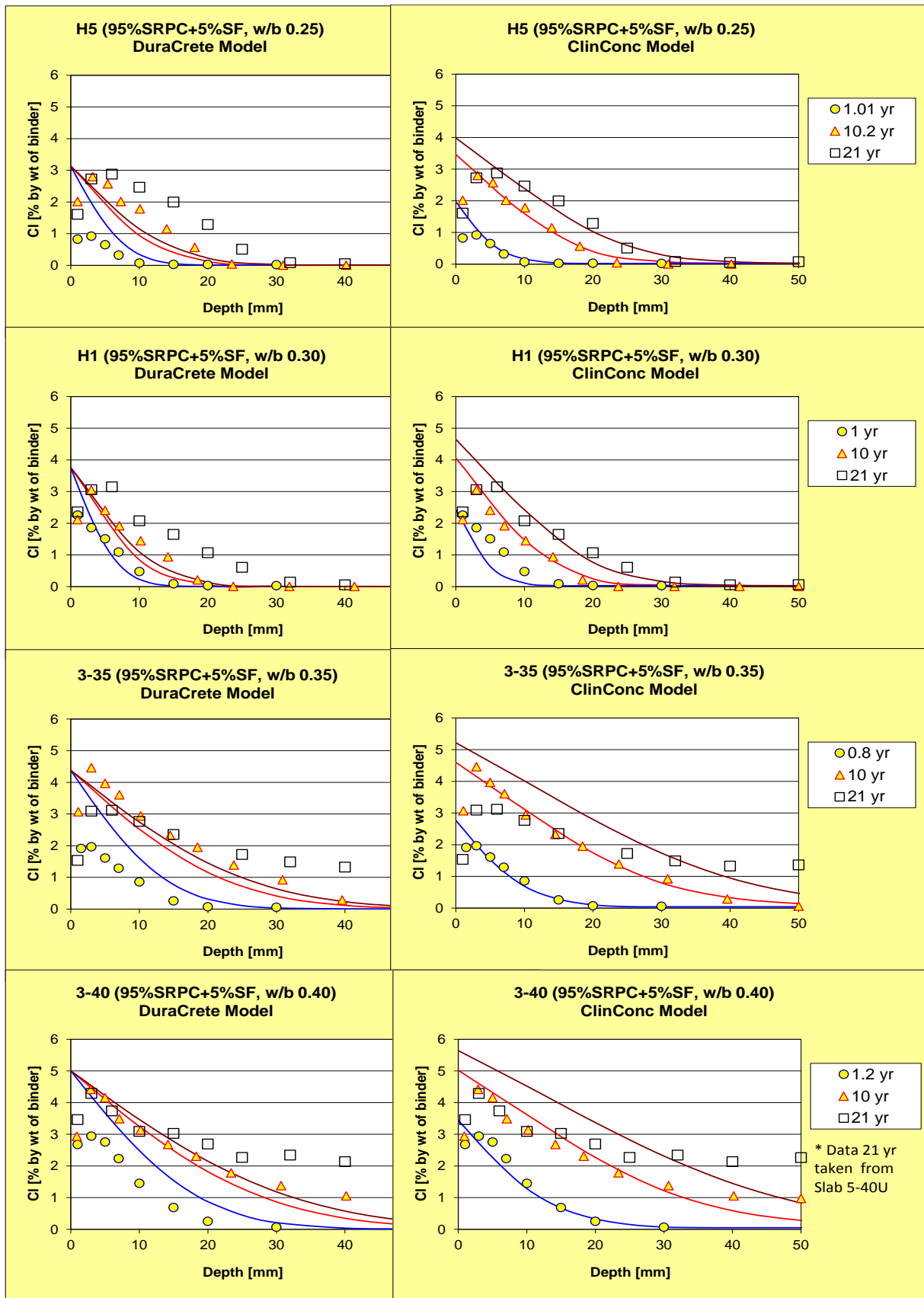


Figure 5.6 Modelled results for the concretes with different water-binder ratios with 95% CEM I (Anl ggningscement) + 5% SF (Microsilica).

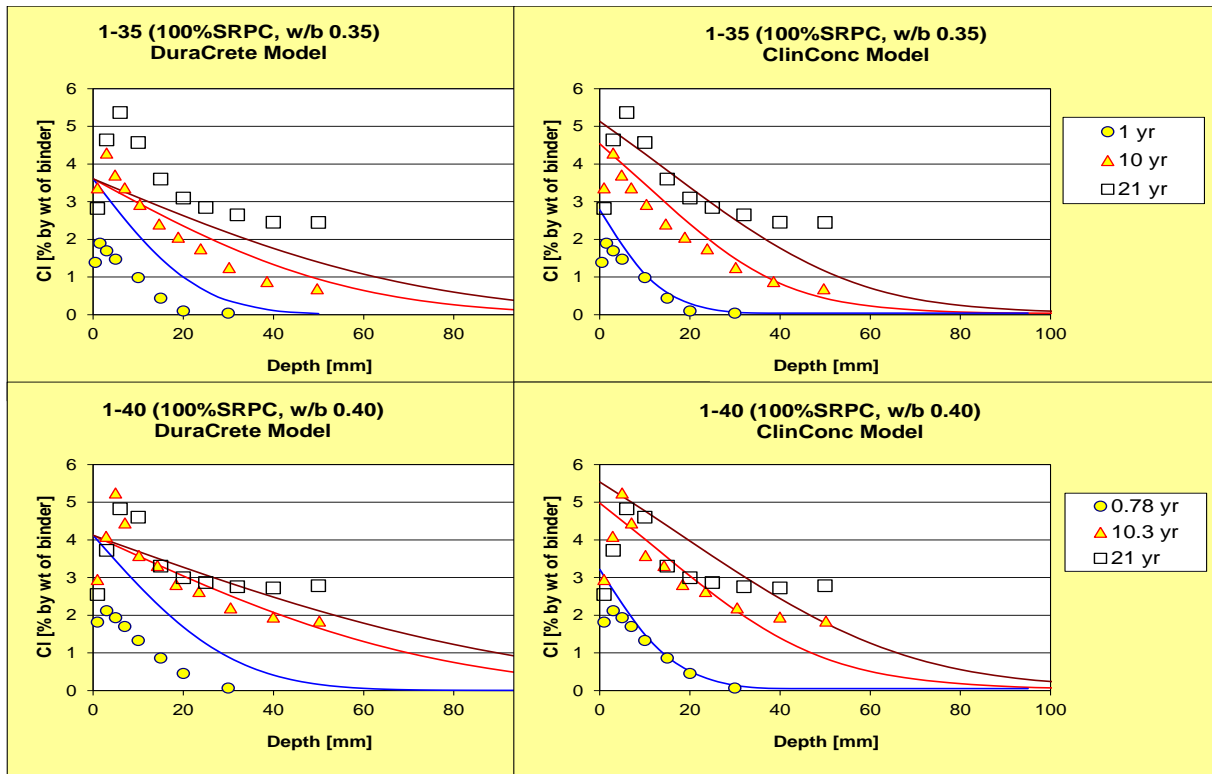


Figure 5.7 Modelled results for the concretes with different water-binder ratios with 100% CEM I (Anlagningscement).

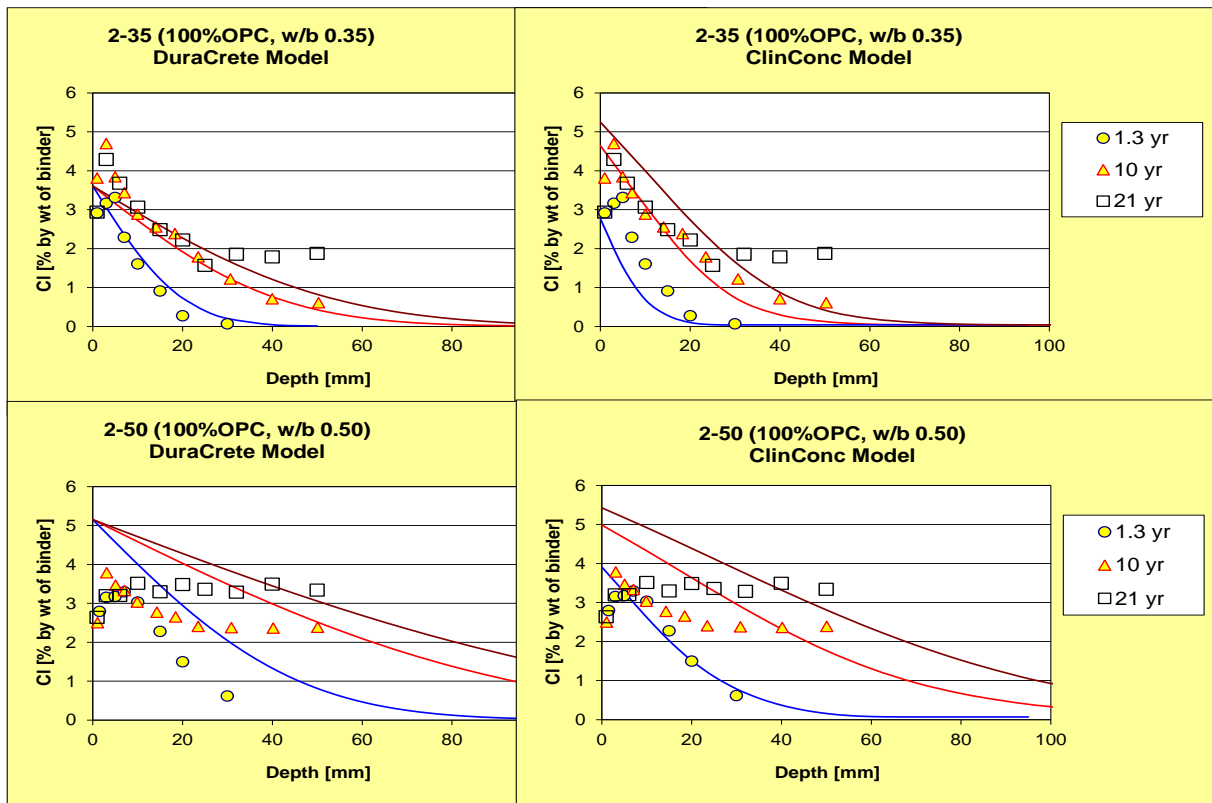


Figure 5.8 Modelled results for the concretes with different water-binder ratios with 100% CEM I (Slite cement).

5.5 Prediction of chloride ingress after 100 years' exposure

From section 5.4 it can be concluded that the ClinConc model fits fairly well to the measured values from one year up to 20 years' field exposure for most types of concrete. Therefore, it is reasonable to use this model to predict chloride ingress in concrete exposed in Swedish west coast seawater. Because the model markedly underestimates the chloride ingress in concrete with 10% silica fume, no prediction for this type of concrete was made in order not to mislead readers of the report. The predicted profiles are shown in Fig. 5.9.

It can be seen from the prediction that, if the chloride threshold value of 1% by weight of binder is assumed, the concrete with plain sulphate resistant Portland cement (SRPC) with water-binder ratio of 0.35 needs a cover thickness of >110 mm to protect the reinforcement for a service life of 100 years. With addition of 5% silica fume and w/b 0.35, it is possible to achieve 100 years' service life with 80 mm cover. The best measure to obtain 100 years' service life with a cover thickness of for example 60 mm is to use either 5% silica fume or 20% fly ash with reduced water-binder ratio ≤ 0.30 , or to use a combination of both fly ash and silica fume (w/b 0.35). It seems that a water-binder ratio lower than 0.30 does not further reduce chloride ingress.

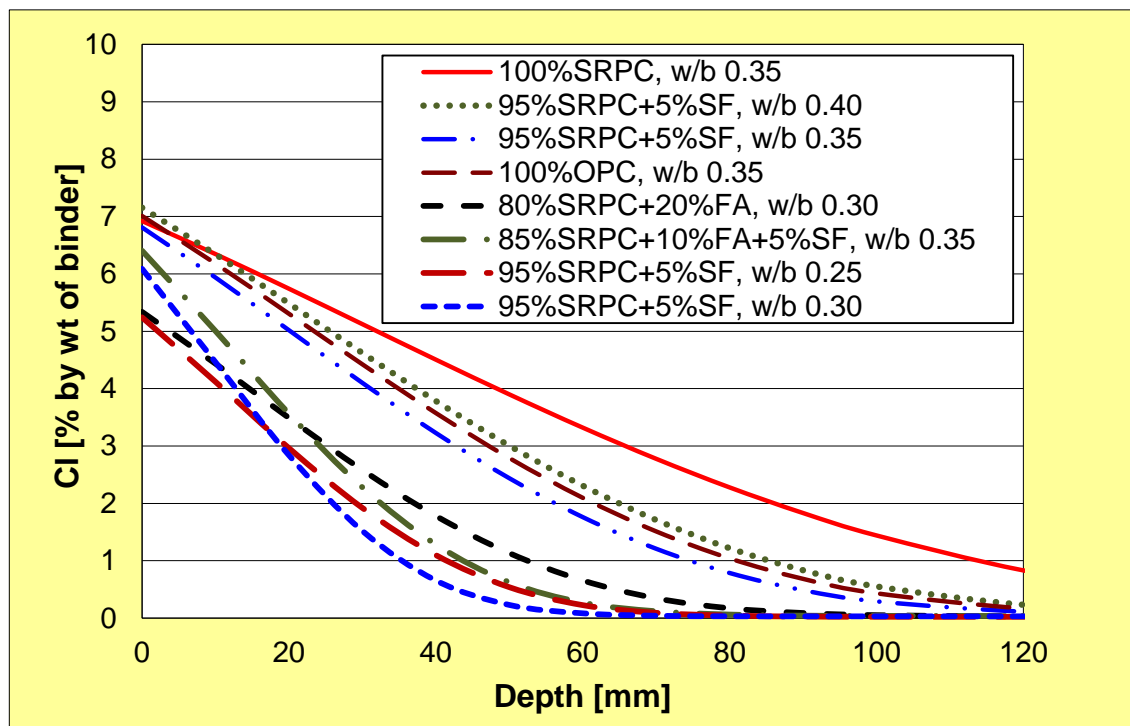


Figure 5.9 Predicted chloride profiles in concrete after 100 years' exposure in Swedish west coast seawater.

6 Chloride induced corrosion

6.1 Measurement Methodology

All corrosion measurements were performed in the laboratory prior to coring for chloride profiles. As can be seen in Fig. 3.1 in most of the exposed slabs three rebars were embedded, one stainless steel and two regular carbon-steel rebars (referred to as Rebar 1 and Rebar 2 in the following). Apart from different binders and water-binder ratios, different steel dimensions and concrete covers were also included as studied parameters. Each rebar was measured at nine positions at an interval of 100 mm from the top edge of the slab.

The commercially available RapiCor instrument based on galvanostatic pulse technique was used to monitor the corrosion. The measuring principle is illustrated in Fig. 6.1.

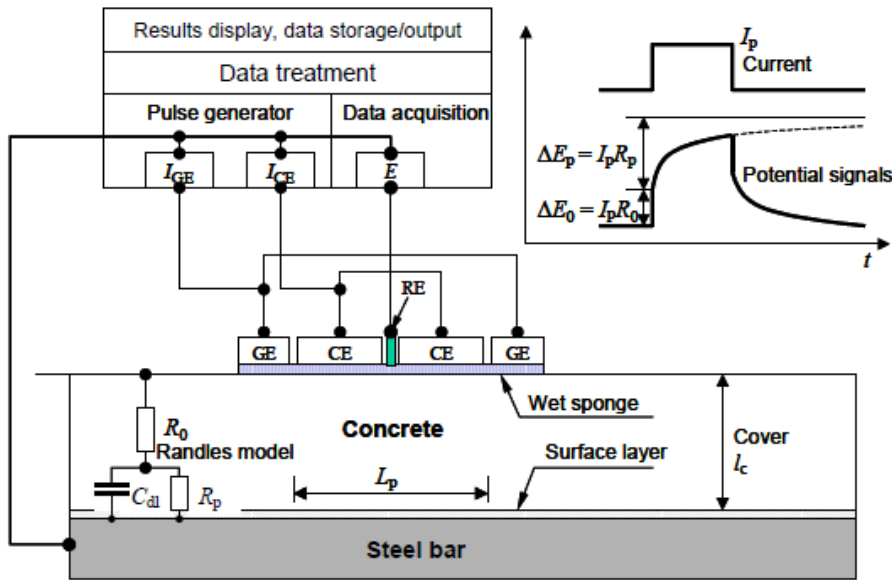


Figure 6.1 Measurement principle for the galvanostatic pulse technique, Tang (2002).

A wet sponge is placed on the concrete surface over the steel to be measured, to improve the contact between the concrete and the electrodes unit. Then the rectangular shaped electrodes unit consisting of two counter electrodes (CE), two guard electrodes (GE) and a reference electrode (RE) is placed on the wet sponge. The instrument measures E_{corr} by means of the RE (silver/silver chloride) placed in the centre of the unit. A galvanostatic current is applied to the CE and another current is applied to the GE, after imposing these currents the potential response is recorded. Modelling the system as a single Randles circuit, from the recorded potential-time curve the polarisation resistance (R_p) is obtained. The R_p is used to calculate the corrosion current density (i_{corr}) using the Stern-Geary equation:

$$i_{\text{corr}} = \frac{B}{AR_p} \quad (6.1)$$

Where, B is assumed to be 26 mV. The instrument gives the corrosion rate in $\mu\text{m}/\text{year}$ assuming uniform corrosion. Further, the instrument gives the corrosion potential (versus the copper/copper sulphate reference electrode) and the concrete resistivity ($\text{k}\Omega\cdot\text{cm}$). A more detailed description of this technique can be found in Tang (2002). It should be noted that the uncertainty in the corrosion rate is large. A factor of 2 (multiplying by 2 for upper and dividing by 2 for lower limits) has normally been adopted (Tang 2002).

After corrosion measurement, for some slabs, one or two rebars were removed for visual examination and confirmation of corrosion status. After the release of the rebar, concrete samples were taken at the depth where the rebar was embedded, see Fig. 6.2.



Figure 6.2 Sampling for chloride analysis.

6.2 Corrosion measurements

The results from the corrosion measurements by RapiCor are listed in Appendix 4.

Initially, after the corrosion measurements five rebars from five different slabs (1-402(I), 1-402(P), 5-40, 7-40 and 8-40(I)) were removed for visual examination, for those rebars chloride profile along the cover level was also measured. The results are summarised in Figs. 6.3-6.7. For the rebars in slabs 5-40, 7-40 and 1-402(I) the measured corrosion rates were above the detection limit of the RapiCor instrument. Once those rebars were removed, severe pitting corrosion was observed at the maximum corrosion rate location. Stains from corrosion products could also be seen externally on the slabs. For the rebar removed from slab 8-40 the measured corrosion rates along the rebar were around $10 \mu\text{m}/\text{year}$. Once opened, no visual corrosion was observed. The measured corrosion rate at the lower end of the rebar in slab 1-402(P) was $55 \mu\text{m}/\text{year}$, severe pitting corrosion was also found in this case, as can be seen in Fig. 6.3. All rebars showed uniform corrosion at the upper part (0~6 cm in the slab) under the insulation tape, but this was not evident in the corrosion rate measurements.

It can be seen in Figs. 6.3-6.7 that the chloride level at the submerged zone for all bars is $\geq 2\%$ by mass of binder. For the rebars in slabs 1-402(I), 5-40 and 7-40, where corrosion initiation occurred at 10 to 20 cm under the sea level, a higher chloride content around the corrosion location can be observed. This is probably due to a damaged concrete cover at those locations because of expanding corroding products.

Previous investigations by Tang et al (2005) have shown that the corrosion rate measurement is the most accurate way to find active corrosion of steel in concrete. Both corrosion potential and resistivity give a greater response to the exposure environment than to the corrosion

process. A corrosion rate of $> 10 \mu\text{m}/\text{year}$ can be considered as high, and represents a higher probability of corrosion initiation.

Generally, the corrosion measurements (appendix 4) showed that pitting corrosion initiation (maximum corrosion rate) was observed mainly at two locations along the rebars, either about 10~20 cm under the sea level or at the lower end of the rebars. The first case is quite expected as the “micro” environment at 10 to 20 cm under the sea level is ideal to support corrosion initiation due to the availability of chlorides, moisture and oxygen. The second case is probably due to the poor interface between the concrete and the mortar spacer. The same observations were made by Tang et al. (2005).

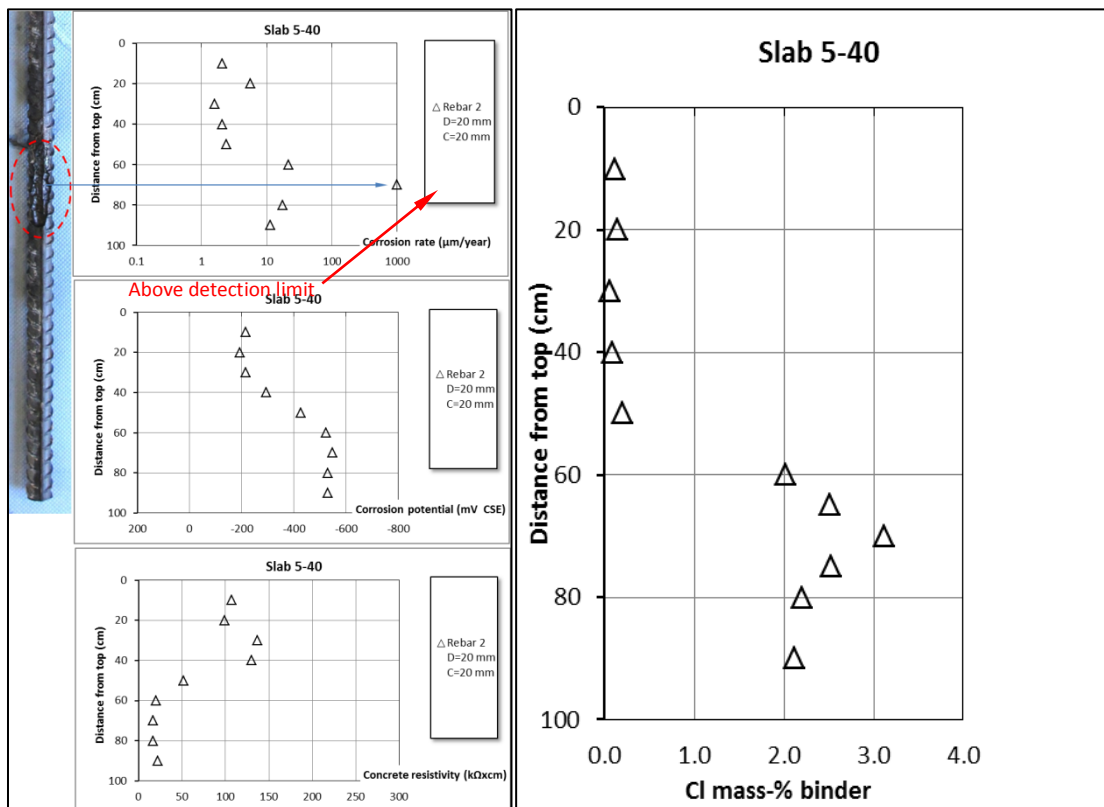


Figure 6.3 Visual examination results, corrosion measurements and chloride content at the cover level of concrete 5-40 (SRPC+5%SF).

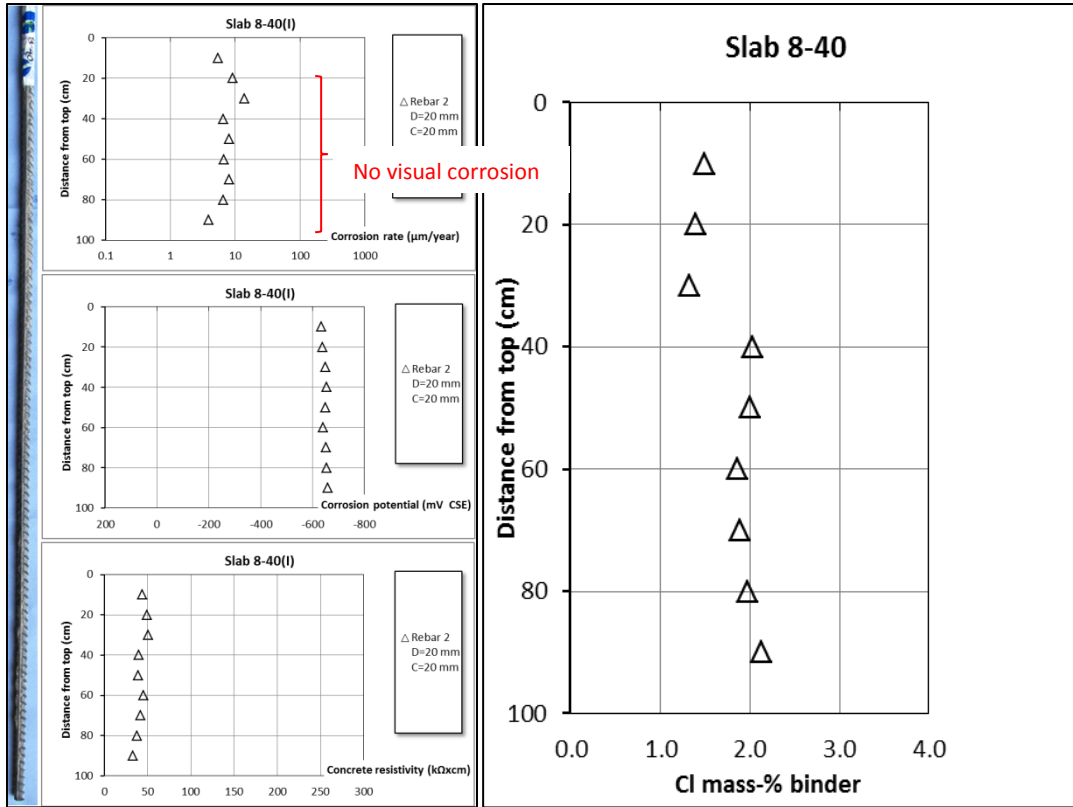


Figure 6.4 Visual examination results, corrosion measurements and chloride content at the cover level of concrete 8-40 (OPC).

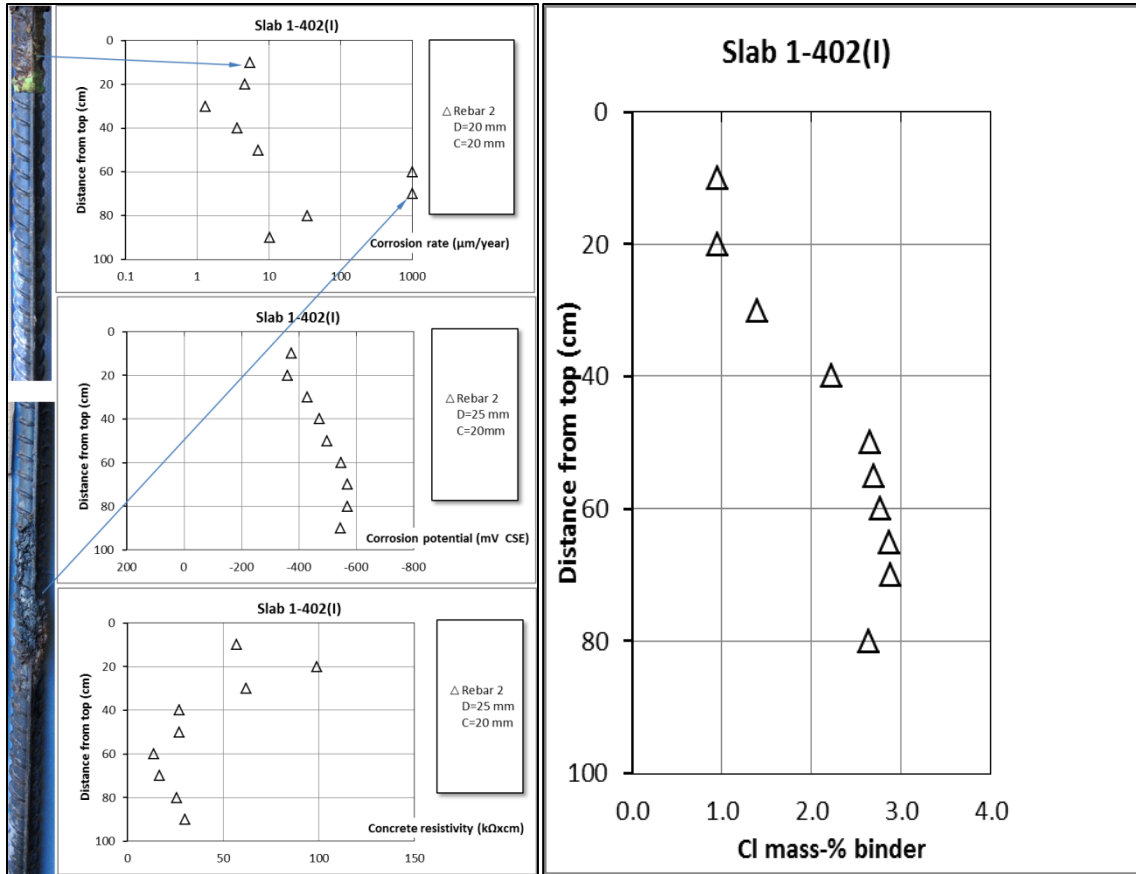


Figure 6.5 Visual examination results, corrosion measurements and chloride content at the cover level of concrete 1-402 (SRPC).

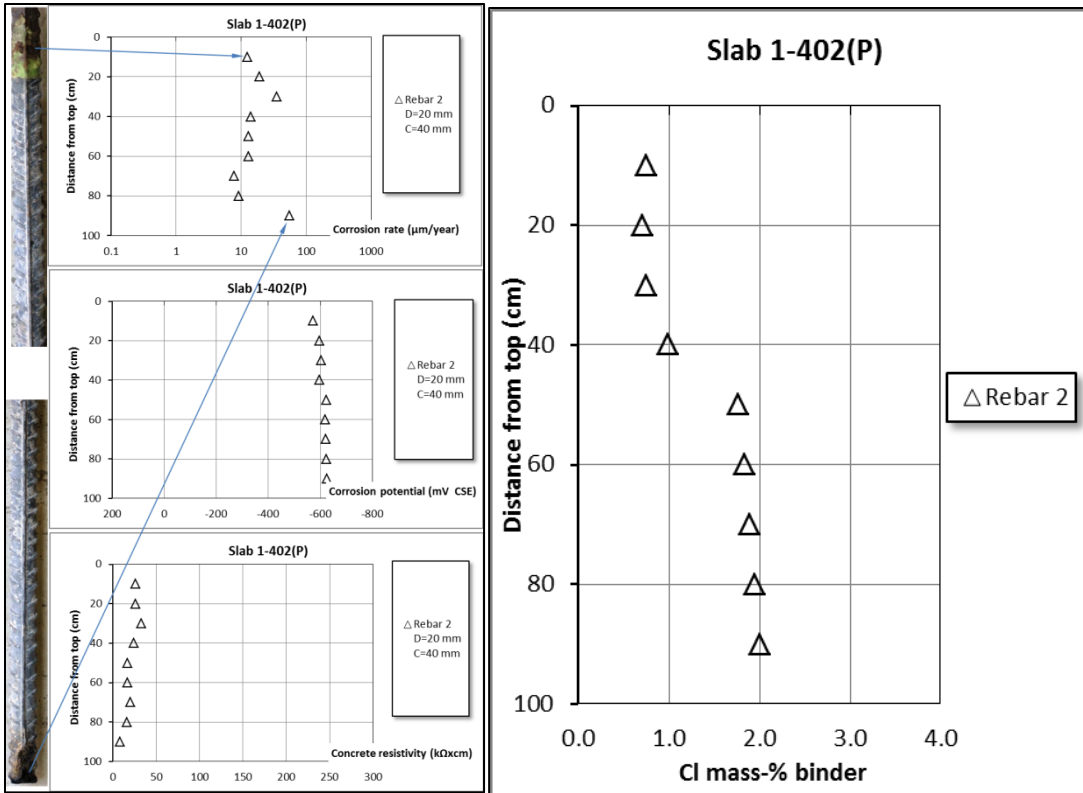


Figure 6.6 Visual examination results, corrosion measurements and chloride content at the cover level of concrete 1-402P (SRPC with a thicker cover of 40 mm).

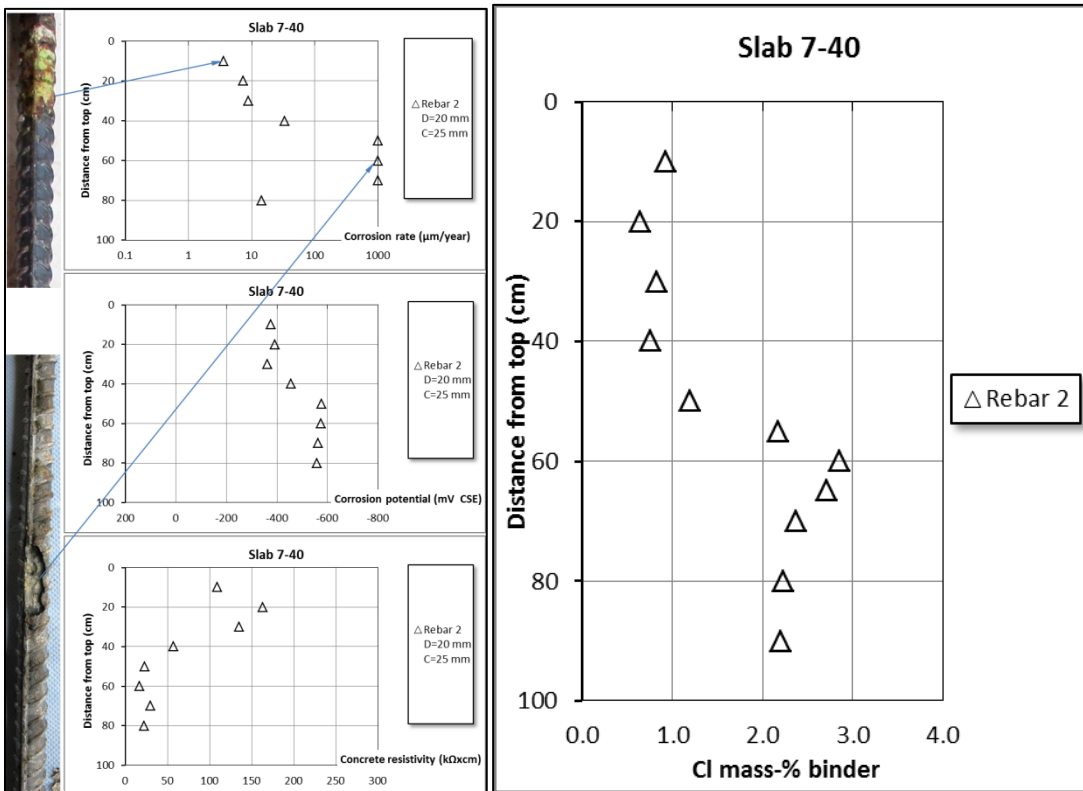


Figure 6.7 Visual examination results, corrosion measurements and chloride content at the cover level of concrete 7-40 (SRPC without air entraining).

6.3 Chloride threshold values for corrosion initiation

A lot of research has been devoted to try to determine the chloride threshold value and several parameters have been identified to affect the threshold level. The exact mechanism of the breakdown (corrosion initiation) of the passive film by chloride ions is not clearly understood. In the recent years comprehensive literature reviews on the subject have been published by Angst et al. (2009); Alonso and Sanchez (2009). Both Angst et al. (2009) and Alonso and Sanchez (2009) found a large scatter in the reported values. Fig. 6.8 shows the scatter in data reported from field and laboratory tests (Alonso and Sanchez 2009).

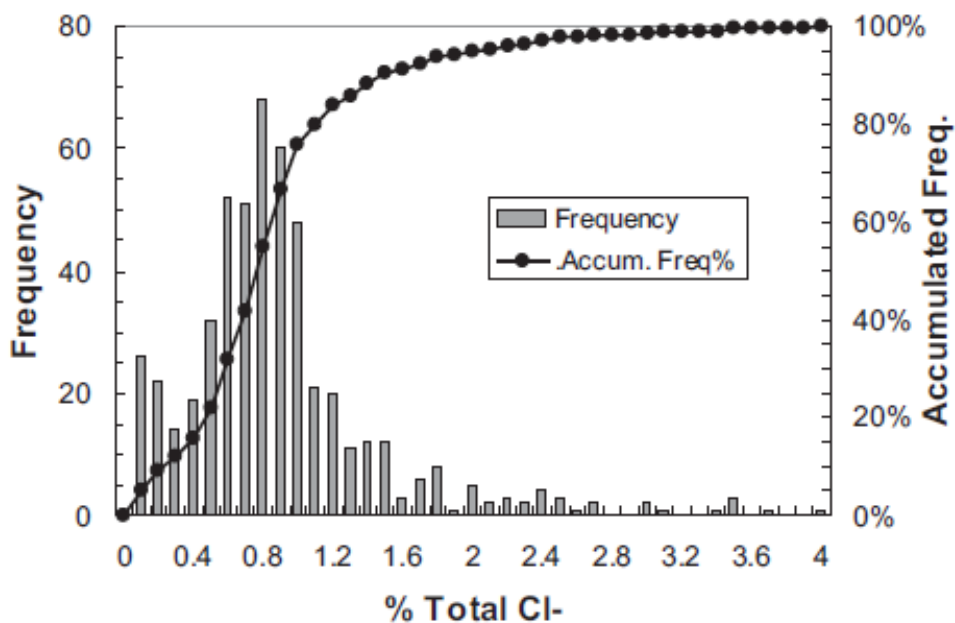


Figure 6.8 Frequency distribution and accumulated frequency of chloride threshold values found in the literature expressed as percent chloride by cement weight (Alonso and Sanchez 2009).

One of the decisive parameters for the chloride threshold value has been identified to be pH of the pore solution which mainly depends on the binder type (Angst et al. 2009). The steel-concrete interface is another identified decisive parameter affecting threshold level (Glass and Buenfeld 1995). The large scatter in the reported data has partially been attributed to the variability in the testing methods Angst et al. (2009), Alonso and Sanchez (2009). So far there is no standard method for testing the chloride threshold values either in the laboratory or in the field. Therefore, the following methodology was used in this project for evaluating the chloride threshold values in concrete exposed in the Träslövsläge field exposure site:

- Mapping the instantaneous corrosion conditions of rebar using the non-destructive test method RapiCor, as described in section 6.1.
- Verifying the above non-destructive test by destructively releasing some rebars under different corrosion conditions for visual examination, as described in section 6.2.
- Evaluating the chloride contents at the cover depth of the rebars showing the instantaneous corrosion rate $> 10 \mu\text{m/yr}$ but $< 100 \mu\text{m/yr}$. The lowest value would be taken as the threshold value, as will be discussed later.

- Verifying the estimated threshold value by destructively releasing some 20 more rebars for visual examination and measurement of chloride content at the cover depth, as will be described in section 6.4.

As mentioned previously, the corrosion measurements by RapiCor carried out in this project provide an indication of the instantaneous corrosion conditions of rebars. Because the corrosion conditions were not monitored during the exposure, it is unknown when the corrosion was initiated. Therefore, it is difficult to estimate the chloride threshold values from the instantaneous corrosion measurements and chloride profiles. However, it might be possible to roughly estimate the threshold from analysis of corrosion conditions and chloride contents at the cover depth after 10 and 20 years exposure. In the analysis those rebars showing severe corrosion at the lower end of the rebar were excluded, because their corrosion was owing to the use of poor distance spacer in the slab casting. Table 6.1 summarised those rebars both 10 and 20 years' field data of corrosion rate and chloride content at the cover depth (based on the chloride profiles) are available. It can be seen that the chloride content at the cover depth is in the most cases larger than 1% by weight of binder. The lowest value 0.9% by weight of binder was found in concrete 6-35 rebar 1, but the value was measured 3 years earlier before the corrosion measurement. Therefore, it is reasonable to state that, to maintain corrosion at a certain rate, at least 1% chloride by weight of binder is needed. From Table 6.1 it can be seen that this threshold value of 1% chloride by weight of binder seems valid for various unitary and binary binder with different water-binder ratios (in a range of 0.3 to 0.5), including SRPC (as 7-35 rebar 1), OPC (as 2-50 rebar 2; 8-40 rebar 1) and SRPC+5% silica fume (as 5-40 rebar 2; 6-35 rebars 1 and 2; H1 (w/b 0.30) rebar 1). It seems that the chloride threshold value for the ternary binder as 12-35 rebars 1 and 2 (with 5% silica fume and 10% fly ash with water binder ratio 0.35) is higher than the unitary or binary binder. The chloride content at the cover depth of concrete 12-35 has already reached 2-3% after 10 years' exposure, but no severe corrosion was observed after over 20 years' exposure. No corrosion of rebars has been detected in concretes H2 and H5 owing to their thicker cover (30-35 mm), low water-binder ratio (0.3-0.25), or high addition of silica fume (10% in H2).

It should be noted that these threshold values have been estimated on specimens with cover thickness of 15-25 mm. In reality, the cover thickness of infrastructural concrete is normally larger than 45 mm according to Swedish requirements for infrastructures exposed to chloride environments. As discussed by Pettersson (1996), corrosion is often promoted by changes in moisture, temperature, oxygen, salinity and so on, because these changes may produce potential difference at the concrete-steel interface and this potential difference can then trigger corrosion at a certain chloride level Silva (2013). Some theoretical considerations of the effect of cover thickness on the chloride threshold value were made by Fagerlund (2011) who proposed a hypothesis that the chloride threshold value exponentially increases with the cover thickness and there is a critical cover thickness beyond that corrosion is impossible. However, this hypothesis has not been verified yet. Fagerlund (2011) also pointed out that the effect of cover thickness on the chloride threshold value has not been thoroughly investigated. Nevertheless, a thicker cover provides a relatively stable micro-climate with less variation in moisture and oxygen, implying that a higher chloride concentration is needed to initiate

corrosion under such a stable climate condition. Therefore, it is reasonable to assume somewhat higher threshold values for steel embedded in concrete with greater cover thickness.

Table 6.1 Chloride contents near the rebars corroding at a certain rate.

Concrete / Rebar	Cover [mm]	Diameter [mm]	Corrosion rate [$\mu\text{m}/\text{yr}$]	Cl% wt of binder ^a	Notes
1-35/Rebar 1	10	12	~50 (~20 ^b)	2.4 (3 ^b)	10 cm under water level
1-402/Rebar 1	15	20	>500 (~20 ^b)	3 (3.3 ^c)	20 cm under water level
1-402/Rebar 2	20	20	>500 (~20 ^b)	3 (2.7 ^c)	20 cm under water level
2-35/Rebar 2	25	20	~40 (~30 ^b)	2 (1.7 ^c)	At water level
2-50/Rebar 1	10	12	~20 (~70 ^b)	2.4 (3 ^c)	20 cm above water level
2-50/Rebar 2	15	12	~15 (~10 ^b)	2 (1.1 ^c)	20 cm above water level
3-351/Rebar 1	20	20	~70 (~40 ^b)	2 (1.8 ^c)	10 cm under water level
3-351/Rebar 2	15	20	>500 (~150 ^b)	2.4 (2.3 ^c)	20 cm under water level
3-352/Rebar 1	10	12	>500 (~10 ^b)	2.8 (2.9 ^c)	30 cm under water level
5-40/Rebar 1	15	20	>500 (~70 ^b)	3 (1.6 ^c)	20 cm under water level
5-40/Rebar 1	20	20	>500 (~100 ^b)	2.7 (1.2 ^c)	20 cm under water level
6-35/Rebar 1	25	20	~15 (~10 ^b)	1.2 (0.9 ^c)	20 cm under water level
6-35/Rebar 2	20	20	~80 (~70 ^b)	1.4 (1.2 ^c)	20 cm under water level
6-40/Rebar 1	15	20	>500 (~70 ^b)	2.6 (1.7 ^c)	20 cm under water level
7-35/Rebar 1	20	20	~30 (~100 ^b)	2.2 (1.1 ^c)	30 cm under water level
7-35/Rebar 2	15	20	~45 (~40 ^b)	2.4 (1.5 ^c)	10 cm under water level
8-40/Rebar 1	20	20	~10 (~5 ^b)	2.3 (1 ^c)	10 cm under water level
12-35/Rebar 1	10	12	~15 (~5 ^b)	3.2 (3 ^c)	30 cm under water level
12-35/Rebar 2	15	12	~10 (<5 ^b)	2.7 (2 ^c)	At water level
H1/Rebar 1	20	12	~20 (<5 ^b)	1.1 (0.5 ^c)	10 cm above water level
H2(II)/Rebar 1	30	12	<5 (<5 ^b)	0.1 (<0.1 ^c)	30 cm under water level
H2(II)/Rebar 2	30	12	<5 (<5 ^b)	0.1 (<0.1 ^c)	30 cm under water level
H5(II)/Rebar 1	35	12	<5 (<5 ^b)	<0.1 (<0.1 ^c)	20 cm under water level
H5(II)/Rebar 2	35	12	<5 (<5 ^b)	<0.1 (<0.1 ^c)	20 cm above water level

^a based on the chloride profiles in the submerged zone.

^b data after 13 years' exposure (Tang et al. 2005).

^c data after 10 years' exposure (Tang 2003b).

6.4 Further visual examination and confirmation of corrosion conditions

Based on the results presented in sections 6.2 to 6.3, it was decided to release as many rebars as possible for visual examination in order to confirm the corrosion conditions measured by the non-destructive RapiCor technique, as well as to check the chloride content at the cover level for possible estimation of chloride threshold values. The results of visual examination including individual comments and supplementary chloride contents at the cover level are attached in Appendix 5. From the results the following remarks can be made:

- The corrosion conditions measured by RapiCor are in most cases confirmed from the visual examination.
- The ongoing corrosion measured by RapiCor on the upper part of the rebars is mainly due to crevice corrosion around or close to the insulation tape, as shown in Fig. 6.9, for example.
- Owing to the polarisation effect of corrosion spots from both the lower and the upper parts of a rebar, it is difficult to accurately estimate the chloride threshold values from the non-corroded part of the rebar. However, it can be seen from rebar 2 in Slab 94-2A that there is a marked shift in half-cell potential at the position of about 40 mm (Fig. 6.10) and no detectable ongoing corrosion in this area of the rebar. The measured chloride content is 0.9% by weight of binder. This may lead to a conclusion that the actual chloride threshold value for this concrete (100% SRPC with w/b 0.35) is higher than 0.9% by weight of binder, which is comparable with the conclusion in section 6.3.

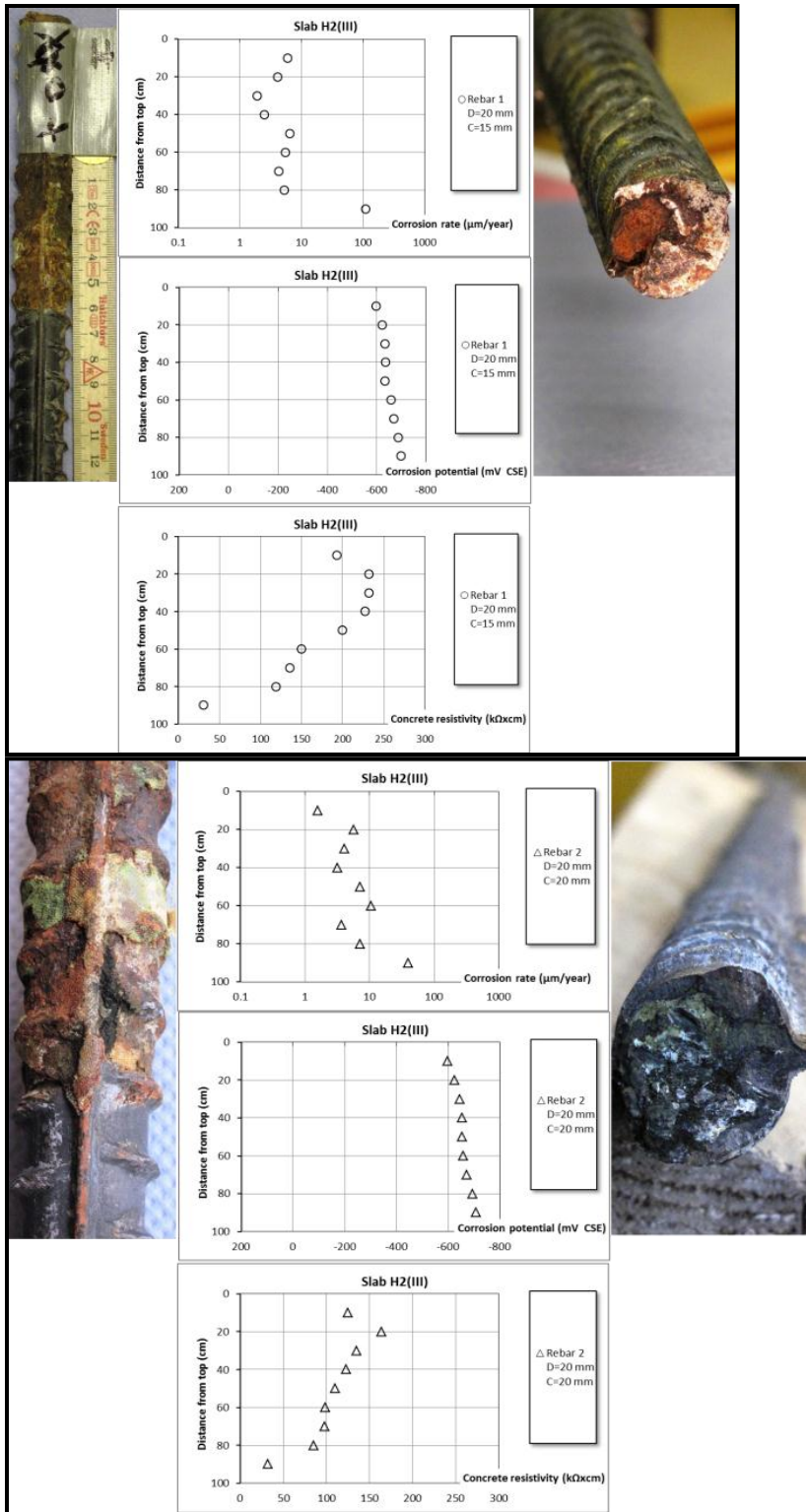


Figure 6.9 Example of confirmation of corrosion by visual examination, rebars 1 (top) and 2 (bottom) in Slab H2 (III).

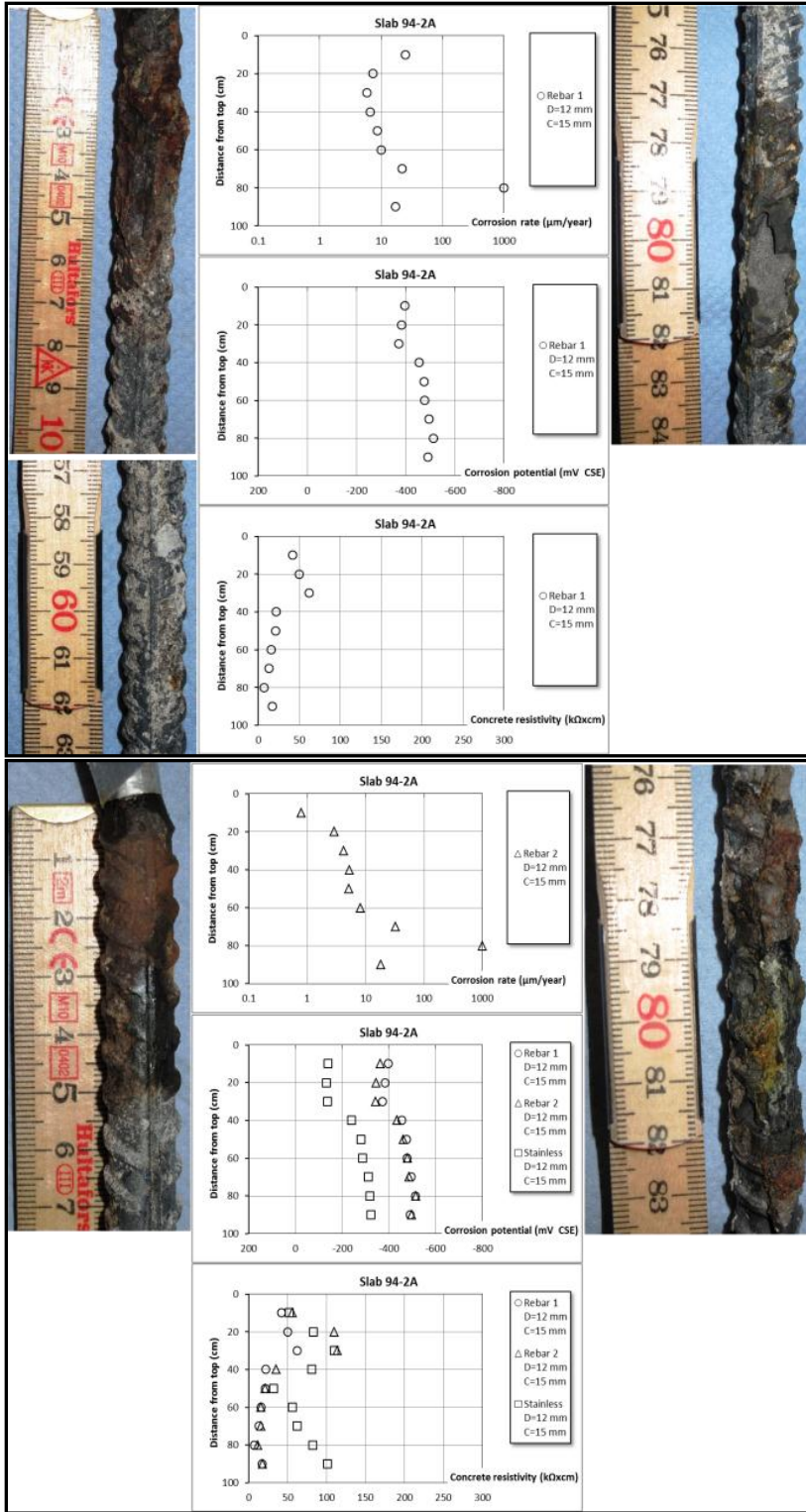


Figure 6.10 Example of potential shift and visual examination, rebars 1 (top) and 2 (bottom) in Slab 94-2A.

7 Concluding Remarks

Based on the investigation of chloride ingress and corrosion conditions after over 20 years' exposure at Träslövsläge field exposure site, the following concluding remarks can be drawn:

- In general the chloride ingress is more severe in the submerged zone than in the other zones, although in some occasional cases the chloride ingress may be severe in the splash zone close to the water level.
- Multi-pozzolanic additions such as fly ash and silica fume can effectively reduce chloride ingress.
- Air entraining in general increases chloride ingress, especially in concrete with SRPC.
- No marked reduction tendency is observed in the apparent chloride diffusion coefficient curve-fitted from the chloride profiles after 10 and 20 years' exposure.
- Chloride ingress in concretes with plain Portland cement $w/c \geq 0.35$ and SRPC with addition of 5% silica fume $w/c \geq 0.4$ reached over 2% by weight of cement at 50 mm depth.
- It is reasonable to assume a chloride threshold value of at least 1% by weight of binder for initiation of corrosion of reinforcement steel embedded in the marine concrete structures considering the actual thickness of cover, although there is a need to develop a reliable laboratory test method for testing the chloride threshold value of various types of binder.
- This threshold value of 1% by weight of binder seems valid for various unitary and binary binders including ordinary Portland cement, sulphate resistance Portland cement and blended cement with 5% silica fume, and also with different water-binder ratios in a range of 0.3 to 0.5.
- For the ternary binder blended with 5% silica fume and 10% fly ash with water binder ratio 0.35, the chloride threshold value can be as high as 2% by weight of binder content.
- The empirical DuraCrete model based on short-term field data underestimates chloride ingress in concrete with low w/b and pozzolanic additions.
- The mechanism-based ClinConc model gives reasonable prediction of chloride ingress from 1 up to 20 years.

From the predictions of the ClinConc model, it has been demonstrated that the best measure to achieve 100 years' service life with a cover thickness of 60 mm is to use either 5% silica fume or 20% fly ash with reduced water-binder ratio down to 0.30, or to use a combination of both fly ash and silica fume. However, the uncertainty in the prediction should be further investigated before this promising model can be applied to the service life design and redesign of reinforced concrete structures exposed to a marine environment.

8 References

Alonso M.C. and Sanchez M. (2009), “Analysis of the variability of chloride threshold values in the literature”, *Mater. Corros.* 60, 631-637.

Angst, U., Elsener B, Larsen, C.K., Vennesland, Ø., (2009), “Critical chloride content in reinforced concrete – A review”, *Cem. and Concr. Res.* 39, 1122-1138.

Bamforth, P.B., Price W.F. and Emerson M. (1997), “An international review of chloride ingress into structural concrete”, Transport Research Laboratory, Contractors Report 359, Edinburgh, Scotland.

Baroghel-Bounya, V., Dierkensb, M., Wanga, X., Soivec, A., Saillioad, M., Thierya M. and Thauvinc, B. (2013), “Ageing and durability of concrete in lab and in field conditions: investigation of chloride penetration”, *Journal of Sustainable Cement-Based Materials* , 2 (2) 67-110.

Betongföreningen (2007), “Guidelines for durability design of concrete structures” (in Swedish), Swedish Concrete Association, Report No. 12, Stockholm, Sweden.

Castellote, M. and Andrade, C. (2001), “Round-Robin test on chloride analysis in concrete - Part I: Analysis of total chloride content”, *Materials and Structures*, 34(243), 532-556.

Duracrete (2000), “General Guidelines for Durability Design and Redesign”, Report R15, in ‘EU Brite-EuRam III project DuraCrete (BE95-1347): Probabilistic Performance Based Durability Design of Concrete Structures’, TNO Netherlands Organisation for Applied Scientific Research, Delft, Netherlands.

Glass, G.K. and Buenfeld, N.R. (1995), “Chloride threshold levels for corrosion induced deterioration of steel in concrete” in: L.O. Nilsson, J.P. Ollivier (Eds.), *Chloride Penetration into Concrete*, RILEM, St-Remy-les-Chevreuse, 429-440.

Fagerlund, G. (2011), “The threshold chloride level for initiation of reinforcement corrosion in concrete - Some theoretical considerations”, Report TVBM-3159, Division of Building Materials, Lund Institute of Technology, p. 49.

Hedenblad, G. and Nilsson, L.-O. (1985), “Degree of Capillary Saturation - A tool for better evaluation of the moisture content in concrete”, LUTVDG/TVBM-7005, Division of Building Materials, Lund Institute of Technology, pp. 13, 1985.

Hobbs, D. W. (2001), “Concrete deterioration: causes, diagnosis, and minimising risk”, *Int. Materials Reviews* (46), 117-143.

Nanukuttan, S., Basheer, P.A.M., Holmes, N., Tang, L. and McCarter, J. (2010), “Use of performance specification and predictive model for concretes exposed to a marine environment”, in *Structural Faults and Repair Conference 2010*, 15-17 June 2010, Edinburgh, Scotland, 12 pages, CDROM.

Nilsson, L.-O. (1980), “Hygroscopic Moisture in Concrete - Drying, Measurements & Related Material Properties”, Report LUTVDG/TVBM-1003, Division of Building Materials, Lund Institute of Technology, p. 162.

Pettersson, K. (1996), “Chloride threshold values in reinforced concrete”, in *Durability of Concrete in Saline Environment*, Cementa AB, Stockholm, pp.95-105.

Sandberg, P. (1996), “Systematic collection of field data for service life prediction of concrete structures”, in *Durability of Concrete in Saline Environment*, Cementa AB, Stockholm.

Silva, N. (2013), “Chloride induced corrosion of reinforcement steel in concrete - Threshold values and ion distributions at the steel-concrete interface”, Chalmers PhD thesis, New series No. 3489, Dept. of Civil and Environmental Engineering, Gothenburg, Sweden.

Tang, L. (1996), “Chloride transport in concrete - Measurement and prediction”, Doctoral thesis, Dept. of Building Materials, Chalmers Universities of Technology, Publication P-96:6, Gothenburg, Sweden.

Tang, L. (1998), “Measurement of chloride content in concrete with blended cement -An evaluation of repeatability and reproducibility of the commonly used test methods, NORDTEST Project No. 1410-98”, SP Report 1998:27, SP Swedish National Testing and Research Institute, Borås, Sweden.

Tang, L. (2002), “Mapping corrosion of steel in reinforced concrete structures”, SP Report 2002:32, SP Swedish National Testing and Research Institute, Borås, Sweden.

Tang, L. (2003a), “Estimation of cement/binder profile parallel to the determination of chloride profile in concrete- Nordtest project No. 1581-02”, SP Report 2003:7, SP Swedish National Testing and Research Institute, Borås, Sweden.

Tang L. (2003b), “Chloride Ingress in Concrete Exposed to Marine Environment – Field Data Up to 10 Years Exposure”, SP Report 2003:16.

Tang L. (2003c), “A Collection of Chloride and Moisture Profiles from the Träslövsläge Field Site – From 0.5 up to 10 years investigations”, Chalmers Publication P-03:3.

Tang, L. (2006), “Service-life prediction based on the rapid migration test and the ClinConc model”, RILEM Proceedings PRO 047: “Performance Based Evaluation and Indicators for Concrete Durability”, ed. by V. Baroghel-Bouny et al., RILEM Publications, pp. 157-164.

Tang, L. (2008), “Engineering expression of the ClinConc model for prediction of free and total chloride ingress in submerged marine concrete”, *Cement and Concrete Research*, 38(8-9), pp. 1092-1097.

Tang, L. and Nilsson, L.-O. (1993), “Chloride binding capacity and binding isotherms of OPC pastes and mortars”, *Cement and Concrete Research*, 23, pp. 347-353.

Tang, L. and Nilsson, L.-O. (1994), “A numerical method for prediction of chloride penetration into concrete structures”, in “The Modelling of Microstructure and its Potential for Studying Transport Properties and Durability”, Kluwer Academic Publisher, pp. 539-552.

Tang, L. and Sandberg, P. (1996), “Chloride penetration into concrete exposed under different conditions”, Proceedings of the 7th International Conference on the Durability of Building Materials and Components, May 19-23, 1996, Stockholm, E & FN Spon, pp.453-461.

Tang, L., Utgenannt,P., Lindvall, A. and Boubitsas, D. (2012), “Validation of models and test methods for assessment of durability of concrete structures in the road environment”, CBI Report 2:2012, Swedish Cement and Concrete Research Institute, Stockholm, Sweden, 2012.

Tang L., Utgenant P. and Fidjestøl P (2005). “Evaluation of Chloride-Induced Corrosion of Steel in Concrete after Lon-Time Exposure in a Marine Environment”, SP Report 2005:54, Borås.

Tuutti, K. (1982) “Corrosion of steel in concrete”, Doctoral thesis, Swedish Cement and Concrete Research Institute, Publication fo 4·82, Stockholm, Sweden.

Appendix 1

**Method for determination of acid soluble chloride
and calcium in concrete**

Procedure for the Extraction of Acid Soluble Chloride and Calcium

- Weigh about 3 g of powdered sample (Note 1) in a 250 ml beaker to the nearest 0.001 g, noted as *m*.
- Add 10 ml demineralised water and swirl to bring the powder into suspension.
- Add 3 ml of concentrated nitric acid, swirl continuously and break up any lumps with a glass rod if necessary.
- Rinse the wall of the beaker and the glass rod with a small portion of water if necessary.
- Dilute the solution in the beaker with demineralised water to about 50 ml.
- Heat the beaker on a hot plate at medium heat to boiling for about 5 minutes.
- Remove the beaker from the hot plate and allow it cool sufficiently to handle.
- Filter the solution into a 250 ml glass or plastic cup, using middle speed filter paper (e.g. MUNKTELL Filter No. 150 or No. 3) pre-wetted with demineralised water.
- Wash and transfer the residue in the beaker into the filter paper with the aid of hot demineralised water.
- Wash the beaker about three times with a small portion of hot demineralised water.
- Wash the filter paper about three times with a small portion of hot demineralised water. The total volume of the filtrate including washings in the cup will be about 100~120 ml.

Note 1: If the expected chloride or calcium content in concrete is high, the size of sample can be reduced to 1 g.

Determination of Chloride Content

Chloride content is determined by potentiometric titration using a chloride or silver selective electrode together with a calomel or Ag/AgCl reference electrode. The silver nitrate solution of 0.01 mol/l is used as titrant. The titration is carried out with an increment of titrant volume 0.1 ml until the significant equivalent point is reached.

The chloride content in a sample can be calculated by the following equation:

$$Cl, \% = \frac{3.545VN}{m}$$

where: *V*: The used amount of silver nitrate solution at the equivalent point, ml;
N: The concentration of silver nitrate solution, mol/l;
m: The mass of the sample, g;

Determination of Calcium Content

Calcium content can be determined by potentiometric titration using a calcium selective electrode together with a calomel or Ag/AgCl reference electrode. The Na₂-EDTA solution of 0.1 mol/l is used as titrant. After the titration for chloride ions,

- Add 5 ml of the 1:2 diluted triethanolamine to the sample solution (Note 2);
- Stir the sample solution and adjust its pH-value to 12~13 using the saturated NaOH solution.
- Carry out the potentiometric titration with an increment of titrant volume 0.1~0.2 ml until the equivalent point is found.

The calcium content in a sample can be calculated by the following equation:

$$CaO, \% = \frac{5.608VN}{m}$$

where: *V*: The used amount of the EDTA solution at the equivalent point, ml;
N: The concentration of the EDTA solution, mol/l;
m: The mass of the sample, g;

Note 2: Dilute one part (by mass) of triethanolamine with two parts of demineralised water.

Appendix 2

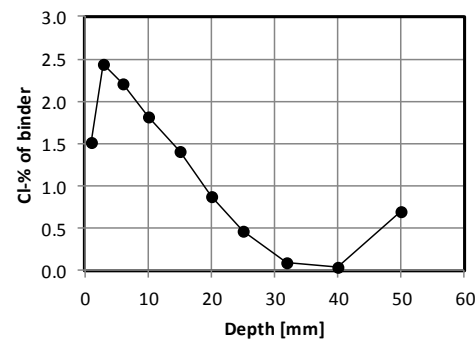
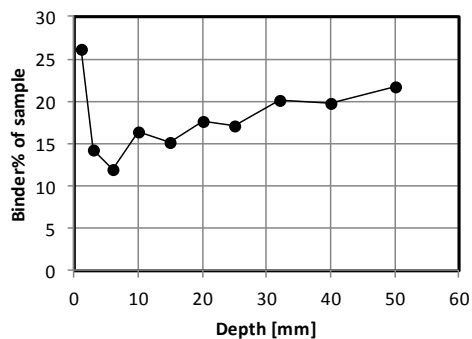
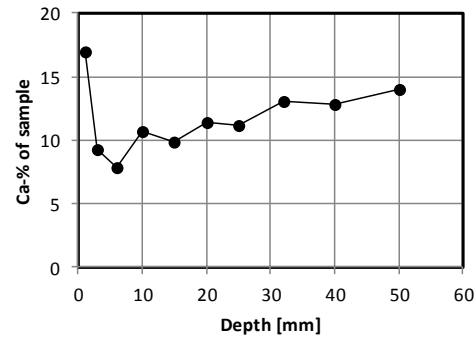
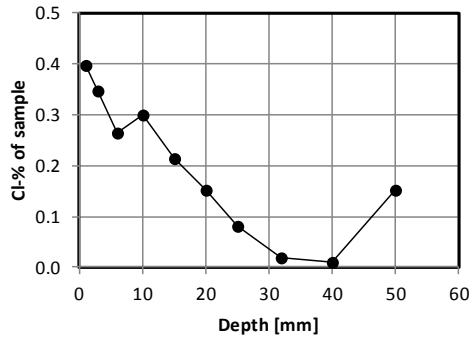
Chloride profiles sampled 2012 (~20 years)

Measurement of chloride ingress in concrete

Concrete ID: 1-351 A	Type of binder: 100% Anl
Casting date: 1992-01-22	w/b: 0.35
Exposure date: 1992-02-05	Exposure zone: Atmospheric
Sampling date: 2012-10-02	Profiling method: Grinding on a lathe
Tested by: LG	Chloride analysis: Potentiometric titration
Tested date: 2013-05-22	Calcium analysis: Potentiometric titration

Raw data and calculations

Exposure duration:		7545 days		CaO% binder:		64.9 %	
Depth from - to (mm)	Mean depth (mm)	Cl% of sample	CaO% of sample	Binder% of sample	Cl% of binder		
0 - 2	1	0.398	16.98	26.17	1.52		
2 - 4	3	0.347	9.23	14.23	2.44		
4 - 8	6	0.266	7.81	12.03	2.21		
8 - 12	10	0.299	10.70	16.48	1.82		
12 - 18	15	0.214	9.81	15.12	1.42		
18 - 22	20	0.153	11.40	17.56	0.87		
22 - 28	25	0.080	11.12	17.13	0.47		
28 - 36	32	0.020	13.11	20.19	0.10		
36 - 44	40	0.009	12.84	19.78	0.05		
44 - 56	50	0.152	14.06	21.66	0.70		

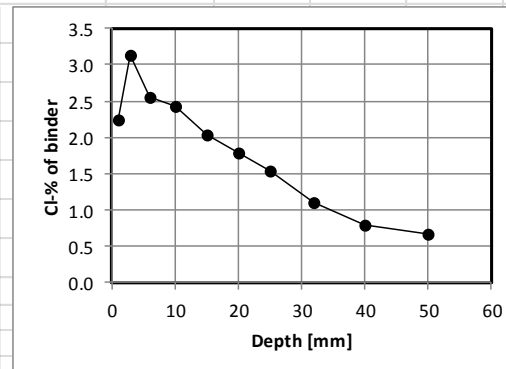
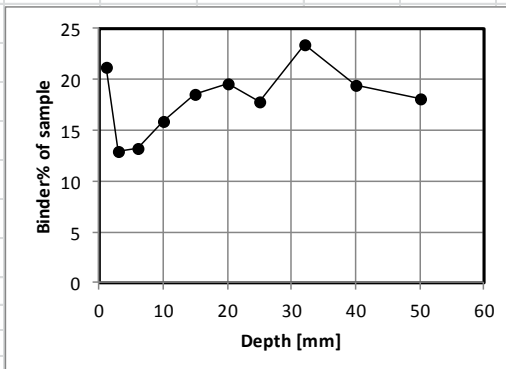
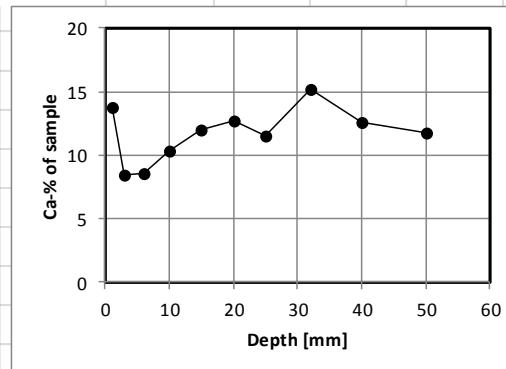
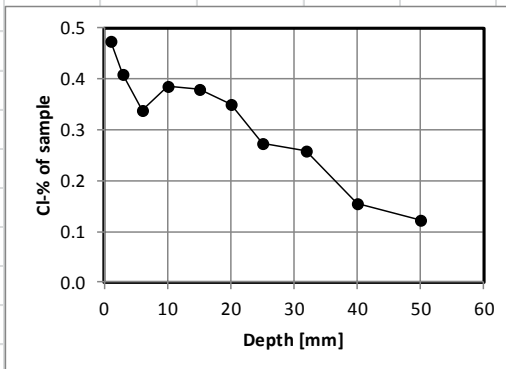


Measurement of chloride ingress in concrete

Concrete ID: 1-351-U	Type of binder: 100% Anl
Casting date: 1992-01-22	w/b: 0.35
Exposure date: 1992-02-05	Exposure zone: Splash
Sampling date: 2012-10-02	Profiling method: Grinding on a lathe
Tested by: LG-IM_LJ	Chloride analysis: Potentiometric titration
Tested date: 2013-05-22	Calcium analysis: Potentiometric titration

Raw data and calculations

Exposure duration:		7545 days		CaO% binder:		64.9 %	
Depth from - to (mm)	Mean depth (mm)	Cl% of sample	CaO% of sample	Binder% of sample	Cl% of binder		
0 - 2	1	0.476	13.79	21.25	2.24		
2 - 4	3	0.408	8.44	13.00	3.14		
4 - 8	6	0.338	8.62	13.29	2.55		
8 - 12	10	0.386	10.32	15.90	2.43		
12 - 18	15	0.378	12.03	18.54	2.04		
18 - 22	20	0.351	12.69	19.55	1.79		
22 - 28	25	0.273	11.54	17.78	1.54		
28 - 36	32	0.259	15.16	23.36	1.11		
36 - 44	40	0.156	12.61	19.43	0.80		
44 - 56	50	0.121	11.79	18.17	0.67		

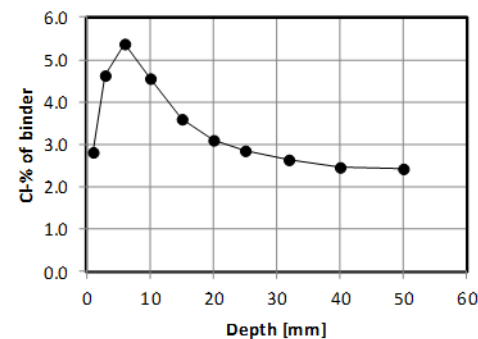
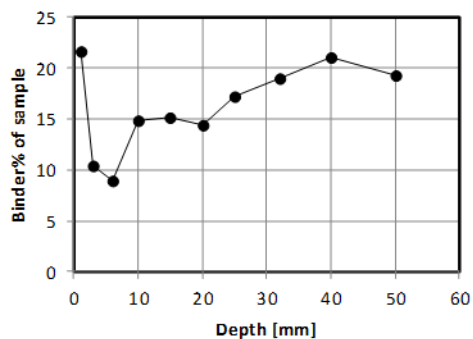
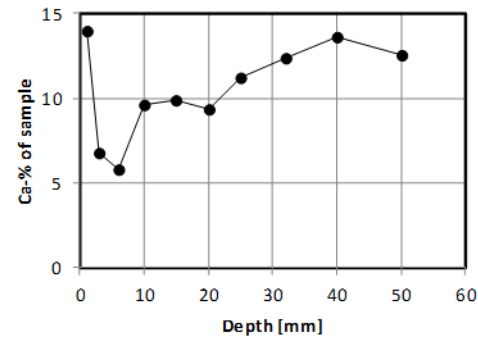
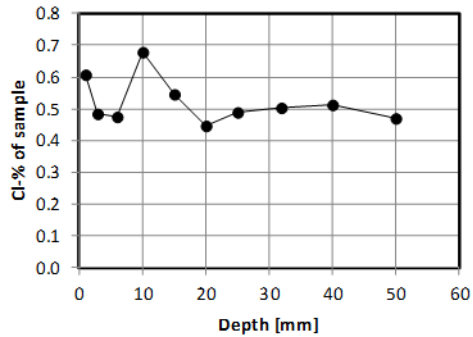


Measurement of chloride ingress in concrete

Concrete ID: 1-351-U	Type of binder: 100% AnI
Casting date: 1992-01-22	w/b: 0.35
Exposure date: 1992-02-05	Exposure zone: Submerged
Sampling date: 2012-10-02	Profiling method: Grinding on a lathe
Tested by: LG-IM_LJ	Chloride analysis: Potentiometric titration
Tested date: 2013-05-22	Calcium analysis: Potentiometric titration

Raw data and calculations

Exposure duration: 7545 days		CaO% binder: 64.9 %			
Depth from - to (mm)	Mean depth (mm)	Cl% of sample	CaO% of sample	Binder% of sample	Cl% of binder
0 - 2	1	0.608	14.01	21.58	2.82
2 - 4	3	0.486	6.81	10.49	4.64
4 - 8	6	0.477	5.77	8.90	5.36
8 - 12	10	0.677	9.63	14.83	4.57
12 - 18	15	0.546	9.86	15.19	3.60
18 - 22	20	0.446	9.35	14.41	3.09
22 - 28	25	0.492	11.21	17.28	2.85
28 - 36	32	0.503	12.34	19.01	2.65
36 - 44	40	0.515	13.64	21.02	2.45
44 - 56	50	0.473	12.54	19.32	2.45

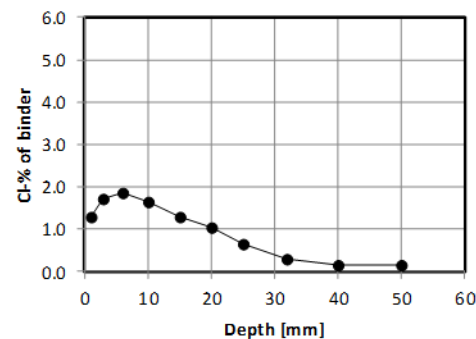
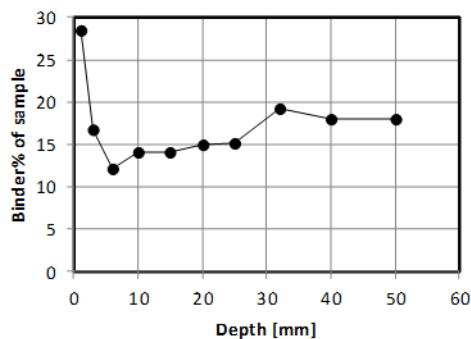
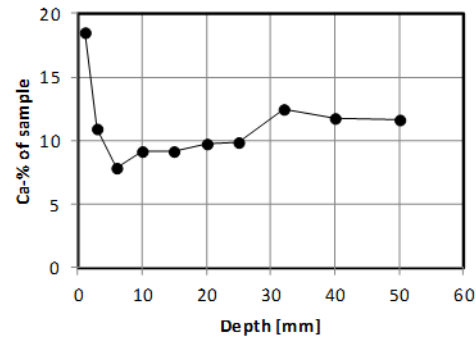
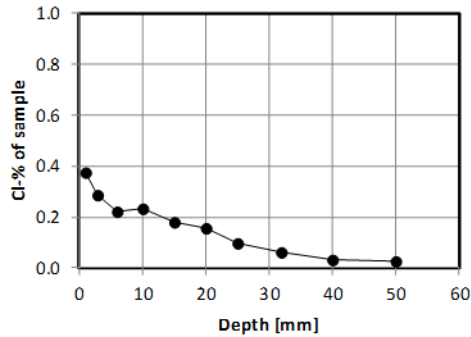


Measurement of chloride ingress in concrete

Concrete ID: 1-402-A	Type of binder: 100% AnI
Casting date: 1992-01-22	w/b: 0.4
Exposure date: 1992-02-05	Exposure zone: Atmospheric
Sampling date: 2012-10-02	Profiling method: Grinding on a lathe
Tested by:	Chloride analysis: Potentiometric titration
Tested date: 2013-05-21	Calcium analysis: Potentiometric titration

Raw data and calculations

Exposure duration: 7545 days		CaO% binder: 64.9 %				
Depth from - to (mm)	Mean depth (mm)	Cl% of sample	CaO% of sample	Binder% of sample	Cl% of binder	
0 - 2	1	0.372	18.45	28.42	1.31	
2 - 4	3	0.286	10.88	16.76	1.71	
4 - 8	6	0.224	7.85	12.09	1.85	
8 - 12	10	0.233	9.16	14.12	1.65	
12 - 18	15	0.180	9.14	14.08	1.28	
18 - 22	20	0.156	9.75	15.03	1.04	
22 - 28	25	0.097	9.82	15.13	0.64	
28 - 36	32	0.061	12.49	19.25	0.32	
36 - 44	40	0.030	11.71	18.04	0.16	
44 - 56	50	0.028	11.70	18.02	0.16	

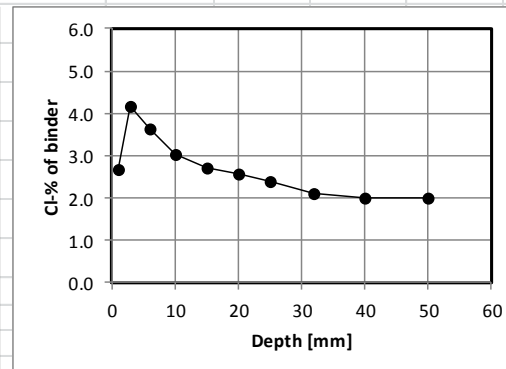
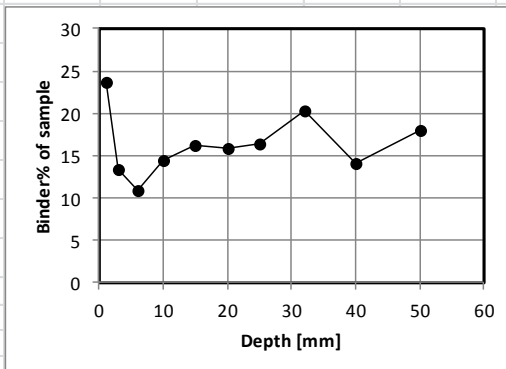
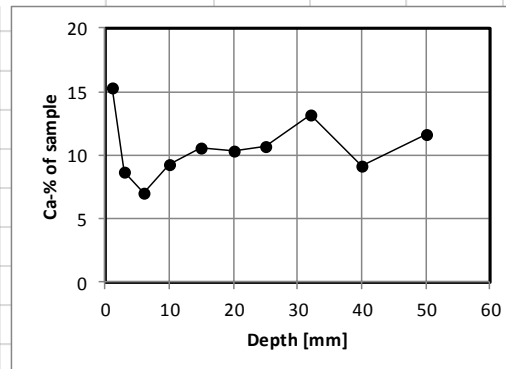
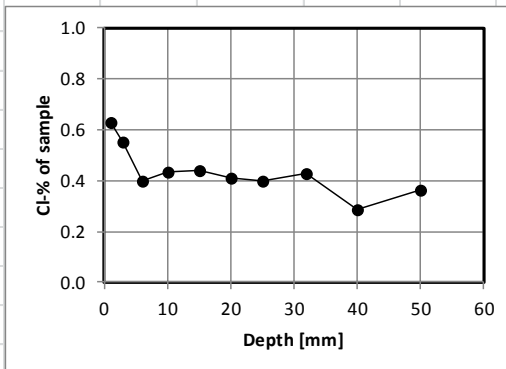


Measurement of chloride ingress in concrete

Concrete ID: 1-402-Sa	Type of binder: 100% Anl
Casting date: 1992-01-22	w/b: 0.4
Exposure date: 1992-02-05	Exposure zone: Splash, Sa
Sampling date: 2012-10-02	Profiling method: Grinding on a lathe
Tested by: IM, LG	Chloride analysis: Potentiometric titration
Tested date: 2013-05-22	Calcium analysis: Potentiometric titration

Raw data and calculations

Exposure duration:		7545 days		CaO% binder:		64.9 %	
Depth from - to (mm)	Mean depth (mm)	Cl% of sample	CaO% of sample	Binder% of sample	Cl% of binder		
0 - 2	1	0.632	15.36	23.67	2.67		
2 - 4	3	0.554	8.65	13.33	4.15		
4 - 8	6	0.398	7.07	10.90	3.65		
8 - 12	10	0.437	9.32	14.36	3.04		
12 - 18	15	0.442	10.54	16.24	2.72		
18 - 22	20	0.409	10.30	15.86	2.58		
22 - 28	25	0.396	10.70	16.49	2.40		
28 - 36	32	0.428	13.13	20.23	2.12		
36 - 44	40	0.285	9.16	14.12	2.02		
44 - 56	50	0.361	11.66	17.96	2.01		

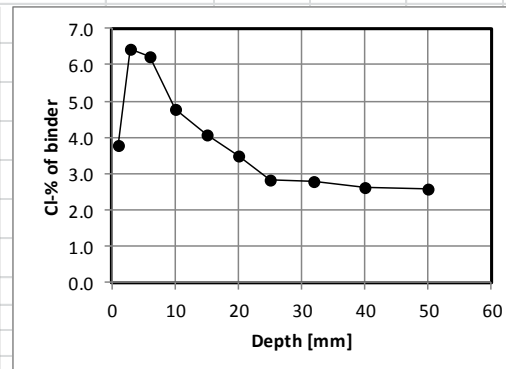
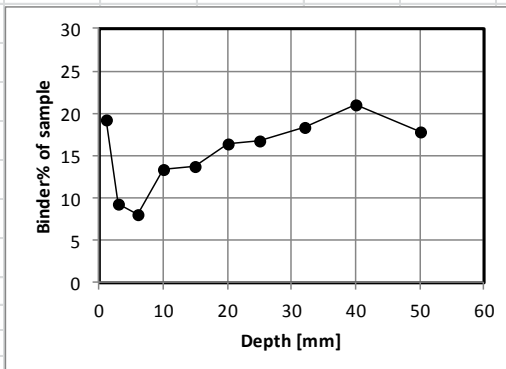
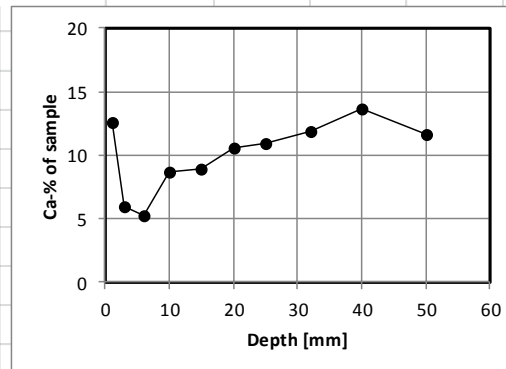
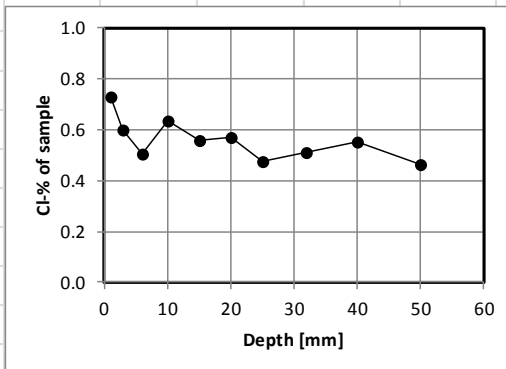


Measurement of chloride ingress in concrete

Concrete ID: 1-402-Su	Type of binder: 100% Anl
Casting date: 1992-01-22	w/b: 0.4
Exposure date: 1992-02-05	Exposure zone: Splash, Su
Sampling date: 2012-10-02	Profiling method: Grinding on a lathe
Tested by: IM, LG	Chloride analysis: Potentiometric titration
Tested date: 2013-05-22	Calcium analysis: Potentiometric titration

Raw data and calculations

Exposure duration:		7545 days		CaO% binder:		64.9 %	
Depth from - to (mm)	Mean depth (mm)	Cl% of sample	CaO% of sample	Binder% of sample	Cl% of binder		
0	2	1	0.732	12.54	19.32	3.79	
2	4	3	0.598	6.01	9.27	6.45	
4	8	6	0.504	5.24	8.07	6.24	
8	12	10	0.635	8.64	13.31	4.77	
12	18	15	0.558	8.93	13.77	4.06	
18	22	20	0.569	10.60	16.33	3.48	
22	28	25	0.477	10.91	16.80	2.84	
28	36	32	0.511	11.92	18.36	2.78	
36	44	40	0.551	13.68	21.08	2.61	
44	56	50	0.464	11.62	17.90	2.59	

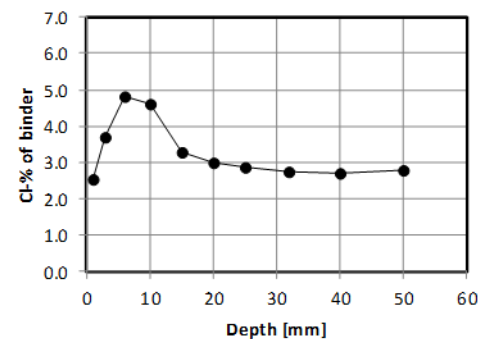
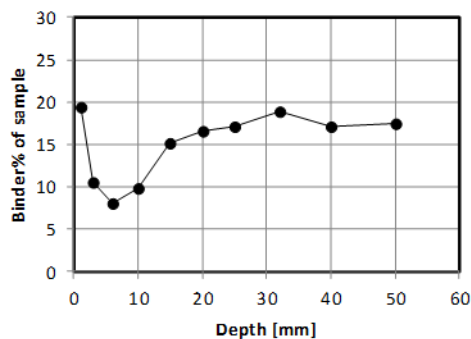
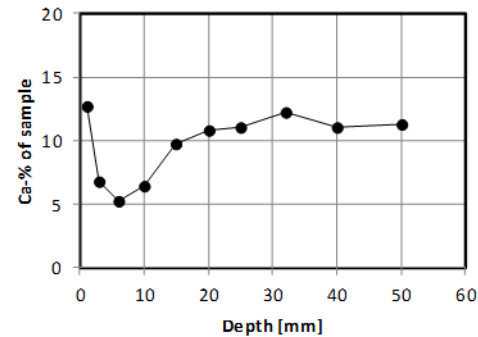
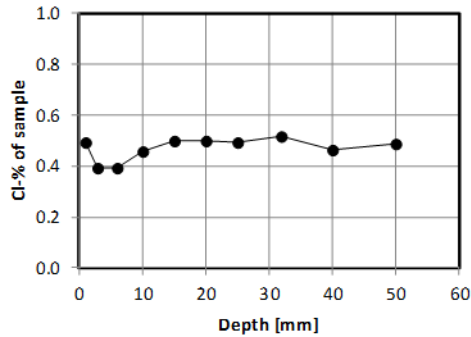


Measurement of chloride ingress in concrete

Concrete ID: 1-402-U	Type of binder: 100% AnI
Casting date: 1992-01-22	w/b: 0.4
Exposure date: 1992-02-05	Exposure zone: Submerged
Sampling date: 2012-10-02	Profiling method: Grinding on a lathe
Tested by: IM, LG, LJ	Chloride analysis: Potentiometric titration
Tested date: 2013-05-23	Calcium analysis: Potentiometric titration

Raw data and calculations

Exposure duration: 7545 days		CaO% binder: 64.9 %				
Depth from - to (mm)	Mean depth (mm)	Cl% of sample	CaO% of sample	Binder% of sample	Cl% of binder	
0 - 2	1	0.496	12.66	19.50	2.54	
2 - 4	3	0.391	6.83	10.52	3.72	
4 - 8	6	0.392	5.27	8.12	4.82	
8 - 12	10	0.456	6.43	9.90	4.60	
12 - 18	15	0.499	9.81	15.11	3.30	
18 - 22	20	0.497	10.77	16.59	2.99	
22 - 28	25	0.491	11.10	17.11	2.87	
28 - 36	32	0.520	12.26	18.89	2.75	
36 - 44	40	0.465	11.10	17.10	2.72	
44 - 56	50	0.485	11.33	17.46	2.78	

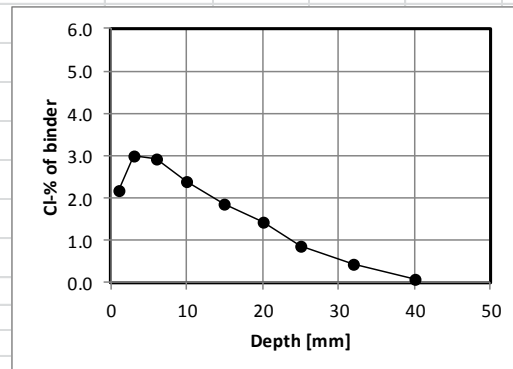
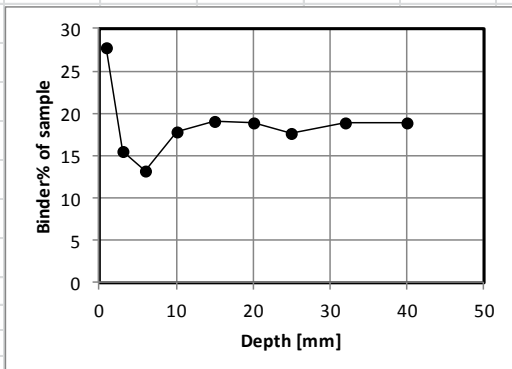
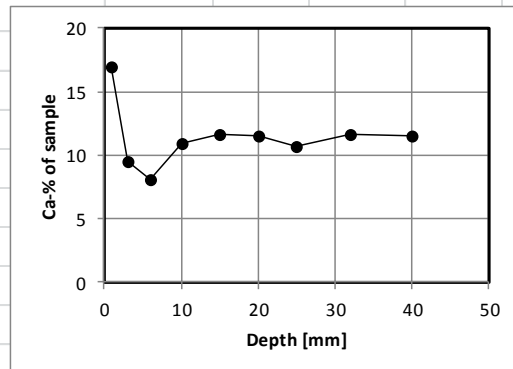
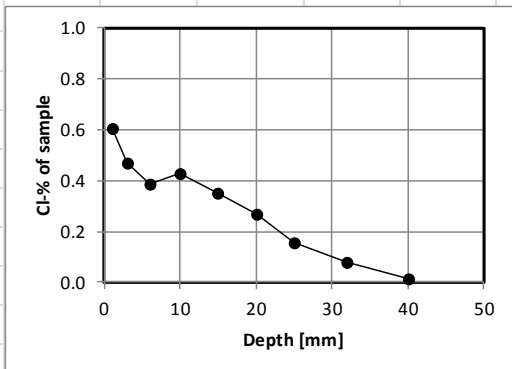


Measurement of chloride ingress in concrete

Concrete ID: 2-352-A	Type of binder: 100% Slite
Casting date: 1991-12-10	w/b: 0.4
Exposure date: 1991-12-19	Exposure zone: Atmospheric
Sampling date: 2012-10-02	Profiling method: Grinding on a lathe
Tested by: IM, LJ, LG	Chloride analysis: Potentiometric titration
Tested date: 2013-05-21	Calcium analysis: Potentiometric titration

Raw data and calculations

Exposure duration:		7593 days		CaO% binder:		61.1 %	
Depth from - to (mm)	Mean depth (mm)	Cl% of sample	CaO% of sample	Binder% of sample	Cl% of binder		
0 - 2	1	0.607	16.98	27.78	2.18		
2 - 4	3	0.468	9.48	15.51	3.01		
4 - 8	6	0.385	8.07	13.21	2.92		
8 - 12	10	0.429	10.93	17.89	2.40		
12 - 18	15	0.353	11.62	19.02	1.85		
18 - 22	20	0.272	11.55	18.90	1.44		
22 - 28	25	0.155	10.74	17.57	0.88		
28 - 36	32	0.082	11.59	18.96	0.43		
36 - 44	40	0.016	11.56	18.92	0.09		

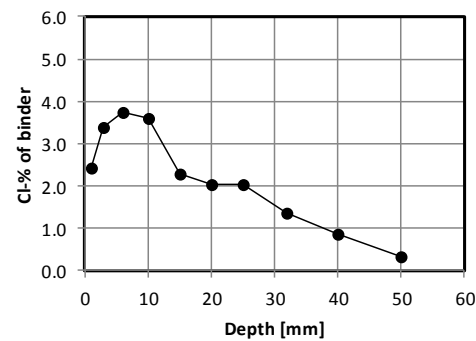
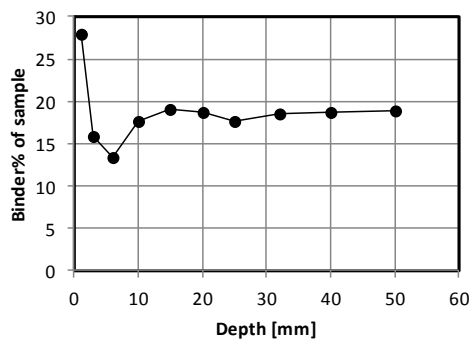
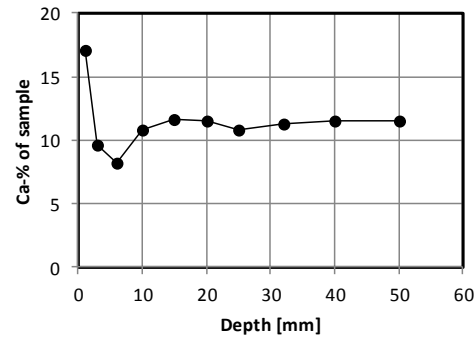
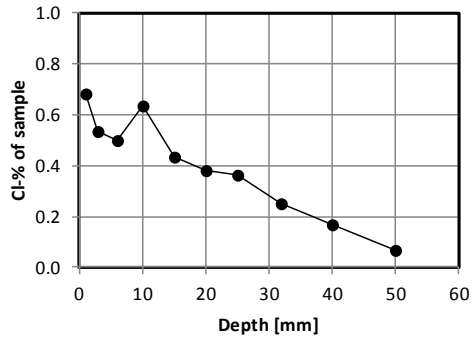


Measurement of chloride ingress in concrete

Concrete ID: 2-352-S	Type of binder: 100% Slite
Casting date: 1991-12-10	w/b: 0.35
Exposure date: 1991-12-19	Exposure zone: Splash
Sampling date: 2012-10-02	Profiling method: Grinding on a lathe
Tested by: IM, LJ, LG	Chloride analysis: Potentiometric titration
Tested date: 2013-05-27	Calcium analysis: Potentiometric titration

Raw data and calculations

Exposure duration:		7593 days		CaO% binder:		61.1 %	
Depth from - to (mm)	Mean depth (mm)	Cl% of sample	CaO% of sample	Binder% of sample	Cl% of binder		
0 - 2	1	0.681	17.08	27.95	2.43		
2 - 4	3	0.537	9.67	15.82	3.39		
4 - 8	6	0.501	8.22	13.45	3.73		
8 - 12	10	0.634	10.77	17.63	3.60		
12 - 18	15	0.435	11.68	19.11	2.28		
18 - 22	20	0.380	11.48	18.79	2.02		
22 - 28	25	0.363	10.81	17.69	2.05		
28 - 36	32	0.253	11.34	18.56	1.37		
36 - 44	40	0.166	11.47	18.77	0.88		
44 - 56	50	0.067	11.57	18.93	0.35		

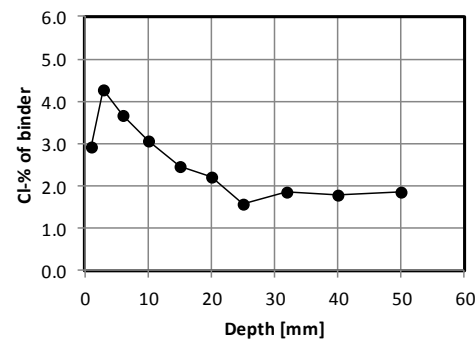
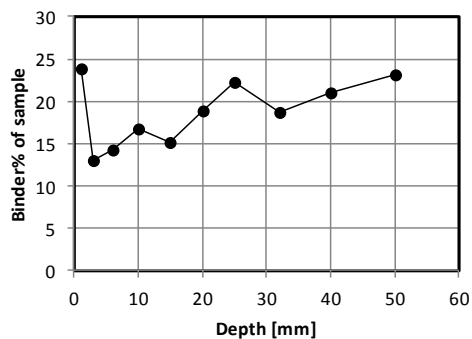
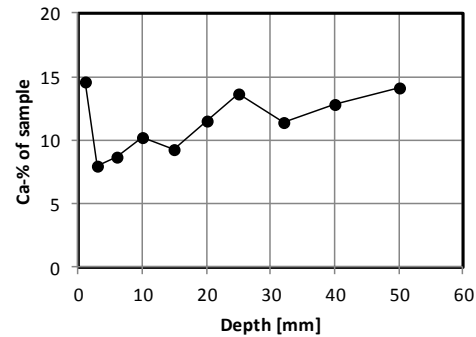
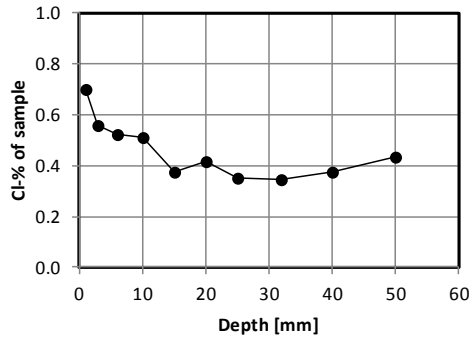


Measurement of chloride ingress in concrete

Concrete ID: 2-352-U	Type of binder: 100% Slite
Casting date: 1991-12-10	w/b: 0.35
Exposure date: 1991-12-19	Exposure zone: Submerged
Sampling date: 2012-10-02	Profiling method: Grinding on a lathe
Tested by: IM, LJ, LG	Chloride analysis: Potentiometric titration
Tested date: 2013-05-27	Calcium analysis: Potentiometric titration

Raw data and calculations

Exposure duration:		7593 days		CaO% binder:		61.1 %	
Depth from - to (mm)	Mean depth (mm)	Cl% of sample	CaO% of sample	Binder% of sample	Cl% of binder		
0 - 2	1	0.701	14.59	23.88	2.94		
2 - 4	3	0.557	7.94	12.99	4.29		
4 - 8	6	0.525	8.72	14.27	3.68		
8 - 12	10	0.511	10.20	16.69	3.06		
12 - 18	15	0.375	9.23	15.11	2.48		
18 - 22	20	0.417	11.49	18.80	2.22		
22 - 28	25	0.349	13.61	22.28	1.57		
28 - 36	32	0.347	11.43	18.71	1.85		
36 - 44	40	0.374	12.79	20.94	1.79		
44 - 56	50	0.432	14.08	23.05	1.87		

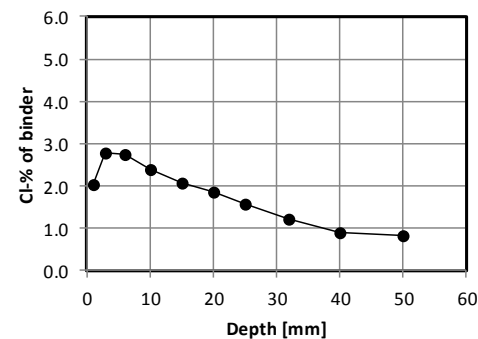
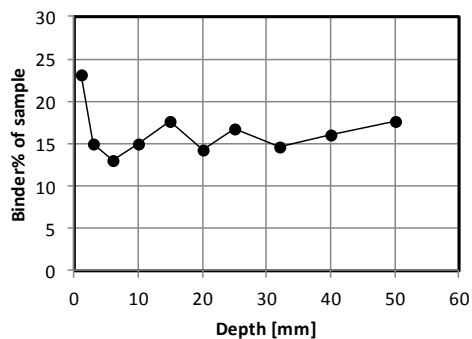
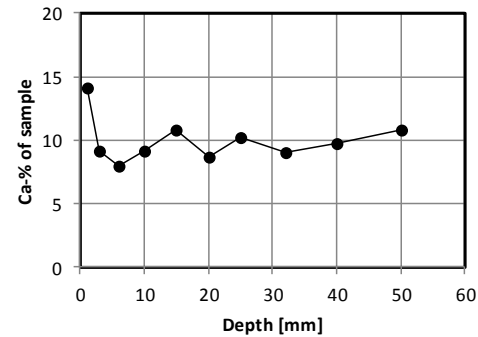
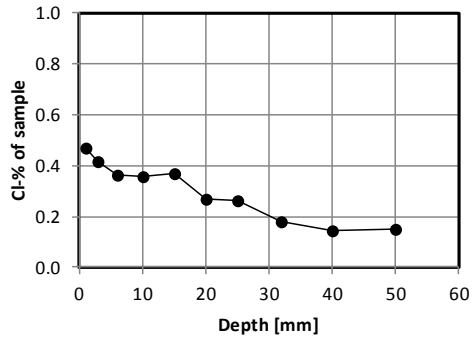


Measurement of chloride ingress in concrete

Concrete ID: 2-50-A	Type of binder: 100% Slite
Casting date: 1991-12-05	w/b: 0.5
Exposure date: 1991-12-19	Exposure zone: Atmos.
Sampling date: 2012-10-02	Profiling method: Grinding on a lathe
Tested by: IM, LJ, LG	Chloride analysis: Potentiometric titration
Tested date: 2013-05-27	Calcium analysis: Potentiometric titration

Raw data and calculations

Exposure duration:		7593 days		CaO% binder:		61.1 %	
Depth from - to (mm)	Mean depth (mm)	Cl% of sample	CaO% of sample	Binder% of sample	Cl% of binder		
0 - 2	1	0.473	14.09	23.06	2.05		
2 - 4	3	0.419	9.17	15.01	2.79		
4 - 8	6	0.362	8.00	13.09	2.76		
8 - 12	10	0.359	9.14	14.95	2.40		
12 - 18	15	0.369	10.80	17.67	2.09		
18 - 22	20	0.266	8.67	14.20	1.88		
22 - 28	25	0.263	10.23	16.75	1.57		
28 - 36	32	0.178	8.99	14.71	1.21		
36 - 44	40	0.142	9.79	16.02	0.89		
44 - 56	50	0.149	10.78	17.64	0.84		

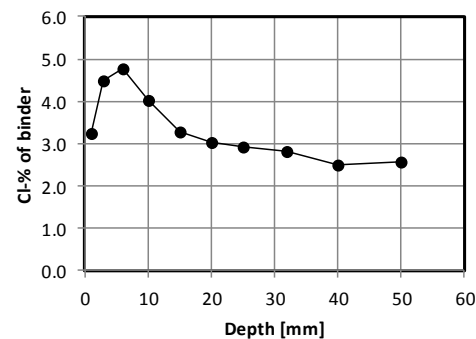
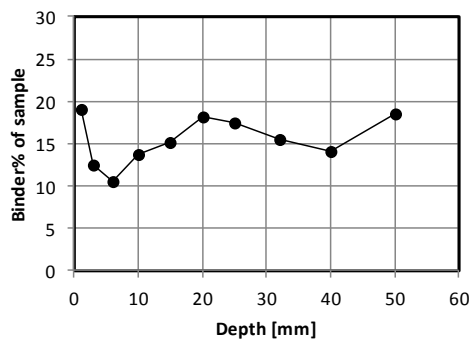
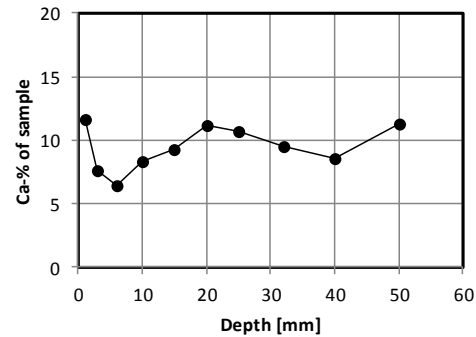
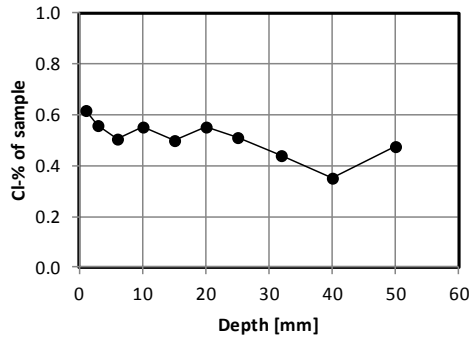


Measurement of chloride ingress in concrete

Concrete ID: 2-50-S	Type of binder: 100% Slite
Casting date: 1991-12-05	w/b: 0.5
Exposure date: 1991-12-19	Exposure zone: Splash
Sampling date: 2012-10-02	Profiling method: Grinding on a lathe
Tested by: IM, LJ, LG	Chloride analysis: Potentiometric titration
Tested date: 2013-05-27	Calcium analysis: Potentiometric titration

Raw data and calculations

Exposure duration:		7593 days		CaO% binder:		61.1 %	
Depth from - to (mm)	Mean depth (mm)	Cl% of sample	CaO% of sample	Binder% of sample	Cl% of binder		
0 - 2	1	0.618	11.65	19.06	3.24		
2 - 4	3	0.560	7.65	12.52	4.47		
4 - 8	6	0.507	6.48	10.61	4.78		
8 - 12	10	0.551	8.39	13.73	4.01		
12 - 18	15	0.501	9.30	15.22	3.29		
18 - 22	20	0.555	11.14	18.23	3.04		
22 - 28	25	0.510	10.69	17.50	2.91		
28 - 36	32	0.442	9.53	15.60	2.83		
36 - 44	40	0.353	8.63	14.12	2.50		
44 - 56	50	0.474	11.29	18.48	2.56		

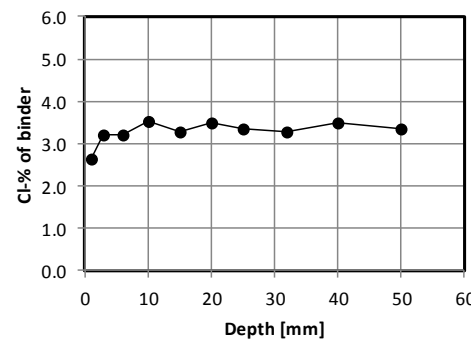
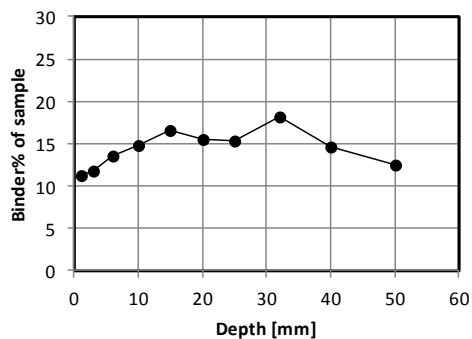
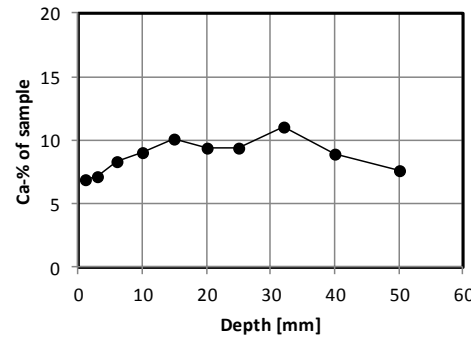
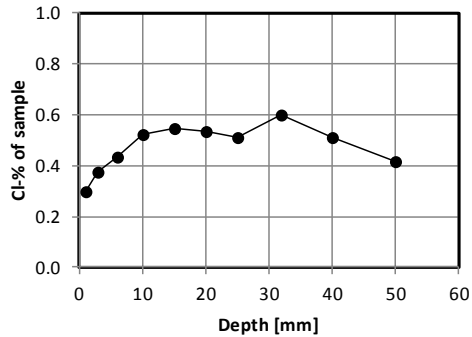


Measurement of chloride ingress in concrete

Concrete ID: 2-50-U	Type of binder: 100% Slite
Casting date: 1991-12-05	w/b: 0.5
Exposure date: 1991-12-19	Exposure zone: Submerged
Sampling date: 2012-10-02	Profiling method: Grinding on a lathe
Tested by: IM, LJ, LG	Chloride analysis: Potentiometric titration
Tested date: 2013-05-27	Calcium analysis: Potentiometric titration

Raw data and calculations

Exposure duration:		7593 days		CaO% binder:		61.1 %	
Depth from - to (mm)	Mean depth (mm)	Cl% of sample	CaO% of sample	Binder% of sample	Cl% of binder		
0 - 2	1	0.299	6.93	11.34	2.63		
2 - 4	3	0.376	7.20	11.78	3.19		
4 - 8	6	0.434	8.30	13.58	3.20		
8 - 12	10	0.522	9.08	14.85	3.51		
12 - 18	15	0.547	10.15	16.62	3.29		
18 - 22	20	0.537	9.43	15.43	3.48		
22 - 28	25	0.514	9.35	15.31	3.36		
28 - 36	32	0.597	11.11	18.18	3.29		
36 - 44	40	0.511	8.96	14.66	3.49		
44 - 56	50	0.420	7.68	12.57	3.34		

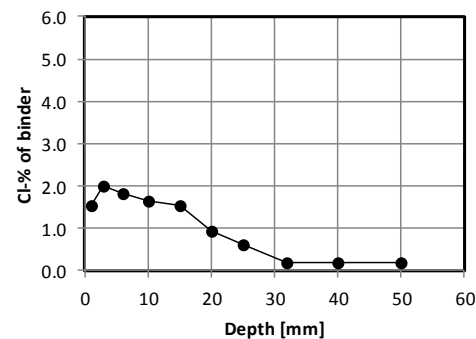
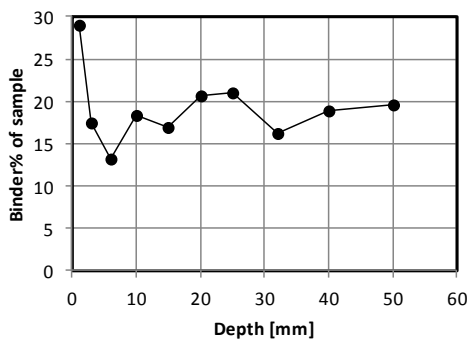
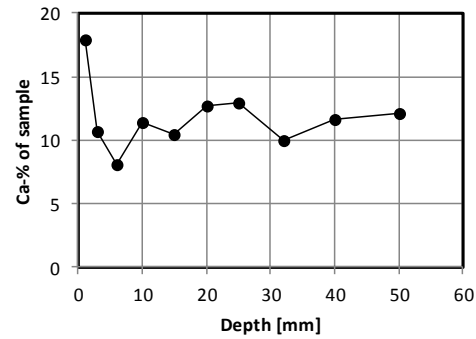
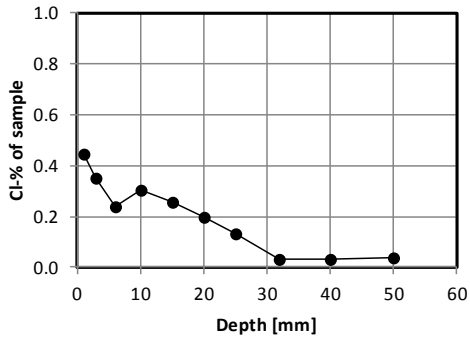


Measurement of chloride ingress in concrete

Concrete ID: 3-351-A	Type of binder: 95%Anl+5%SF
Casting date: 1992-01-27	w/b: 0.35
Exposure date: 1992-02-05	Exposure zone: Atmospheric
Sampling date: 2012-10-02	Profiling method: Grinding on a lathe
Tested by: IM, LG	Chloride analysis: Potentiometric titration
Tested date: 2013-06-03	Calcium analysis: Potentiometric titration

Raw data and calculations

Exposure duration:		7545 days		CaO% binder:		61.7 %	
Depth from - to (mm)	Mean depth (mm)	Cl% of sample	CaO% of sample	Binder% of sample	Cl% of binder		
0	2	1	0.446	17.87	28.97	1.54	
2	4	3	0.349	10.73	17.39	2.01	
4	8	6	0.241	8.12	13.15	1.83	
8	12	10	0.303	11.36	18.41	1.64	
12	18	15	0.260	10.45	16.93	1.53	
18	22	20	0.198	12.76	20.68	0.96	
22	28	25	0.133	12.97	21.03	0.63	
28	36	32	0.030	10.03	16.26	0.19	
36	44	40	0.035	11.70	18.96	0.18	
44	56	50	0.038	12.08	19.58	0.19	

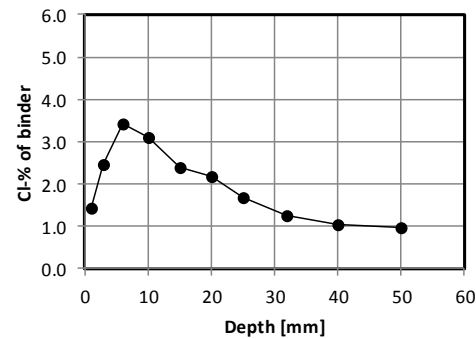
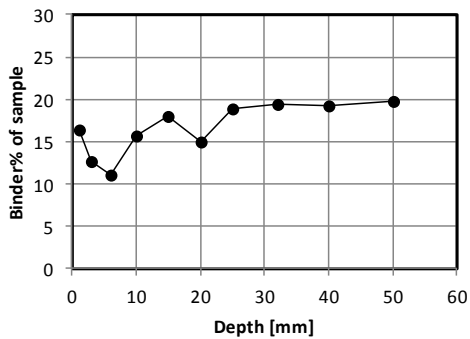
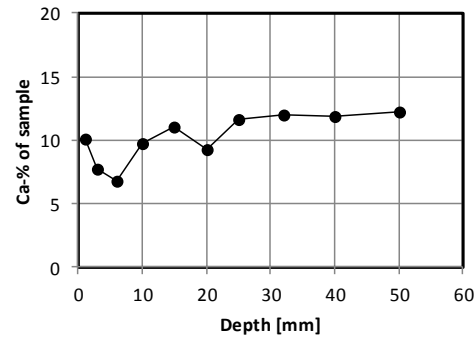
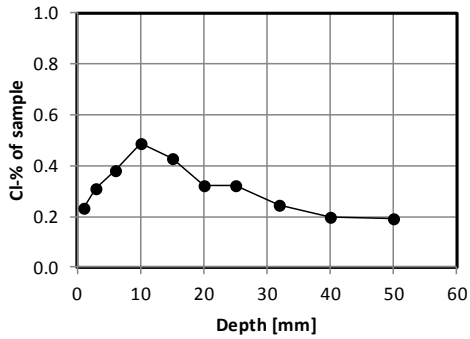


Measurement of chloride ingress in concrete

Concrete ID: 3-351-S	Type of binder: 95%Anl+5%SF
Casting date: 1992-01-27	w/b: 0.35
Exposure date: 1992-02-05	Exposure zone: Splash
Sampling date: 2012-10-02	Profiling method: Grinding on a lathe
Tested by: LG	Chloride analysis: Potentiometric titration
Tested date: 2013-06-04	Calcium analysis: Potentiometric titration

Raw data and calculations

Exposure duration:		7545 days		CaO% binder:		61.7 %	
Depth from - to (mm)	Mean depth (mm)	Cl% of sample	CaO% of sample	Binder% of sample	Cl% of binder		
0 - 2	1	0.235	10.14	16.43	1.43		
2 - 4	3	0.311	7.78	12.61	2.47		
4 - 8	6	0.379	6.84	11.09	3.42		
8 - 12	10	0.489	9.72	15.75	3.11		
12 - 18	15	0.430	11.08	17.95	2.39		
18 - 22	20	0.325	9.22	14.94	2.17		
22 - 28	25	0.322	11.69	18.94	1.70		
28 - 36	32	0.244	12.02	19.49	1.25		
36 - 44	40	0.200	11.84	19.19	1.04		
44 - 56	50	0.191	12.18	19.75	0.97		

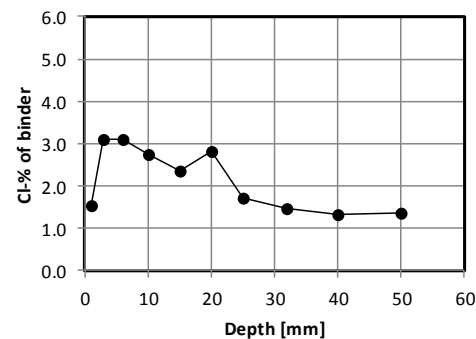
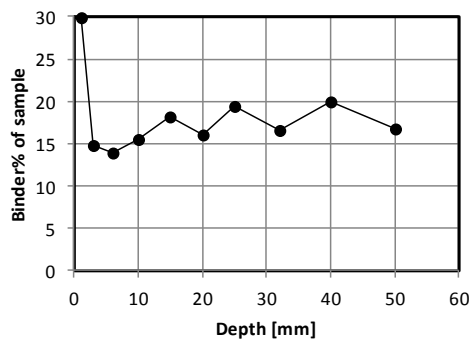
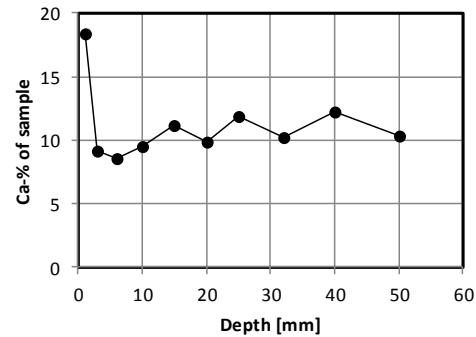
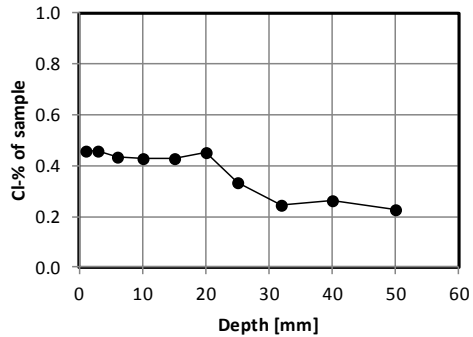


Measurement of chloride ingress in concrete

Concrete ID: 3-351-S	Type of binder: 95%Anl+5%SF
Casting date: 1992-01-27	w/b: 0.35
Exposure date: 1992-02-05	Exposure zone: Submerged
Sampling date: 2012-10-02	Profiling method: Grinding on a lathe
Tested by: LG	Chloride analysis: Potentiometric titration
Tested date: 2013-06-04	Calcium analysis: Potentiometric titration

Raw data and calculations

Exposure duration:		7545 days		CaO% binder:		61.7 %	
Depth from - to (mm)	Mean depth (mm)	Cl% of sample	CaO% of sample	Binder% of sample	Cl% of binder		
0	2	1	0.457	18.39	29.81	1.53	
2	4	3	0.457	9.13	14.80	3.09	
4	8	6	0.432	8.56	13.87	3.12	
8	12	10	0.429	9.57	15.51	2.76	
12	18	15	0.426	11.17	18.10	2.35	
18	22	20	0.451	9.90	16.05	2.81	
22	28	25	0.332	11.93	19.34	1.72	
28	36	32	0.245	10.19	16.51	1.49	
36	44	40	0.264	12.28	19.91	1.32	
44	56	50	0.226	10.29	16.68	1.36	

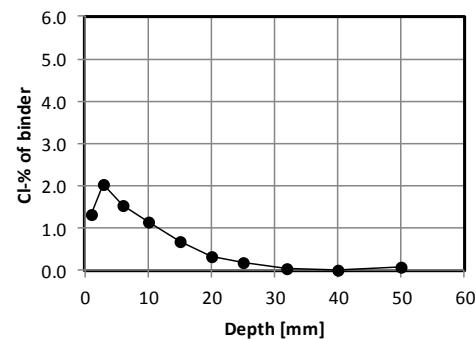
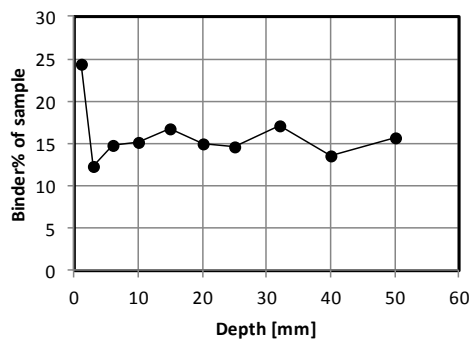
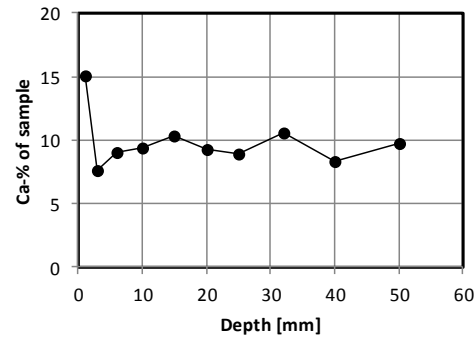
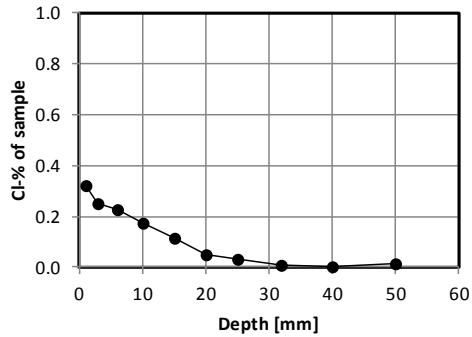


Measurement of chloride ingress in concrete

Concrete ID: 5-40-A	Type of binder: 95%AnI+5%SF
Casting date: 1992-01-25	w/b: 0.4
Exposure date: 1992-03-16	Exposure zone: Atmospheric
Sampling date: 2012-10-02	Profiling method: Grinding on a lathe
Tested by: LG	Chloride analysis: Potentiometric titration
Tested date: 2013-06-10	Calcium analysis: Potentiometric titration

Raw data and calculations

Exposure duration:		7505 days		CaO% binder:		61.7 %	
Depth from - to (mm)	Mean depth (mm)	Cl% of sample	CaO% of sample	Binder% of sample	Cl% of binder		
0 - 2	1	0.323	15.02	24.35	1.32		
2 - 4	3	0.252	7.62	12.35	2.04		
4 - 8	6	0.227	9.09	14.73	1.54		
8 - 12	10	0.173	9.35	15.15	1.14		
12 - 18	15	0.116	10.33	16.74	0.69		
18 - 22	20	0.051	9.28	15.05	0.34		
22 - 28	25	0.030	8.98	14.55	0.21		
28 - 36	32	0.008	10.56	17.11	0.05		
36 - 44	40	0.003	8.37	13.56	0.02		
44 - 56	50	0.013	9.73	15.77	0.08		

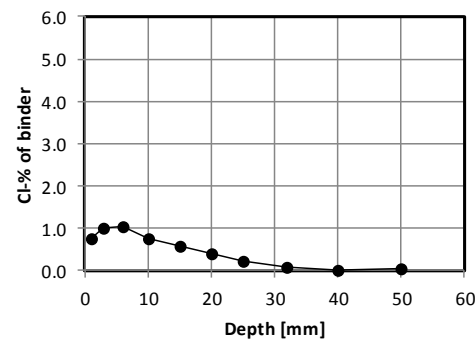
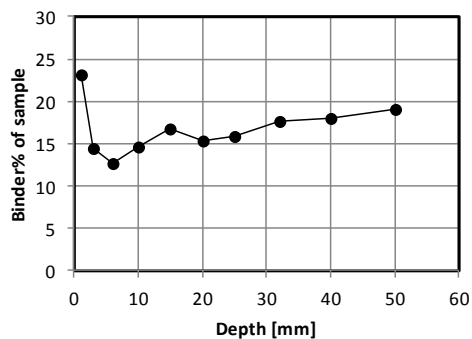
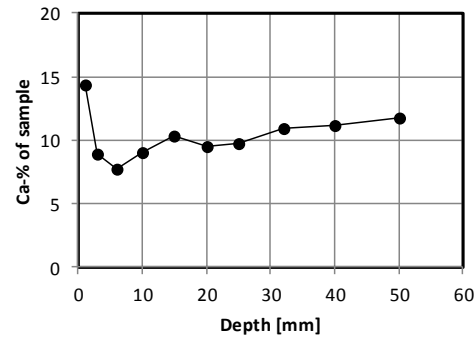
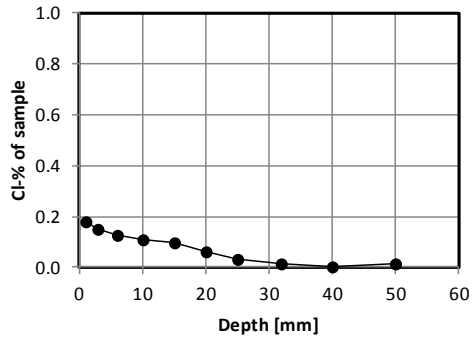


Measurement of chloride ingress in concrete

Concrete ID: 5-40-Sa	Type of binder: 95%Anl+5%SF
Casting date: 1992-01-27	w/b: 0.35
Exposure date: 1992-02-05	Exposure zone: Splash, Sa
Sampling date: 2012-10-02	Profiling method: Grinding on a lathe
Tested by: LJ, LG, NS	Chloride analysis: Potentiometric titration
Tested date: 2013-06-10	Calcium analysis: Potentiometric titration

Raw data and calculations

Exposure duration:		7545 days		CaO% binder:		61.7 %	
Depth from - to (mm)	Mean depth (mm)	Cl% of sample	CaO% of sample	Binder% of sample	Cl% of binder		
0 - 2	1	0.178	14.30	23.18	0.77		
2 - 4	3	0.148	8.91	14.43	1.03		
4 - 8	6	0.130	7.79	12.63	1.03		
8 - 12	10	0.111	9.02	14.62	0.76		
12 - 18	15	0.097	10.30	16.69	0.58		
18 - 22	20	0.063	9.48	15.37	0.41		
22 - 28	25	0.034	9.80	15.88	0.21		
28 - 36	32	0.017	10.92	17.71	0.10		
36 - 44	40	0.005	11.13	18.04	0.03		
44 - 56	50	0.012	11.72	18.99	0.06		

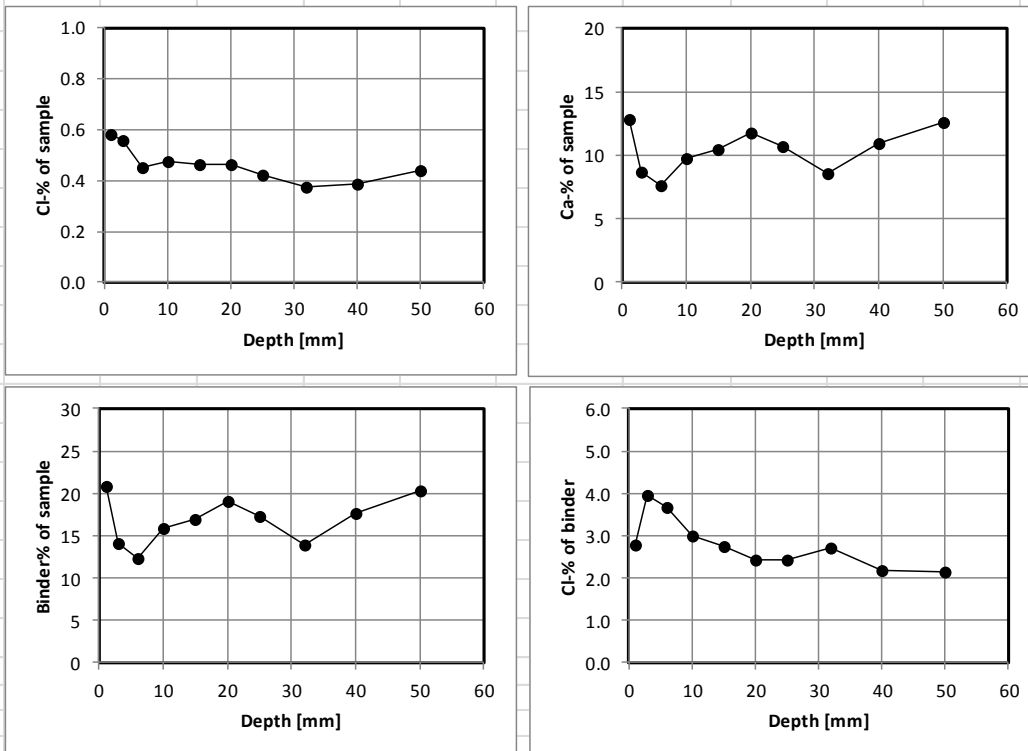


Measurement of chloride ingress in concrete

Concrete ID: 5-40-Sa	Type of binder: 95%Anl+5%SF
Casting date: 1992-01-27	w/b: 0.35
Exposure date: 1992-02-05	Exposure zone: Splash, Su
Sampling date: 2012-10-02	Profiling method: Grinding on a lathe
Tested by: LJ, LG, NS	Chloride analysis: Potentiometric titration
Tested date: 2013-06-11	Calcium analysis: Potentiometric titration

Raw data and calculations

Exposure duration:		7545 days		CaO% binder:		61.7 %	
Depth from - to (mm)	Mean depth (mm)	Cl% of sample	CaO% of sample	Binder% of sample	Cl% of binder		
0 - 2	1	0.582	12.84	20.81	2.79		
2 - 4	3	0.558	8.70	14.10	3.96		
4 - 8	6	0.455	7.64	12.38	3.67		
8 - 12	10	0.473	9.75	15.80	2.99		
12 - 18	15	0.466	10.46	16.96	2.75		
18 - 22	20	0.464	11.75	19.05	2.44		
22 - 28	25	0.421	10.70	17.35	2.43		
28 - 36	32	0.376	8.59	13.92	2.70		
36 - 44	40	0.386	10.92	17.70	2.18		
44 - 56	50	0.438	12.58	20.38	2.15		

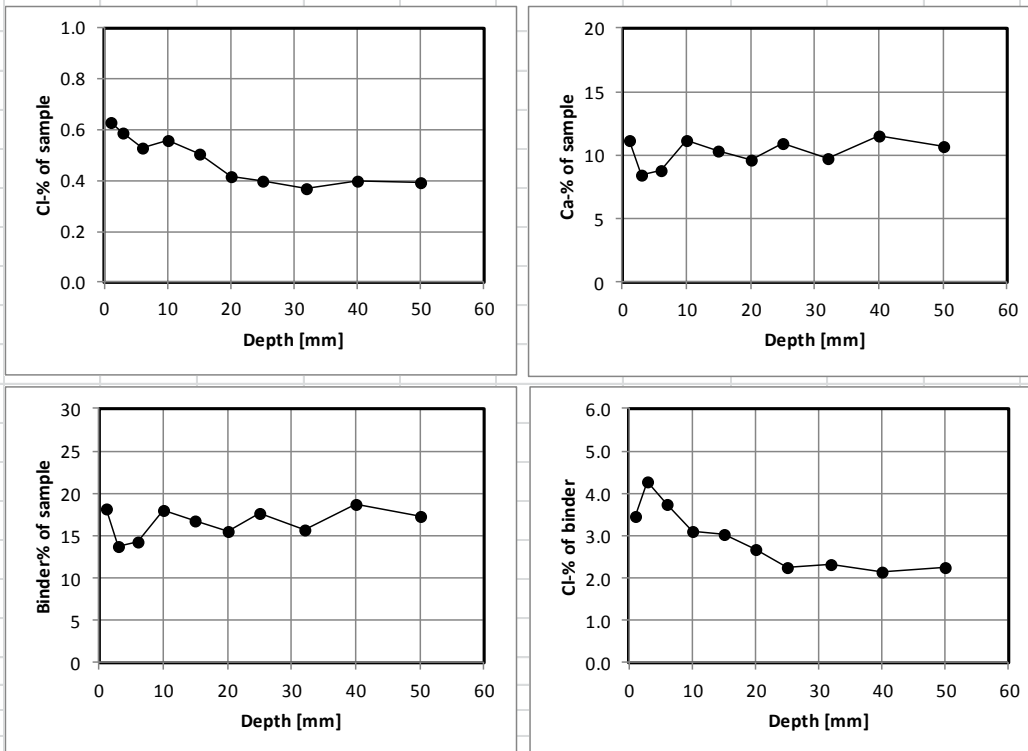


Measurement of chloride ingress in concrete

Concrete ID: 5-40-U	Type of binder: 95%AnI+5%SF
Casting date: 1992-01-27	w/b: 0.35
Exposure date: 1992-02-05	Exposure zone: Submerged
Sampling date: 2012-10-02	Profiling method: Grinding on a lathe
Tested by: LJ, LG, NS	Chloride analysis: Potentiometric titration
Tested date: 2013-06-11	Calcium analysis: Potentiometric titration

Raw data and calculations

Exposure duration:		7545 days		CaO% binder:		61.7 %	
Depth from - to (mm)	Mean depth (mm)	Cl% of sample	CaO% of sample	Binder% of sample	Cl% of binder		
0 - 2	1	0.629	11.22	18.18	3.46		
2 - 4	3	0.591	8.50	13.77	4.29		
4 - 8	6	0.530	8.76	14.21	3.73		
8 - 12	10	0.556	11.12	18.02	3.09		
12 - 18	15	0.508	10.36	16.80	3.02		
18 - 22	20	0.419	9.61	15.58	2.69		
22 - 28	25	0.402	10.93	17.71	2.27		
28 - 36	32	0.368	9.69	15.71	2.34		
36 - 44	40	0.399	11.52	18.67	2.13		
44 - 56	50	0.392	10.70	17.34	2.26		

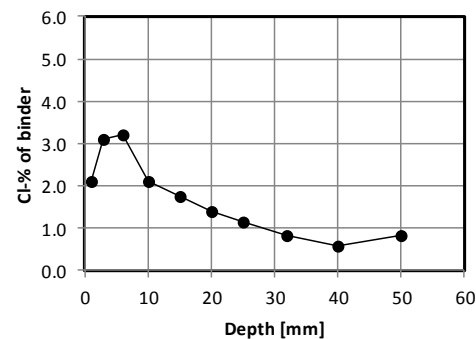
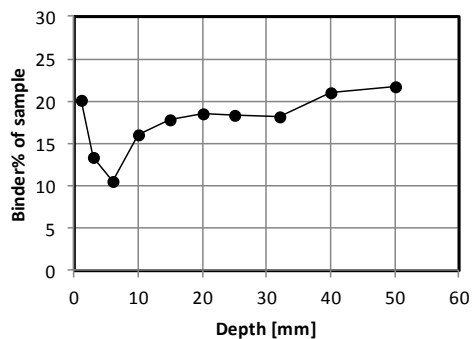
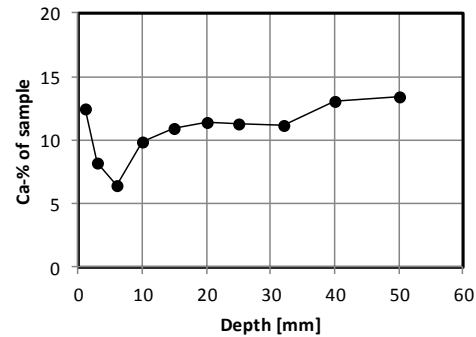
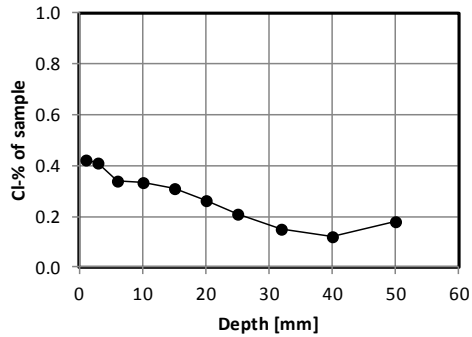


Measurement of chloride ingress in concrete

Concrete ID: 6-35-U	Type of binder: 95%AnI+5%SF
Casting date: 1992-01-25	w/b: 0.35
Exposure date: 1992-03-16	Exposure zone: Submerged
Sampling date: 2012-10-02	Profiling method: Grinding on a lathe
Tested by: LJ, LG	Chloride analysis: Potentiometric titration
Tested date: 2013-06-12	Calcium analysis: Potentiometric titration

Raw data and calculations

Exposure duration:		7505 days		CaO% binder:		61.7 %	
Depth from - to (mm)	Mean depth (mm)	Cl% of sample	CaO% of sample	Binder% of sample	Cl% of binder		
0	2	1	0.424	12.41	20.12	2.11	
2	4	3	0.411	8.22	13.32	3.09	
4	8	6	0.338	6.50	10.53	3.21	
8	12	10	0.337	9.88	16.01	2.10	
12	18	15	0.313	10.95	17.75	1.76	
18	22	20	0.261	11.45	18.56	1.40	
22	28	25	0.212	11.27	18.27	1.16	
28	36	32	0.153	11.16	18.09	0.84	
36	44	40	0.121	13.01	21.09	0.57	
44	56	50	0.177	13.40	21.72	0.82	

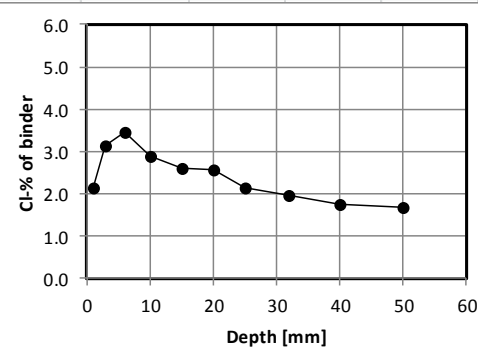
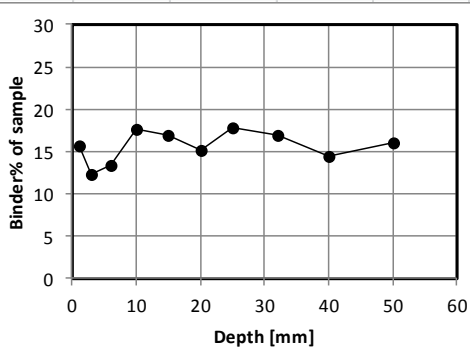
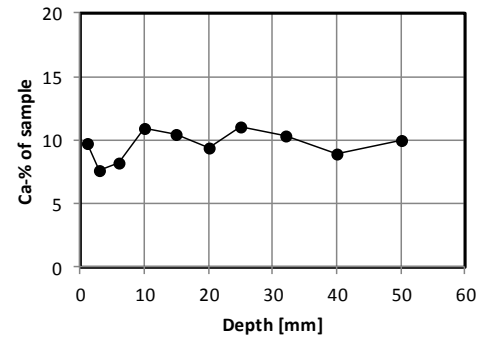
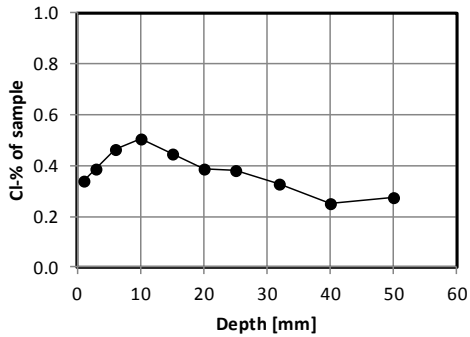


Measurement of chloride ingress in concrete

Concrete ID: 6-40-U	Type of binder: 95%Anl+5%SF
Casting date: 1992-01-25	w/b: 0.4
Exposure date: 1992-03-16	Exposure zone: Submerged
Sampling date: 2012-10-02	Profiling method: Grinding on a lathe
Tested by: LJ, LG	Chloride analysis: Potentiometric titration
Tested date: 2013-06-12	Calcium analysis: Potentiometric titration

Raw data and calculations

Exposure duration:		7505 days		CaO% binder:		61.7 %	
Depth from	- to (mm)	Mean depth (mm)	Cl% of sample	CaO% of sample	Binder% of sample	Cl% of binder	
0	2	1	0.340	9.72	15.75	2.16	
2	4	3	0.387	7.58	12.29	3.15	
4	8	6	0.462	8.23	13.33	3.47	
8	12	10	0.508	10.88	17.64	2.88	
12	18	15	0.443	10.45	16.94	2.62	
18	22	20	0.389	9.38	15.20	2.56	
22	28	25	0.383	11.02	17.86	2.14	
28	36	32	0.330	10.40	16.86	1.96	
36	44	40	0.253	8.88	14.40	1.76	
44	56	50	0.273	9.93	16.10	1.70	

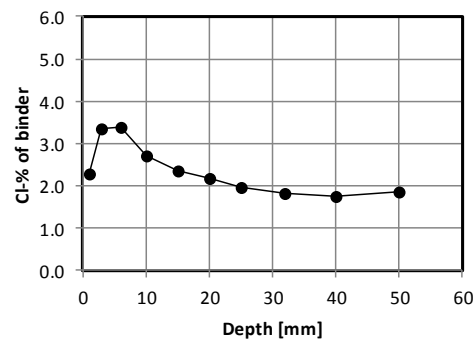
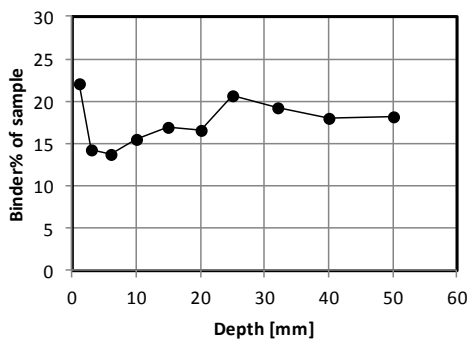
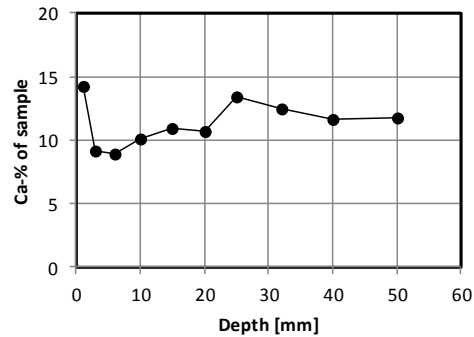
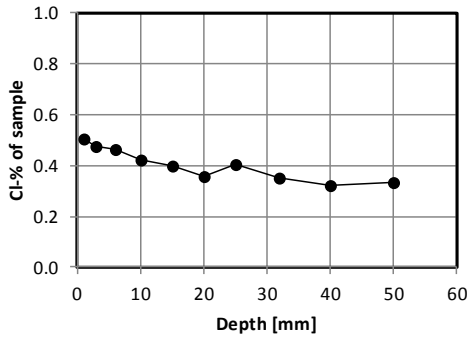


Measurement of chloride ingress in concrete

Concrete ID: 7-35-U	Type of binder: 100%Anl.
Casting date: 1992-01-25	w/b: 0.35
Exposure date: 1992-03-16	Exposure zone: Submerged
Sampling date: 2012-10-02	Profiling method: Grinding on a lathe
Tested by: LJ, LG	Chloride analysis: Potentiometric titration
Tested date: 2013-06-13	Calcium analysis: Potentiometric titration

Raw data and calculations

Exposure duration:		7505 days		CaO% binder:		64.9 %	
Depth from - to (mm)	Mean depth (mm)	Cl% of sample	CaO% of sample	Binder% of sample	Cl% of binder		
0 - 2	1	0.504	14.29	22.01	2.29		
2 - 4	3	0.477	9.22	14.20	3.36		
4 - 8	6	0.462	8.88	13.68	3.38		
8 - 12	10	0.421	10.12	15.60	2.70		
12 - 18	15	0.399	10.99	16.93	2.36		
18 - 22	20	0.359	10.75	16.57	2.17		
22 - 28	25	0.405	13.41	20.67	1.96		
28 - 36	32	0.352	12.45	19.18	1.83		
36 - 44	40	0.319	11.70	18.03	1.77		
44 - 56	50	0.336	11.78	18.15	1.85		

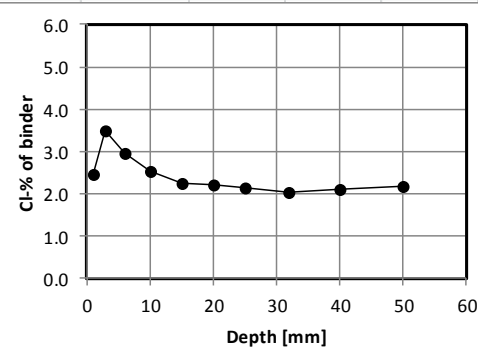
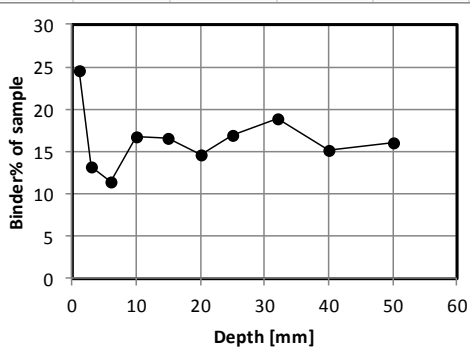
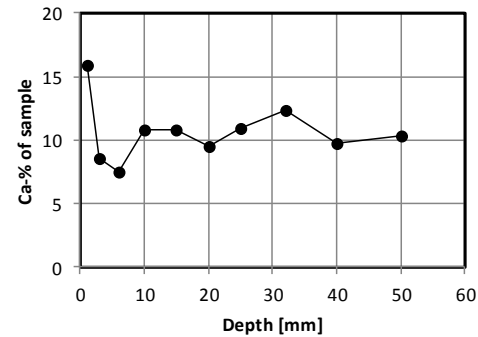
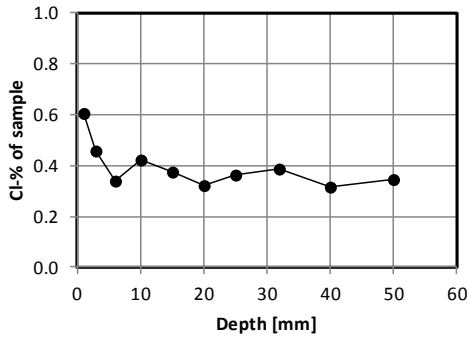


Measurement of chloride ingress in concrete

Concrete ID: 7-40-U	Type of binder: 100%Anl.
Casting date: 1992-01-25	w/b: 0.4
Exposure date: 1992-03-16	Exposure zone: Submerged
Sampling date: 2012-10-02	Profiling method: Grinding on a lathe
Tested by: LJ, NS	Chloride analysis: Potentiometric titration
Tested date: 2013-06-18	Calcium analysis: Potentiometric titration

Raw data and calculations

Exposure duration:		7505 days		CaO% binder:		64.9 %	
Depth from	- to (mm)	Mean depth (mm)	Cl% of sample	CaO% of sample	Binder% of sample	Cl% of binder	
0	2	1	0.608	15.91	24.51	2.48	
2	4	3	0.458	8.54	13.15	3.48	
4	8	6	0.339	7.45	11.48	2.95	
8	12	10	0.422	10.87	16.75	2.52	
12	18	15	0.377	10.79	16.63	2.27	
18	22	20	0.323	9.46	14.58	2.21	
22	28	25	0.365	10.98	16.92	2.16	
28	36	32	0.387	12.31	18.96	2.04	
36	44	40	0.317	9.79	15.09	2.10	
44	56	50	0.348	10.39	16.01	2.17	

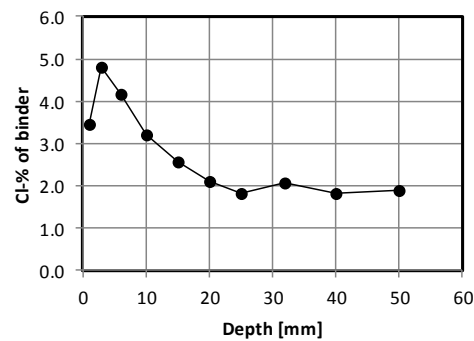
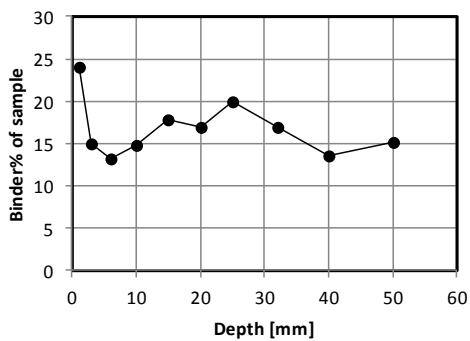
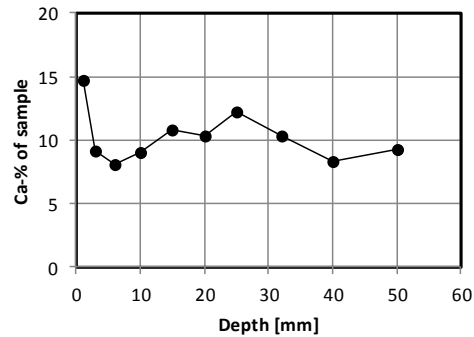
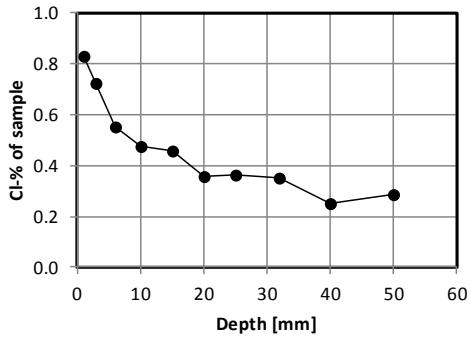


Measurement of chloride ingress in concrete

Concrete ID: 8-35-U	Type of binder: 100%Slite
Casting date: 1992-12-03	w/b: 0.35
Exposure date: 1992-12-19	Exposure zone: Submerged
Sampling date: 2012-10-02	Profiling method: Grinding on a lathe
Tested by: LJ, NS	Chloride analysis: Potentiometric titration
Tested date: 2013-06-18	Calcium analysis: Potentiometric titration

Raw data and calculations

Exposure duration: 7227 days			CaO% binder: 61.1 %			
Depth from - to (mm)	Mean depth (mm)	Cl% of sample	CaO% of sample	Binder% of sample	Cl% of binder	
0	2	1	0.831	14.70	24.06	3.45
2	4	3	0.723	9.20	15.06	4.80
4	8	6	0.554	8.09	13.25	4.18
8	12	10	0.476	9.09	14.87	3.20
12	18	15	0.460	10.87	17.79	2.59
18	22	20	0.357	10.34	16.92	2.11
22	28	25	0.365	12.23	20.01	1.82
28	36	32	0.349	10.32	16.89	2.07
36	44	40	0.249	8.28	13.55	1.84
44	56	50	0.287	9.26	15.16	1.89

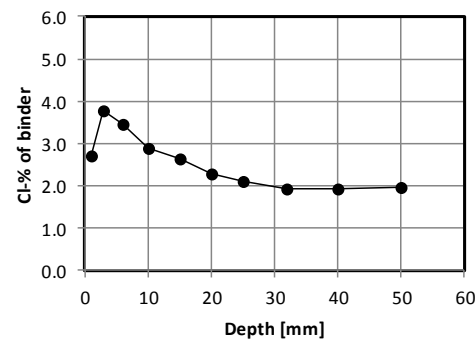
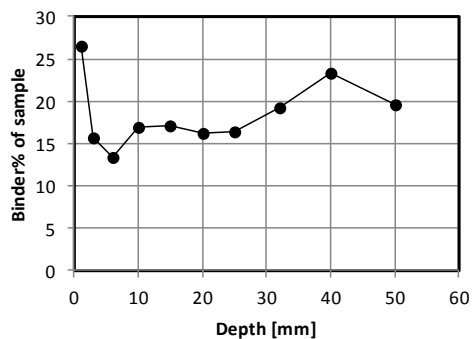
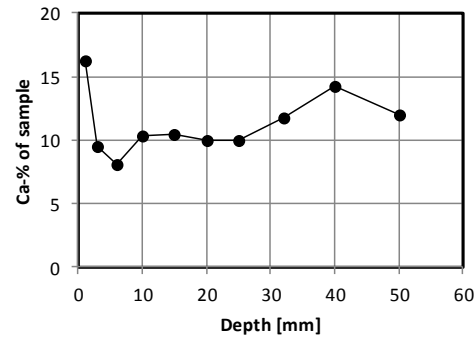
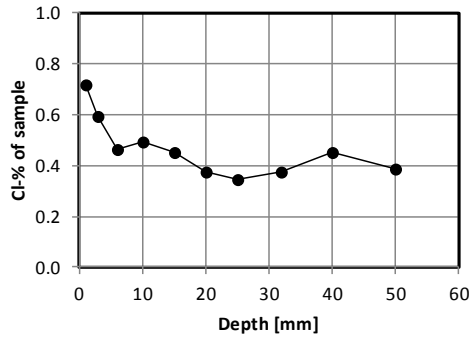


Measurement of chloride ingress in concrete

Concrete ID: 8-40-U	Type of binder: 100%Slite
Casting date: 1992-12-03	w/b: 0.4
Exposure date: 1992-12-19	Exposure zone: Submerged
Sampling date: 2012-10-02	Profiling method: Grinding on a lathe
Tested by: LG, IM	Chloride analysis: Potentiometric titration
Tested date: 2013-06-18	Calcium analysis: Potentiometric titration

Raw data and calculations

Exposure duration:		7227 days		CaO% binder:		61.1 %	
Depth from - to (mm)	Mean depth (mm)	Cl% of sample	CaO% of sample	Binder% of sample	Cl% of binder		
0	2	1	0.717	16.20	26.51	2.70	
2	4	3	0.593	9.55	15.62	3.79	
4	8	6	0.462	8.15	13.34	3.47	
8	12	10	0.491	10.39	17.01	2.89	
12	18	15	0.449	10.46	17.11	2.63	
18	22	20	0.374	9.95	16.28	2.30	
22	28	25	0.344	10.01	16.39	2.10	
28	36	32	0.376	11.79	19.29	1.95	
36	44	40	0.451	14.22	23.28	1.94	
44	56	50	0.386	11.98	19.61	1.97	

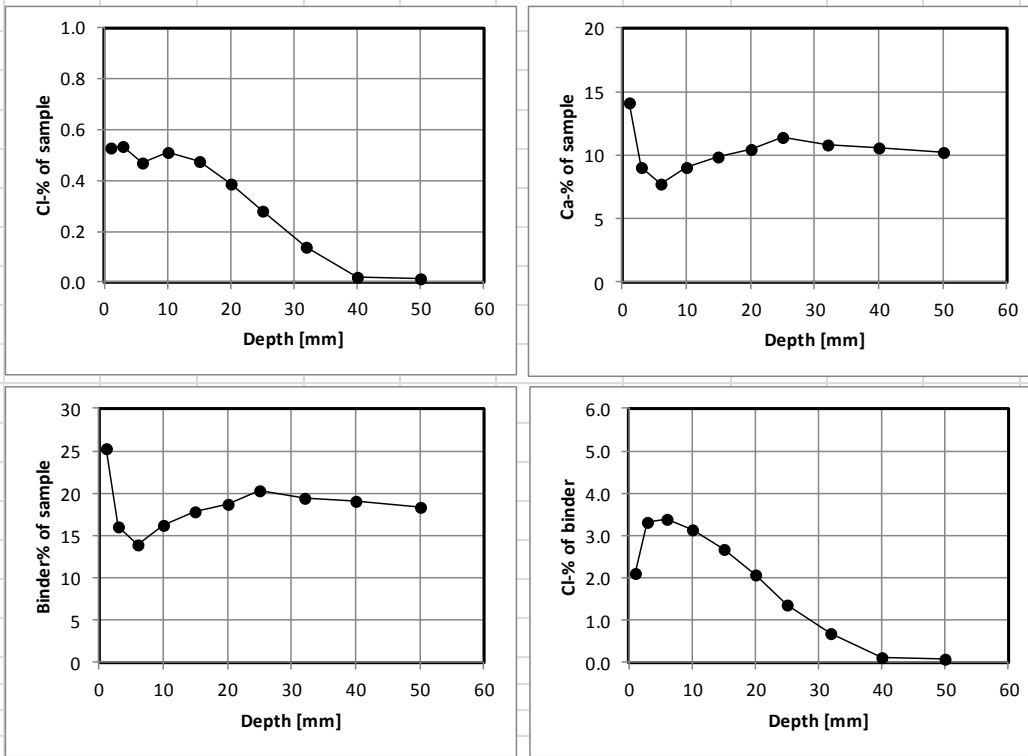


Measurement of chloride ingress in concrete

Concrete ID: 12-35-U	Type of binder: 85%Anl+10%FA+5%SF
Casting date: 1992-02-26	w/b: 0.35
Exposure date: 1992-03-16	Exposure zone: Submerged
Sampling date: 2012-10-02	Profiling method: Grinding on a lathe
Tested by: LG, IM	Chloride analysis: Potentiometric titration
Tested date: 2013-06-13	Calcium analysis: Potentiometric titration

Raw data and calculations

Exposure duration:		7505 days		CaO% binder:		55.7 %	
Depth from - to (mm)	Mean depth (mm)	Cl% of sample	CaO% of sample	Binder% of sample	Cl% of binder		
0	2	1	0.530	14.07	25.26	2.10	
2	4	3	0.535	8.99	16.13	3.32	
4	8	6	0.469	7.74	13.89	3.37	
8	12	10	0.512	9.05	16.26	3.15	
12	18	15	0.478	9.91	17.80	2.69	
18	22	20	0.387	10.44	18.74	2.06	
22	28	25	0.279	11.35	20.38	1.37	
28	36	32	0.137	10.80	19.38	0.71	
36	44	40	0.021	10.59	19.01	0.11	
44	56	50	0.017	10.19	18.29	0.09	

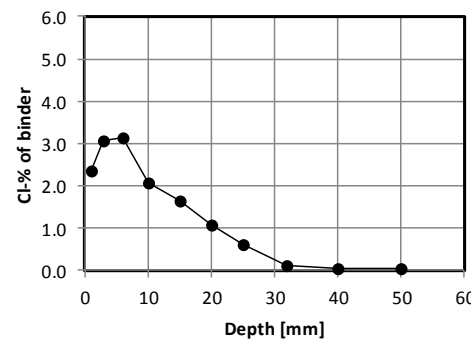
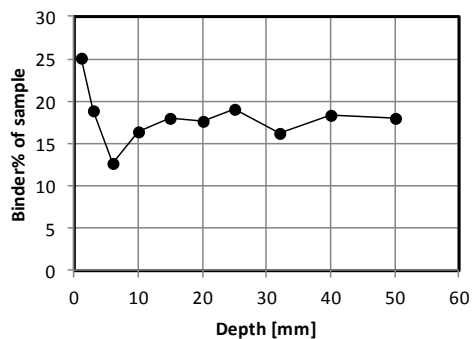
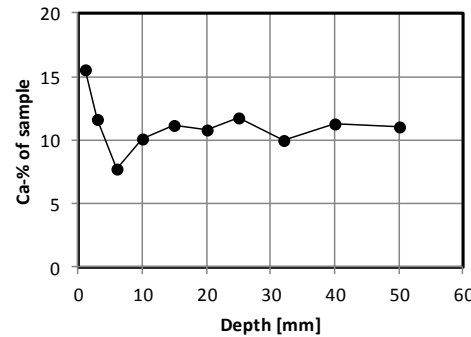
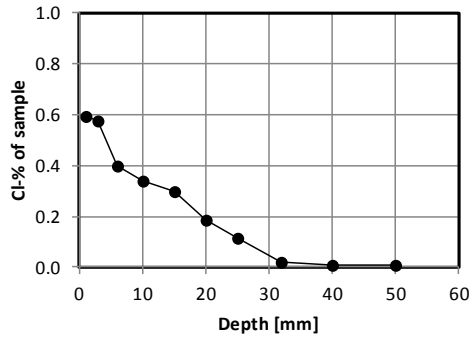


Measurement of chloride ingress in concrete

Concrete ID: H1-U	Type of binder: 95%AnI+5%SF
Casting date: 1992-04-02	w/b: 0.3
Exposure date: 1992-04-14	Exposure zone: Submerged
Sampling date: 2012-10-02	Profiling method: Grinding on a lathe
Tested by: LG, JW	Chloride analysis: Potentiometric titration
Tested date: 2013-06-25	Calcium analysis: Potentiometric titration

Raw data and calculations

Exposure duration:		7476 days		CaO% binder:		61.7 %	
Depth from - to (mm)	Mean depth (mm)	Cl% of sample	CaO% of sample	Binder% of sample	Cl% of binder		
0 - 2	1	0.592	15.52	25.16	2.36		
2 - 4	3	0.579	11.69	18.94	3.06		
4 - 8	6	0.398	7.80	12.64	3.14		
8 - 12	10	0.339	10.09	16.35	2.07		
12 - 18	15	0.297	11.14	18.05	1.65		
18 - 22	20	0.188	10.84	17.57	1.07		
22 - 28	25	0.116	11.80	19.13	0.61		
28 - 36	32	0.023	10.01	16.22	0.14		
36 - 44	40	0.010	11.30	18.31	0.06		
44 - 56	50	0.011	11.06	17.93	0.06		

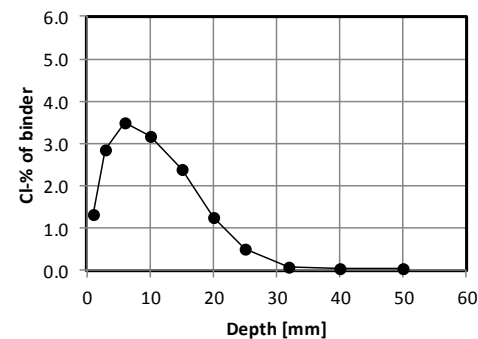
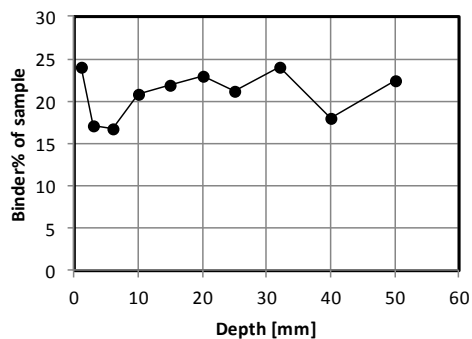
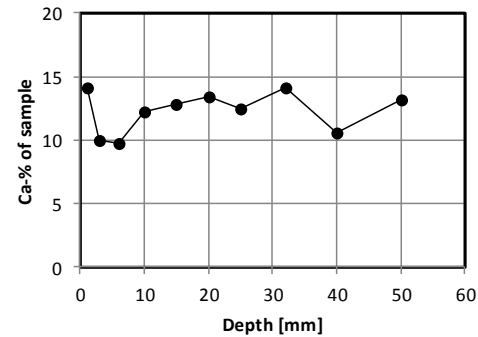
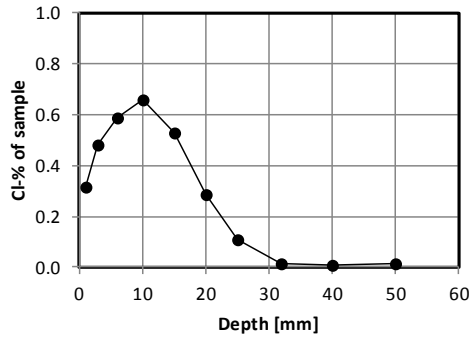


Measurement of chloride ingress in concrete

Concrete ID: H2-U	Type of binder: 90%Anl+10%SF
Casting date: 1992-04-02	w/b: 0.3
Exposure date: 1992-04-14	Exposure zone: Submerged
Sampling date: 2012-10-02	Profiling method: Grinding on a lathe
Tested by: LG, JW, NS	Chloride analysis: Potentiometric titration
Tested date: 2013-06-25	Calcium analysis: Potentiometric titration

Raw data and calculations

Exposure duration:		7476 days		CaO% binder:		58.6 %	
Depth from - to (mm)	Mean depth (mm)	Cl% of sample	CaO% of sample	Binder% of sample	Cl% of binder		
0	2	1	0.318	14.12	24.10	1.32	
2	4	3	0.484	9.98	17.03	2.84	
4	8	6	0.586	9.79	16.70	3.51	
8	12	10	0.661	12.18	20.79	3.18	
12	18	15	0.526	12.83	21.89	2.41	
18	22	20	0.288	13.43	22.91	1.26	
22	28	25	0.110	12.42	21.19	0.52	
28	36	32	0.018	14.09	24.04	0.07	
36	44	40	0.012	10.60	18.08	0.06	
44	56	50	0.014	13.19	22.52	0.06	

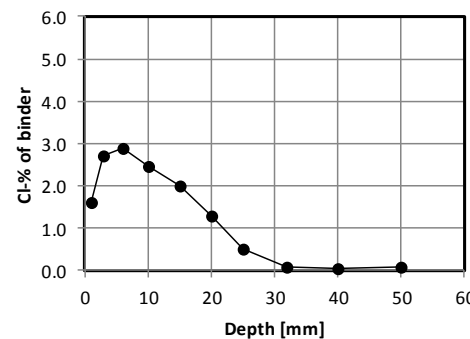
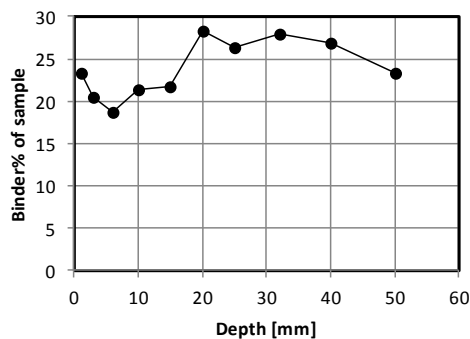
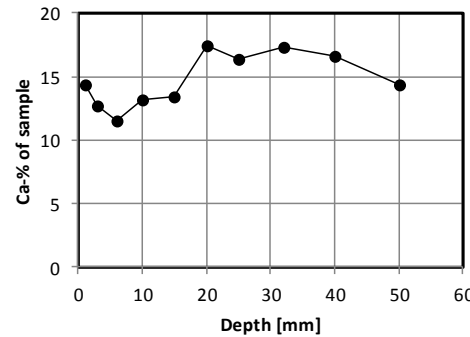
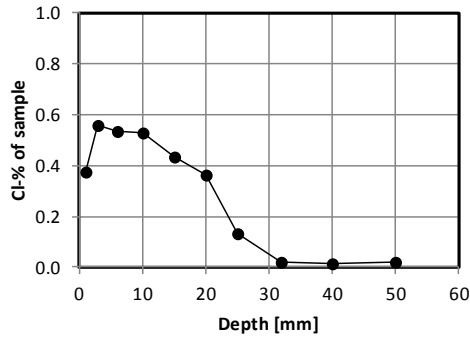


Measurement of chloride ingress in concrete

Concrete ID: H5-U	Type of binder: 95%Anl+5%SF
Casting date: 1992-04-02	w/b: 0.25
Exposure date: 1992-04-14	Exposure zone: Submerged
Sampling date: 2012-10-02	Profiling method: Grinding on a lathe
Tested by: LG, JW, NS	Chloride analysis: Potentiometric titration
Tested date: 2013-06-25	Calcium analysis: Potentiometric titration

Raw data and calculations

Exposure duration:		7476 days		CaO% binder:		61.9 %	
Depth from - to (mm)	Mean depth (mm)	Cl% of sample	CaO% of sample	Binder% of sample	Cl% of binder		
0 - 2	1	0.375	14.41	23.28	1.61		
2 - 4	3	0.558	12.67	20.47	2.72		
4 - 8	6	0.537	11.56	18.67	2.87		
8 - 12	10	0.526	13.23	21.37	2.46		
12 - 18	15	0.434	13.46	21.74	1.99		
18 - 22	20	0.363	17.48	28.23	1.28		
22 - 28	25	0.134	16.34	26.40	0.51		
28 - 36	32	0.023	17.31	27.97	0.08		
36 - 44	40	0.013	16.62	26.85	0.05		
44 - 56	50	0.018	14.41	23.28	0.08		

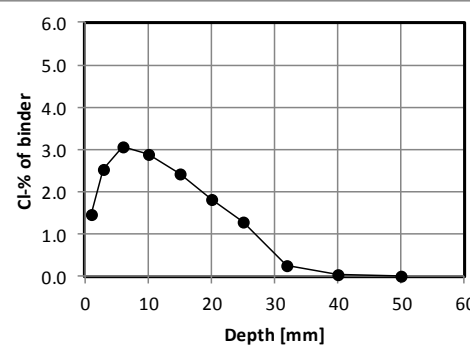
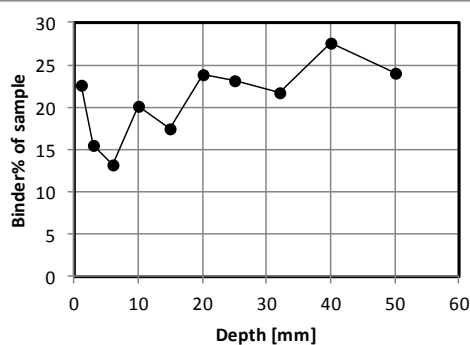
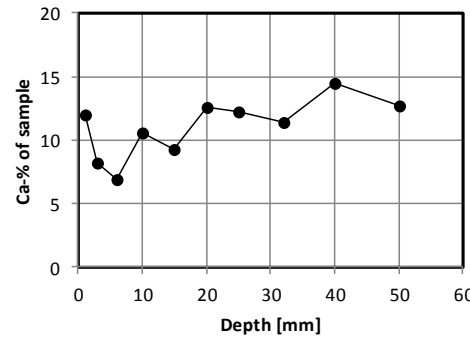
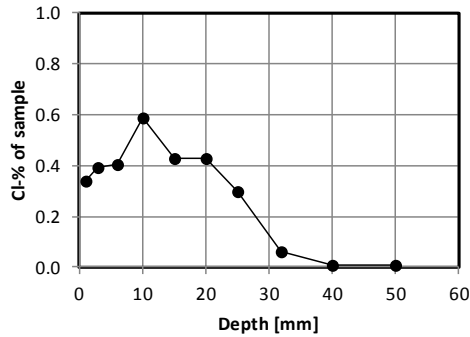


Measurement of chloride ingress in concrete

Concrete ID: H8-U	Type of binder: 80%AnI+20%SF
Casting date: 1992-04-02	w/b: 0.3
Exposure date: 1992-04-14	Exposure zone: Submerged
Sampling date: 2012-10-02	Profiling method: Grinding on a lathe
Tested by: LG, JW, LJ	Chloride analysis: Potentiometric titration
Tested date: 2013-06-28	Calcium analysis: Potentiometric titration

Raw data and calculations

Exposure duration:		7476 days		CaO% binder:		52.7 %	
Depth from - to (mm)	Mean depth (mm)	Cl% of sample	CaO% of sample	Binder% of sample	Cl% of binder		
0 - 2	1	0.338	11.96	22.69	1.49		
2 - 4	3	0.393	8.20	15.56	2.53		
4 - 8	6	0.405	6.95	13.19	3.07		
8 - 12	10	0.585	10.61	20.13	2.91		
12 - 18	15	0.427	9.24	17.54	2.43		
18 - 22	20	0.431	12.56	23.83	1.81		
22 - 28	25	0.300	12.18	23.12	1.30		
28 - 36	32	0.060	11.46	21.75	0.27		
36 - 44	40	0.011	14.53	27.57	0.04		
44 - 56	50	0.008	12.67	24.03	0.03		

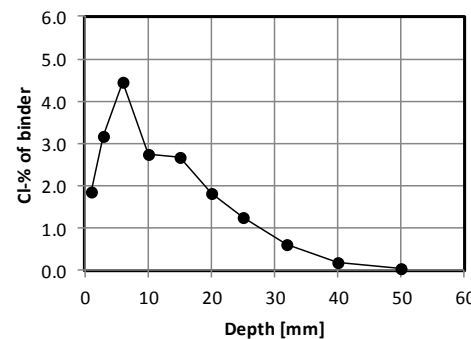
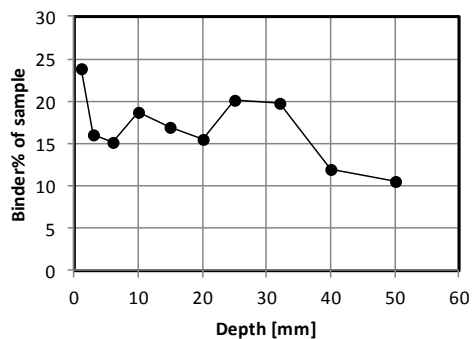
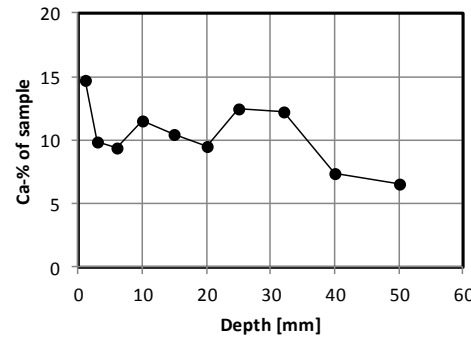
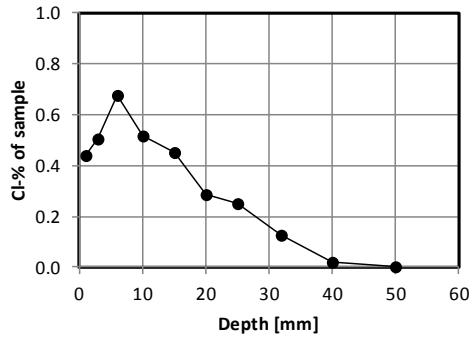


Measurement of chloride ingress in concrete

Concrete ID: H1-Air-30-5	Type of binder: 95%Anl+5%SF
Casting date: 1993-05-10	w/b: 0.3
Exposure date: 1993-06-04	Exposure zone: Submerged
Sampling date: 2012-10-02	Profiling method: Grinding on a lathe
Tested by: LG, NS	Chloride analysis: Potentiometric titration
Tested date: 2013-06-20	Calcium analysis: Potentiometric titration

Raw data and calculations

Exposure duration:		7060 days		CaO% binder:		61.7 %	
Depth from - to (mm)	Mean depth (mm)	Cl% of sample	CaO% of sample	Binder% of sample	Cl% of binder		
0 - 2	1	0.439	14.67	23.77	1.85		
2 - 4	3	0.506	9.85	15.97	3.17		
4 - 8	6	0.676	9.39	15.22	4.44		
8 - 12	10	0.515	11.51	18.66	2.76		
12 - 18	15	0.452	10.46	16.96	2.67		
18 - 22	20	0.285	9.53	15.45	1.84		
22 - 28	25	0.253	12.43	20.14	1.26		
28 - 36	32	0.125	12.18	19.73	0.63		
36 - 44	40	0.022	7.39	11.97	0.19		
44 - 56	50	0.005	6.52	10.57	0.05		

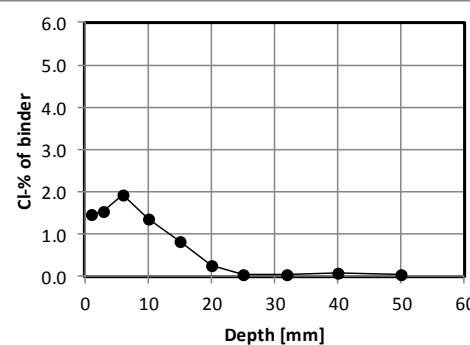
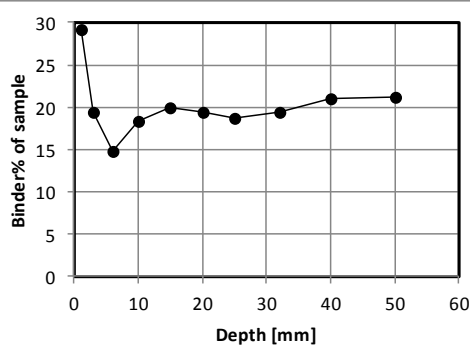
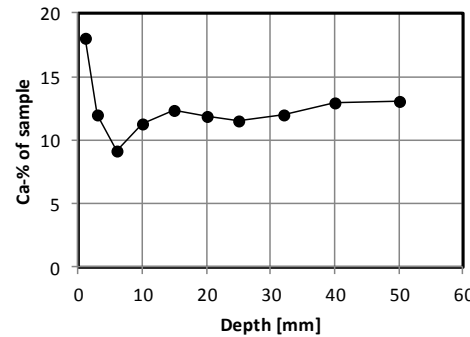
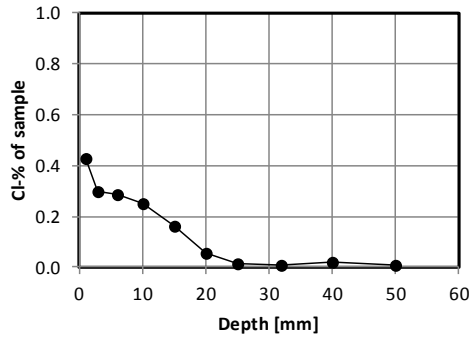


Measurement of chloride ingress in concrete

Concrete ID: H1-Air-35-5	Type of binder: 95%Anl+5%SF
Casting date: 1993-05-10	w/b: 0.35
Exposure date: 1993-06-04	Exposure zone: Atmospheric
Sampling date: 2012-10-02	Profiling method: Grinding on a lathe
Tested by: LG, NS	Chloride analysis: Potentiometric titration
Tested date: 2013-06-20	Calcium analysis: Potentiometric titration

Raw data and calculations

Exposure duration:		7060 days		CaO% binder:		61.7 %	
Depth from - to (mm)	Mean depth (mm)	Cl% of sample	CaO% of sample	Binder% of sample	Cl% of binder		
0 - 2	1	0.431	17.98	29.15	1.48		
2 - 4	3	0.299	11.98	19.42	1.54		
4 - 8	6	0.288	9.13	14.80	1.95		
8 - 12	10	0.249	11.30	18.31	1.36		
12 - 18	15	0.165	12.30	19.94	0.83		
18 - 22	20	0.054	11.93	19.34	0.28		
22 - 28	25	0.012	11.57	18.75	0.07		
28 - 36	32	0.007	11.98	19.41	0.04		
36 - 44	40	0.019	12.97	21.02	0.09		
44 - 56	50	0.010	13.11	21.24	0.05		

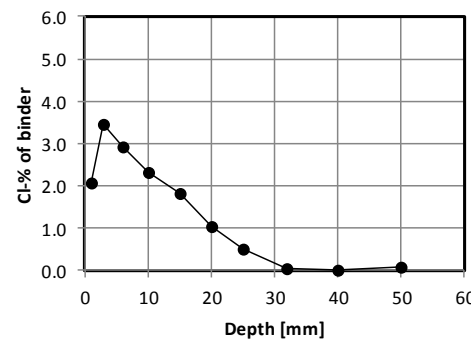
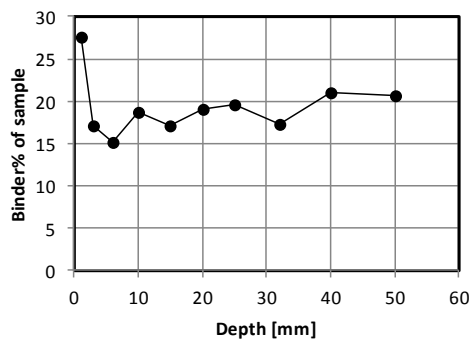
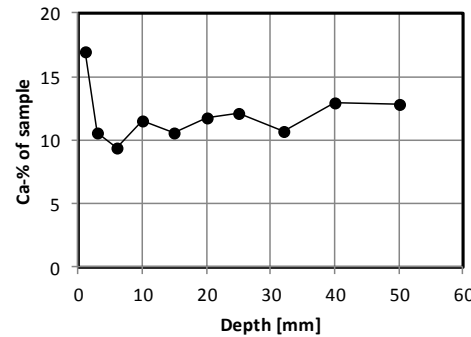
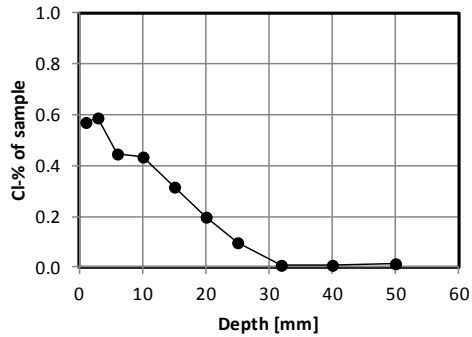


Measurement of chloride ingress in concrete

Concrete ID: H1-Air-35-5	Type of binder: 95%AnI+5%SF
Casting date: 1993-05-10	w/b: 0.35
Exposure date: 1993-06-04	Exposure zone: Splash
Sampling date: 2012-10-02	Profiling method: Grinding on a lathe
Tested by: LG, NS	Chloride analysis: Potentiometric titration
Tested date: 2013-06-20	Calcium analysis: Potentiometric titration

Raw data and calculations

Exposure duration:		7060 days		CaO% binder:		61.7 %	
Depth from - to (mm)	Mean depth (mm)	Cl% of sample	CaO% of sample	Binder% of sample	Cl% of binder		
0	2	1	0.571	16.97	27.51	2.08	
2	4	3	0.588	10.53	17.06	3.45	
4	8	6	0.444	9.41	15.24	2.91	
8	12	10	0.436	11.56	18.73	2.33	
12	18	15	0.315	10.55	17.11	1.84	
18	22	20	0.200	11.76	19.07	1.05	
22	28	25	0.099	12.08	19.58	0.51	
28	36	32	0.011	10.72	17.37	0.06	
36	44	40	0.007	12.95	21.00	0.03	
44	56	50	0.018	12.77	20.70	0.09	

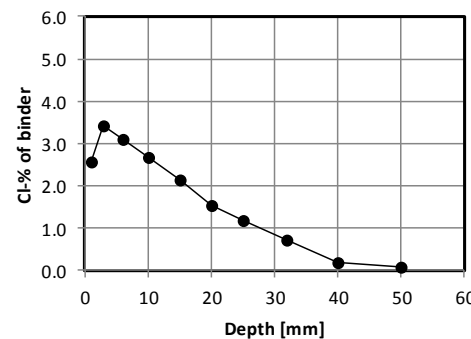
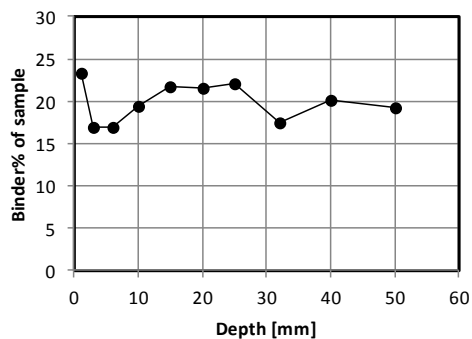
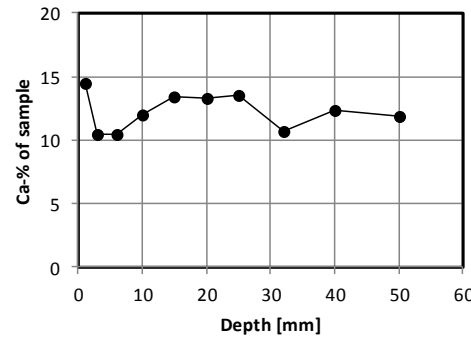
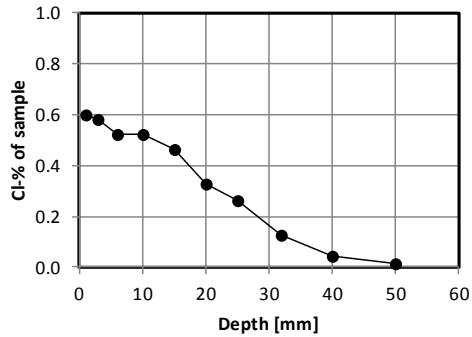


Measurement of chloride ingress in concrete

Concrete ID: H1-Air-35-5	Type of binder: 95%AnI+5%SF
Casting date: 1993-05-10	w/b: 0.35
Exposure date: 1993-06-04	Exposure zone: Submerged
Sampling date: 2012-10-02	Profiling method: Grinding on a lathe
Tested by: LG, LJ	Chloride analysis: Potentiometric titration
Tested date: 2013-06-10	Calcium analysis: Potentiometric titration

Raw data and calculations

Exposure duration:		7060 days		CaO% binder:		61.7 %	
Depth from - to (mm)	Mean depth (mm)	Cl% of sample	CaO% of sample	Binder% of sample	Cl% of binder		
0 - 2	1	0.599	14.44	23.40	2.56		
2 - 4	3	0.582	10.44	16.92	3.44		
4 - 8	6	0.522	10.41	16.87	3.10		
8 - 12	10	0.523	12.02	19.49	2.69		
12 - 18	15	0.461	13.38	21.69	2.13		
18 - 22	20	0.327	13.24	21.46	1.53		
22 - 28	25	0.261	13.57	21.99	1.19		
28 - 36	32	0.126	10.74	17.40	0.72		
36 - 44	40	0.042	12.38	20.06	0.21		
44 - 56	50	0.017	11.87	19.24	0.09		

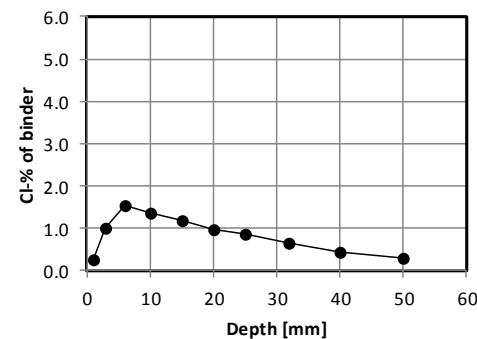
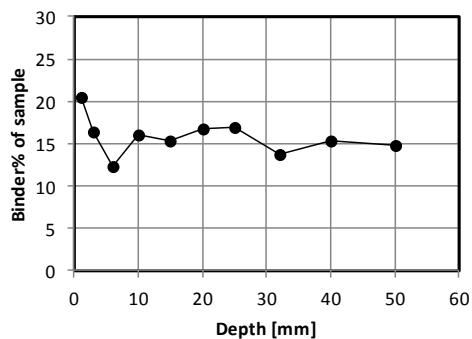
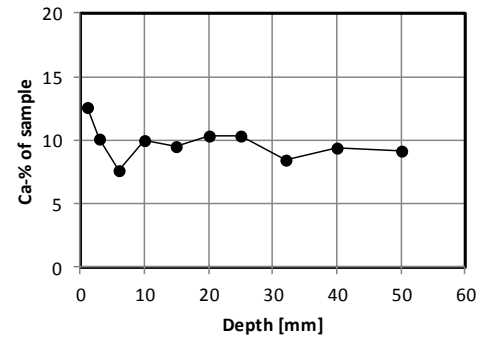
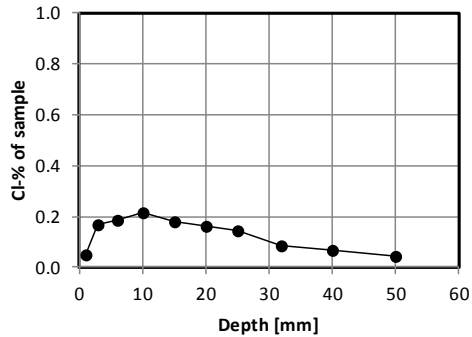


Measurement of chloride ingress in concrete

Concrete ID: H1-Air-50-5	Type of binder: 95%Anl+5%SF
Casting date: 1993-05-13	w/b: 0.5
Exposure date: 1993-06-04	Exposure zone: Atmospheric
Sampling date: 2012-10-02	Profiling method: Grinding on a lathe
Tested by: LG, IM	Chloride analysis: Potentiometric titration
Tested date: 2013-06-19	Calcium analysis: Potentiometric titration

Raw data and calculations

Exposure duration:		7060 days		CaO% binder:		61.7 %	
Depth from - to (mm)	Mean depth (mm)	Cl% of sample	CaO% of sample	Binder% of sample	Cl% of binder		
0 - 2	1	0.052	12.62	20.45	0.26		
2 - 4	3	0.169	10.12	16.40	1.03		
4 - 8	6	0.188	7.57	12.27	1.53		
8 - 12	10	0.218	9.95	16.12	1.35		
12 - 18	15	0.182	9.46	15.33	1.19		
18 - 22	20	0.164	10.30	16.69	0.98		
22 - 28	25	0.143	10.40	16.85	0.85		
28 - 36	32	0.088	8.51	13.79	0.64		
36 - 44	40	0.068	9.43	15.28	0.45		
44 - 56	50	0.043	9.11	14.76	0.29		



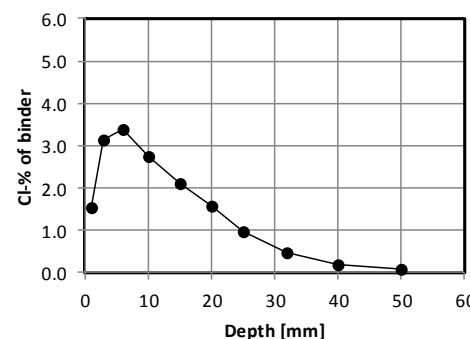
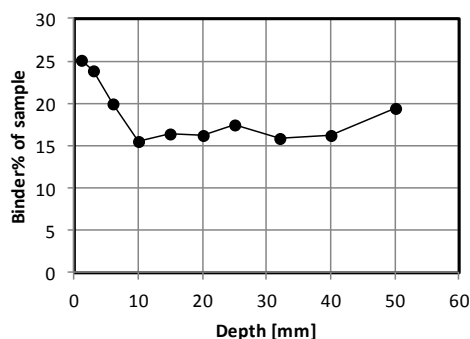
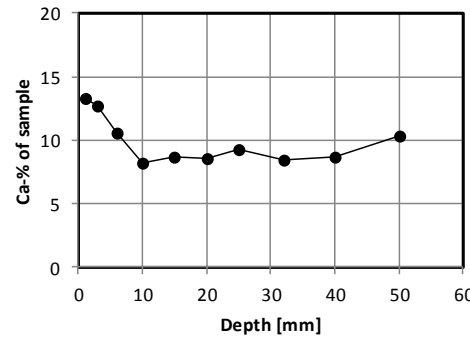
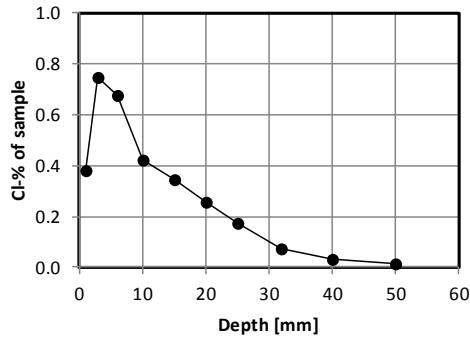
Measurement of chloride ingress in concrete

Concrete ID: 94-1- B	Type of binder: Slagcement
Casting date: 1994-04-26	w/b: 0.35
Exposure date: 1994-05-11	Exposure zone: Submerged
Sampling date: 2012-10-02	Profiling method: Grinding on a lathe
Tested by:	Chloride analysis: Potentiometric titration
Tested date: 2013-06-24	Calcium analysis: Potentiometric titration

Artificial cracks

Raw data and calculations

Exposure duration:		6719 days		CaO% binder:		53.0 %	
Depth from - to (mm)	Mean depth (mm)	Cl% of sample	CaO% of sample	Binder% of sample	Cl% of binder		
0 - 2	1	0.384	13.31	25.11	1.53		
2 - 4	3	0.748	12.68	23.92	3.13		
4 - 8	6	0.675	10.57	19.94	3.38		
8 - 12	10	0.425	8.25	15.57	2.73		
12 - 18	15	0.345	8.65	16.32	2.11		
18 - 22	20	0.254	8.59	16.22	1.57		
22 - 28	25	0.172	9.22	17.40	0.99		
28 - 36	32	0.076	8.46	15.96	0.48		
36 - 44	40	0.031	8.64	16.31	0.19		
44 - 56	50	0.014	10.29	19.41	0.07		

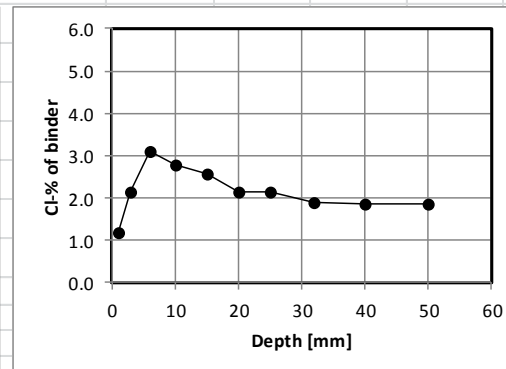
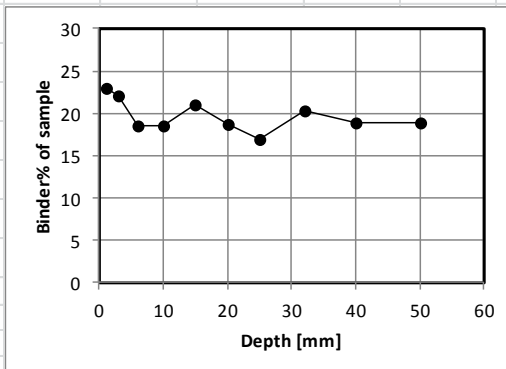
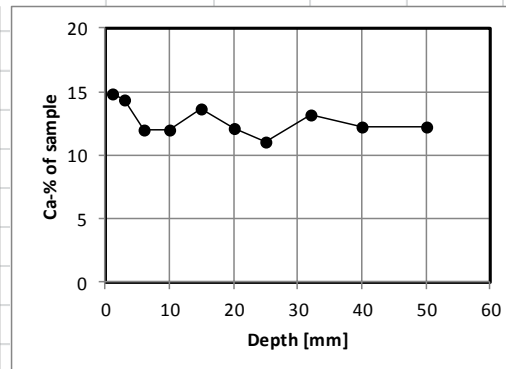
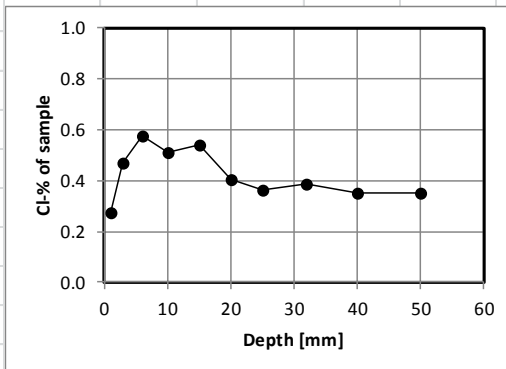


Measurement of chloride ingress in concrete

Concrete ID: 94-2-C	Type of binder: 100% Anl.
Casting date: 1994-04-26	w/b: 0.35
Exposure date: 1994-05-11	Exposure zone: Submerged
Sampling date: 2012-10-02	Profiling method: Grinding on a lathe
Tested by: LJ, LG	Chloride analysis: Potentiometric titration
Tested date: 2013-06-13	Calcium analysis: Potentiometric titration

Raw data and calculations

Exposure duration:		6719 days		CaO% binder:		64.9 %	
Depth from - to (mm)	Mean depth (mm)	Cl% of sample	CaO% of sample	Binder% of sample	Cl% of binder		
0 - 2	1	0.273	14.89	22.94	1.19		
2 - 4	3	0.473	14.31	22.05	2.14		
4 - 8	6	0.578	12.03	18.54	3.12		
8 - 12	10	0.514	12.06	18.58	2.77		
12 - 18	15	0.539	13.69	21.10	2.56		
18 - 22	20	0.404	12.11	18.66	2.16		
22 - 28	25	0.361	11.01	16.97	2.13		
28 - 36	32	0.385	13.16	20.27	1.90		
36 - 44	40	0.353	12.21	18.81	1.88		
44 - 56	50	0.352	12.27	18.91	1.86		

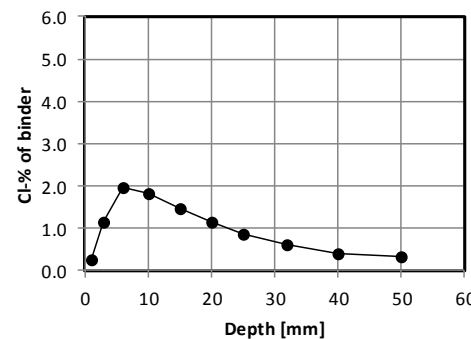
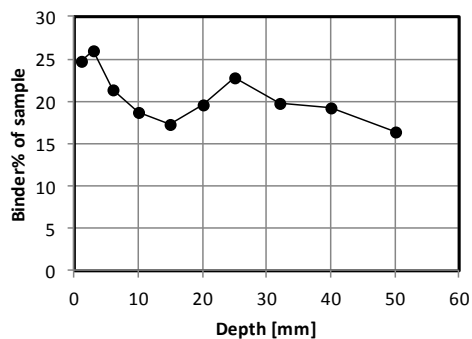
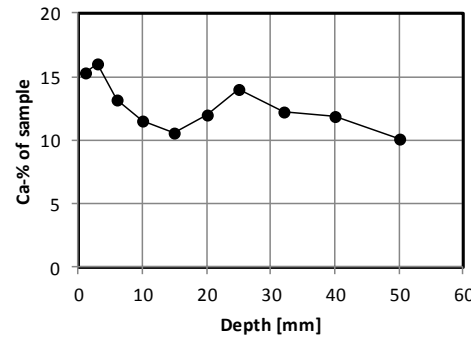
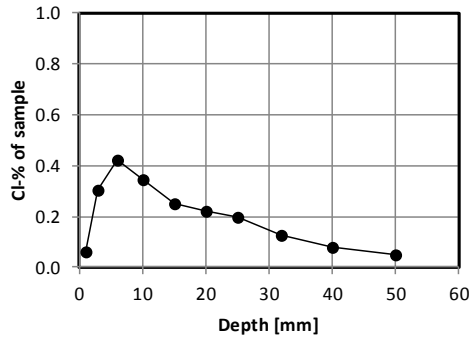


Measurement of chloride ingress in concrete

Concrete ID: 94-3-C	Type of binder: 95% Anl.+5%SF
Casting date: 1994-04-27	w/b: 0.35
Exposure date: 1994-05-11	Exposure zone: Submerged (holes)
Sampling date: 2012-10-02	Profiling method: Grinding on a lathe
Tested by: LJ, LG	Chloride analysis: Potentiometric titration
Tested date: 2013-06-13	Calcium analysis: Potentiometric titration

Raw data and calculations

Exposure duration:		6719 days		CaO% binder:		61.7 %	
Depth from - to (mm)	Mean depth (mm)	Cl% of sample	CaO% of sample	Binder% of sample	Cl% of binder		
0 - 2	1	0.063	15.27	24.76	0.25		
2 - 4	3	0.301	16.06	26.04	1.16		
4 - 8	6	0.423	13.18	21.36	1.98		
8 - 12	10	0.344	11.54	18.70	1.84		
12 - 18	15	0.253	10.63	17.23	1.47		
18 - 22	20	0.223	12.04	19.52	1.14		
22 - 28	25	0.200	14.05	22.78	0.88		
28 - 36	32	0.125	12.22	19.80	0.63		
36 - 44	40	0.082	11.91	19.30	0.42		
44 - 56	50	0.053	10.09	16.36	0.32		

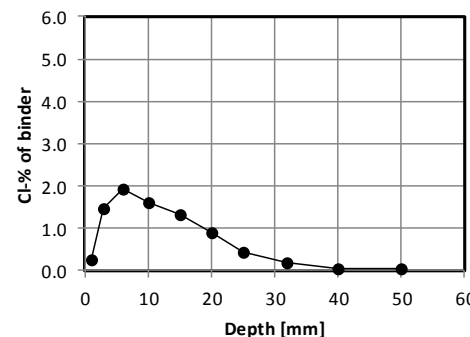
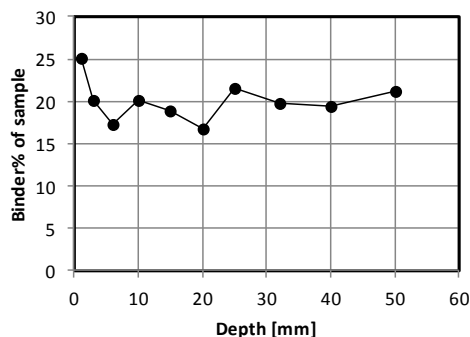
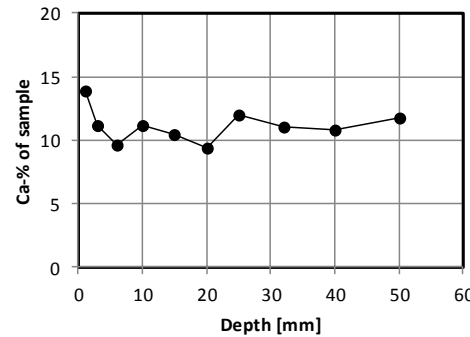
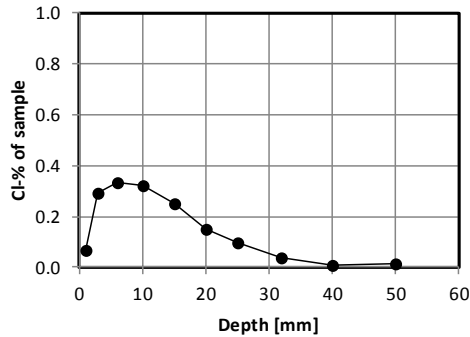


Measurement of chloride ingress in concrete

Concrete ID: 94-4-C	Type of binder: 95% Anl.+5%SF+10FA
Casting date: 1994-04-27	w/b: 0.35
Exposure date: 1994-05-11	Exposure zone: Submerged
Sampling date: 2012-10-02	Profiling method: Grinding on a lathe
Tested by: NS, LG	Chloride analysis: Potentiometric titration
Tested date: 2013-06-24	Calcium analysis: Potentiometric titration

Raw data and calculations

Exposure duration:		6719 days		CaO% binder:		55.7 %	
Depth from - to (mm)	Mean depth (mm)	Cl% of sample	CaO% of sample	Binder% of sample	Cl% of binder		
0 - 2	1	0.069	13.95	25.04	0.28		
2 - 4	3	0.293	11.18	20.06	1.46		
4 - 8	6	0.332	9.59	17.21	1.93		
8 - 12	10	0.323	11.18	20.06	1.61		
12 - 18	15	0.250	10.48	18.81	1.33		
18 - 22	20	0.152	9.36	16.81	0.90		
22 - 28	25	0.097	12.04	21.61	0.45		
28 - 36	32	0.039	11.00	19.74	0.20		
36 - 44	40	0.012	10.84	19.47	0.06		
44 - 56	50	0.013	11.78	21.16	0.06		

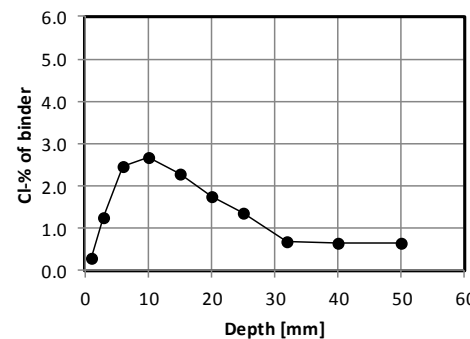
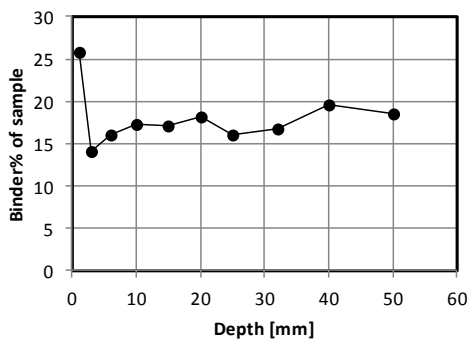
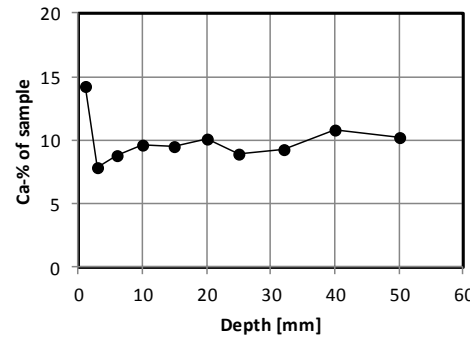
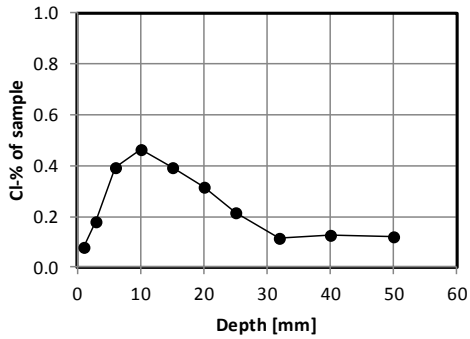


Measurement of chloride ingress in concrete

Concrete ID: RHA2	Type of binder: 85%Anl.+15%RA
Casting date: 1994-08-22	w/b: 0.35
Exposure date: 1994-09-06	Exposure zone: Submerged
Sampling date: 2012-10-02	Profiling method: Grinding on a lathe
Tested by: NS, JW	Chloride analysis: Potentiometric titration
Tested date: 2013-06-27	Calcium analysis: Potentiometric titration

Raw data and calculations

Exposure duration:		6601 days		CaO% binder:		55.2 %	
Depth from - to (mm)	Mean depth (mm)	Cl% of sample	CaO% of sample	Binder% of sample	Cl% of binder		
0 - 2	1	0.081	14.26	25.83	0.31		
2 - 4	3	0.181	7.82	14.17	1.27		
4 - 8	6	0.395	8.81	15.97	2.48		
8 - 12	10	0.465	9.59	17.37	2.68		
12 - 18	15	0.394	9.49	17.19	2.29		
18 - 22	20	0.319	10.06	18.22	1.75		
22 - 28	25	0.217	8.87	16.06	1.35		
28 - 36	32	0.117	9.28	16.81	0.70		
36 - 44	40	0.130	10.83	19.61	0.66		
44 - 56	50	0.119	10.19	18.46	0.64		



Appendix 3**Curve-fitted parameters D_{F2} and C_s**

Mix No.	$D_{F2} \times 10^{-12} \text{ m}^2/\text{s}$, submerged zone					
	0.6-0.9 y	1-1.3 y	2-2.3 y	5.1-5.4 y	10.1-10.5y	20.5-20.8 y
1-35	2.89				1.13*	1.07*
1-40	4.55	3.2	3.27	2.51*	1.95*	1.30*
2-35		1.61			1.01*	0.96*
2-50	6.56	5.02			3.44*	5.43*
3-35	1.91				0.72	1.02*
5-40					0.82	1.36*
6-35					0.63	0.53*
6-40					0.98	1.3*
7-35					1.03*	1.35*
7-40					2.17*	1.73*
8-35					1.01	0.92
8-40					1.44*	1.34*
12-35	1.86		0.8	0.76	0.75	0.39*
H1		0.92	0.64**	0.5	0.19	0.21*
H2		0.43	0.47**	0.14	0.2	0.23
H5		0.45	0.52**	0.21	0.27	0.26
H8		1.52	1.05**	0.51	0.4	0.4

* According to Eq. (5.2) for two-sides exposure boundary.

** Measured by AEC Laboratory.

Mix No.	C _s mass% of binder, submerged zone					
	0.6-0.9 y	1-1.3 y	2-2.3 y	5.1-5.4 y	10.1-10.5y	20.5-20.8 y
1-35	2.14				4.37*	5.65*
1-40	2.58	3.28	3.33	5.19*	5.00*	5.14*
2-35		4.32			4.67*	4.18*
2-50	1.94	4.64			3.65*	3.49
3-35	2.64				4.45	3.46*
5-40					3.19	4.14*
6-35					3.84	3.51*
6-40					3.96	3.67*
7-35					2.95*	3.41*
7-40					3.28*	3.22*
8-35					3.90*	4.67*
8-40					2.15*	3.75*
12-35	1.86		3.45	5.18	4.51	4.75*
H1		2.77	3.90**	4.74	3.81	4.26
H2		1.67	2.49**	4.87	3.54	5.23*
H5		1.63	2.95**	4.38	3.61	4.11*
H8		3.01	2.90**	5.28	4.29	4.26*

* According to Eq. (5.2) for two-sides exposure boundary.

** Measured by AEC Laboratory.

Mix No.	$D_{F2} \times 10^{-12} \text{ m}^2/\text{s}$, splash zone							
	0.6-0.9 y	1-1.3 y	2-2.3 y	5.1-5.4 y	10.1-10.5y	20.5-20.8 y		
						S	Sa	Su
1-35	1.47					0.73*		
1-40	1.98		2.01	1.31	1.43*		1.27*	0.93*
2-35		1.09				0.55*		
2-50	2.94					1.34*		
3-35	0.71					0.73*		
5-40							0.24	1.53*
6-35								
6-40								
7-35								
7-40								
8-35								
8-40								
12-35	0.95		0.98	0.28				
H1		0.26		0.19				
H2		0.25		0.12				
H5		0.20		0.20				
H8		0.96		0.31				

* According to Eq. (5.2) for two-sides exposure boundary.

Mix No.	$C_s \times 10^{-12} \text{ m}^2/\text{s}$, splash zone							
	0.6-0.9 y	1-1.3 y	2-2.3 y	5.1-5.4 y	10.1-10.5y	20.5-20.8 y		
						S	Sa	Su
1-35	1.50					3.25*		
1-40	1.48		1.96	1.92	5.72*		4.03*	6.64*
2-35		2.85				4.70*		
2-50	2.56					4.88*		
3-35	1.30					4.02*		
5-40							1.38	3.88*
6-35								
6-40								
7-35								
7-40								
8-35								
8-40								
12-35	0.99		2.73	1.63				
H1				1.92				
H2				1.17				
H5		1.34						
H8		2.39			3.08			

* According to Eq. (5.2) for two-sides exposure boundary.

Mix No.	$D_{F2} \times 10^{-12} \text{ m}^2/\text{s}$, atmospheric zone					
	0.6-0.9 y	1-1.3 y	2-2.3 y	5.1-5.4 y	10.1-10.5y	20.5-20.8 y
1-35	1.43				0.39	0.26
1-40	1.95		0.81	1.08	0.53	0.36*
2-35		0.84			0.42	0.36
2-50	2.37				1.44*	0.84*
3-35	0.75				0.15	0.40
5-40					0.10	0.14
6-35					0.04	
6-40					0.13	
7-35					0.21	
7-40					0.25	
8-35					0.15	
8-40					0.21	
12-35	1.23		0.63	0.20	0.23	
H1		0.38		0.15	0.07	
H2		0.40		0.08	0.04	
H5		0.50		0.16	0.04	
H8		0.51		0.26	0.12	

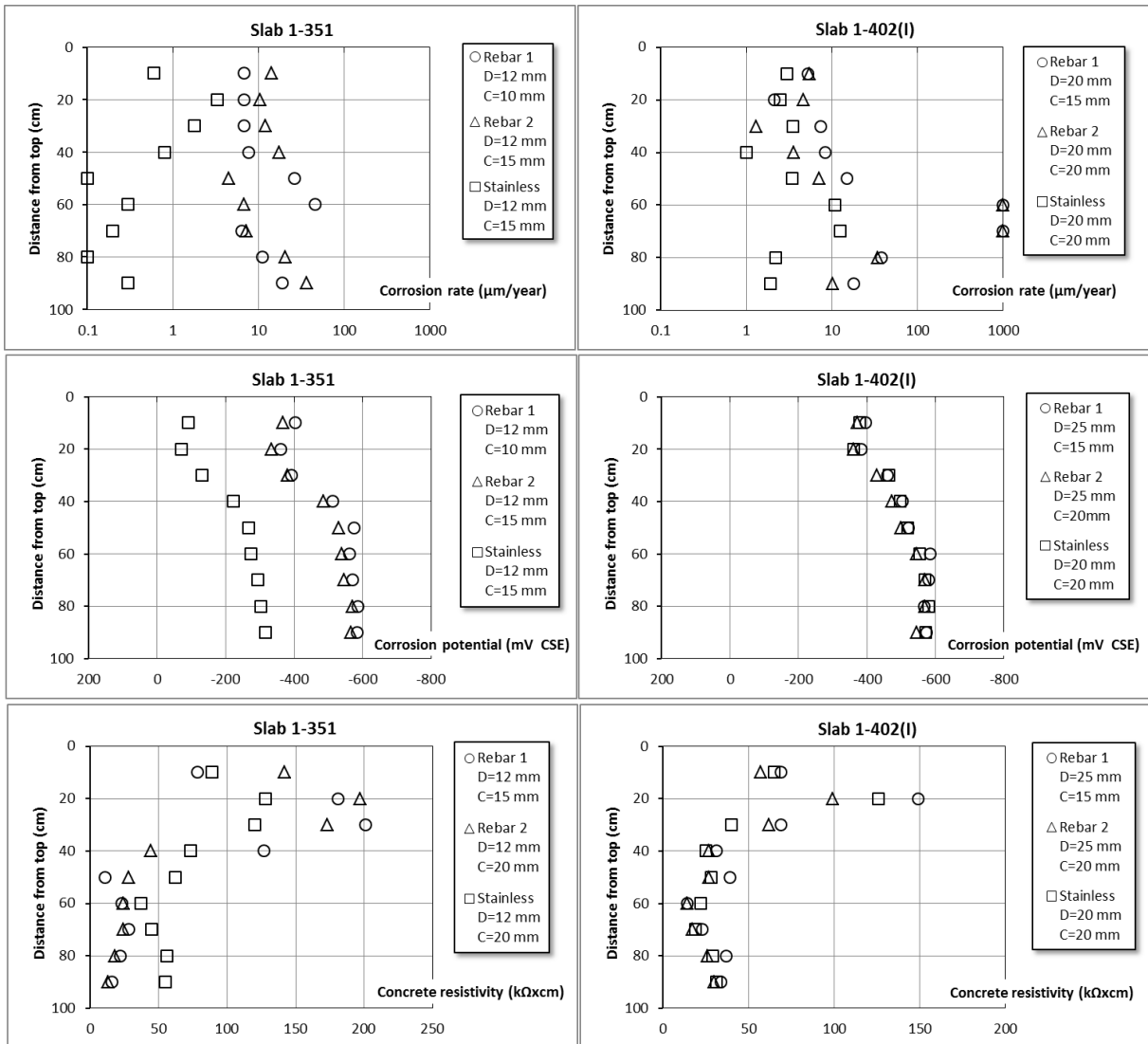
* According to Eq. (5.2) for two-sides exposure boundary.

Mix No.	$C_s \times 10^{-12} \text{ m}^2/\text{s}$, atmospheric zone					
	0.6-0.9 y	1-1.3 y	2-2.3 y	5.1-5.4 y	10.1-10.5y	20.5-20.8 y
1-35	1.19				1.51	2.93
1-40	1.1		1.22	1.44	1.25	2.48*
2-35		1.66			1.57	3.59*
2-50	1.19				1.73*	3.13*
3-35	1.03				1.38	2.37
5-40					0.67	2.42
6-35					1.53	
6-40					1.27	
7-35					0.85	
7-40					0.76	
8-35					0.92	
8-40					2.48	
12-35	1.39		0.76	1.65	2.3	
H1		0.88		1.6	3.51	
H2		1.02		2.02	1.04	
H5		0.84		1.96	2.36	
H8		1.53		3.53	2.88	

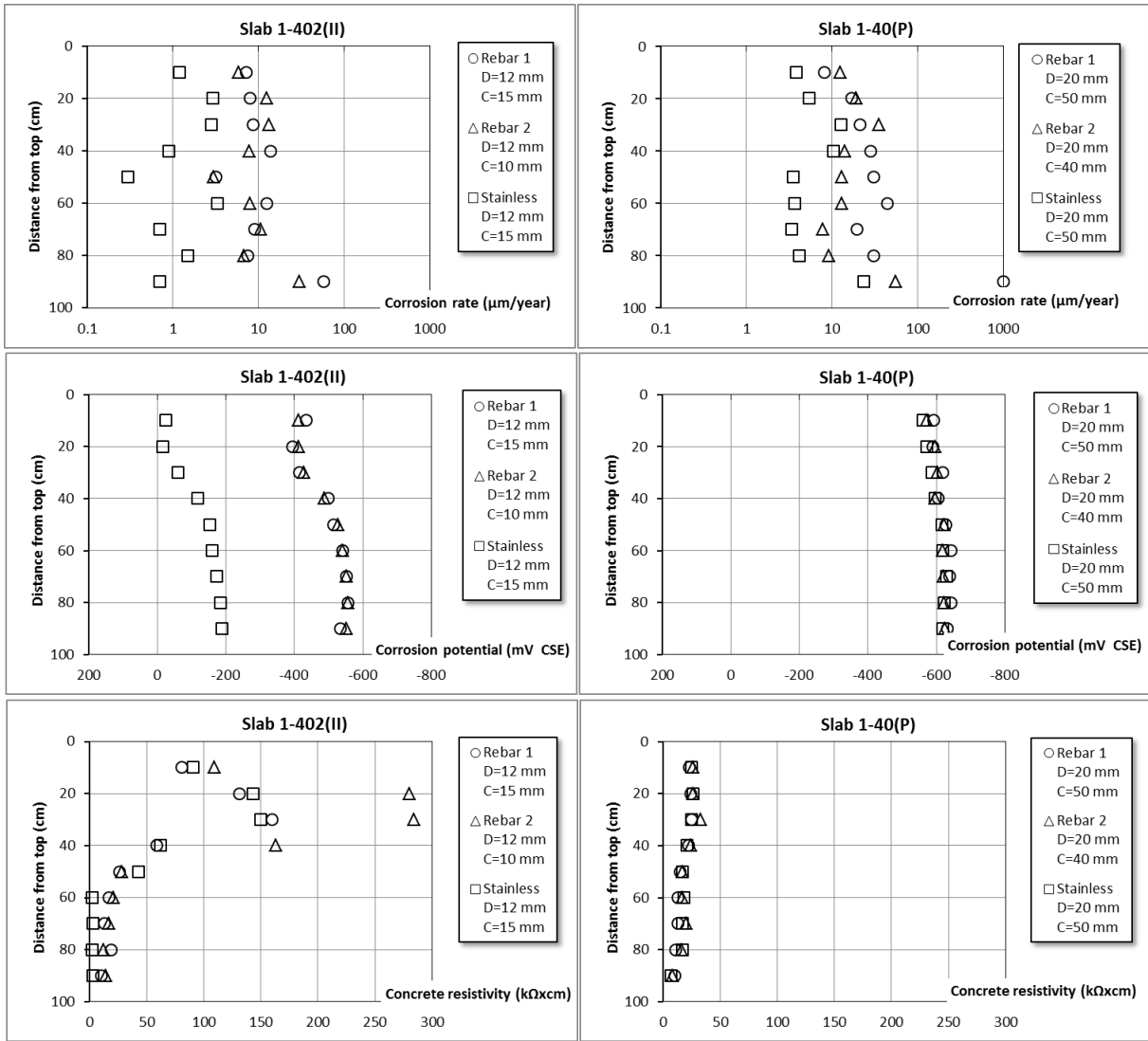
* According to Eq. (5.2) for two-sides exposure boundary.

Appendix 4 Data from corrosion measurements

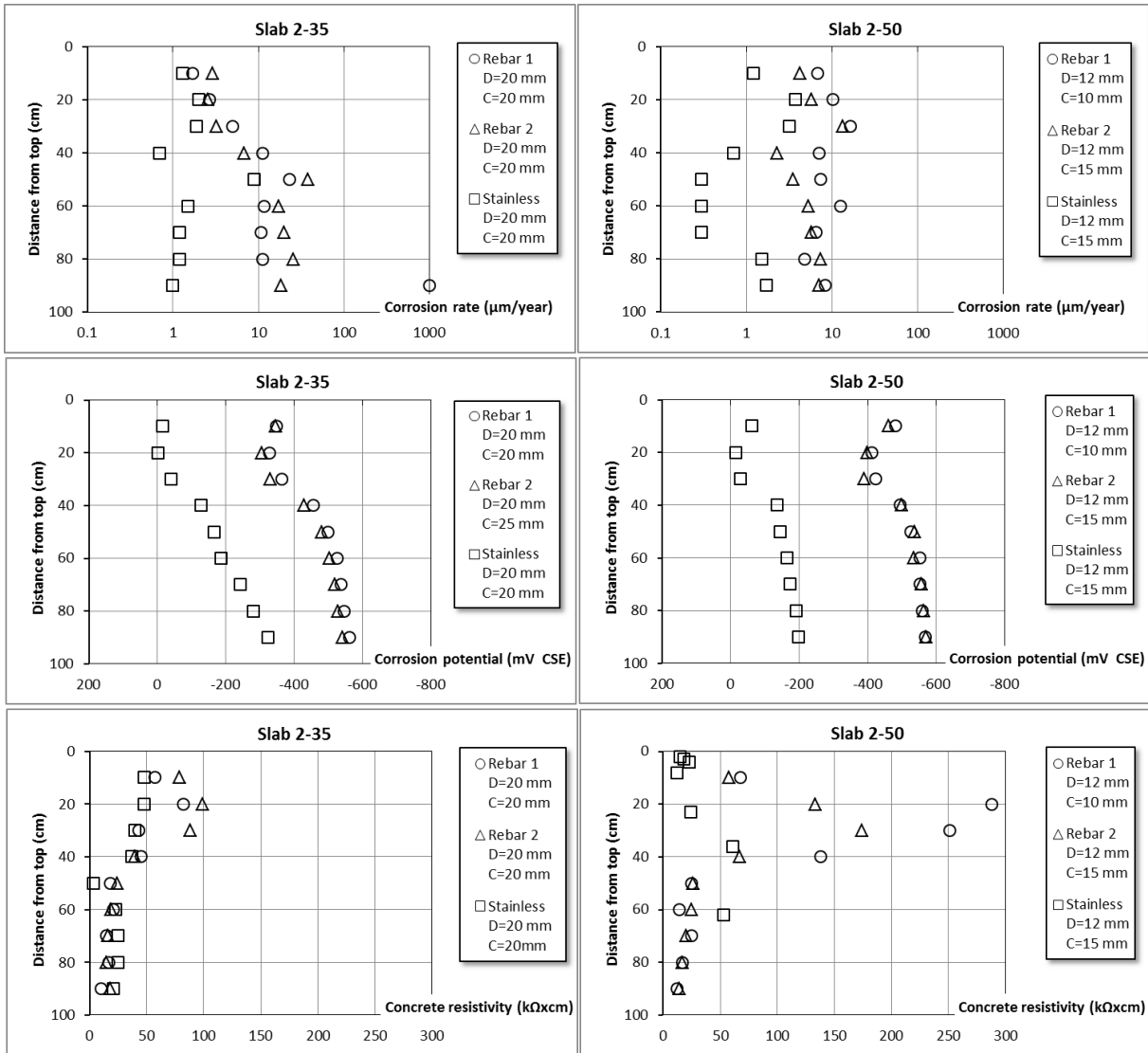
In the tables below in this appendix the maximum corrosion rate (“Corr. max”) is given together with its location as distance from the top of the slab (“Distance from top”). The chloride level (“Cl”) at the same location is also given if this is known (from chloride profiles). Further, if corrosion products were observed externally on the slab (“Visual corr.”) is also noted.



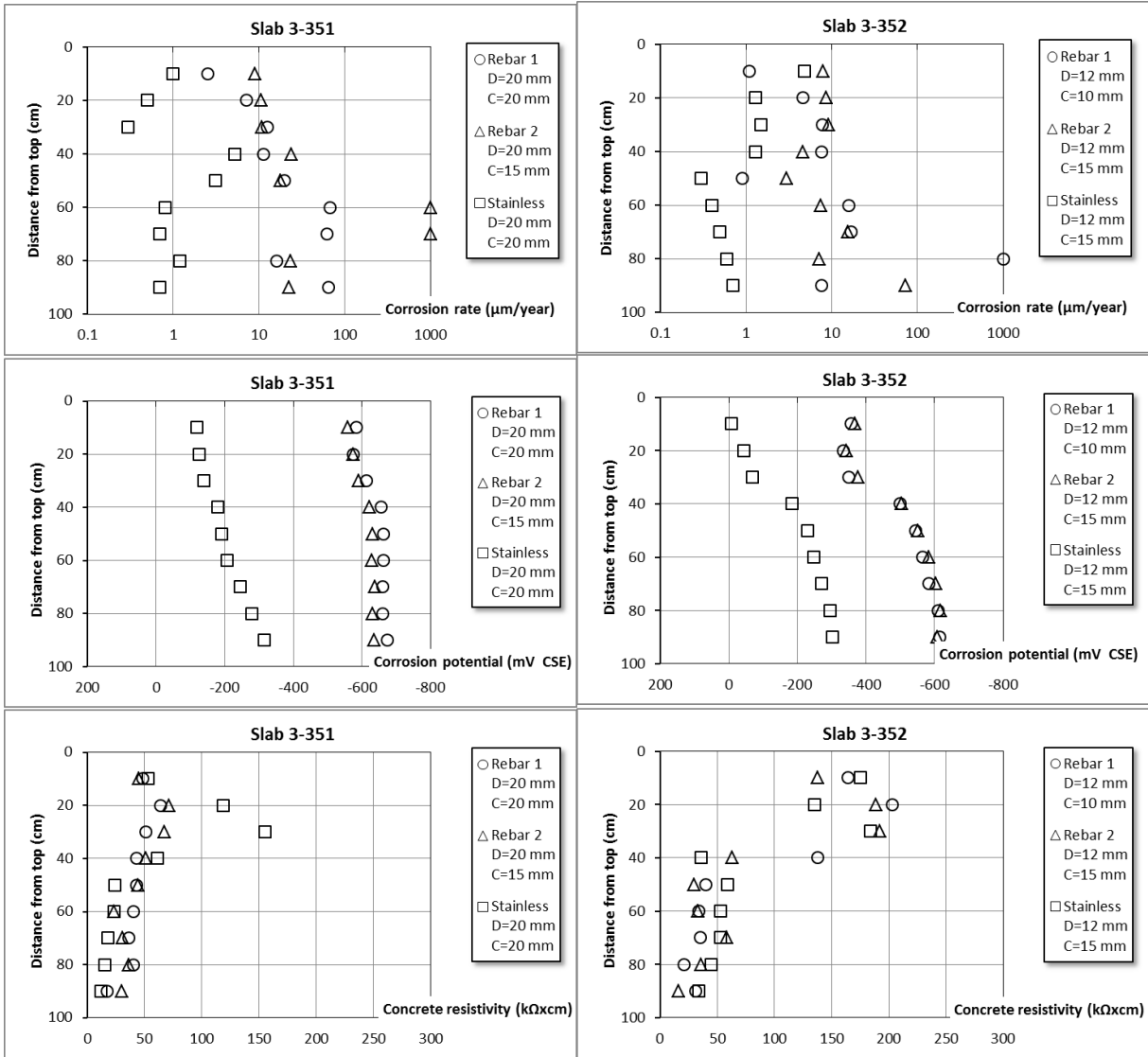
Mix	Rebar	Diameter (mm)	Cover (mm)	After 20 years				After 13 years		After 10 years
				Corr. max (µm/year)	Cl (mass % binder)	Distance from top (cm)	Visual corr.	Corr. max (µm/year)	Distance from top (cm)	Cl (mass % binder)
1-351	1	12	10	46	2.4	60	Yes	22.9	50	3
	2	12	15	36.9	3.6	90	Yes	15.4	90	2.4
	Stainless	12	15	3.3	1.4	20	No	1.8	30	0.4
1-402(I)	1	20	15	>500	3.3	70	Yes	17.6	70	3.3
	2	20	20	>500	3	70	Yes	24.4	70	2.7
	Stainless	20	20	12.5	3	70	No	8.2	60	-



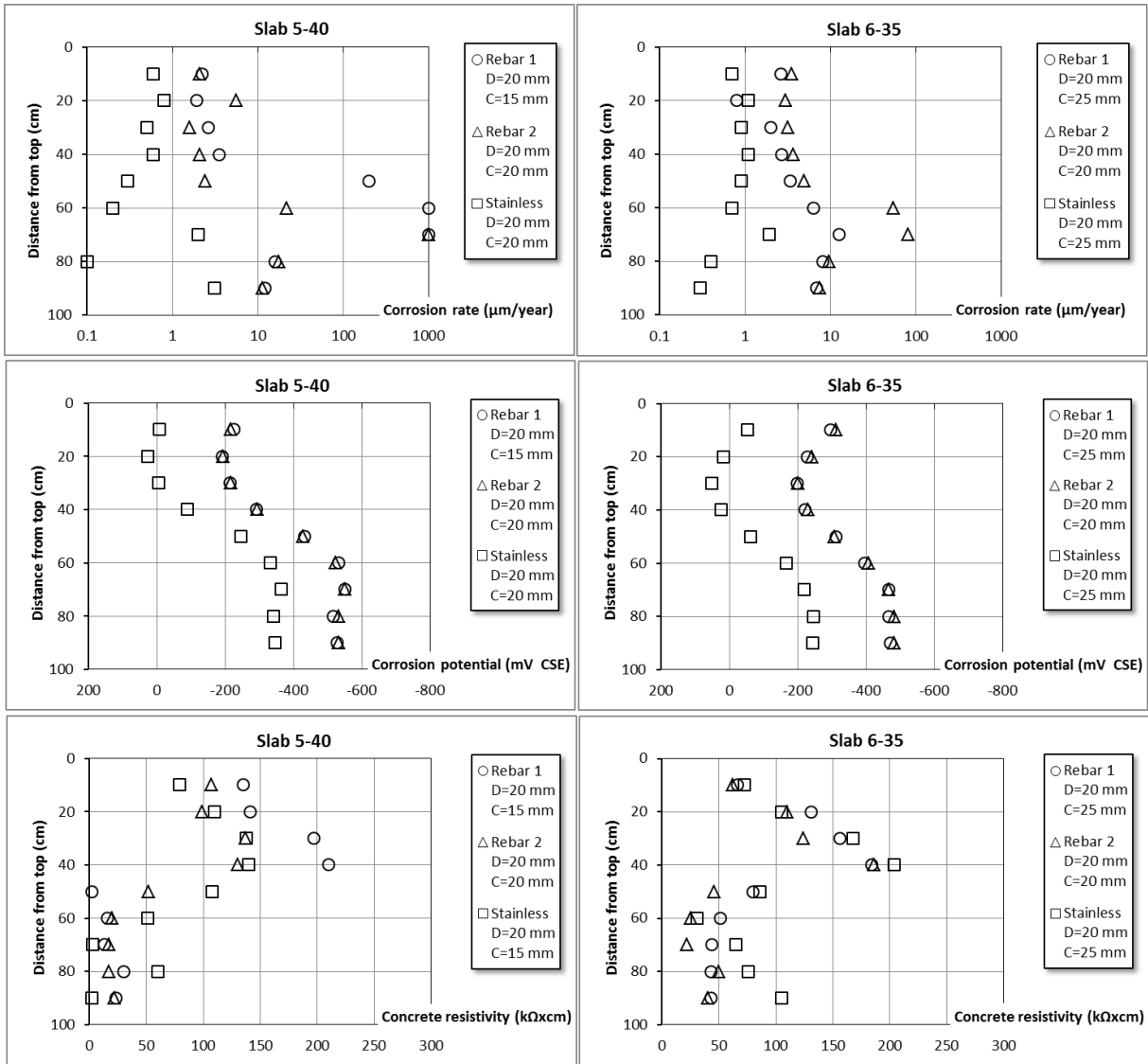
Mix	Rebar	Diameter (mm)	Cover (mm)	After 20 years				After 13 years		After 10 years
				Corr. max ($\mu\text{m/year}$)	Cl (mass % binder)	Distance from top (cm)	Visual corr.	Corr. max ($\mu\text{m/year}$)	Distance from top (cm)	Cl (mass % binder)
1-402(II)	1	12	15	57.1	3.3	90	Yes	28.5	90	3.2
	2	12	10	29.9	4.6	90	Yes	15.1	90	3.6
	Stainless	12	15	2.9	1.3	20	No	1.7	20	0.6
1-402(P)	1	20	50	>500		90	No			
	2	20	40	55.1	2	90	Yes			
	Stainless	20	50	23.6		90	No			



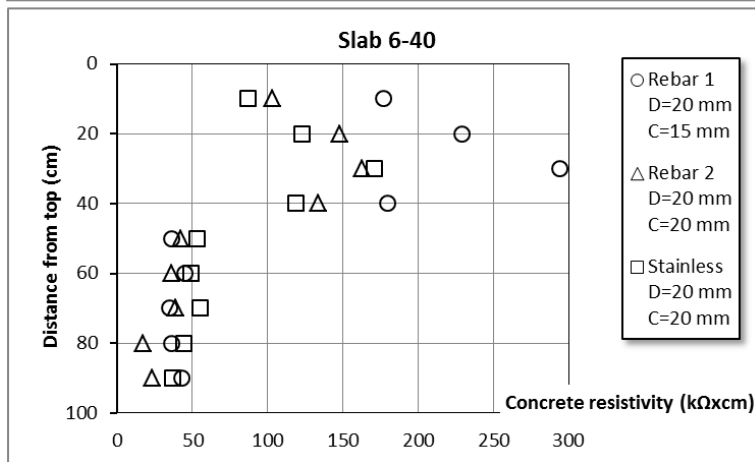
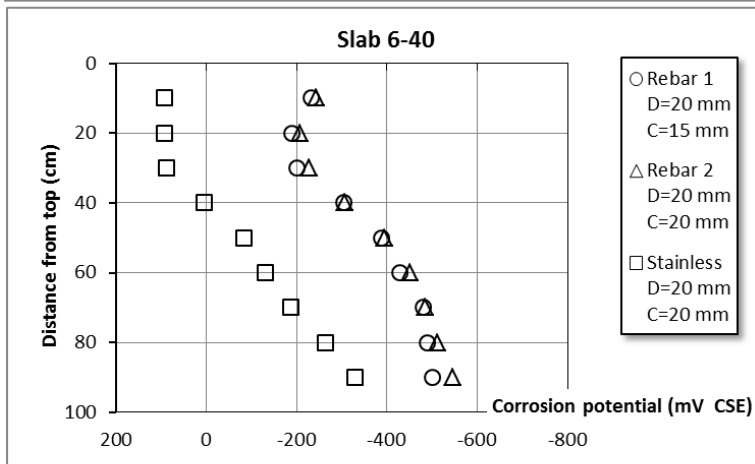
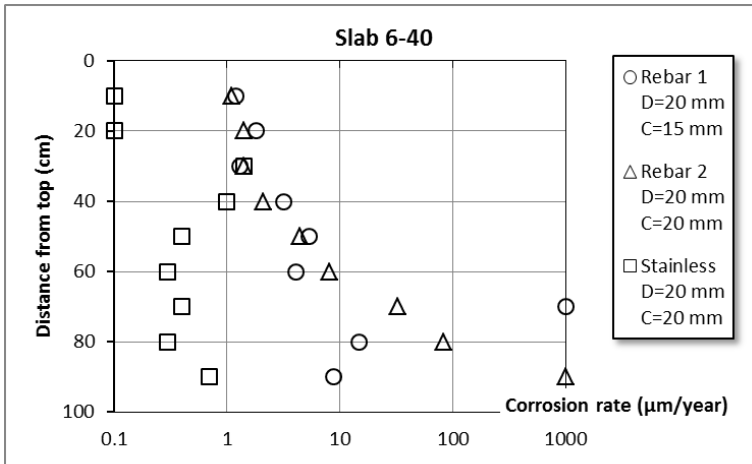
Mix	Rebar	Diameter (mm)	Cover (mm)	After 20 years				After 13 years		After 10 years
				Corr. max (µm/year)	Cl (mass % binder)	Distance from top (cm)	Visual corr.	Corr. max (µm/year)	Distance from top (cm)	Cl (mass % binder)
2-352	1	20	20	>500	2.2	90	Yes	37.9	90	2.2
	2	20	25	38.3	2	50	Yes	28	50	1.7
	Stainless	20	20	9	2	50	No	1.5	10	0.07
2-50	1	12	10	16.4	2.4	30	Yes	73.7	60	3
	2	12	15	13.4	2	30	No	11.2	20	1.1
	Stainless	12	15	3.7	2	20	No	1.3	20	1.1



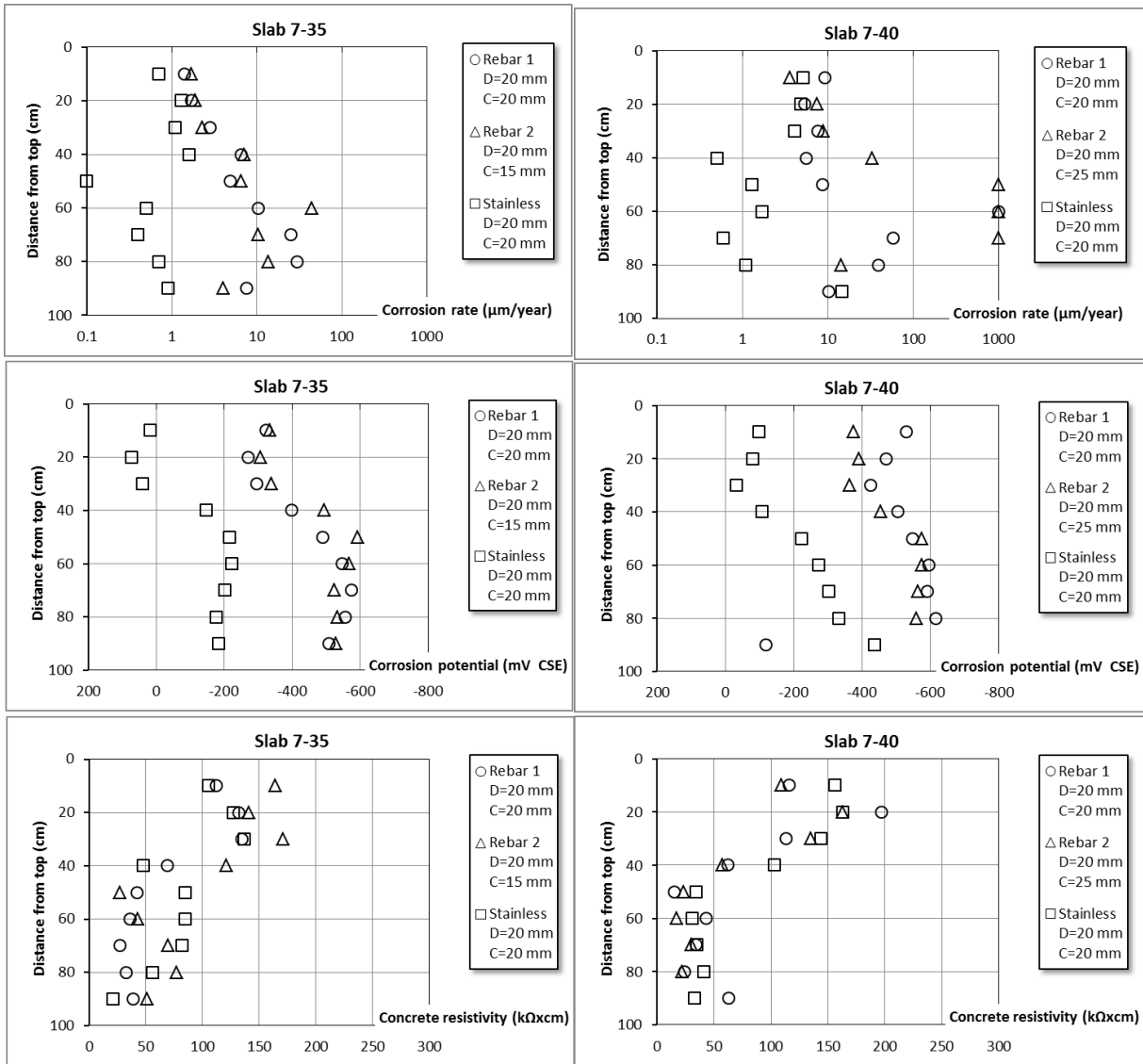
Mix	Rebar	Diameter (mm)	Cover (mm)	After 20 years				After 13 years		After 10 years
				Corr. max ($\mu\text{m/year}$)	CI (mass % binder)	Distance from top (cm)	Visual corr.	Corr. max ($\mu\text{m/year}$)	Distance from top (cm)	CI (mass % binder)
3-351	1	20	20	67.3	2	60	Yes	39.9	60	1.8
	2	20	15	>500	2.4	70	Yes	164	70	2.3
	Stainless	20	15	5.2	0.96	40	No	1.5	30	
3-352	1	12	10	>500	2.8	80	Yes	7.5	80	2.9
	2	12	15	71.8	2.4	90	Yes	19.3	90	2.3
	Stainless	12	15	4.8	1.5	10	No	1.2	30	0.1



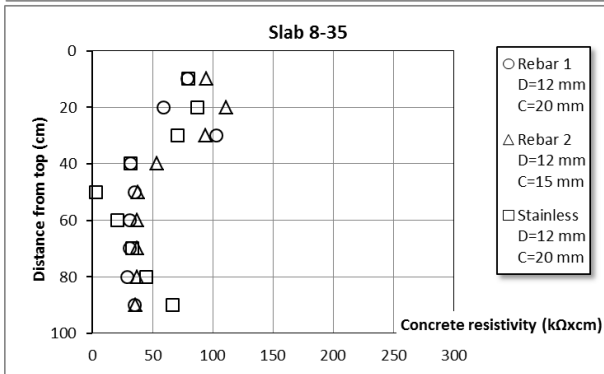
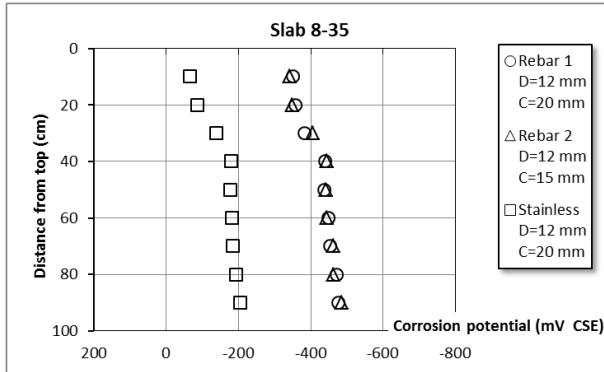
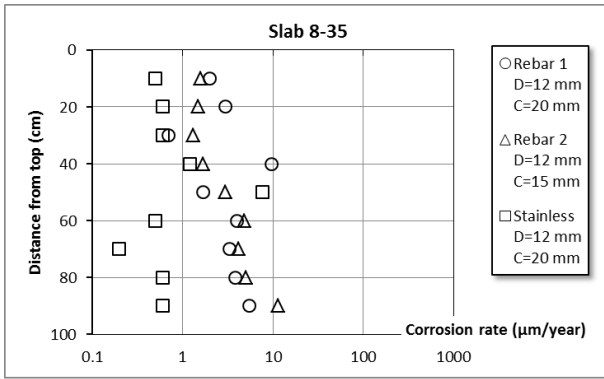
Mix	Rebar	Diameter (mm)	Cover (mm)	After 20 years				After 13 years		After 10 years
				Corr. max (µm/year)	Cl (mass % binder)	Distance from top (cm)	Visual corr.	Corr. max (µm/year)	Distance from top (cm)	Cl (mass % binder)
5-40	1	20	15	>500	3	70	Yes	71.5	70	1.6
	2	20	20	>500	2.7	70	Yes	96.6	70	1.2
	Stainless	20	20	3.1	2.7	90	No	1.5	40	~0
6-35	1	20	25	12.6	1.2	70	No	10.2	70	0.9
	2	20	20	81	1.4	70	Yes	69.1	70	1.2
	Stainless	20	25	1.9	1.2	70	No	1.8	70	0.9



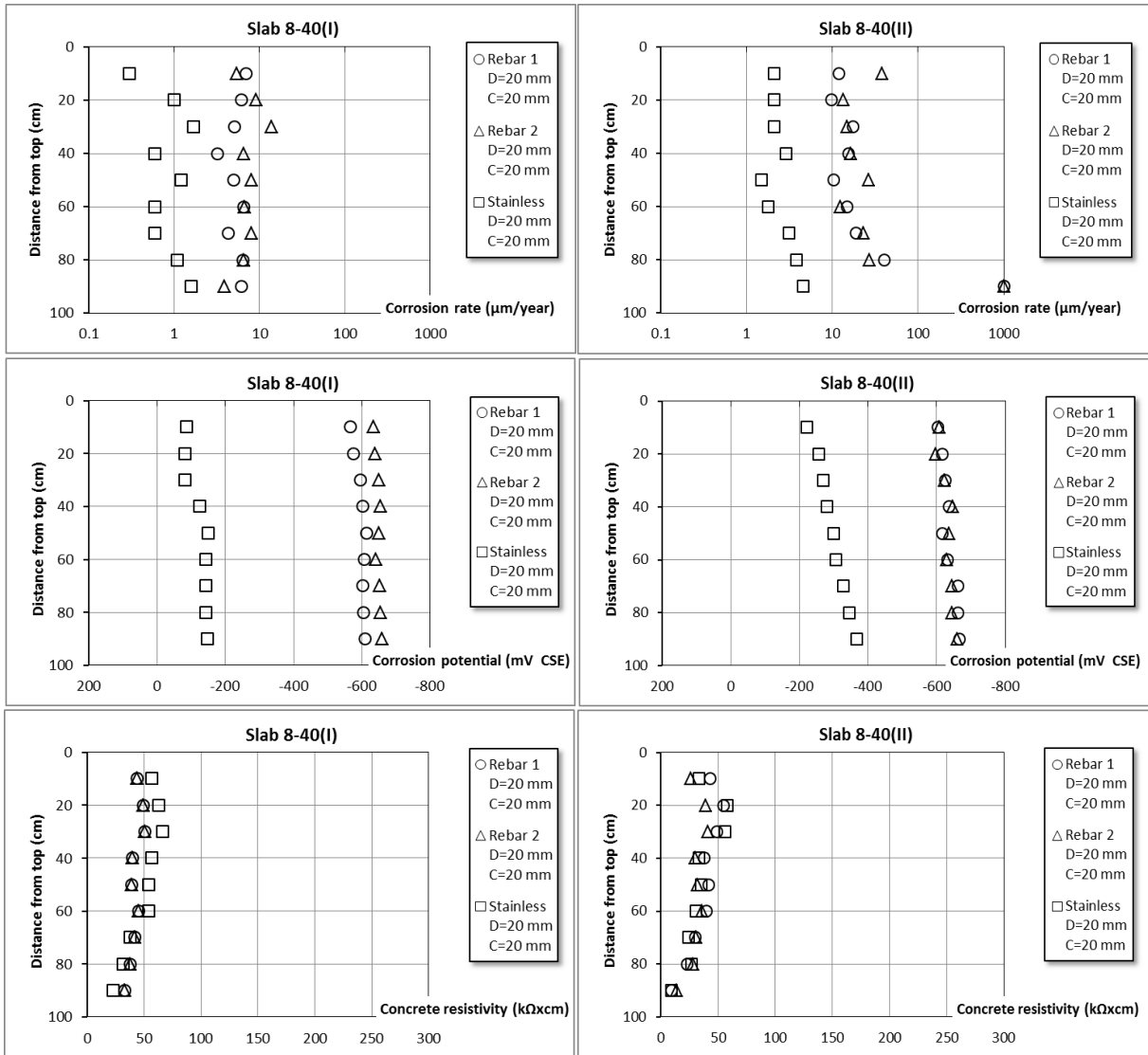
Mix	Rebar	Diameter (mm)	Cover (mm)	After 20 years				After 13 years		After 10 years
				Corr. max ($\mu\text{m}/\text{year}$)	Cl (mass % binder)	Distance from top (cm)	Visual corr.	Corr. max ($\mu\text{m}/\text{year}$)	Distance from top (cm)	Cl (mass % binder)
6-40	1	20	15	>500	2.6	70	Yes	70.7	70	1.7
	2	20	20	>500	2.6	90	Yes	40	90	1.7
	Stainless	20	20	1.4		30	No	1.7	30	0.01



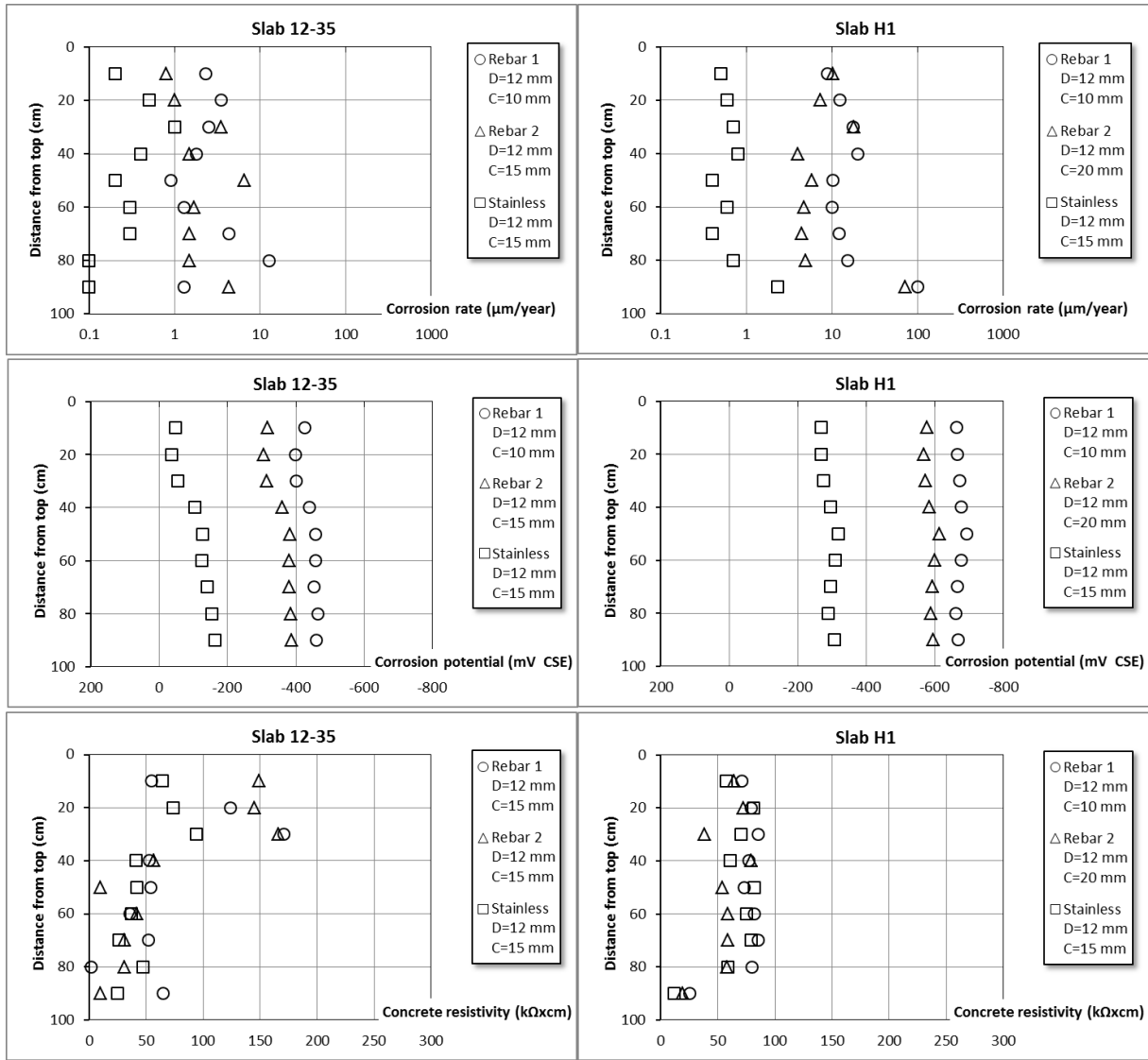
Mix	Rebar	Diameter (mm)	Cover (mm)	After 20 years				After 13 years		After 10 years
				Corr. max ($\mu\text{m}/\text{year}$)	Cl (mass % binder)	Distance from top (cm)	Visual corr.	Corr. max ($\mu\text{m}/\text{year}$)	Distance from top (cm)	Cl (mass % binder)
7-35	1	20	20	29.9	2.2	80	Yes	120.1	70	1.1
	2	20	15	44.7	2.4	60	No	42.2	50	1.5
	Stainless	20	20	1.6		40	No	1.7	20	0
7-40	1	20	20	>500	2.2	60	Yes			
	2	20	20	>500	2.2	60	Yes			
	Stainless	20	20	14.5	2.2	90	No			



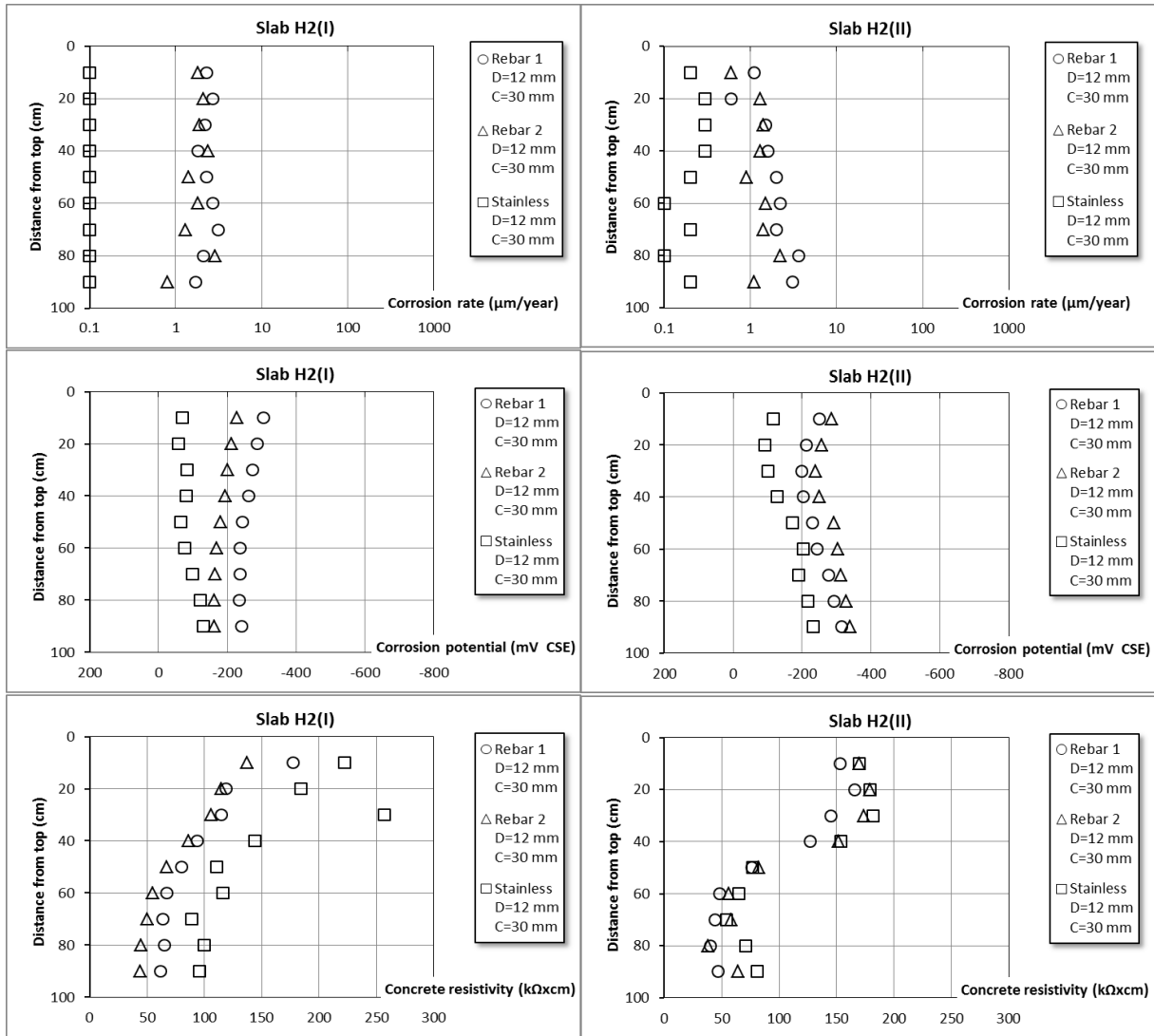
Mix	Rebar	Diameter (mm)	Cover (mm)	After 20 years				After 13 years		After 10 years
				Corr. max ($\mu\text{m}/\text{year}$)	Cl (mass % binder)	Distance from top (cm)	Visual corr.	Corr. max ($\mu\text{m}/\text{year}$)	Distance from top (cm)	Cl (mass % binder)
8-35	1	12	20	5.5	2.1	90	Yes	16.2	70	1.8
	2	12	15	11.3	2.6	90	No	6.5	60	2.2
	Stainless	12	20	6.9		50	No	1.1	30	0



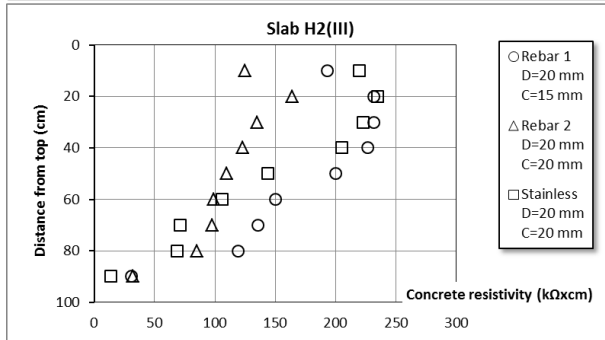
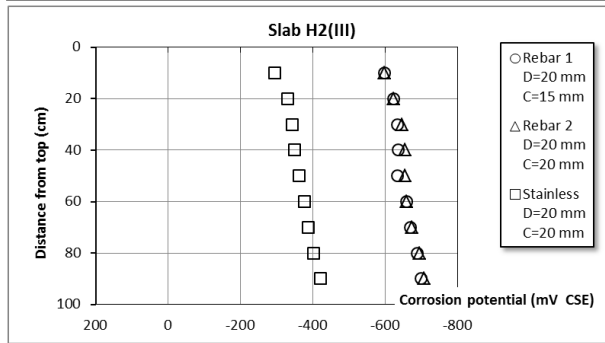
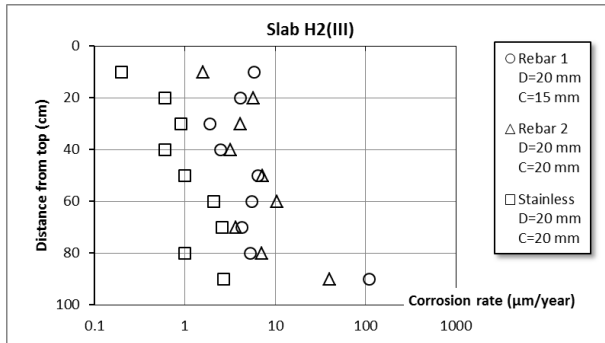
Mix	Rebar	Diameter (mm)	Cover (mm)	After 20 years				After 13 years		After 10 years
				Corr. max (µm/year)	Cl (mass % binder)	Distance from top (cm)	Visual corr.	Corr. max (µm/year)	Distance from top (cm)	Cl (mass % binder)
8-40 (I)	1	20	20	6.5	2.3	60	No	5.6	60	1
	2	20	20	14		30	No	4	90	1
	Stainless	20	20	1.7		30	No	0.8	90	1
8-40 (II)	1	20	15	>500	2.6	90	Yes	90.1	50	
	2	20	20	>500	2.3	90	Yes	22.9	90	1
	Stainless	20	20	4.6	2.3	90	No	1.8	90	1



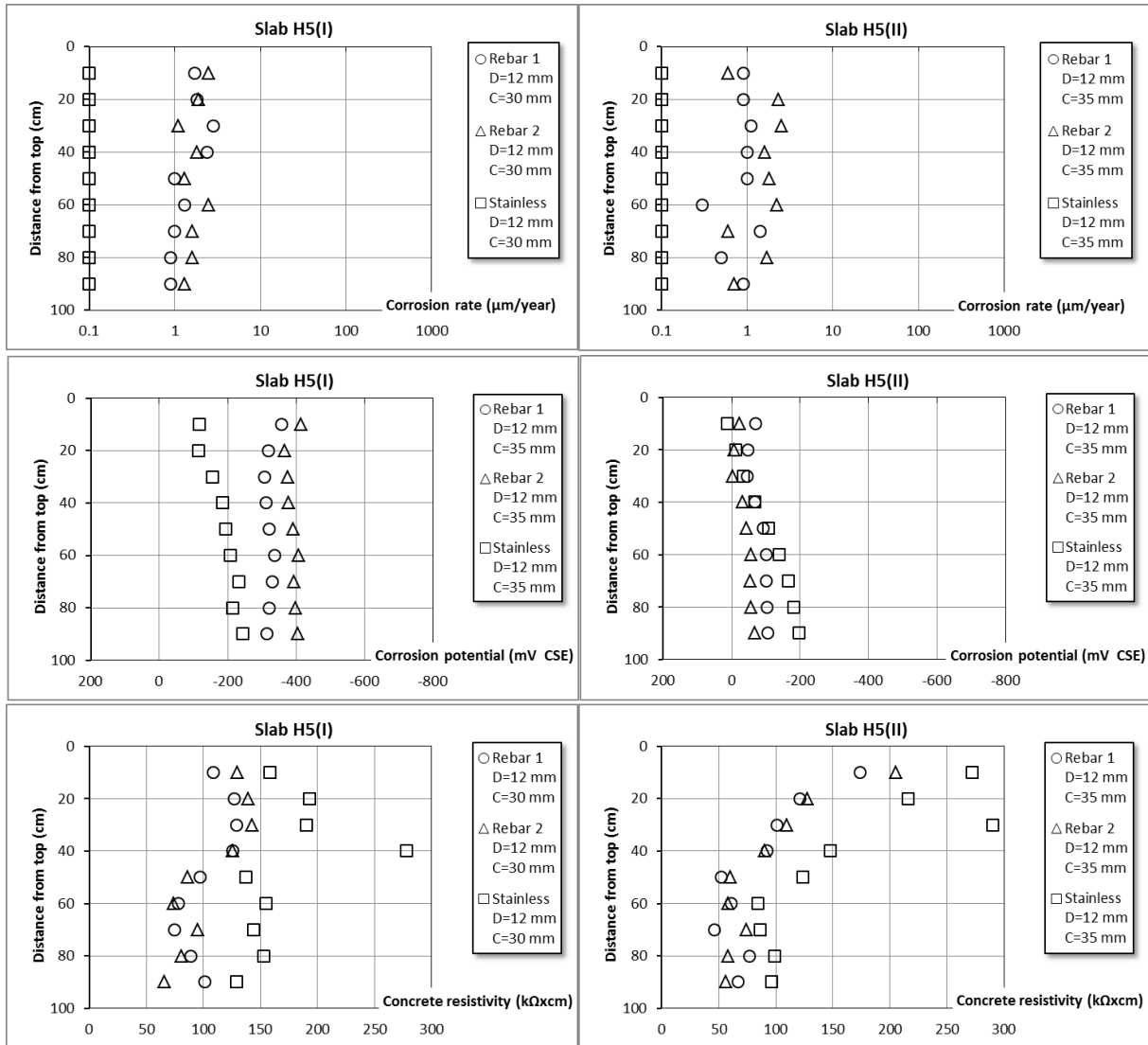
Mix	Rebar	Diameter (mm)	Cover (mm)	After 20 years				After 13 years		After 10 years
				Corr. max (µm/year)	CI (mass % binder)	Distance from top (cm)	Visual corr.	Corr. max (µm/year)	Distance from top (cm)	CI (mass % binder)
12-35	1	12	10	12.8	3.2	80	Yes	3.7	70	3
	2	12	15	6.6		50	No	2.6	70	2
	Stainless	12	15	1		30	No	1	20	0.5
H1	1	12	10	101	2.1	90	Yes	31.1	90	0.9
	2	12	20	72.1	1.1	90	Yes	20	90	0.9
	Stainless	12	15	2.3	1.7	90	No	1.4	10	0



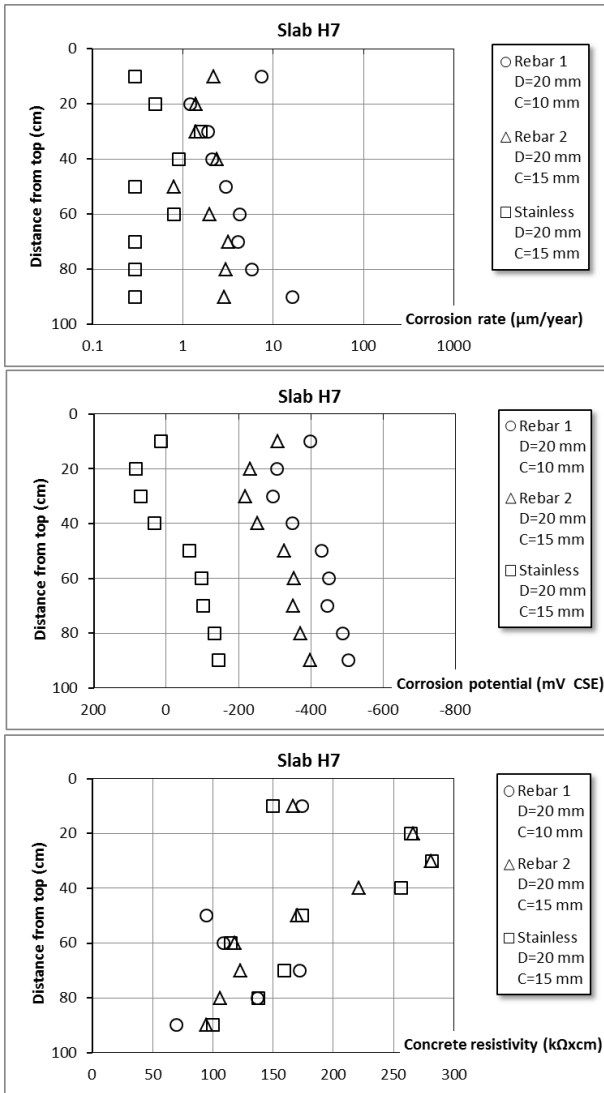
Mix	Rebar	Diameter (mm)	Cover (mm)	After 20 years				After 13 years		After 10 years
				Corr. max (µm/year)	Cl (mass % binder)	Distance from top (cm)	Visual corr.	Corr. max (µm/year)	Distance from top (cm)	Cl (mass % binder)
H2 (I)	1	12	30	2.5	0.1	70	No			
	2	12	30	2.4	0.1	80	No			
	Stainless	12	30	0.1	0.1	-	No			
H2 (II)	1	12	30	3.6	0.1	80	No	5.5	60	0
	2	12	30	2.2	0.1	80	No	5.5	50	0
	Stainless	12	30	0.3	0.1	70	No	1	20	0



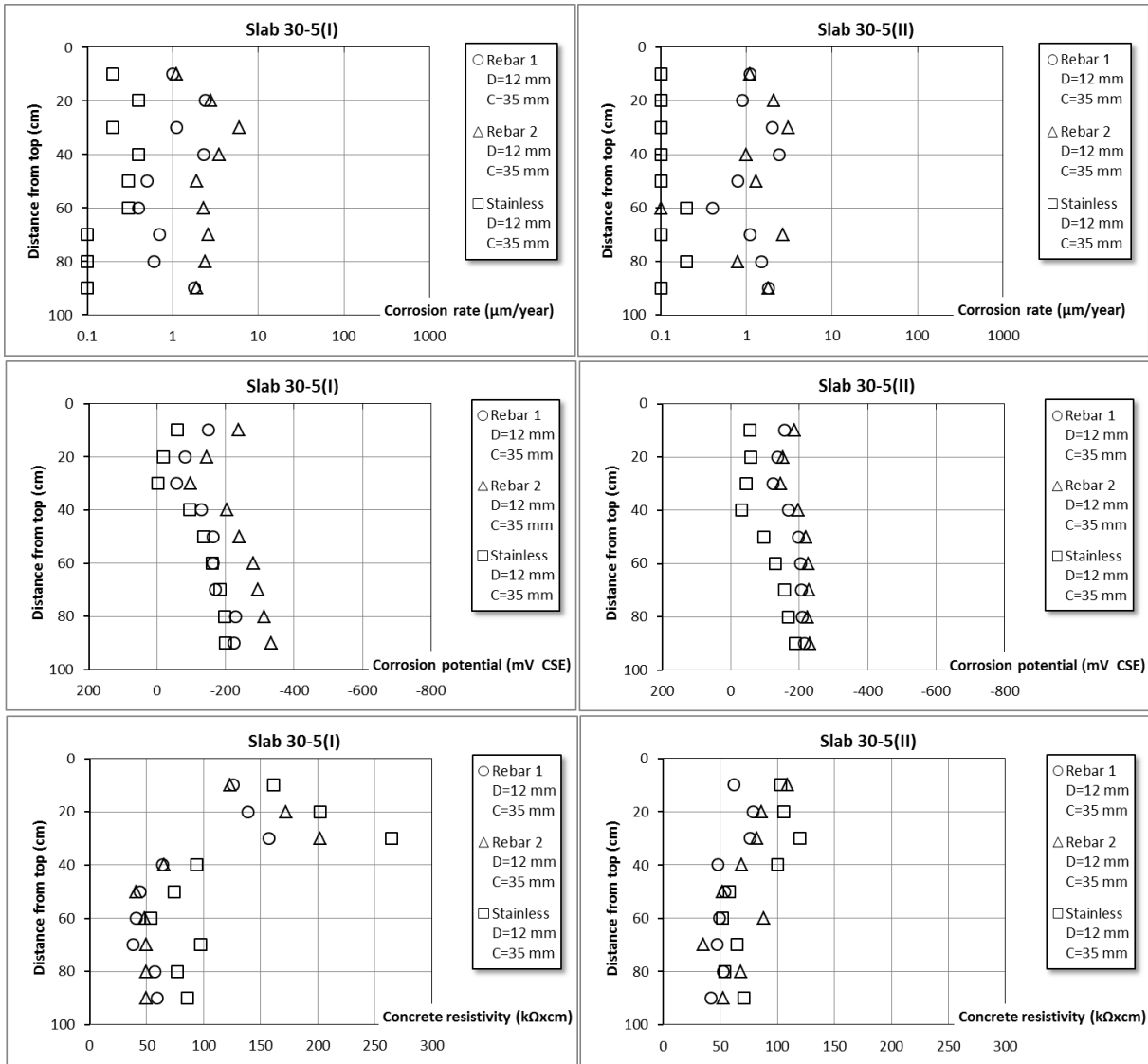
Mix	Rebar	Diameter (mm)	Cover (mm)	After 20 years				After 13 years		After 10 years
				Corr. max ($\mu\text{m}/\text{year}$)	Cl (mass % binder)	Distance from top (cm)	Visual corr.	Corr. max ($\mu\text{m}/\text{year}$)	Distance from top (cm)	Cl (mass % binder)
H2 (III)	1	20	15	110.1	2.4	90	No	12.3	90	0.7
	2	20	20	40	1.3	90	No	11.8	70	0.5
	Stainless	20	20	2.7	1.3	90	No	0.6	70	0.5



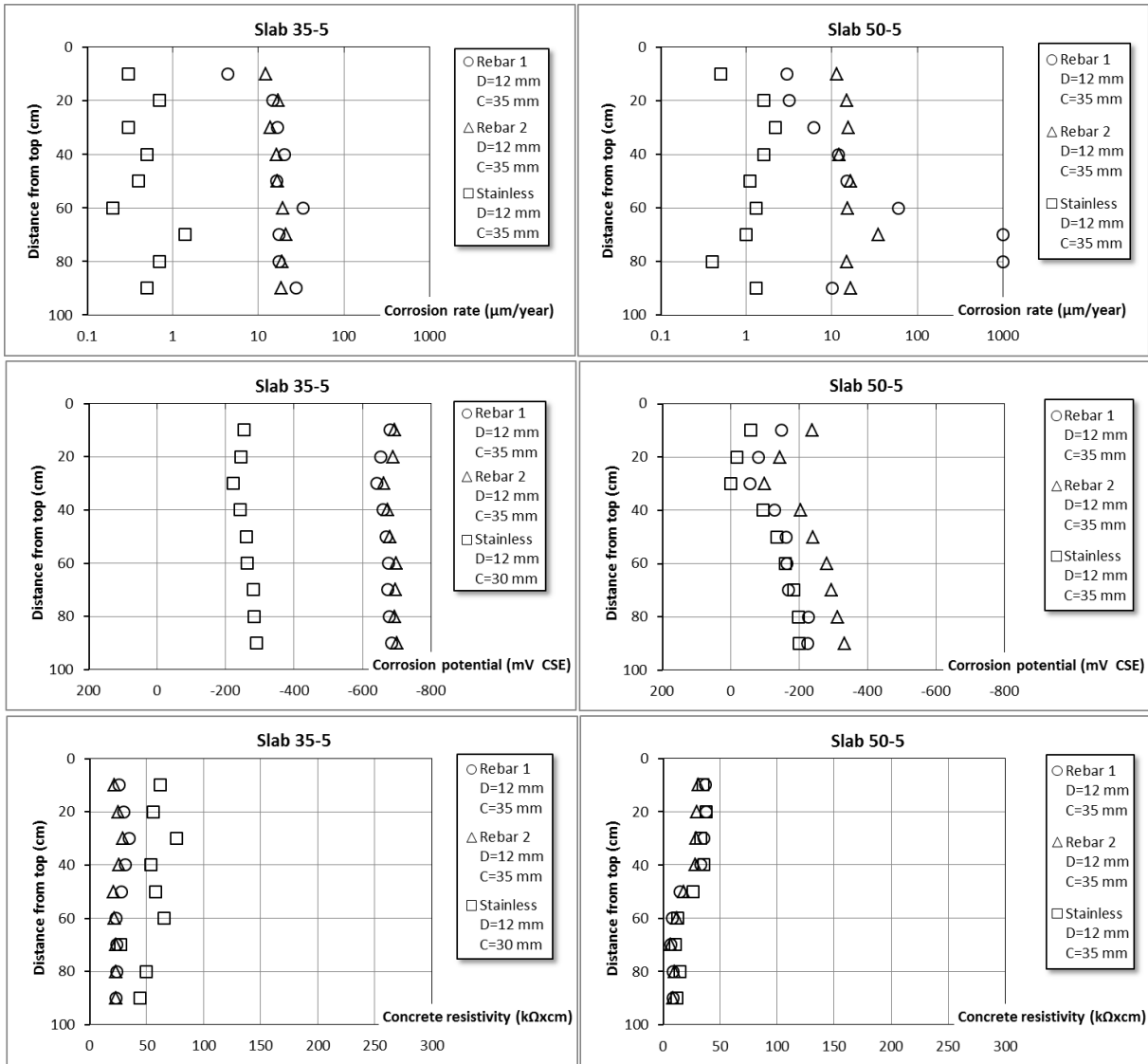
Mix	Rebar	Diameter (mm)	Cover (mm)	After 20 years				After 13 years		After 10 years
				Corr. max (µm/year)	Cl (mass % binder)	Distance from top (cm)	Visual corr.	Corr. max (µm/year)	Distance from top (cm)	Cl (mass % binder)
H5 (I)	1	12	30	2.8		30	No			
	2	12	30	2.5	0.08	60	No			
	Stainless	12	30	0.1	0.08	10-90	No			
H5(II)	1	12	35	1.4	0.07	70	No	4.4	50	0
	2	12	35	2.5		30	No	5.7	60	0
	Stainless	12	35	0.1	0.07	10-90	No	0.5	40	0



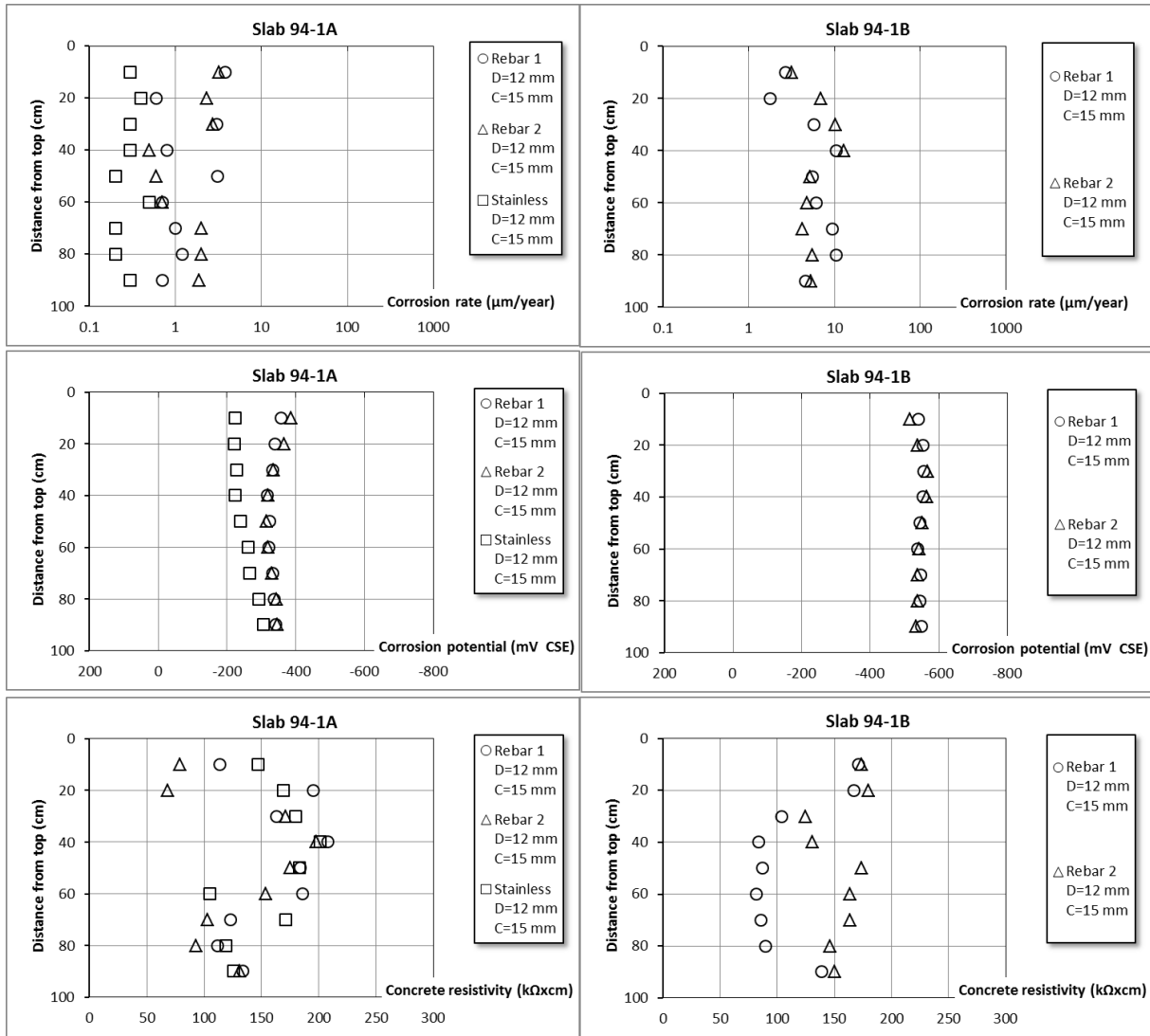
Mix	Rebar	Diameter (mm)	Cover (mm)	After 20 years			After 13 years		After 10 years	
				Corr. max (µm/year)	Cl (mass % binder)	Distance from top (cm)	Visual corr.	Corr. max (µm/year)	Distance from top (cm)	Cl (mass % binder)
H7	1	20	10	16.4		90	Yes	45.1	90	2.5
	2	20	15	3.2		70	No	7.5	80	1.8
	Stainless	20	15	1.6		30	No	2.1	10	0



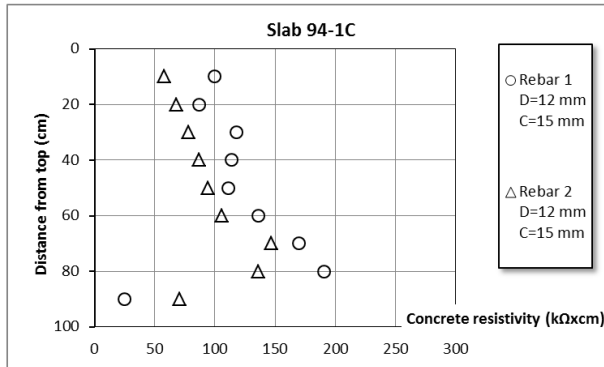
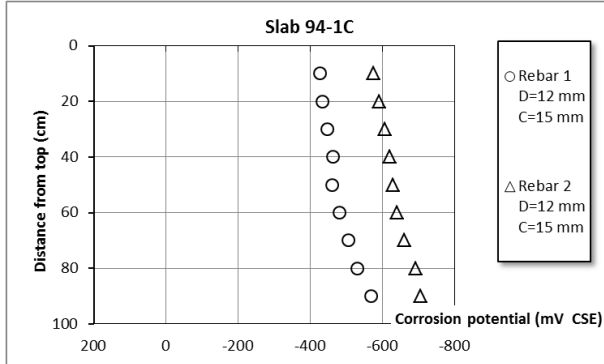
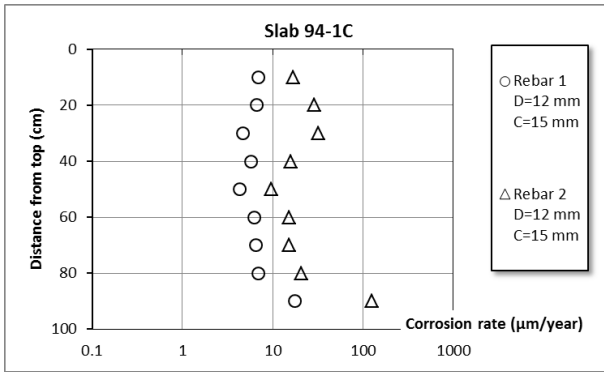
Mix	Rebar	Diameter (mm)	Cover (mm)	After 20 years				After 13 years		After 10 years
				Corr. max (µm/year)	CI (mass % binder)	Distance from top (cm)	Visual corr.	Corr. max (µm/year)	Distance from top (cm)	CI (mass % binder)
30-5 (I)	1	12	35	2.4		20	No			
	2	12	35	6		30	No			
	Stainless	12	35	0.4		20	No			
30-5 (II)	1	12	35	2.4		40	No			
	2	12	35	3.1		30	No			
	Stainless	12	35	0.2	0.5	60	No			



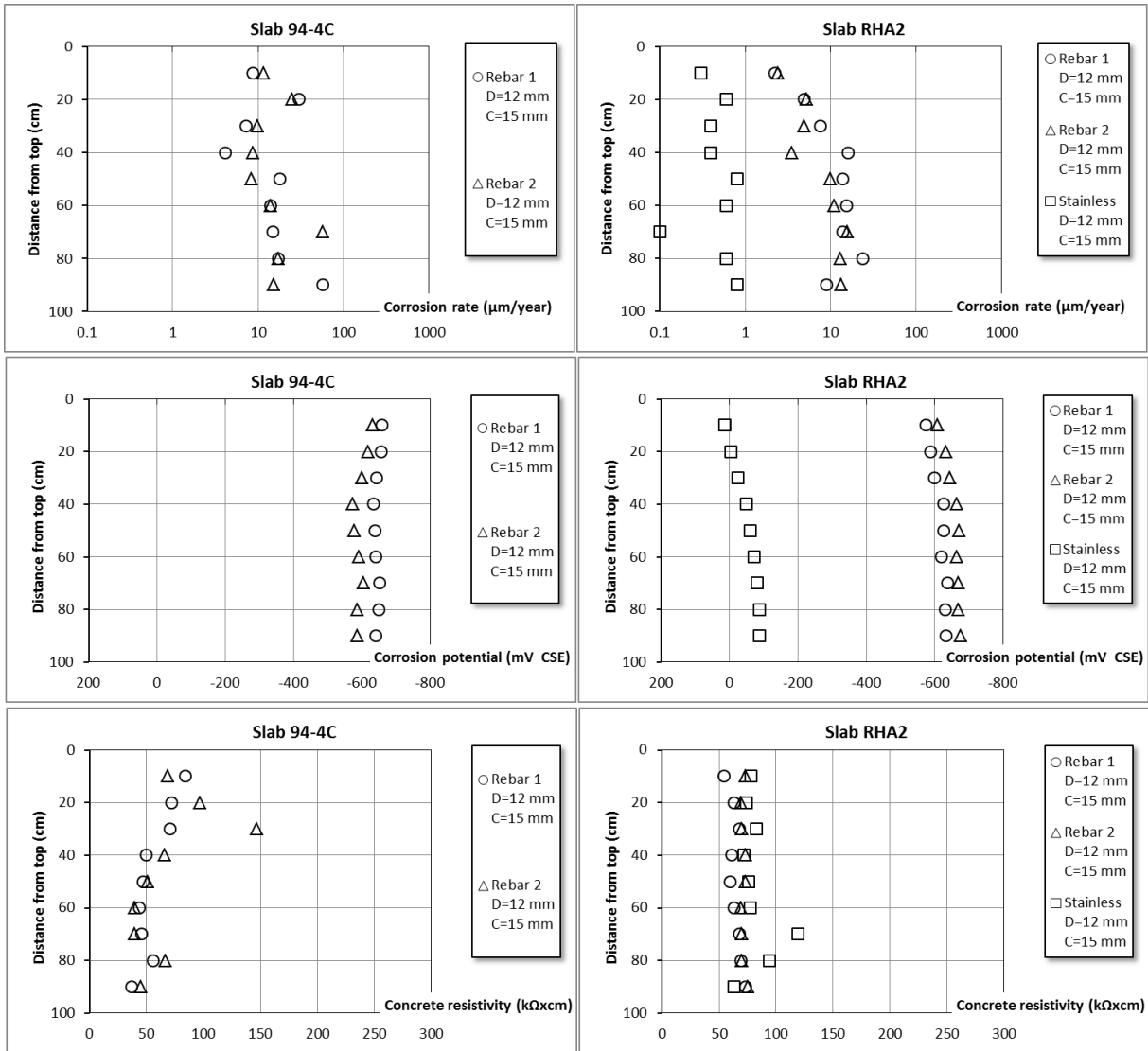
Mix	Rebar	Diameter (mm)	Cover (mm)	After 20 years			After 13 years		After 10 years
				Corr. max (µm/year)	CI (mass % binder)	Distance from top (cm)	Visual corr.	Corr. max (µm/year)	Distance from top (cm)
35-5	1	12	35	33.2	0.5	60	No		
	2	12	35	21.2	0.5	70	No		
	Stainless	12	30	1.4	0.8	70	No		
50-5	1	12	35	>500		70	No		
	2	12	35	35.4		70	No		
	Stainless	12	35	2.2		30	No		



Mix	Rebar	Diameter (mm)	Cover (mm)	After 20 years				After 13 years		After 10 years
				Corr. max (µm/year)	Cl (mass % binder)	Distance from top (cm)	Visual corr.	Corr. max (µm/year)	Distance from top (cm)	Cl (mass % binder)
94-1A	1	12	15	3.8		10	No			
	2	12	15	3.2		10	No			
	Stainless	12	15	0.5		60	No			
94-1B	1	12	15	10.4	2.1	80	Yes			
	2	12	15	13		40	Yes			



Mix	Rebar	Diameter (mm)	Cover (mm)	After 20 years				After 13 years		After 10 years
				Corr. max ($\mu\text{m/year}$)	Cl (mass % binder)	Distance from top (cm)	Visual corr.	Corr. max ($\mu\text{m/year}$)	Distance from top (cm)	Cl (mass % binder)
94-1C	1	12	15	17.5		90	Yes			
	2	12	15	124.6		90	Yes			



Mix	Rebar	Diameter (mm)	Cover (mm)	After 20 years				After 13 years		After 10 years
				Corr. max (µm/year)	Cl (mass % binder)	Distance from top (cm)	Visual corr.	Corr. max (µm/year)	Distance from top (cm)	Cl (mass % binder)
94-4C	1	12	15	57.1	1.3	90	Yes			
	2	12	15	57.3	1.3	70	Yes			
	Stainless									
RHA2	1	12	15	23.9	2.3	80	No			
	2	12	15	15.5	2.3	70	Yes			
	Stainless	12	15	0.8	2.3	90	No			

Appendix 5

Visual examination and confirmation of corrosion conditions

In this section the RapiCor measurements are compared with visual examinations. Further, the chloride levels at the reinforcement, both from chloride profiling and from samples taken direct at the reinforcement after opening of the specimens are presented.

Fig. 1 shows various types of corrosion which will be referred to in the text.




 <p>Uniform corrosion</p> <p>The reaction starts at the surface and proceeds uniformly.</p>	 <p>Localized corrosion (pitting corrosion)</p> <p>The basis metal is eaten away and perforated in places in the manner of holes, the rest of the surface being affected only slightly or not at all.</p>	 <p>Wide pitting corrosion</p> <p>The corrosion causes localized scarring.</p>
---	---	--

Figure 1. Various types of corrosion.

Slab 94-1B

Table 1. Maximum corrosion rate and chloride content (taken from profiles) after 18 years

Rebar	Diameter (mm)	Cover (mm)	Corr. Max ($\mu\text{m}/\text{year}$)	Cl (profile) (mass % binder)	Distance from top (cm)	Extern. visual corr.
1	12	15	10.4	2.1/-	80/40	Yes
2	12	15	13	-	40	Yes

Rebar 1

The visual examination showed some corrosion products in the cracks. After removing the rebar from the slab two distinct wide pitting corrosion positions were observed, one at distance 35 cm from the top, and the other 77-80 cm from the top (see Fig. 2). This is consistent with the maximum corrosion rate measurements as can be seen in Table 1 and Fig. 2.

Rebar 2

The visual examination showed some corrosion products in the cracks. After removing the rebar from the slab several corrosion initiation sites were observed. Between 0-6 cm, (under the protective tape) uniform corrosion was observed at the surface (see Fig. 2). From 10 cm to about 40 cm several corrosion spots were observed of the type of wide pitting corrosion (see Fig. 2). No corrosion had occurred under 40 cm from the top, this is consistent with the corrosion rate measurements in Fig. 2.

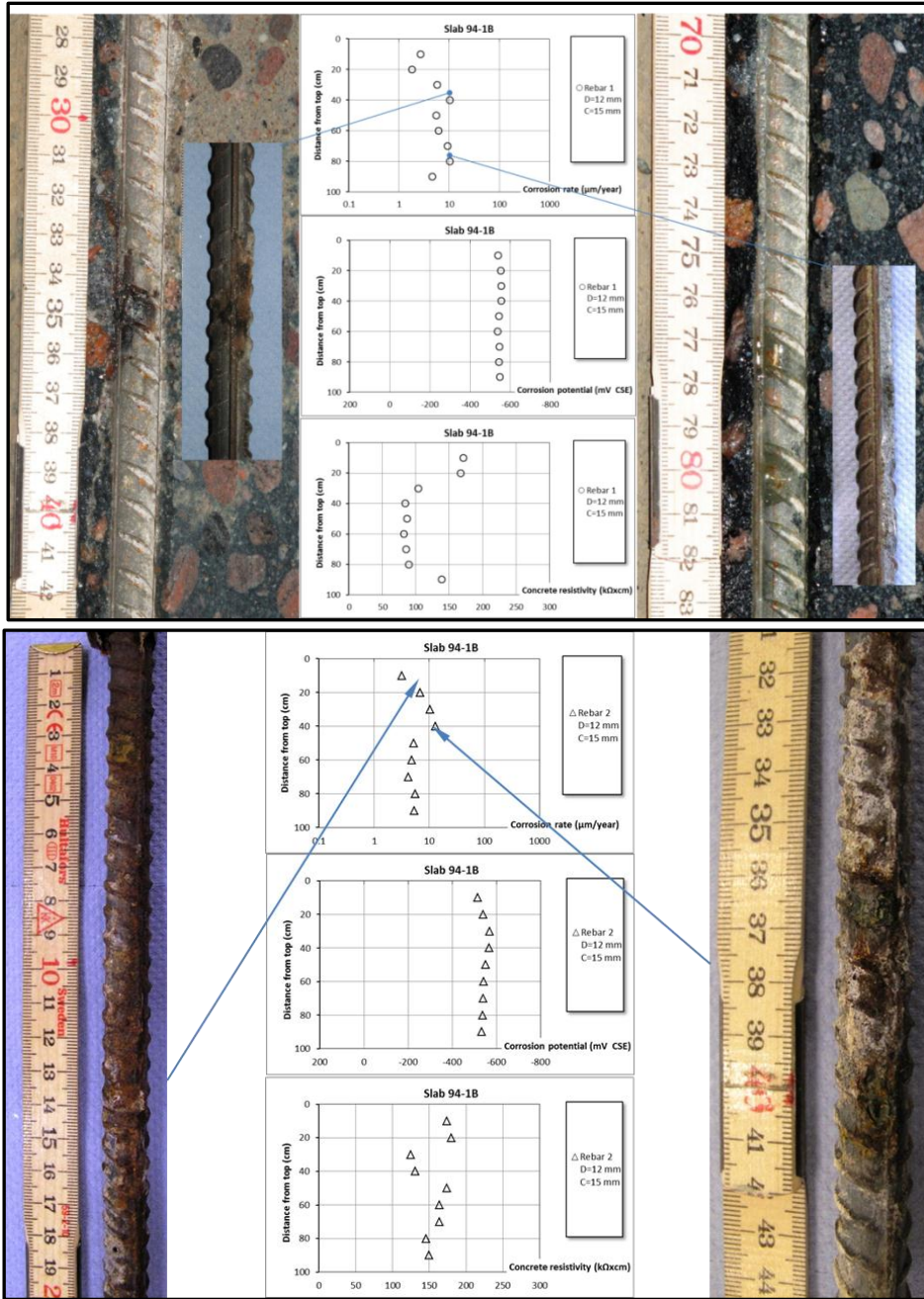


Figure 2. Visual examination and corrosion measurements for rebar in slab 94-1B.

Table 2 Chloride content at cover level after removal of the rebar.

Rebar 1		Rebar 2	
Dist. from top (cm)	Cl (mass % binder)	Dist. form top (cm)	Cl (mass % binder)
33	1.8	35	1.9
35 (corr. point)	2.2	37 (corr. point)	1.7
37	1.9		

Slab 2-50

Table 3. Maximum corrosion rate and chloride content (taken from profiles) after 20 years.

Rebar	Diameter (mm)	Cover (mm)	Corr. Max ($\mu\text{m}/\text{year}$)	Cl (profile) (mass % binder)	Distance from top (cm)	Extern. visual corr.
2	12	15	13.4	2	30	No

Rebar 2

Two pitting corrosion sites were observed, one at distance 6 cm from the top, and the other at the lower end of the rebar (see Fig. 3.). Further, severe uniform corrosion was observed between 0 to 6 cm from the top (see Fig. 3), this part was under the protective tape. The visual observations in this case are not consistent with the corrosion rate measurements as can be seen in Fig. 3. An explanation to this discrepancy can be that it was not possible to make a proper corrosion measurement for either of the two pitting corrosion spots. In the first case because the corrosion spot (at 6 cm from top) was partially under the protective tape, and in the second case because it was a small corrosion spot at the cutting edge of the rebar. Why maximum corrosion rate was measured 30 cm from the top without observing any corrosion on the rebar is difficult to explain.

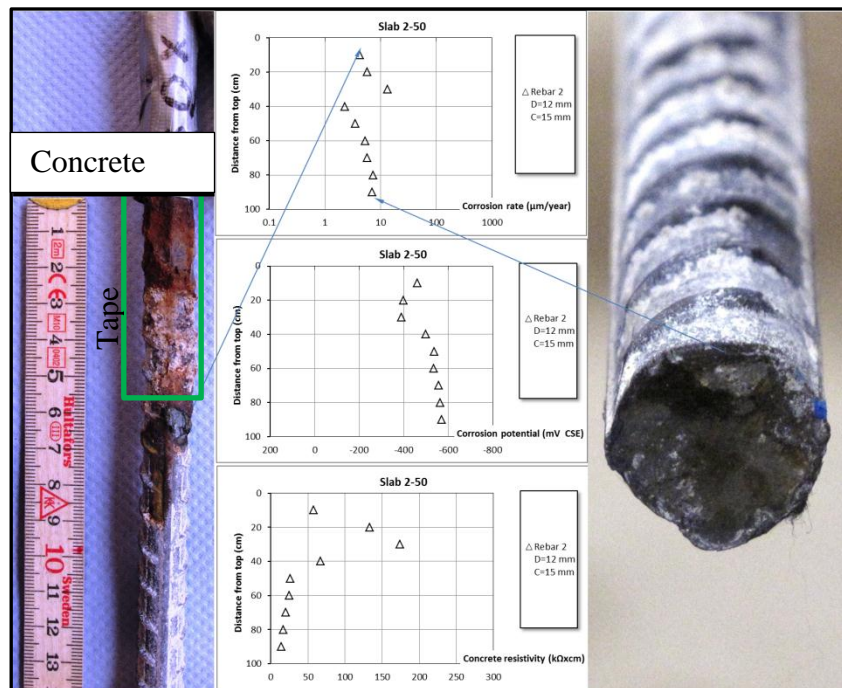


Figure 5.3. Visual examination and corrosion measurements for rebar 2 in slab 2-50.

Table 4. Chloride content at cover level after removal of the rebar.

Rebar 2	
Dist. form top (cm)	Cl (mass % binder)
25	1.43

Slab H7

Table 5. Maximum corrosion rate and chloride content (taken from profiles) at the rebars.

Rebar	Diameter (mm)	Cover (mm)	Corr. Max ($\mu\text{m}/\text{year}$)	Cl (profile) (mass % binder)	Distance from top (cm)	Extern. visual corr.
1	20	10	16.4	-	90	Yes

Rebar 1

Three corrosion sites were observed on the rebar (see Fig. 4). Severe uniform corrosion was observed from 0 to 7 cm from the top (under the protective tape). Further, wide pitting corrosion was observed at the lower end of the rebar, and a small pitting corrosion spot was located 54 cm from the top. The visual observations were consistent with the corrosion rate measurements except for the corrosion spot located 54 cm from the top, where a higher measured corrosion rate would be expected (see Fig. 4).

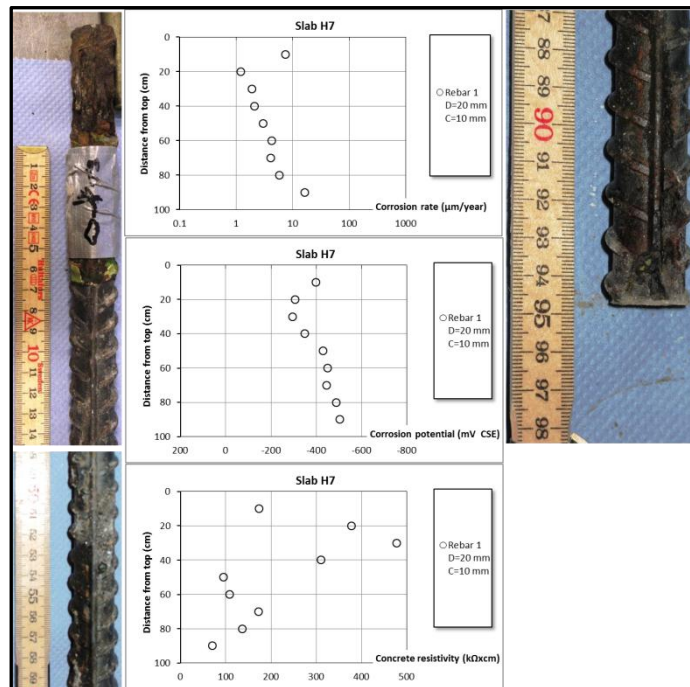


Figure 4. Visual examination and corrosion measurements for rebar 1 in slab H7

Table 6. Chloride content at cover level after removal of the rebars.

Rebar 1	
Dist. from top (cm)	Cl (mass % binder)
92	0.61
94 (corr.)	0.87
96 (spacer)	2.15

Slab 8-40II

Table 7. Maximum corrosion rate and chloride content (taken from profiles) after 20 years.

Rebar	Diameter (mm)	Cover (mm)	Corr. Max ($\mu\text{m}/\text{year}$)	Cl (profile) (mass % binder)	Distance from top (cm)	Extern. visual corr.
1	20	15	>500	2.6	90	Yes
2	20	20	>500	2.3	90	Yes

Rebar 1

Several corrosion sites along the rebar were observed as can be seen in Fig. 5. At the atmospheric zone (0-40 cm) only uniform corrosion was observed from 0 to 7 cm from the top (under the protective tape). The severest corrosion site was located at the lower end of the rebar, where the diameter was reduces to about half of its original size. The corrosion measurement reflect quite good the visual observations, with the exception that the corrosion rate measurement shows higher values then expected between 20 to 40 cm from the top.

Rebar 2

Only two corrosion sites were observed (see Fig. 5), one about 3 cm from the top (under the protective tape) and the other at the lower end of the rebar. Both corrosion sites were of the wide pitting corrosion type. The visual observations were consistence with the corrosion rate measurements.

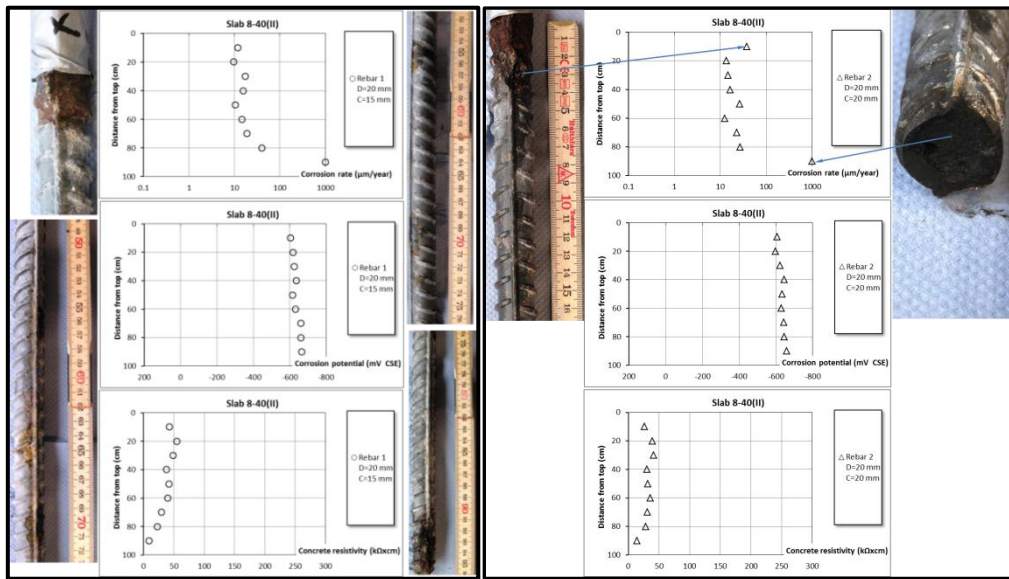


Figure 5. Visual examination and corrosion measurements for rebars 1 and 2 in slab 8-40(II).

Table 8. Chloride content at cover level after removal of the rebars.

Rebar 1		Rebar 2	
Dist. from top (cm)	Cl (mass % binder)	Dist. from top (cm)	Cl (mass % binder)
70	2.1	25	0.36
		94	2.7

Slab H2III

Table 7. Maximum corrosion rate and chloride content (taken from profiles) after 20 years.

Rebar	Diameter (mm)	Cover (mm)	Corr. Max ($\mu\text{m}/\text{year}$)	Cl (profile) (mass % binder)	Distance from top (cm)	Extern. visual corr.
1	20	15	110.1	2.4	90	No
2	20	20	40	1.3	90	No

Rebar 1

Two corrosion sites were observed (see Fig. 6). Uniform corrosion was observed from 0 to 7 cm from the top under the protective tape, and a wide spot of pitting corrosion type was observed at the lower end of the rebar. The visual observations were consistent with the corrosion rate measurements.

Rebar 2

Two corrosion sites were observed (see Fig. 6). Uniform corrosion was observed from 0 to 7 cm from the top under the protective tape including also pitting corrosion about 6 cm from the top. Pitting corrosion was also observed at the lower end of the rebar. The visual observations were quite consistent with the corrosion rate measurements in Fig. 6. The reason why not a higher corrosion was measured close to the upper corrosion site can be that this site was under the protective tape.

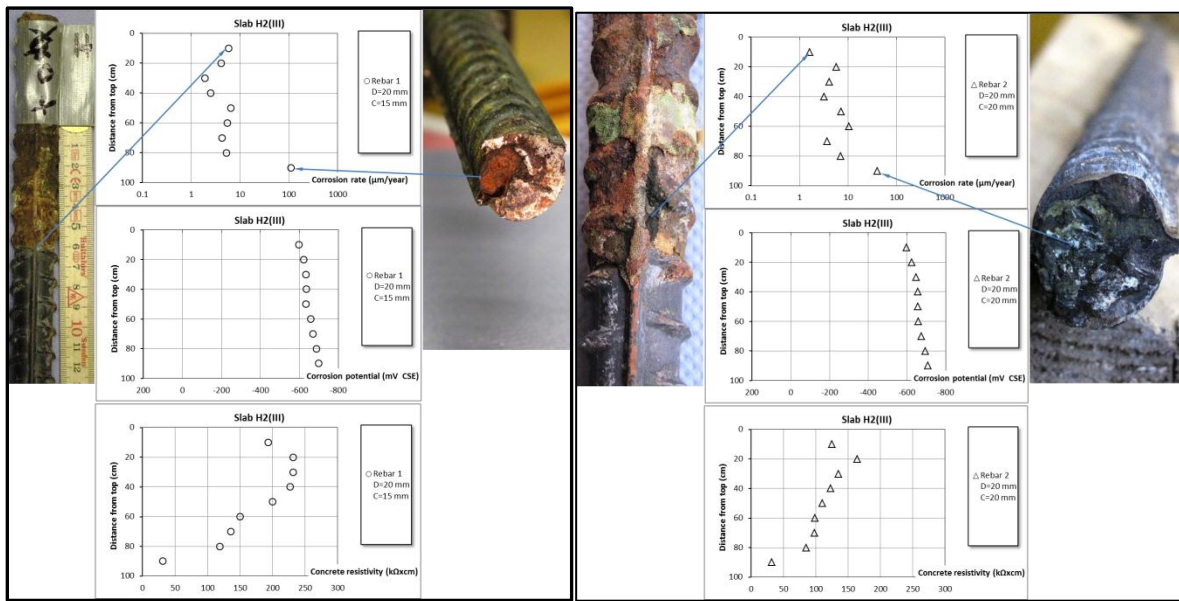


Figure 6. Visual examination and corrosion measurements for rebars 1 and 2 in slab H2 (III).

Table 8. Chloride content at cover level after removal of the rebars.

Rebar 1		Rebar 2	
Dist. from top (cm)	Cl (mass % binder)	Dist. from top (cm)	Cl (mass % binder)
25	0.14	25	0.11

Slab 1-351

Table 9. Maximum corrosion rate and chloride content (taken from profiles) after 20 years.

Rebar	Diameter (mm)	Cover (mm)	Corr. Max ($\mu\text{m}/\text{year}$)	Cl (profile) (mass % binder)	Distance from top (cm)	Extern. visual corr.
2	12	15	36.9	3.6	90	Yes

Rebar 2

Except for the uniform corrosion at the top under the protective tape, three different pitting corrosion sites were observed, placed at 63 cm and 80 cm from the top, and at the lower end of the bar. Despite quite high measured corrosion rates in the atmospheric zone no corrosion was observed at that area.

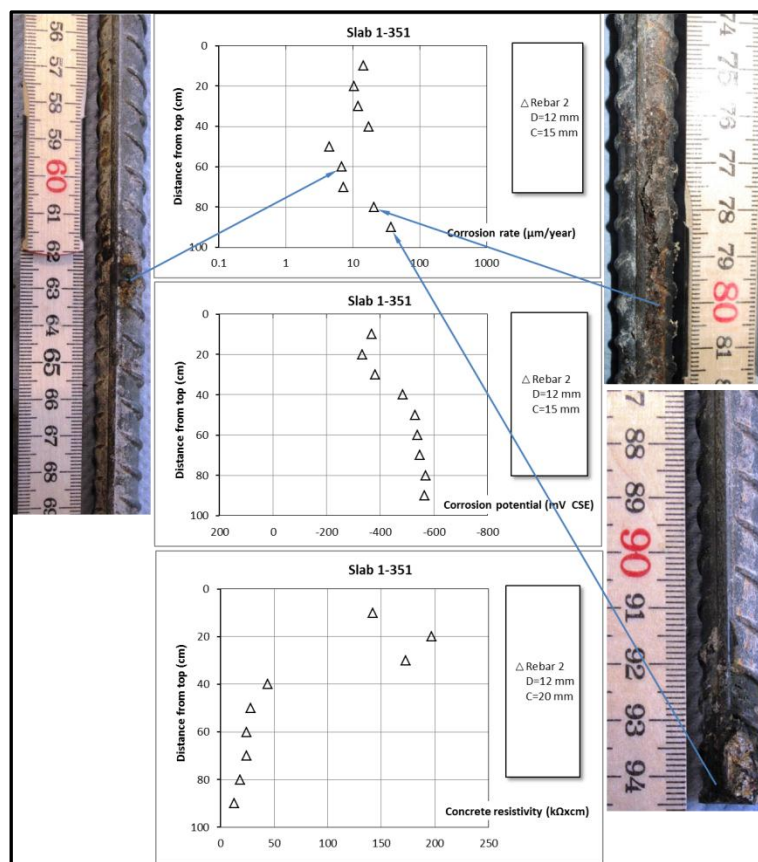


Figure 7. Visual examination and corrosion measurements for rebar 2 in slab 1-351.

Table 10. Chloride content at cover level after removal of the rebar.

Rebar 2	
Dist. form top (cm)	Cl (mass % binder)
25	0.6
76	3.2

Slab 94-2A

Table 11. Maximum corrosion rate and chloride content (taken from profiles) after 18 years.

Rebar	Diameter (mm)	Cover (mm)	Corr. Max ($\mu\text{m}/\text{year}$)	Cl (profile) (mass % binder)	Distance from top (cm)	Extern. visual corr.
1	12	15	>500	-	80	Yes
2	12	15	>500	-	80	Yes

Rebar 1

Three corrosion sites were observed (see Fig. 8). Severe uniform corrosion was observed from 0 to 5 cm from the top under the protective tape, and a wide spot of severe pitting corrosion was observed at 80 cm distance from top. Further, a minor pitting corrosion was observed about 60 cm from the top. The visual observations were consistent with the corrosion rate measurements.

Rebar 2

Uniform corrosion was observed from 0 to 5 cm from the top under the protective tape (see Fig. 8). Several minor pitting corrosion sites were observed along the rebar at 17, 22, 60 and 67 cm from the top. The severest pitting corrosion was observed at 80 cm distance from top (see Fig. 8). The visual observations were quite consistent with the corrosion rate measurements.

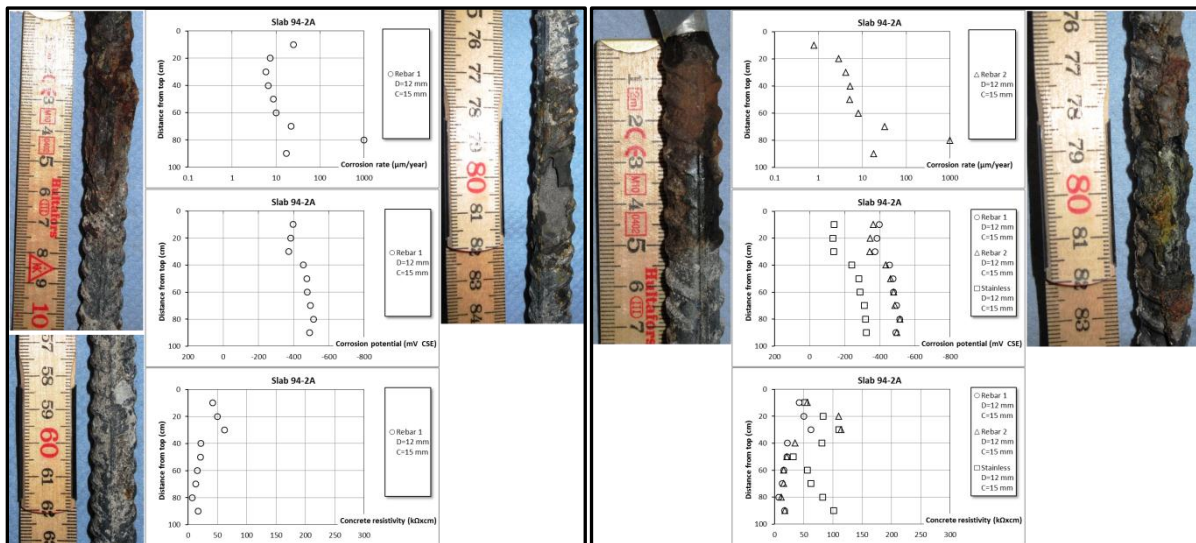


Figure 8. Visual examination and corrosion measurements for rebars 1 and 2 in slab 94-2A.

Table 12. Chloride content at cover level after removal of the rebars.

Rebar 1		Rebar 2	
Dist. from top (cm)	Cl (mass % binder)	Dist. from top (cm)	Cl (mass % binder)
25	0.8	25	0.9

Slab 94-3A

Table 11. Maximum corrosion rate and chloride content (taken from profiles) after 18 years.

Rebar	Diameter (mm)	Cover (mm)	Corr. Max ($\mu\text{m}/\text{year}$)	Cl (profile) (mass % binder)	Distance from top (cm)	Extern. visual corr.
1	12	15	>500	-	90	Yes
2	12	15	>500	-	60	No

Rebar 1

Three corrosion sites were observed (see Fig. 9). Minor uniform corrosion was observed from 0 to 5 cm from the top under the protective tape, and a wide spot of severe pitting corrosion was observed at 90 cm distance from top. Further, a minor pitting corrosion was observed about 28 cm from the top. The visual observations were consistence with the corrosion rate measurements.

Rebar 2

Uniform corrosion was observed from 0 to 5 cm from the top under the protective tape (see Fig. 9). Minor pitting corrosion sites were observed about 18 cm from the top, and severe pitting corrosion was observed at 58 cm from top (see Fig. 9). The visual observations were quite consistence with the corrosion rate measurements.

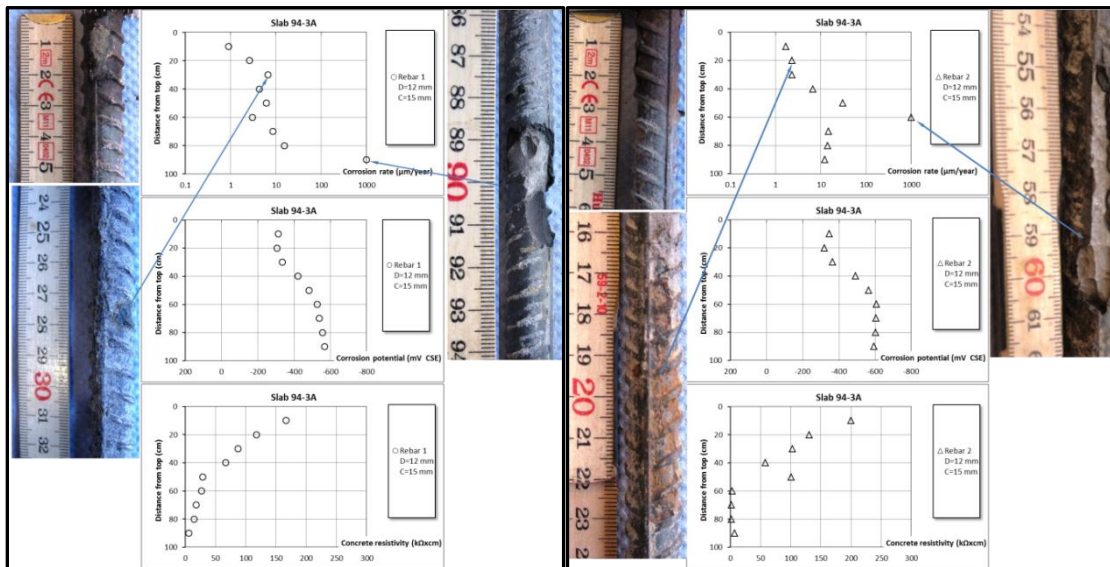


Figure 9. Visual examination and corrosion measurements for rebars 1 and 2 in slab 94-3A.

Table 12. Chloride content at cover level after removal of the rebars.

Rebar 1		Rebar 2	
Dist. from top (cm)	Cl (mass % binder)	Dist. form top (cm)	Cl (mass % binder)
28	2.8	18	0.5
		58	3.4
		90	2.7

Slab 50-5

Table 13. Maximum corrosion rate and chloride content (taken from profiles) after 20 years.

Rebar	Diameter (mm)	Cover (mm)	Corr. Max ($\mu\text{m}/\text{year}$)	Cl (profile) (mass % binder)	Distance from top (cm)	Extern. visual corr.
1	12	35	>500	-	70	No
2	12	35	>35.4	-	70	No

Rebar 1

Minor uniform corrosion was observed from 0 to 6 cm from the top under the protective tape, and a wide spot of severe pitting corrosion was observed at 70 cm distance from top. Further, minor pitting corrosion was observed at 86 cm (back side) from the top. The visual observations were consistency with the corrosion rate measurements.

Rebar 2

Minor uniform corrosion was observed from 0 to 6 cm from the top under the protective tape, and a wide spot of severe pitting corrosion was observed at 67 cm distance from top. Further, minor pitting corrosion spots were observed between 70 to 72 cm from the top. The visual observations were consistency with the corrosion rate measurements.

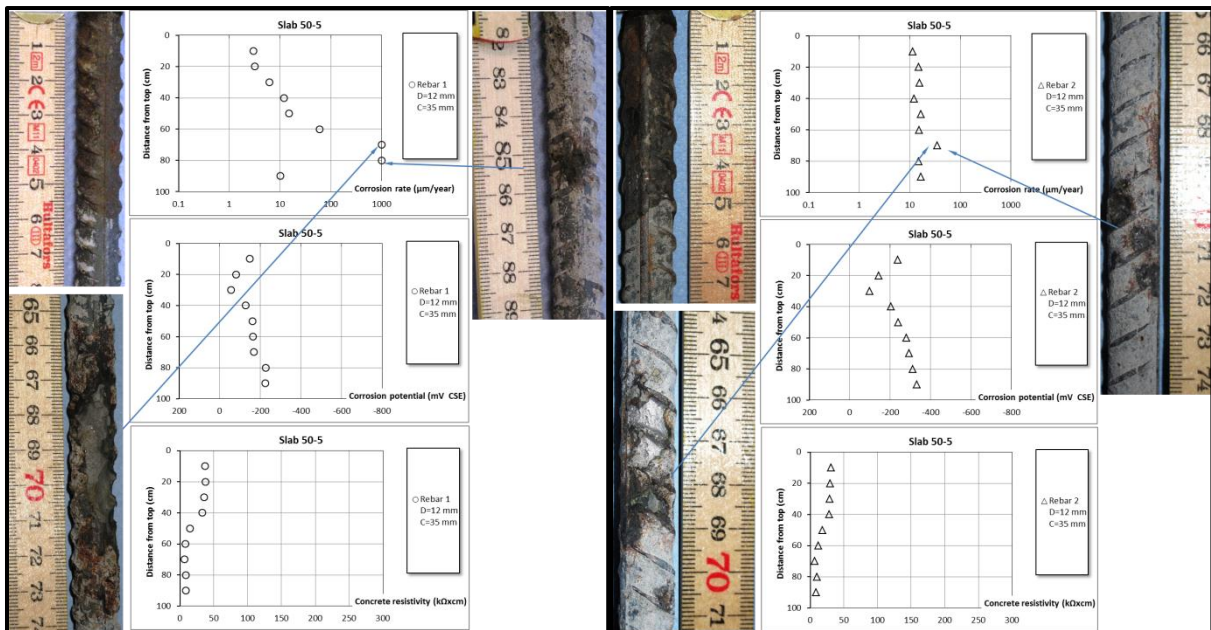


Figure 10. Visual examination and corrosion measurements for rebars 1 and 2 in slab 50-5.

Table 14. Chloride content at cover level after removal of the rebars.

Rebar 1		Rebar 2	
Dist. from top (cm)	Cl (mass % binder)	Dist. form top (cm)	Cl (mass % binder)
25	0.4	25	0.5
70	5.4	75	2.84

Slab RHA2

Table 15. Maximum corrosion rate and chloride content (taken from profiles) after 18 years.

Rebar	Diameter (mm)	Cover (mm)	Corr. Max ($\mu\text{m}/\text{year}$)	Cl (profile) (mass % binder)	Distance from top (cm)	Extern. visual corr.
1	12	15	23.9	2.3	80	No

Rebar 1

Minor pitting corrosion was observed at 83 cm from the top.

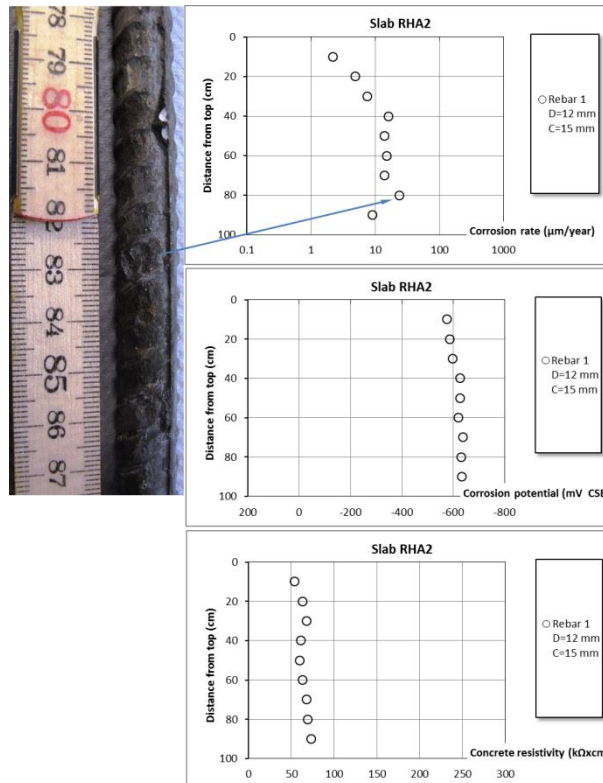


Figure 11. Visual examination and corrosion measurements for rebars 1 and 2 in slab RHA2.

Table 16. Chloride content at cover level after removal of the rebar.

Rebar 2	
Dist. form top (cm)	Cl (mass % binder)
25	0.43
80	1.7

Slab 35-5

Table 17. Maximum corrosion rate and chloride content (taken from profiles) after 20 years.

Rebar	Diameter (mm)	Cover (mm)	Corr. Max ($\mu\text{m}/\text{year}$)	Cl (profile) (mass % binder)	Distance from top (cm)	Extern. visual corr.
1	12	35	33.2	0.5	60	No
2	12	35	21.2	0.5	70	No

Rebar 1

Minor uniform corrosion was observed from 0 to 6 cm from the top under the protective tape and minor pitting corrosion was observed at the lower end side of the rebar (see Fig. 12). Further, it was unclear if corrosion was initiated at about 60 cm from the top.

Rebar 2

Minor uniform corrosion was observed at the top of the rebar under the protective tape. Minor corrosion spots were also observed at 56 and 91 cm from the top of the rebar, in both these case it was difficult to distinguish the corrosion type.

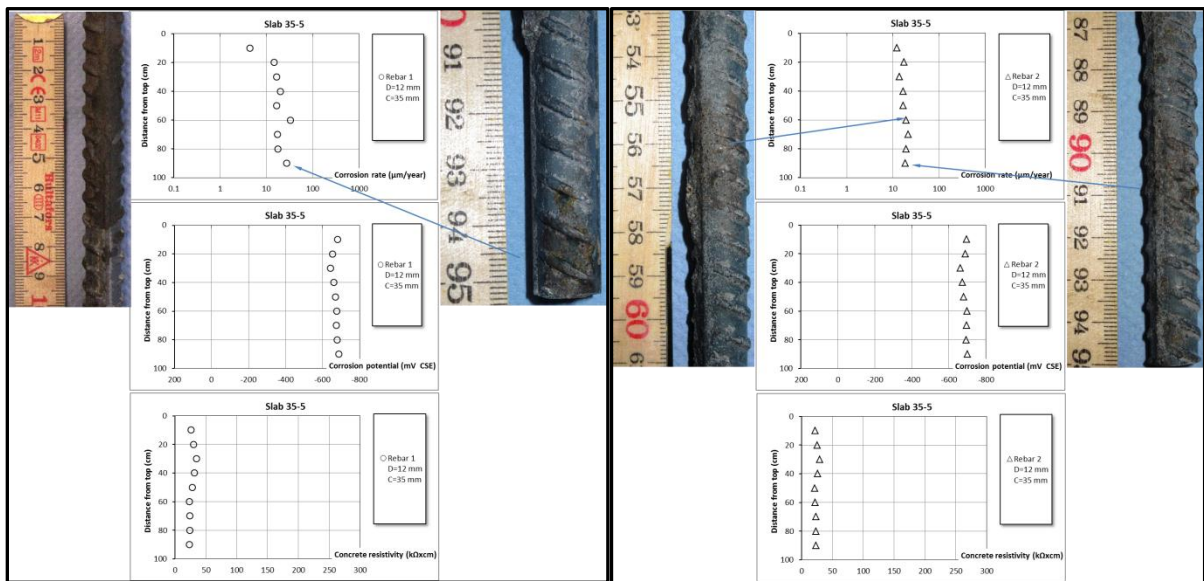


Figure 12. Visual examination and corrosion measurements for rebars 1 and 2 in slab 35-5.

Table 18. Chloride content at cover level after removal of the rebars.

Rebar 1		Rebar 2	
Dist. from top (cm)	Cl (mass % binder)	Dist. from top (cm)	Cl (mass % binder)
25	0.03	25	0.02

Slab 2-35

Table 19. Maximum corrosion rate and chloride content (taken from profiles) after 20 years.

Rebar	Diameter (mm)	Cover (mm)	Corr. Max ($\mu\text{m}/\text{year}$)	Cl (Sub.-profile) (mass % binder)	Distance from top (cm)	Extern. visual corr.
1	20	20	>500	2.2	90	Yes

Rebar 1

Severe uniform corrosion was observed from 1 to 3 cm from the top under the protective tape and severe pitting corrosion was observed at the lower end side of the rebar (see Fig. 13). Further, minor corrosion (surface type) was observed about 45 cm from the top.

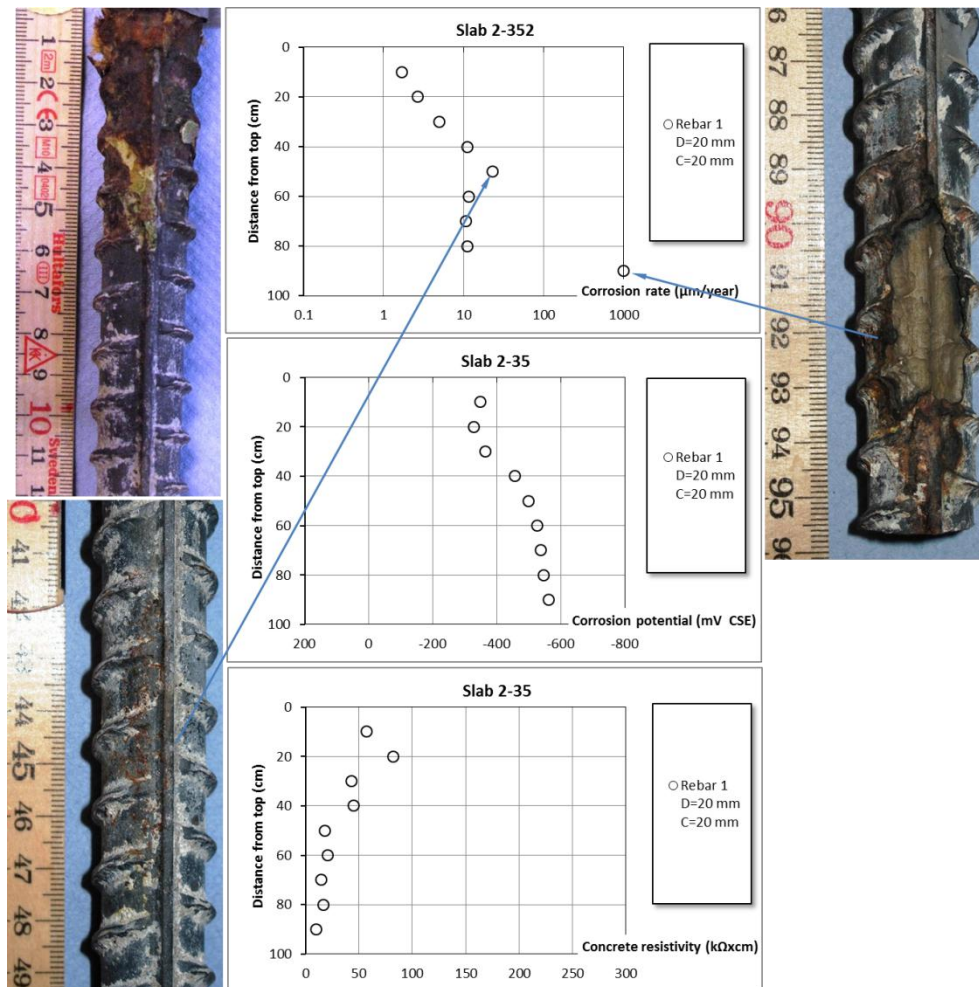


Figure 13. Visual examination and corrosion measurements for rebar 1 in slab 2-35.

Table 20. Chloride content at the rebar level from chloride profiles.

Rebar 1	
Dist. from top (cm)	Cl (mass % binder)
Atm. zone	1.4
Splash zone	2.0

Slab 12-35

Table 21. Maximum corrosion rate and chloride content (taken from profiles) after 20 years.

Rebar	Diameter (mm)	Cover (mm)	Corr. Max ($\mu\text{m}/\text{year}$)	Cl (Spl.-profile) (mass % binder)	Distance from top (cm)	Extern. visual corr.
2	12	15	6.6	-	50	No

Rebar 1

Uniform corrosion was observed from 0 to 6 cm from the top under the protective tape and several pitting corrosion sites along the rebar from about 54 cm to 90 cm from the top (see Fig. 14).

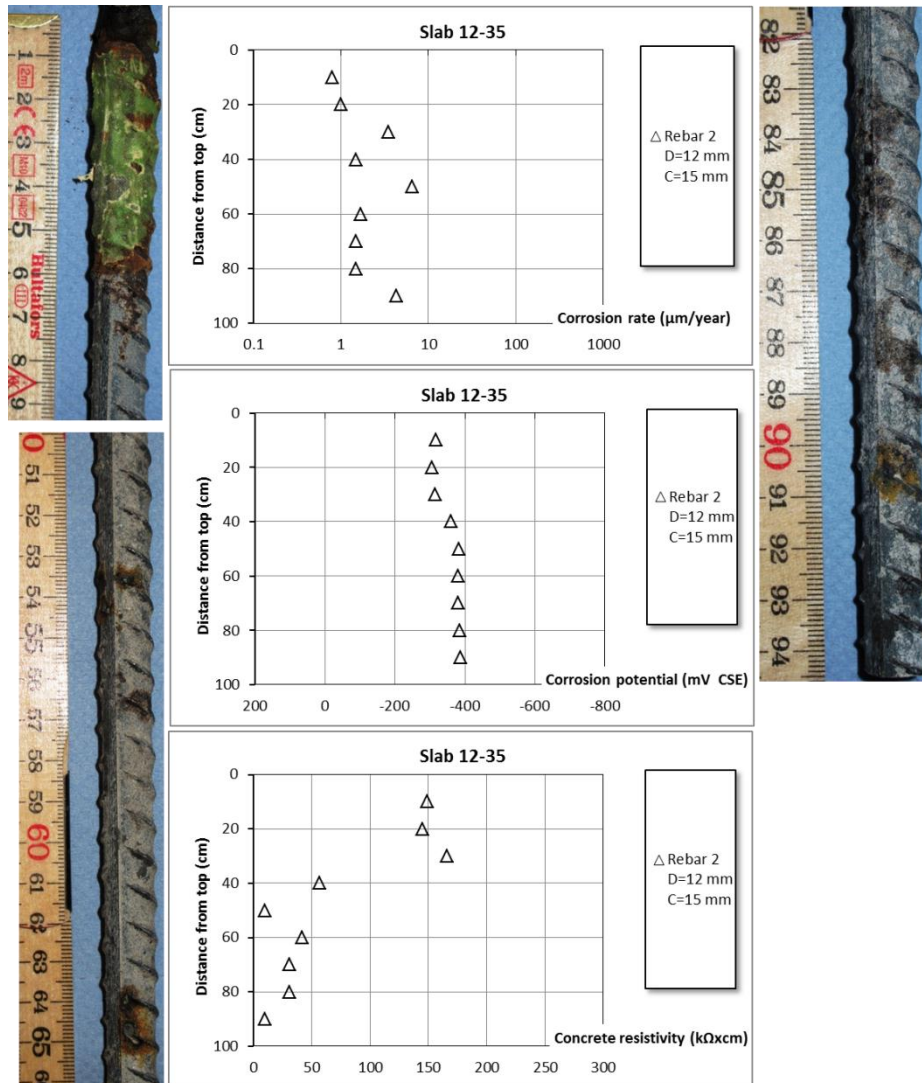


Figure 14. Visual examination and corrosion measurements for rebar 2 in slab 12-35.

Table 22. Chloride content at the rebar level from chloride profiles.

Rebar 2	
Dist. from top (cm)	Cl (mass % binder)
Sub. zone	2.7